frontiers | Research Topics

The physiology, molecular biology and biochemistry in ripening and stored fruit

Edited by
Shifeng Cao, Kaituo Wang, C. Watkins and Zhenfeng Yang

Published in
Frontiers in Plant Science

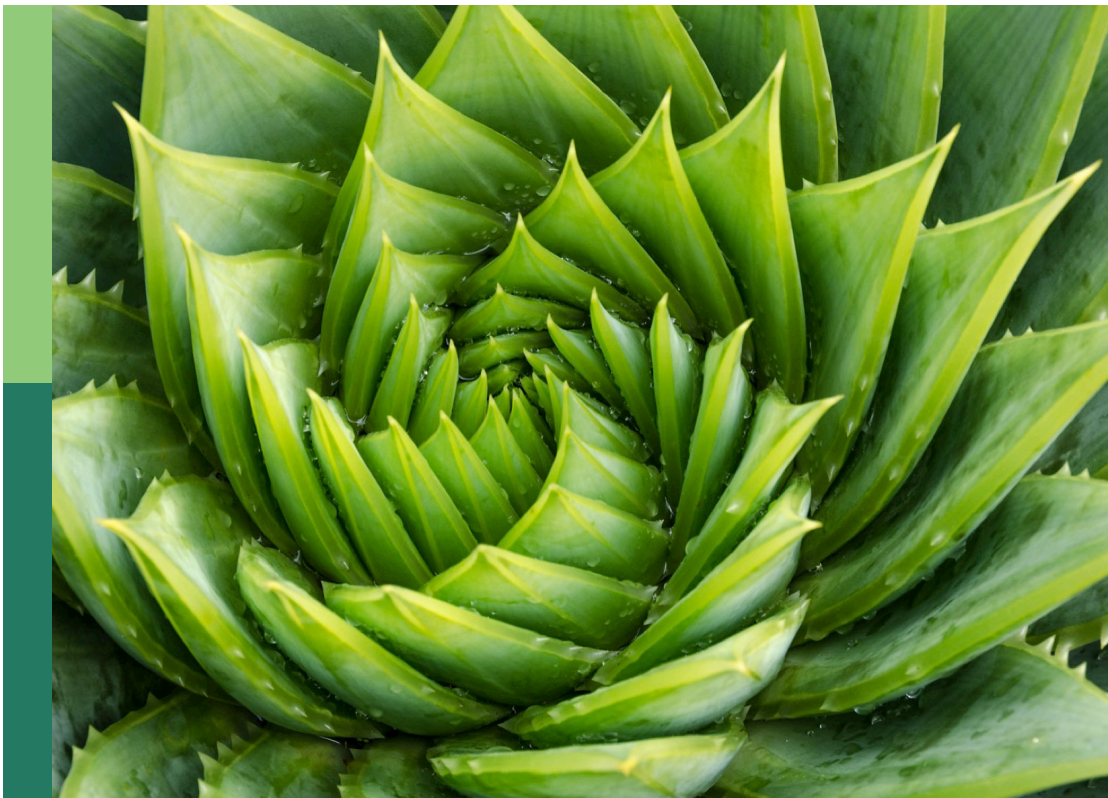

ISSN 1664-8714
ISBN 978-2-8325-3707-7
DOI 10.3389/978-2-8325-3707-7

About Frontiers

Frontiers is more than just an open access publisher of scholarly articles: it is a pioneering approach to the world of academia, radically improving the way scholarly research is managed. The grand vision of Frontiers is a world where all people have an equal opportunity to seek, share and generate knowledge. Frontiers provides immediate and permanent online open access to all its publications, but this alone is not enough to realize our grand goals.

Frontiers journal series

The Frontiers journal series is a multi-tier and interdisciplinary set of open-access, online journals, promising a paradigm shift from the current review, selection and dissemination processes in academic publishing. All Frontiers journals are driven by researchers for researchers; therefore, they constitute a service to the scholarly community. At the same time, the *Frontiers journal series* operates on a revolutionary invention, the tiered publishing system, initially addressing specific communities of scholars, and gradually climbing up to broader public understanding, thus serving the interests of the lay society, too.

Dedication to quality

Each Frontiers article is a landmark of the highest quality, thanks to genuinely collaborative interactions between authors and review editors, who include some of the world's best academicians. Research must be certified by peers before entering a stream of knowledge that may eventually reach the public - and shape society; therefore, Frontiers only applies the most rigorous and unbiased reviews. Frontiers revolutionizes research publishing by freely delivering the most outstanding research, evaluated with no bias from both the academic and social point of view. By applying the most advanced information technologies, Frontiers is catapulting scholarly publishing into a new generation.

What are Frontiers Research Topics?

Frontiers Research Topics are very popular trademarks of the *Frontiers journals series*: they are collections of at least ten articles, all centered on a particular subject. With their unique mix of varied contributions from Original Research to Review Articles, Frontiers Research Topics unify the most influential researchers, the latest key findings and historical advances in a hot research area.

Find out more on how to host your own Frontiers Research Topic or contribute to one as an author by contacting the Frontiers editorial office: frontiersin.org/about/contact

The physiology, molecular biology and biochemistry in ripening and stored fruit

Topic editors

Shifeng Cao — Zhejiang Wanli University, China
Kaituo Wang — Chongqing Three Gorges University, China
C. Watkins — Cornell University, United States
Zhenfeng Yang — Zhejiang Wanli University, China

Citation

Cao, S., Wang, K., Watkins, C., Yang, Z., eds. (2023). *The physiology, molecular biology and biochemistry in ripening and stored fruit*. Lausanne: Frontiers Media SA. doi: 10.3389/978-2-8325-3707-7

Table of contents

frontiers | Frontiers in Plant Science

TYPE Editorial
PUBLISHED 29 September 2023
DOI 10.3389/fpls.2023.1296816

OPEN ACCESS

EDITED AND REVIEWED BY
Claudio Bonghi,
University of Padua, Italy

*CORRESPONDENCE
Kaituo Wang
wangkaituo83@gmail.com

RECEIVED 19 September 2023
ACCEPTED 26 September 2023
PUBLISHED 29 September 2023

CITATION
Li C, Cao S, Yang Z, Watkins CB and Wang K (2023) Editorial: The physiology, molecular biology and biochemistry in ripening and stored fruit.
Front. Plant Sci. 14:1296816.
doi: 10.3389/fpls.2023.1296816

Editorial: The physiology, molecular biology and biochemistry in ripening and stored fruit

Chunhong Li[1,2], Shifeng Cao[2], Zhenfeng Yang[2], Christopher B. Watkins[3] and Kaituo Wang[1,4]*

[1]Institute of Fruit Function and Disease Management, Department of Public Health and Management, Chongqing Three Gorges Medical College, Chongqing, China, [2]College of Biological and Environmental Sciences, Zhejiang Wanli University, Ningbo, China, [3]Horticulture Section, School of Integrative Plant Science, College of Agriculture and Life Sciences, Cornell University, Ithaca, NY, United States, [4]College of Biology and Food Science, Chongqing Three Gorges University, Chongqing, China

KEYWORDS

fruit, ripening, chilling injury, phytohormone, transcription factor

Editorial on the Research Topic
The physiology, molecular biology and biochemistry in ripening and stored fruit

Introduction

The ripening process of fruits is complicated and coordinated and is characterized by obvious changes in pericarp color (green color loss and non-photosynthetic pigment increases), flesh texture (modulating by cell wall-degrading enzymes), taste (variation of sugars and organic acids), and aroma flavour (volatile productions) of fleshy fruits (Giovannoni, 2001). Specifically, most horticultural fruits of tropical origin suffer from physiological injury when exposed to cold temperature (Wang, 1989). A comprehensive understanding of the mechanism of phytohormone-mediated protection and the transcriptional regulation network may provide strategies to maintain fruit quality and reduce cold stress-induced losses. Hence, efforts to unravel the mechanisms of alleviation in fruit ripening and mitigation in chilling injury (CI) are pivotal contributing solutions to regulate postharvest fruit quality. Eleven original research articles that focus on the regulatory mechanisms of fruit ripening and chilling injury or offer effective strategies to retard fruit ripening and alleviate chilling injury were included in this Research Topic.

Quality formation and ripening regulation of horticultural fruits

The material basis and regulator underlying fruit development and ripening still remain challenges. Teixeira et al. showed that the exocarp of green and mature grape berries is rich in chloroplasts, and they applied proteomic analysis of chloroplasts from the

two phases. The authors observed that proteins associated with the Calvin cycle were stimulated in green berries, while those related to energy-generating metabolism were enriched in mature berries. Wang et al. systematically identified a batch of lignin biosynthesis-related genes and constructed a co-expression network of these genes via weighted gene co-expression network analysis. Specifically, they found the major lignin biosynthesis genes involved in ripening process and stress resistance in banana. Liu et al. reviewed NAC transcription factors, which show extensive participation in fruit yield and quality and regulate fruit ripening by directly acting on critical genes related to the biosynthesis and signal transduction of the plant hormones abscisic acid (ABA) and ethylene (ET). These articles provide the basis for the improvement of fruit development and ripening.

Postharvest ripening and senescence restrict the shelf life of horticultural crops. Both Huang et al. and Jiang et al. reported that salicylic acid (SA) treatment could maintain the organoleptic quality and postharvest storability of pummelo and blueberry. Li et al. recorded that pear had a greasy coating and yellowing process during postharvest storage, while 1-methylcyclopropene (1-MCP) could decrease the wax content of postharvest pear and delay the development of peel greasiness and yellowing by suppressing the transcription of a series of cluster genes associated with ethylene synthesis, ethylene signal transduction, wax accumulation, and chlorophyll degradation. Choi et al. investigated the molecular details of kiwifruit ripening using ethylene and its action inhibitor 1-MCP. Through a time-course transcriptomic analysis, they found that the genes related to ET synthesis and signalling suffered from opposite influence from postharvest application of 1-MCP and ET, conversely, in the process of kiwifruit ripening. They identified that the ET transcription factor *AcEIL* might exhibit an essential function in ET-induced kiwifruit ripening. These articles suggest a practical foundation for improving the protective mechanisms in relation to fruit ripening and senescence.

Chilling injury alleviation in horticultural crops

Sensitivity to chilling can influence plant growth in the field and storability and quality during the postharvest storage period (Morris, 1982). Accordingly, the recognition of the phenomenon and the investigation of the improvement measures of chilling injury are of concern. Lin et al. compared two cultivars of hardy kiwifruit that have high frost hardiness and show similar trends in antioxidant capacities and nutritional compounds. The authors noted that the antioxidant capacity of the two hardy kiwifruit cultivars decreased but glucose increased progressively during maturation, in which the conversion from starch to total sugar was dominantly due to the expression of sucrose phosphate synthase (SPS) and fructokinase (FK). The predominant acids in the two hardy kiwifruit cultivars were quinic acid and citric acid from the early developmental to late maturity stages, respectively. These findings are conducive to a wider understanding of the physiological and biochemical basis of hardy kiwifruit for the cultivation of chilling-tolerant cultivars.

Lin et al. assessed the effect of fucoidan application on cold storage quality, reactive oxygen species (ROS) homeostasis, and energy metabolism in cucumber fruit. The authors determined that the optimum concentration of coated fucoidan was 15 g/L, which could increase DPPH and -OH scavenging rates and reduce H_2O_2 accumulation. The authors suggested that the improved chilling tolerance in cucumbers with fucoidan treatment may be related to the increased antioxidant enzyme activities and ROS scavenging rates, as well as high levels of ATP, ADP, and energy charge. In accordance with the effects of fucoidan in cucumbers, Zhou et al. confirmed that γ-aminobutyric acid (GABA) could lighten CI symptoms in peach fruit and that the reduction efficiency of GABA on chilling injury was associated with the accumulation of ascorbic acid (AsA) and glutathione (GSH) contents and the amplified expression profiles of AsA-GSH recycling-related genes. Moreover, the authors indicated that several ERF transcription factors, which are potentiated by GABA treatment in peach fruit, regulate AsA and GSH contents to reduce chilling injury. Overall, the authors proposed potential strategies of fucoidan coating and GABA immersion in alleviating CI symptoms in postharvest horticultural crops.

Genetic improvement of cold tolerance in horticultural crops

In general, microRNAs (miRNAs) are a class of small, non-protein coding RNA molecules that function as negative regulators of target gene messages (Hinske et al., 2010), and their negative modulations on target genes are essential for enhancing cold tolerance (Zhao et al., 2022). Xing et al. investigated the mechanism of action of Sly-miR171d on chilling injury in tomato fruit. They found that down-regulated Sly-miR171d promotes GRAS24 expression, which obviously increased gibberellin production and C-repeat binding factor (CBF) expression and maintained cell membrane stability, therefore enhancing the chilling tolerance of tomato fruit. This study sheds light on the genetic improvement of postharvest tomato to chilling injury.

In summary, the articles in this Research Topic provide advanced information on ripening and chilling injury alleviation in horticultural crops. New insights into phytohormones, transcription factors and epigenetic modifications will impel our future applied research in the alleviation of crop ripening and chilling injury.

Author contributions

CL: Conceptualization, Writing – original draft. ZY: Supervision, Validation, Writing – review & editing. SC: Writing – review & editing. CW: Supervision, Writing – review & editing. KW: Conceptualization, Writing – review & editing.

Funding

This work was supported by the National Natural Science Foundation of China (No. 32302161) and the Start-up Fund for

High-level Talents of Chongqing Three Gorges Medical College (No. XJ2022000401).

Acknowledgments

We thank all the authors that contributed to this Research Topic.

Conflict of interest

The authors declare that the research was conducted in the absence of any commercial or financial relationships that could be construed as a potential conflict of interest.

The author(s) declared that they were an editorial board member of Frontiers, at the time of submission. This had no impact on the peer review process and the final decision.

Publisher's note

References

Giovannoni, J. (2001). Molecular biology of fruit maturation and ripening. *Annu. Rev. Plant Physiol. Plant Mol. Biol.* 52, 725–749. doi: 10.1146/annurev.arplant.52.1.725

Hinske, L. C. G., Galante, P. A. F., Kuo, W. P., and Ohno-MaChado, L. (2010). A potential role for intragenic miRNAs on their hosts' interactome. *BMC Genomics* 11, 533–545. doi: 10.1186/1471-2164-11-533

Morris, L. L. (1982). Chilling injury of horticultural crops: an overview. *HortScience* 17 (2), 161–162. doi: 10.21273/HORTSCI.17.2.161

Wang, C. Y. (1989). Chilling injury of fruits and vegetables. *Food Rev. Int.* 5 (2), 209–236. doi: 10.1080/87559128909540850

Zhao, K. Y., Chen, R. L., Duan, W. H., Meng, L. H., Song, H. M., Wang, Q., et al. (2022). Chilling injury of tomato fruit was alleviated under low-temperature storage by silencing Sly-miR171e with short tandem target mimic technology. *Front. Nutr.* 9. doi: 10.3389/fnut.2022.906227

frontiers | Frontiers in Plant Science

TYPE Original Research
PUBLISHED 09 September 2022
DOI 10.3389/fpls.2022.1006940

OPEN ACCESS

EDITED BY
Zhenfeng Yang,
Zhejiang Wanli University, China

REVIEWED BY
Feng Xu,
Ningbo University, China
Yuquan Duan,
Chinese Academy of Agricultural Sciences (CAAS), China

*CORRESPONDENCE
Xiangbin Xu
xbxuibcas@126.com
Songbai Liu
liusongbai@126.com

SPECIALTY SECTION
This article was submitted to Crop and Product Physiology, a section of the journal Frontiers in Plant Science

RECEIVED 29 July 2022
ACCEPTED 23 August 2022
PUBLISHED 09 September 2022

CITATION
Xing Z, Huang T, Zhao K, Meng L, Song H, Zhang Z, Xu X and Liu S (2022) Silencing of Sly-miR171d increased the expression of *GRAS24* and enhanced postharvest chilling tolerance of tomato fruit. *Front. Plant Sci.* 13:1006940. doi: 10.3389/fpls.2022.1006940

Silencing of Sly-miR171d increased the expression of *GRAS24* and enhanced postharvest chilling tolerance of tomato fruit

Zengting Xing[1], Taishan Huang[1], Keyan Zhao[1], Lanhuan Meng[1], Hongmiao Song[1], Zhengke Zhang[1], Xiangbin Xu[1]* and Songbai Liu[1,2]*

[1]School of Food Science and Engineering, Hainan University, Haikou, China, [2]Suzhou Key Laboratory of Medical Biotechnology, Suzhou Vocational Health College, Suzhou, China

The role of Sly-miR171d on tomato fruit chilling injury (CI) was investigated. The results showed that silencing the endogenous Sly-miR171d effectively delayed the increase of CI and electrolyte leakage (EL) in tomato fruit, and maintained fruit firmness and quality. After low temperature storage, the expression of target gene *GRAS24* increased in STTM-miR171d tomato fruit, the level of GA_3 anabolism and the expression of *CBF1*, an important regulator of cold resistance, both increased in STTM-miR171d tomato fruit, indicated that silencing the Sly-miR171d can improve the resistance ability of postharvest tomato fruit to chilling tolerance.

KEYWORDS

Sly-miR171d, tomato, chilling tolerance, GRAS, GA

Introduction

Low temperature storage technology can reduce respiratory metabolism and is widely used in prolonging fruit storage period (Duan et al., 2022). However, fruit from subtropical and tropical regions stored below the temperature of 12°C are susceptible to the risk of chilling injury (CI), resulting in lower product quality and lower sales (Ding et al., 2021). Tomato fruit is the major contributors of minerals, dietary fiber, sugars, essential amino acids, and vitamins in the daily diet (Bai et al., 2020). It widely distributes in tropical and subtropical regions. However, tomato fruit stored at low temperature below 10°C (green ripening stage) and 5°C (red ripening stage) for a long time are susceptible to CI. During storage at low temperatures, incipient CI in tomato is not generally apparent. After returning the fruit to room temperature, CI is very obvious, such as failure to ripen properly, indentation of the surface or damage, discoloration, decay and increased water loss (Tian et al., 2022). CI sharply led to

a decline in tomato quality and consumer acceptance, which ultimately led to huge economic losses (Luengwilai et al., 2012). Hence, controlling the postharvest CI of fruit is essential to ensure good quality and minimize losses.

MicroRNAs (miRNAs) is a class of endogenous non-coding small RNAs with a length of about 18–25 nt (Bartel, 2004). The miRNAs binds to mRNA molecules through base pairing, resulting in translation inhibition or cleavage of its target mRNA (Barciszewska-Pacak et al., 2015). Negative regulation of target genes by miRNAs is critical for coordinating the plant responses to cold stress (Zhao et al., 2022b). In recent years, miRNAs has attracted more and more attention in their important role in the post-transcriptional or translational regulation of gene expression and plant stress tolerance (Sunkar et al., 2007). In rice (*Oryza sativa*), overexpression of miR156 reduced the expression of *OsWRKY71*, resulting in enhanced expression of *MYB2* and *MYB3R-2*, thereby enhanced cold tolerance (Zhou and Tang, 2019). In Switchgrass (*Panicum virgatum*), overexpression of miR393 enhanced low temperature tolerance by regulating the auxin signaling pathway in switchgrass (Liu et al., 2017a). In tomato, Sha-miR319d enhances the cold tolerance by reducing the expression of *GAMYB-like1* and further changing ROS, heat and cold signal transduction (Shi et al., 2019). In citrus (*Citrus reticulata*), miR171 plays a key role in the adaptation to long-term B toxicity by regulating the expression of *SCARECROW* (Huang et al., 2019). In apples (*Malus pumila*), miR171i and its target gene *SCARECROW-LIKE PROTEINS26.1* improves drought stress tolerance by regulating antioxidant gene expression and ascorbic acid metabolism (Wang et al., 2020a). The miR171 regulates members of the *GRAS* gene family (Huang et al., 2017). GRAS proteins are widely taken part in signal transduction, growth and development, and stress in plants (Peng et al., 1997). In rice, *OsGRAS23* increases the transcription of genes related to stress response, especially the protein protection and antioxidant genes, and positively regulates the drought tolerance (Xu et al., 2015). In tomato, overexpression of *SlGRAS40* enhances drought resistance and salt resistance by regulating gibberellin (GAs) and auxin homeostasis (Liu et al., 2017b). The down-regulation of *SlGRAS10* improves the tolerance of abiotic stresses by regulating complex stress-induced gene expression in physiological modifications (Habib et al., 2021) and overexpression of *SlGRAS4* induces the expression of *SlCBF* and enhances the low temperature tolerance of tomato (Liu et al., 2020). *SlGRAS24* is the target gene of miR171d and involved in GAs signal transduction (Huang et al., 2017). Plant-specific GRAS protein family contains important regulatory parts of GA signaling that coordinately participate in plant growth and development (Shan et al., 2012). GRAS proteins have a subgroup that is a GA signaling repressor whose amino acid sequence in the N-terminal region is identical and is therefore called DELLA proteins (Chen et al., 2019). GAs induces the degradation of DELLA repressor protein and controls responses to cold stress (Lantzouni et al., 2020).

To further understand the function of miR171d in tomato, we obtained the up-regulated and down-regulated transgenic lines of Sly-miR171d by constructing the overexpression vector and the short tandem target mimic (STTM) vector. The results revealed the mechanism of Sly-miR171d in promoting cold resistance in tomato through GAs signal and provided help for cultivating stress tolerant germplasm.

Materials and methods

Plant expression vector construction and transformation

Silencing of mature Sly-miR171d was performed with STTM according to the method developed by Yan et al. (2012). The overexpression vector of Sly-miR171d was constructed according to the methods of Zhao et al. (2022a). After sequencing confirmation, all the correct constructs were transformed to Micro-Tom *via Agrobacterium*-mediated method. All primers and sequences are listed in **Supplementary 1**, **2**.

Sample treatment

Tomato (*Solanum lycopersicum* cv. Micro-Tom) plant materials used in this study were all homozygous T3 lines of Micro-Tom (MT). The plant growth chamber conditions were as follows: the ambient temperature was maintained at 23 ± 2°C; 16 h light/8 h dark alternate lighting; 60% humidity. Wild-type (WT) Micro-Tom tomato seeds were purchased with Nanjing Fengshuo Horticultural Co., Ltd. All fruit were selected with the same shape and size, without defect and disease. The fruit surface was soaked in 2% (V/V) sodium hypochlorite for 60 s to disinfect, washer with steam water, and dried. Green and red ripening tomato fruit (STTM-miR171d, WT, and miR171d-OE lines) with the same size, maturity and no mechanical damage were selected. The green ripening fruit were stored at 9°C for 30 days and randomly selected every 5 days. The shelf life was simulated at room temperature (25°C storage). Red ripening fruit were stored at 4°C for 25 days and randomly detected every 5 days. Each experiment was repeated two times.

Chilling injury index

Chilling injury index was divided into five grades: 1 = no CI; 2 = slight damage (pitting covered <5% of fruit surface);

3 = moderate damage (pitting covers less than 25%, but >5% of the surface); 4 = severe damage (pitting coverage less than 50% but >25% of the surface); 5 = very severe damage (depression covers 50% of the surface). The CI was expressed as

$$CI = [\sum(\text{CI scale}) \times \text{fruit number at that scale}]/(4 \times \text{total number of fruit in the group}).$$

Each group selected 12 tomato fruit to evaluate the degree of CI.

Electrolyte leakage, firmness, and total soluble solids of tomato fruit

Electrolyte leakage (EL) was detected according to the method of Li et al. (2016). FE30 conductivity meter (Mettler Toledo Instrument Co., Ltd., China) was used to measure the EL of fruit. Select 10 circular pulp tissues (10 mm straight × 4 mm thick in diameter) from the equatorial region of five tomato fruit and measure P_1 by shaking in 30 ml of distilled water for 20 min. P_2 is then measured after the sample has been boiled for 15 min. where P_1 is the initial conductivity value and P_2 is the final conductivity value.

Fruit firmness was detected according to the method of El-Mogy et al. (2018). Measuring fruit firmness with a texture analyzer (TA; XT Plus, Stable Micro Systems, United Kingdom) by a 2 mm flat probe at 3 points in the equatorial region, with hardness values of three fruit repeated at a time.

Total soluble solids (TSS) was detected according to the method of Shan et al. (2022). TSS in tomato pulp was determined at room temperature using a hand-held refractometer (WY032R; Chengdu Optical Instrument Factory, China). The results are expressed as %.

Determination of GA_3 content

The tomato samples were ground to homogenate and determined according to plant GA_3 ELISA kit (Jiangsu Meibiao Biotechnology Co., Ltd., China).

RNA isolation and quantitative real-time PCR analysis

The kits (Tiangen, Beijing, China) were used for total RNA extraction, first-strand cDNA synthesis and real-time quantitative PCR. The expression of Sly-miR171d, *SlGRAS24*, *COR*, *CBF1*, *GA20ox1*, *GA3ox1*, *GA2ox1*, and *GAI* were calculated by the $2^{-\Delta\Delta Ct}$ method. The internal reference gene is *Actin*. The qRT-PCR primers are supplemented in **Supplementary Table 1**. Two grams of fruit pulp tissue were taken from three tomato fruit, ground in liquid nitrogen, and RNA was extracted according to the kit.

Statistical analysis

Values were expressed as means ± standard deviation (SD). Data analysis using SPSS 20.0 (SPSS, Chicago, IL, United States). A one-way analysis of variance (ANOVA) was performed to test significant differences among the means ($P < 0.05$).

Results

Characterization of STTM-miR171d and miR171d-OE fruit

Stable transformation of tomato plant STTM-miR171d and miR171d-OE lines were produced by *Agrobacterium*-mediated method. A total of 25 independent tomato transgenic lines (16 STTM-miR171d and 9 miR171d-OE plants) were detected in the T1 generation. After PCR amplification with *hygromycin* (STTM-miR171d lines) and *kanamycin* (miR171d-OE lines), cell lines with target bands were detected by agarose gel electrophoresis (**Supplementary 1**). This indicated that the vector had been successfully integrated into the tomato chromosome. Expression analysis of miR171d-OE and STTM-miR171d in T3 transgenic plants and identify them as transgenic fruit, and selected as experimental materials. Green tomato fruit was harvested at 35 dpa and red tomato fruit was harvested at 45 dpa.

Chilling injury index

Silencing of Sly-miR171d with STTM delayed CI symptoms in fruit compared to WT (**Figures 1A**, **2A**). The red miR171d-OE tomato showed obvious epidermal atrophy on the 20 days under the condition of 4°C. With the storage time Prolonged, the phenomenon of skin atrophy deepened. WT tomato fruit showed CI symptoms after 20 days, and the symptoms worsened at 25 days, while STTM-miR171d fruit did not show obvious abnormalities on the surface of fruit after 25 days of storage. During the green ripening stage, the miR171d-OE tomato fruit were stored at 9°C for 30 days, and the skin wrinkles appeared after the 12 days of the shelf life. WT tomato fruit and STTM-miR171d fruit did not show obvious symptoms of CI.

In the red ripening stage, at 4°C for 25 days, the CI of miR171d-OE, STTM-miR171d, and WT tomato fruit were 71.80, 52.02, and 64.30%. The CI of WT tomato fruit was 12.28% higher than that of STTM-miR171d (**Figure 1B**). The CI of miR171d-OE, STTM-miR171d, and WT tomato fruit were 35.89, 25.96, and 30.53%, respectively, when green tomato fruit

10.3389/fpls.2022.1006940

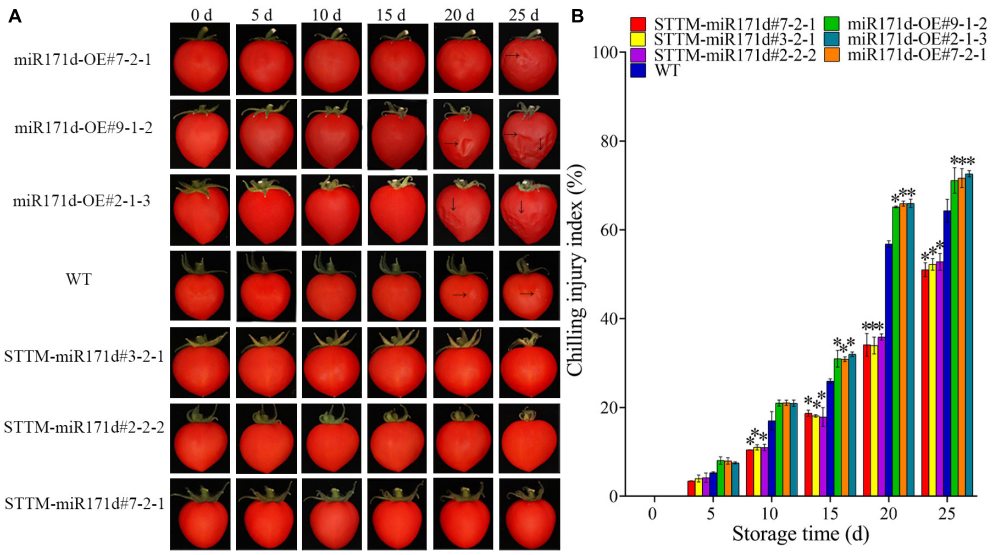

FIGURE 1
Surface CI symptoms and CI index of red ripe tomato fruit. **(A)** Symptoms of CI on the surface of tomato fruit. **(B)** CI index. The error bar represents the independent repeat SDs (n = 3). The asterisk indicates that the data difference with $P < 0.05$ is statistically significant.

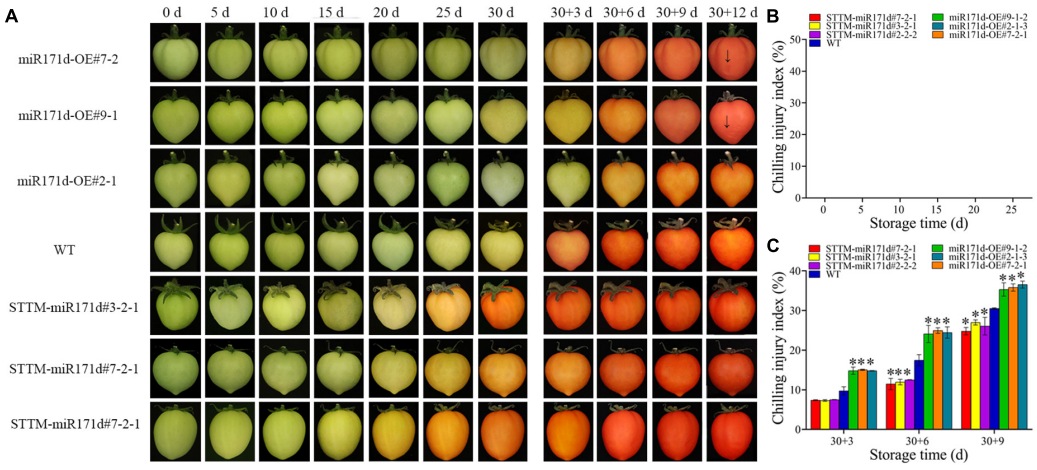

FIGURE 2
Surface CI symptoms and CI index of green ripe tomato fruit. **(A)** Symptoms of CI on the surface of tomato fruit. **(B,C)** CI index. The error bar represents the independent repeat SDs (n = 3). The asterisk indicates that the data difference with $P < 0.05$ is statistically significant.

were refrigerated and stored at 25°C for 9 days. The CI of WT tomato fruit was 4.57% higher than that of STTM-miR171d (Figure 2C).

Electrolyte leakage, firmness, total soluble solids, and GA_3 content of tomato fruit

The accumulation of EL in red and green fruit increased under low temperature stress. At 4°C for 25 days, The EL of miR171d-OE tomato red fruit was 4.18 higher than WT, and that of STTM-miR171d tomato was 7.09 lower than WT. After the green tomato fruit was refrigerated and stored at 9°C, the EL content of STTM-miR171d fruit was 4.83 lower than WT. The EL content of miR171d-OE fruit was 5.23 higher than WT (Figure 3).

In tomato fruit, firmness decreased gradually with storage time. After 25 days of low temperature stress, the firmness of red STTM-miR171d tomato fruit decreased to 5.65 N. The hardness of miR171d-OE decreased to 3.32 N and that of WT was 4.38 N. The firmness of STTM-miR171d fruit was 1.29 times that of

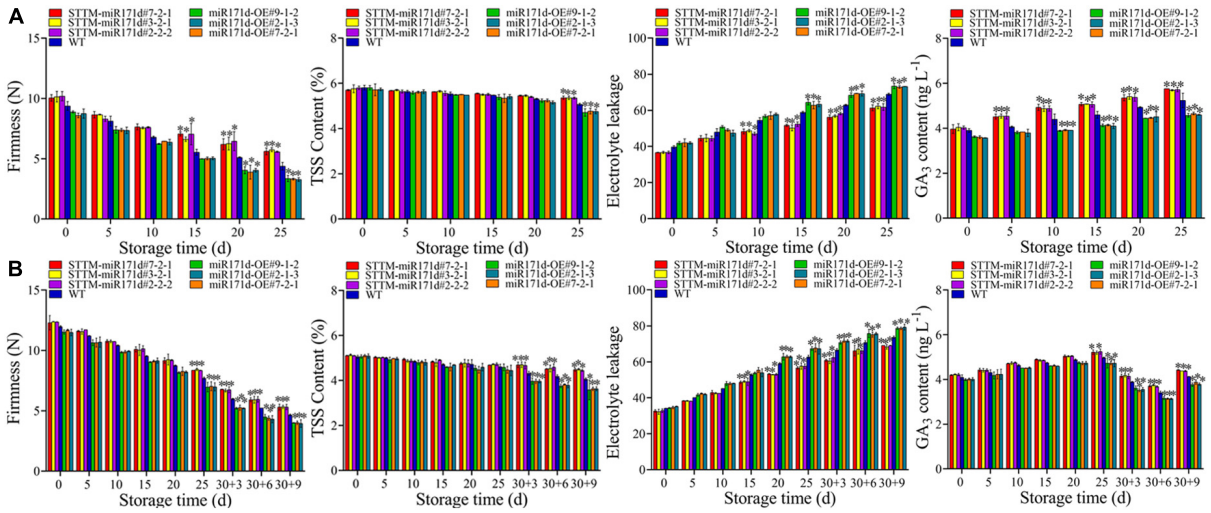

FIGURE 3
Electrolyte leakage, Firmness, TSS, and GA_3 content of tomato fruit in red ripening stage **(A)** and green ripening stage **(B)**. The error bar represents the independent repeat SDs (n = 3). The asterisk indicates that the data difference with $P < 0.05$ is statistically significant.

WT. After storage at 25°C for 9 days at green ripening stage, fruit hardness of STTM-miR171d, miR171d-OE, and WT were 5.32, 3.99, and 4.66 N (Figure 3).

The TSS in tomato fruit gradually decreased. The red fruit is stored for 25 days, miR171d-OE fruit decreased from 5.75 to 4.74%, and WT fruit decreased from 5.81 to 5.07%, while STTM-miR171d fruit still maintained 5.36% at 25 days. The TSS content of green tomato fruit showed significant differences after the shelf life, miR171d-OE fruit decreased from 5.08 to 3.61%, WT fruit decreased from 5.05 to 4.06%, while STTM-miR171d fruit remained at 4.48% at the end (Figure 3).

During low temperatures, the GA_3 content of red tomato fruit showed an overall upward trend, but the content of miR171d-OE was lower than that of STTM-miR171d. After 25 days of storage, the contents of STTM-miR171d, WT, and miR171d-OE increased to 5.73, 5.24, and 4.61 ng L^{-1}. The GA_3 content of green tomato fruit showed an increasing trend throughout the storage period and gradually decreased during the shelf life. During the shelf life, the fruit content of STTM-miR171d decreased from 5.23 to 4.40 ng L^{-1}, and the fruit content of WT decreased from 4.97 to 4.13 ng L^{-1}. The fruit content of miR171d-OE decreased from 4.73 to 3.81 ng L^{-1}, and the content of STTM-miR171d was 6.54% higher than WT (Figure 3).

The expressions of *CBF1* and *COR* in tomato

In red tomato fruit, the expression of *COR* genes and *CBF1* genes showed an upward trend from 0 to 15 days and then sharply decreased, as shown in Figure 4A. At 25 days, the *CBF1* gene expression levels of STTM-miR171d#7-2-1, STTM-miR171d#3-2-1, and STTM-miR171d#2-2-2 were 2.55, 2.65, and 2.62 times than WT. The *COR* gene expression of STTM-miR171d#7-2-1, STTM-miR171d#3-2-1, and STTM-miR171d#2-2-2 were 1.75, 1.90, and 1.83 times than WT, respectively. *CBF1* and *COR* genes in green tomato fruit showed an increasing trend during storage, but sharply decreased during shelf life, as shown in Figure 4B. At the end of 9 days shelf life, the *CBF1* gene expression levels of STTM-miR171d#7-2-1, STTM-miR171d#3-2-1, and STTM-miR171d#2-2-2 were 1.61, 1.59, and 1.63 times than WT. The *COR* gene expression of STTM-miR171d#7-2-1, STTM-miR171d#3-2-1, and STTM-miR171d#2-2-2 were 1.56, 1.38, and 1.48 times than WT (Figure 4).

The expressions of miR171d and *SlGRAS24* in tomato

During the low temperature, the expression level of *miR171d* in STTM-miR171d fruit was not significant and lower than that in WT fruit. Red tomato fruit was refrigerated at 4°C, STTM-miR171d#7-2-1, STTM-miR171d#3-2-1, and STTM-miR171d#2-2-2 the expression of miR171d were 0.34, 0.30, and 0.34. After green tomato fruit was refrigerated at 9°C and stored at 25°C for 9 days, the expression levels of miR171d in STTM-miR171d#7-2-1, STTM-miR171d#3-2-1, and STTM-miR171d#2-2-2 were 0.35, 0.36, and 0.31. The miR171d gene was significantly expressed in tomato fruit miR171d-OE, and the gene expression decreased with an extended storage period. At

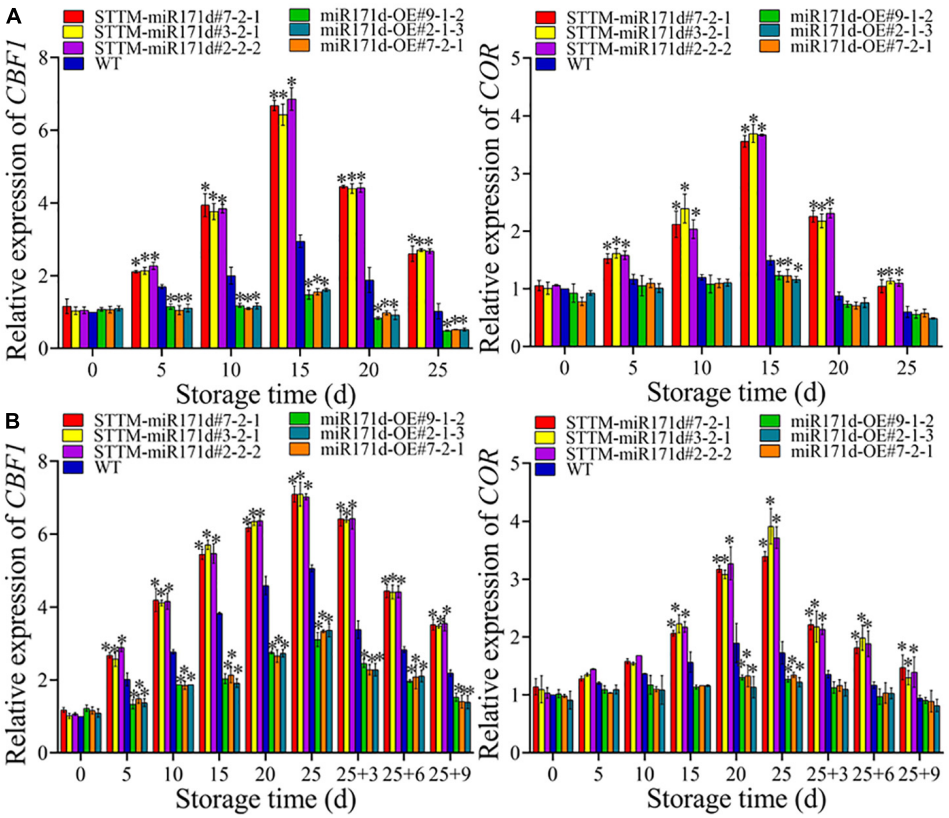

FIGURE 4
The expression levels of *CBF1* and *COR* genes in red ripe tomato fruit **(A)** and green ripe tomato fruit **(B)**. The error bar represents the independent repeat SDs (n = 3). The asterisk indicates that the data difference with $P < 0.05$ is statistically significant.

25 days in red tomato fruit, the miR171d of miR171d-OE#9-1-2, miR171d-OE#7-2-1, and miR171d-OE#2-1-3 were 9.76, 9.74, and 9.50 times that of WT. After the shelf life of green tomato fruit, the miR171d in miR171d-OE#9-1-2, miR171d-OE#7-2-1, and miR171d-OE#2-1-3 were 9.52, 9.34, and 9.59 times than WT (Figure 5).

In red STTM-miR171d tomato fruit the expression of *GRAS24* gene increased with storage time under low temperature stress. Red tomato fruit after 25 days, the expression of *GRAS24* in STTM-miR171d#7-2-1, STTM-miR171d#3-2-1, STTM-miR171d#2-2-2, and WT were 61.89, 63.38, 59.49, and 40.06. The expression levels of *GRAS24* in red fruit of miR171d-OE#9-1-2, miR171d-OE#7-2-1, and miR171d-OE#2-1-3 were 21.78, 22.07, and 21.15. Under low temperature stress in green STTM-miR171d tomato, the expression of *GRAS24* gene increased with the storage time during the storage period, and the shelf life decreased gradually. At the end of the shelf life at 25°C, the expression of *GRAS24* in STTM-miR171d#7-2-1, STTM-miR171d#3-2-1, STTM-miR171d#2-2-2, and WT were 26.06, 25.50, 26.65, and 14.78. The expression levels of *GRAS24* in green fruit of miR171d-OE#9-1-2, miR171d-OE#7-2-1, and miR171d-OE#2-1-3 were 8.20, 9.76, and 9.07 (Figure 5).

The expressions of *GA20ox1*, *GA3ox1*, *GA2ox1*, and *GAI* in tomato

GA20ox1, *GA3ox1*, and *GA2ox1* are key genes that affect bioactive GA levels in plants. *GA20ox1* and *GA3ox1* are synthetic genes, and *GA2ox1* is the catabolic gene. At 25 days in red tomato fruit, the expression of *GA20ox1* and *GA3ox1* genes in STTM-miR171d were 1.24 and 1.12 times that of WT. After 9 days of shelf life, the expression of *GA20ox1* and *GA3ox1* genes in STTM-miR171d were 1.23 and 1.38 times that of WT. The expression of the *GA2ox1* gene increased rapidly and then decreased during the storage period. At 25 days of red tomato fruit, the *GA2ox1* gene expression level in STTM-miR171d fruit was 1.50 times that of WT. Green tomato after 9 days of shelf life, the expression level of *GA2ox1* gene in STTM-miR171d fruit was 1.25 times that of WT (Figure 6).

In tomato fruit the expression of the *GAI* gene first increased and then decreased. The expression of *GAI* in red tomato fruit reached the peak at 15 days. On 25 days, miR171d-OE #9-1-2, miR171d-OE #7-2-1, and miR171d-OE #2-1-3 were 1.26, 1.25, and 1.21 times than those in WT fruit, respectively.

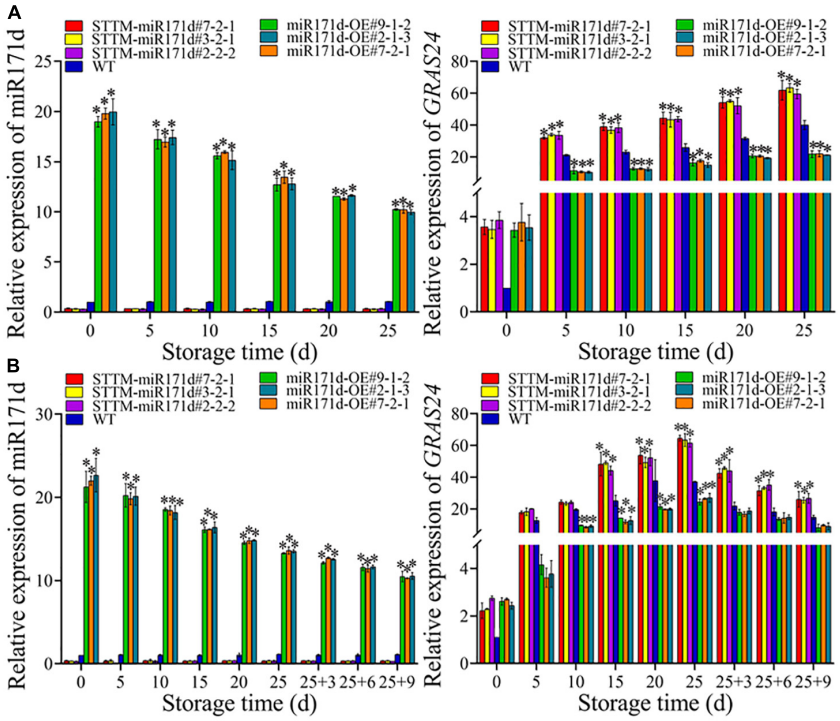

FIGURE 5
The expression levels of Sly-miR171d and *SlGRAS24* genes in red ripe tomato fruit **(A)** and green ripe tomato fruit **(B)**. The error bar represents the independent repeat SDs (n = 3). The asterisk indicates that the data difference with $P < 0.05$ is statistically significant.

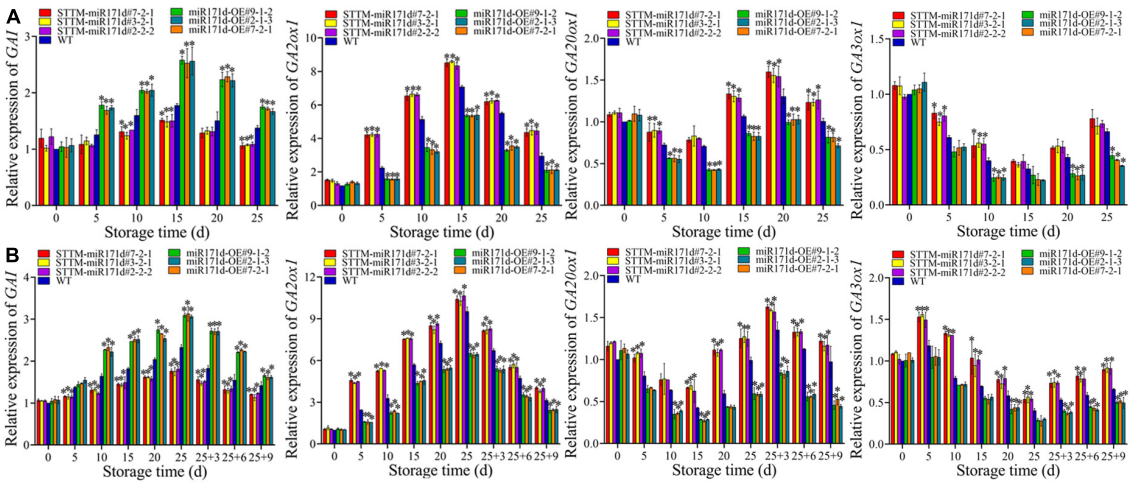

FIGURE 6
The expression levels of *GA20ox1*, *GA3ox1*, *GA2ox1*, and *GAI* genes in red ripe tomato fruit **(A)** and green ripe tomato fruit **(B)**. The error bar represents the independent repeat SDs (n = 3). The asterisk indicates that the data difference with $P < 0.05$ is statistically significant.

The expression of *GAI* in green tomato fruit reached its peak at the end of storage period. After 9 days of shelf life, miR171d-OE #9-1-2, miR171d-OE #7-2-1, and miR171d-OE #2-1-3 were 1.18, 1.14, and 1.14 times than WT, respectively (**Figure 6**).

Discussion

Refrigeration is currently the most commonly used technique for extending the shelf life of postharvest fruit. However, most tropical and subtropical fruit are susceptible

to CI during refrigeration (Wang et al., 2021). As important regulatory factors of various physiological processes in plants, miRNA also plays a significant role in plants resistance to cold tolerance (Zhou and Tang, 2019). Low temperature stress can increase membrane permeability and damage the membrane system, leading to cell metabolism and dysfunction in plants (Mekontso et al., 2021; Wang et al., 2022). EL is one of the main outcomes caused by CI, and elevated EL is considered an important marker of cell membrane damage, with lower EL indicating higher membrane integrity (Duan et al., 2022). CI index reflects the degree of CI symptoms and judges cold tolerance, and the development of CI symptoms increases with long-term storage (Zhang et al., 2022). The contents of TSS reflects the intracellular mass and solute concentration, and is a protective substance in the cells under the conditions of CI, and its content is positively correlated with the cold resistance of most plants (Jia et al., 2018). The present results showed that STTM-miR171d tomato fruit surface did not change significantly, WT fruit showed epidermis shrank, while miR171d-OE tomato fruit showed epidermis atrophy and surface depression. The accumulation of EL in tomato fruit increased with storage time, and the accumulation of EL in STTM-miR171d fruit did not increase significantly. TSS content in STTM-miR171d fruit was higher than that of miR171d-OE and WT fruit, and remained at a higher level. Inhibition of Sly-miR171d can slow down the development of CI symptoms in tomato fruit, reduce the accumulation of EL, maintain high cell membrane integrity and high TSS content to delay the decline of fruit tissue firmness. Therefore, silencing Sly-miR171d improved the cold resistance of tomato fruit.

GA_3 is a natural plant hormone that plays a crucial role in various abiotic stresses (Alonso-Ramírez et al., 2009). GA inactivation and positive and negative feedback regulation of GA biosynthesis to maintain GA homeostasis (Hedden and Thomas, 2012). The down-regulation of GA biosynthesis genes *GA20ox1* and *GA3ox1* in tomato fruit stored at low temperature is related to the decrease of GA content (Zhu et al., 2016). Exogenous SA treatment of tomato fruit induced *GA3ox1* expression, increased GA_3 content, stimulated the degradation of DELLA protein, and alleviated CI symptoms in tomato fruit (Ding et al., 2015). GRAS transcription factors are essential in plant responses to stress. DELLA belongs to the GRAS protein family, and GA can stimulate DELLA accumulation, inhibit protein degradation, and control key developmental processes to enhance stress tolerance (Achard et al., 2008). Exogenous GA_3 may resist phytoplasma infection of potato purple top disease by down-regulating the *DELLA* gene (Ding et al., 2013). Under cold stress, *SlPIF4* activates the *SlDELLA* gene and inhibits GA biosynthesis to partially enhance the cold tolerance of tomato plants (Wang et al., 2020b). Overexpression of tomato transcription factor *SlGRAS40* affects auxin and GA pathways in the process of tomato nutrition and reproduction, promotes the accumulation of DELLA protein, and enhances

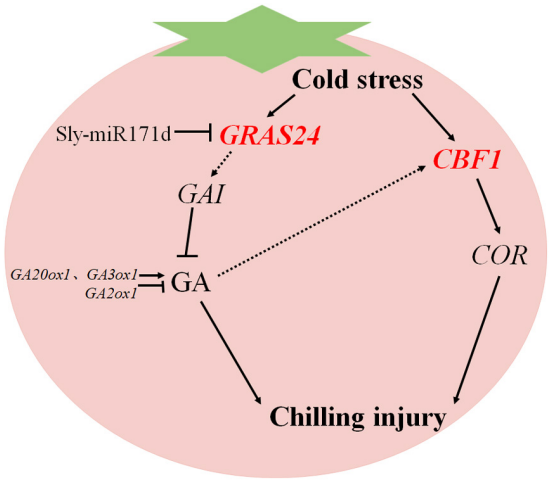

FIGURE 7
A simplified model of the regulatory mechanism of Sly-miR171d on cold tolerance of tomato fruit stored at low temperature.

plants stress resistance (Liu et al., 2017b). In the study, the expression levels of key GA metabolizing genes and signal transduction genes in red and green ripe tomato fruit were analyzed. After low temperature storage, the expression level of target gene *GRAS24* was positively correlated with GA biosynthesis key genes *GA20ox1*, *GA3ox1*, and *GA2ox1*. It was negatively correlated with the DELLA protein gene *GAI*. These results suggested that Sly-miR171d negatively regulated target gene *GRAS24*, increased GA content in tomato fruit and down-regulated DELLA protein gene *GAI*. Conversely, the expression of key genes *GA20ox1* and *GA3ox1* for GA biosynthesis and the GA decomposition gene *GA2ox1* were up-regulated. The target gene *GRAS24* may inhibit growth by downregulating the relative expression of *GAI* or degrading DELLA protein, thereby activating the cold tolerance of tomato fruit (**Figure 7**).

The CBF pathway is essential in plant resistance to cold stress. The transcript level of *CBF1* is positively correlated with tomato chilling resistance and negatively correlated with tomato CI index, which is for assessing the chilling resistance of tomato (Zhao et al., 2011). The expression of CBF-related genes in *Arabidopsis thaliana* can actively regulate low temperature stress resistance (Jiang et al., 2020). Overexpression of *CmICE2* in *Arabidopsis* induced up-regulation of *CBF* and *COR* genes, and enhanced the response to freezing stress (Zhang et al., 2020). Overexpression of *AtCBF1* in potato induces physiological modifications associated with cold adaptation to enhance freezing resistance (Pino et al., 2008). CBF has been shown to fully activate *COR* gene expression and induce resistance to low temperature stress (Stockinger et al., 1997). Application of exogenous GA_3 increased the expression of the *CBF1* gene and improved low temperature tolerance of tomato fruit by regulating GA catabolism through the CBF pathway

(Zhu et al., 2016). Exogenous SA induced the expression of *CBF1*, which in turn induced the expression of the *GA2ox1* gene, thereby activated the biosynthesis of GA and alleviated the CI of tomato fruit during low temperature storage (Ding et al., 2016). In this study, *CBF1* and *COR* were higher expressed in STTM-miR171d than that in miR171-OE and WT fruit, which was consistent with their phenotype. The expression patterns of *CBF1* and *GA2ox1* are similar, and the *CBF* pathway may enhance the low temperature tolerance of tomato fruit by regulating GA catabolism (**Figure 7**).

Conclusion

In conclusion, silencing of Sly-miR171d and enhancing the expression of target gene *GRAS24* effectively maintained the stability of cell membrane and increased the GA_3 level in tomato fruit under low temperature, thereby improved postharvest chilling tolerance of tomato fruit.

Data availability statement

The datasets presented in this study can be found in online repositories. The names of the repository/repositories and accession number(s) can be found in the article/**Supplementary material**.

Author contributions

ZX, XX, and SL conceived and designed the experiments. ZX, TH, and KZ conducted the experiments. ZX, TH, KZ, LM, HS, ZZ, XX, and SL wrote and edited the manuscript. All authors approved the publication of final version of the manuscript.

Funding

This study was supported by the National Natural Science Foundation of China (31872160), the Hainan Provincial Natural Science Foundation of China (2019RC127, 321RC1025, and 322RC565), Jiangsu Higher Education Institution Innovative Research Team for Science and technology (2021), and Qing-Lan Project of Jiangsu Province in China (2021 and 2022).

Conflict of interest

The authors declare that the research was conducted in the absence of any commercial or financial relationships that could be construed as a potential conflict of interest.

Publisher's note

All claims expressed in this article are solely those of the authors and do not necessarily represent those of their affiliated organizations, or those of the publisher, the editors and the reviewers. Any product that may be evaluated in this article, or claim that may be made by its manufacturer, is not guaranteed or endorsed by the publisher.

Supplementary material

The Supplementary Material for this article can be found online at: https://www.frontiersin.org/articles/10.3389/fpls.2022.1006940/full#supplementary-material

References

Achard, P., Renou, J. P., Berthomé, R., Harberd, N. P., and Genschik, P. (2008). Plant DELLAs restrain growth and promote survival of adversity by reducing the levels of reactive oxygen species. *Curr. Biol.* 18, 656–660. doi: 10.1016/j.cub.2008.04.034

Alonso-Ramírez, A., Rodríguez, D., Reyes, D., Jiménez, J. A., Nicolás, G., López-Climent, M., et al. (2009). Evidence for a role of gibberellins in salicylic acid-modulated early plant responses to abiotic stress in *Arabidopsis* seeds. *Plant Physiol.* 150, 1335–1344. doi: 10.1104/pp.109.139352

Bai, C., Zheng, Y., Watkins, C. B., Fu, A., Ma, L., Gao, H., et al. (2020). Revealing the specific regulations of brassinolide on tomato fruit chilling injury by integrated Multi-Omics. *Front. Nutr.* 8:769715. doi: 10.3389/fnut.2021.769715

Barciszewska-Pacak, M., Milanowska, K., Knop, K., Bielewicz, D., Nuc, P., Plewka, P., et al. (2015). *Arabidopsis* microRNA expression regulation in a wide range of abiotic stress responses. *Front Plant Sci.* 6:410. doi: 10.3389/fpls.2015.00410

Bartel, D. P. (2004). MicroRNAs: Genomics, biogenesis, mechanism, and function. *Cell* 116, 281–297. doi: 10.1016/S0092-8674(04)00045-5

Chen, H., Li, H. H., Lu, X. Q., Chen, L. Z., Liu, J., and Wu, H. (2019). Identification and expression analysis of GRAS transcription factors to elucidate candidate genes related to stolons, fruit ripening and abiotic stresses in woodland strawberry (*Fragaria vesca*). *Int. J. Mol. Sci.* 20:4593. doi: 10.3390/ijms20184593

Ding, F., Ren, L., Xie, F., Wang, M., and Zhang, S. (2021). Jasmonate and melatonin act synergistically to potentiate cold tolerance in tomato plants. *Front. Plant Sci.* 12:763284. doi: 10.3389/fpls.2021.763284

Ding, Y., Sheng, J. P., Li, S. Y., Nie, Y., Zhao, J. H., Zhu, Z., et al. (2015). The role of gibberellins in the mitigation of chilling injury in cherry tomato (*Solanum lycopersicum* L.) fruit. *Postharvest Biol. Technol.* 101, 88–95. doi: 10.1016/j.postharvbio.2014.12.001

Ding, Y., Wei, W., Wu, W., Davis, R. E., Jiang, Y., Lee, I. M., et al. (2013). Role of gibberellic acid in tomato defence against potato purple top phytoplasma infection. *Ann. Appl. Biol.* 162, 191–199. doi: 10.1111/aab.12011

Ding, Y., Zhao, J. H., Nie, Y., Fan, B., Wu, S. J., Zhang, Y., et al. (2016). Salicylic-acid-induced chilling-and oxidative-stress tolerance in relation to gibberellin homeostasis, C-repeat/dehydration-responsive element binding factor pathway,

and antioxidant enzyme systems in cold-stored tomato fruit. *J. Agric. Food Chem.* 64, 8200–8206. doi: 10.1021/acs.jafc.6b02902

Duan, W. H., Mekontso, F. N., Li, W., Tian, J. X., Li, J. K., Wang, Q., et al. (2022). Alleviation of postharvest rib-edge darkening and chilling injury of carambola fruit by brassinolide under low temperature storage. *Sci. Hortic.* 299:111015. doi: 10.1016/j.scienta.2022.111015

El-Mogy, M. M., Garchery, C., and Stevens, R. (2018). Irrigation with salt water affects growth, yield, fruit quality, storability and marker-gene expression in cherry tomato. *Acta Agric. Scand. B Soil Plant Sci.* 68, 727–737. doi: 10.1080/09064710.2018.1473482

Habib, S., Lwin, Y. Y., and Li, N. (2021). Down-Regulation of SlGRAS10 in tomato confers abiotic stress tolerance. *Gene* 12:623. doi: 10.3390/genes12050623

Hedden, P., and Thomas, S. G. (2012). Gibberellin biosynthesis and its regulation. *Biochem. J.* 444, 11–25. doi: 10.1042/BJ20120245

Huang, J. H., Lin, X. J., Zhang, L. Y., Wang, X. D., Fan, G. C., and Chen, L. S. (2019). MicroRNA sequencing revealed Citrus adaptation to long-term boron toxicity through modulation of root development by miR319 and miR171. *Int. J. Mol. Sci.* 20:1422. doi: 10.3390/ijms20061422

Huang, W., Peng, S. Y., Xian, Z. Q., Lin, D. B., Hu, G. J., Yang, L., et al. (2017). Overexpression of a tomato miR171 target gene *SlGRAS24* impacts multiple agronomical traits *via* regulating gibberellin and auxin homeostasis. *Plant Biotechnol. J.* 15, 472–488. doi: 10.1111/pbi.12646

Jia, B., Zheng, Q. L., Zuo, J. H., Gao, L. P., Wang, Q., Guan, W. Q., et al. (2018). Application of postharvest putrescine treatment to maintain the quality and increase the activity of antioxidative enzyme of cucumber. *Sci. Hortic.* 239, 210–215. doi: 10.1016/j.scienta.2018.05.043

Jiang, B. C., Shi, Y. T., Peng, Y., Jia, Y. X., Yan, Y., Dong, X. J., et al. (2020). Cold-induced CBF–PIF3 interaction enhances freezing tolerance by stabilizing the phyB thermosensor in Arabidopsis. *Mol. Plant* 13, 894–906. doi: 10.1016/j.molp.2020.04.006

Lantzouni, O., Alkofer, A., Falter-Braun, P., and Schwechheimer, C. (2020). GROWTH-REGULATING FACTORS interact with DELLAs and regulate growth in cold stress. *Plant Cell* 32, 1018–1034. doi: 10.1105/tpc.19.00784

Li, P. Y., Yin, F., Song, L. J., and Zheng, X. L. (2016). Alleviation of chilling injury in tomato fruit by exogenous application of oxalic acid. *Food Chem.* 202, 125–132. doi: 10.1016/j.foodchem.2016.01.142

Liu, Y. D., Huang, W., Xian, Z. Q., Hu, N., Lin, D. B., Ren, H., et al. (2017b). Overexpression of SlGRAS40 in tomato enhances tolerance to abiotic stresses and influences auxin and gibberellin signaling. *Front. Plant Sci.* 8:1659. doi: 10.3389/fpls.2017.01659

Liu, Y. D., Shi, Y., Zhu, N., Zhong, S. L., Bouzayen, M., and Li, Z. G. (2020). SlGRAS4 mediates a novel regulatory pathway promoting chilling tolerance in tomato. *Plant Biotechnol. J.* 18, 1620–1633. doi: 10.1111/pbi.13328

Liu, Y. R., Wang, K., Li, D. Y., Yan, J. P., and Zhang, W. J. (2017a). Enhanced cold tolerance and tillering in switchgrass (*Panicum virgatum* L.) by heterologous expression of Osa-miR393a. *Plant Cell Physiol.* 58, 2226–2240. doi: 10.1093/pcp/pcx157

Luengwilai, K., Beckles, D. M., and Saltveit, M. E. (2012). Chilling-injury of harvested tomato (*Solanum lycopersicum* L.) cv. Micro-Tom fruit is reduced by temperature pre-treatments. *Postharvest Biol. Technol.* 63, 123–128. doi: 10.1016/j.postharvbio.2011.06.017

Mekontso, F. N., Duan, W. H., Cisse, E. H. M., Chen, T. Y., and Xu, X. B. (2021). Alleviation of postharvest chilling injury of carambola fruit by γ-aminobutyric acid: Physiological, biochemical, and structural characterization. *Front. Nutr.* 752:538. doi: 10.3389/fnut.2021.752583

Peng, J. R., Carol, P., Richards, D. E., King, K. E., Cowling, R. J., Murphy, G. P., et al. (1997). The Arabidopsis GAI gene defines a signaling pathway that negatively regulates gibberellin responses. *Genes Dev.* 11, 3194–3205. doi: 10.1101/gad.11.23.3194

Pino, M. T., Skinner, J. S., Jeknić, Z., Hayes, P. M., Soeldner, A. H., Thomashow, M. F., et al. (2008). Ectopic AtCBF1 over-expression enhances freezing tolerance and induces cold acclimation-associated physiological modifications in potato. *Plant Cell Environ.* 31, 393–406. doi: 10.1111/j.1365-3040.2008.01776.x

Shan, S. S., Wang, Z. Q., Pu, H. L., Duan, W. H., Song, H. M., Li, J. K., et al. (2022). DNA methylation mediated by melatonin was involved in ethylene signal transmission and ripening of tomato fruit. *Sci. Hortic.* 291:110566. doi: 10.1016/j.scienta.2021.110566

Shan, X. Y., Yan, J. B., and Xie, D. X. (2012). Comparison of phytohormone signaling mechanisms. *Curr. Opin. Plant Biol.* 15, 84–91. doi: 10.1016/j.pbi.2011.09.006

Shi, X. P., Jiang, F. L., Wen, J. Q., and Wu, Z. (2019). Overexpression of Solanum habrochaites microRNA319d (sha-miR319d) confers chilling and heat stress tolerance in tomato (S. lycopersicum). *BMC Plant Biol.* 19:214. doi: 10.1186/s12870-019-1823-x

Stockinger, E. J., Gilmour, S. J., and Thomashow, M. F. (1997). Arabidopsis thaliana *CBF1* encodes an AP2 domain-containing transcriptional activator that binds to the C-repeat/DRE, a cis-acting DNA regulatory element that stimulates transcription in response to low temperature and water deficit. *Proc. Natl. Acad. Sci. U.S.A.* 94, 1035–1040. doi: 10.1073/pnas.94.3.1035

Sunkar, R., Chinnusamy, V., Zhu, J. H., and Zhu, J. K. (2007). Small RNAs as big players in plant abiotic stress responses and nutrient deprivation. *Trends Plant Sci.* 12, 301–309. doi: 10.1016/j.tplants.2007.05.001

Tian, J. X., Xie, S. Y., Zhang, P., Wang, Q., Li, J. K., and Xu, X. B. (2022). Attenuation of postharvest peel browning and chilling injury of banana fruit by Astragalus polysaccharides. *Postharvest Biol. Technol.* 184:111783. doi: 10.1016/j.postharvbio.2021.111783

Wang, F., Chen, X. X., Dong, S. J., Jiang, X. C., Wang, L. Y., Yu, J. Q., et al. (2020b). Crosstalk of PIF4 and DELLA modulates CBF transcript and hormone homeostasis in cold response in tomato. *Plant Biotechnol. J.* 18, 1041–1055. doi: 10.1111/pbi.13272

Wang, Y. T., Feng, C., Zhai, Z. F., Peng, X., Wang, Y. Y., Sun, Y. T., et al. (2020a). The apple microR171i-SCARECROW-LIKE PROTEINS26. 1 module enhances drought stress tolerance by integrating ascorbic acid metabolism. *Plant Physiol.* 184, 194–211. doi: 10.1104/pp.20.00476

Wang, Z. Q., Pu, H. L., Shan, S. S., Zhang, P., Li, J. K., Song, H. M., et al. (2021). Melatonin enhanced chilling tolerance and alleviated peel browning of banana fruit under low temperature storage. *Postharvest Biol Technol.* 179:111571. doi: 10.1016/j.postharvbio.2021.111571

Wang, Z. Q., Zhang, L., Duan, W. H., Li, W., Wang, Q., Li, J. K., et al. (2022). Melatonin maintained higher contents of unsaturated fatty acid and cell membrane structure integrity in banana peel and alleviated postharvest chilling injury. *Food Chem.* 397:133836. doi: 10.1016/j.foodchem.2022.133836

Xu, K., Chen, S. J., Li, T. F., Ma, X. S., Liang, X. H., Ding, X. F., et al. (2015). OsGRAS23, a rice GRAS transcription factor gene, is involved in drought stress response through regulating expression of stress-responsive genes. *BMC Plant Biol.* 15:141. doi: 10.1186/s12870-015-0532-3

Yan, J., Gu, Y. Y., Jia, X. Y., Kang, W. J., Pan, S. J., Tang, X. Q., et al. (2012). Effective small RNA destruction by the expression of a short tandem target mimic in *Arabidopsis*. *Plant Cell* 24, 415–427. doi: 10.1105/tpc.111.094144

Zhang, L., Cao, X., Wang, Z. Q., Zhang, Z. K., Li, J. K., Wang, Q., et al. (2022). Brassinolide alleviated chilling injury of banana fruit by regulating unsaturated fatty acids and phenolic compounds. *Sci Hortic.* 297:110922. doi: 10.1016/j.scienta.2022.110922

Zhang, Z. H., Zhu, L., Song, A. P., Wang, H. B., Chen, S. M., Jiang, J. F., et al. (2020). Chrysanthemum (Chrysanthemum morifolium) CmICE2 conferred freezing tolerance in *Arabidopsis*. *Plant Physiol. Biochem.* 146, 31–41. doi: 10.1016/j.plaphy.2019.10.041

Zhao, K. Y., Chen, R. L., Duan, W. H., Meng, L. H., Song, H. M., Wang, Q., et al. (2022b). Chilling injury of tomato fruit was alleviated under low-temperature storage by silencing Sly-miR171e with short tandem target mimic technology. *Front. Nutr.* 9:906227. doi: 10.3389/fnut.2022.906227

Zhao, K. Y., Song, H. M., Wang, Z. Q., Xing, Z. T., Tian, J. X., Wang, Q., et al. (2022a). Knockdown of Sly-miR164a by short tandem target mimic (STTM) enhanced postharvest chilling tolerance of tomato fruit under low temperature storage. *Postharvest Biol. Technol.* 187:111872. doi: 10.1016/j.postharvbio.2022.111872

Zhao, R. R., Sheng, J. P., Lv, S. N., Zheng, Y., Zhang, J., Yu, M. M., et al. (2011). Nitric oxide participates in the regulation of LeCBF1 gene expression and improves cold tolerance in harvested tomato fruit. *Postharvest Biol. Technol.* 62, 121–126. doi: 10.1016/j.postharvbio.2011.05.013

Zhou, M. Q., and Tang, W. (2019). MicroRNA156 amplifies transcription factor-associated cold stress tolerance in plant cells. *Mol. Genet. Genomics* 294, 379–393. doi: 10.1007/s00438-018-1516-4

Zhu, Z., Ding, Y., Zhao, J. H., Nie, Y., Zhang, Y., Sheng, J. P., et al. (2016). Effects of postharvest gibberellic acid treatment on chilling tolerance in cold-stored tomato (*Solanum lycopersicum* L.) fruit. *Food Bioproc. Tech.* 9, 1202–1209. doi: 10.1007/s11947-016-1712-3

frontiers | Frontiers in Plant Science

TYPE Original Research
PUBLISHED 17 October 2022
DOI 10.3389/fpls.2022.1024909

OPEN ACCESS

EDITED BY
Christopher B. Watkins,
Cornell University, United States

REVIEWED BY
Morteza Soleimani Aghdam,
Imam Khomeini International University, Iran
Zhenfeng Yang,
Zhejiang Wanli University, China

*CORRESPONDENCE
Haiyan Gao
spsghy@163.com
Ruiling Liu
ruilingliu2005@163.com

†These authors contributed equally to this work

SPECIALTY SECTION
This article was submitted to Crop and Product Physiology, a section of the journal Frontiers in Plant Science

RECEIVED 22 August 2022
ACCEPTED 26 September 2022
PUBLISHED 17 October 2022

CITATION
Jiang B, Fang X, Fu D, Wu W, Han Y, Chen H, Liu R and Gao H (2022) Exogenous salicylic acid regulates organic acids metabolism in postharvest blueberry fruit. *Front. Plant Sci.* 13:1024909. doi: 10.3389/fpls.2022.1024909

Exogenous salicylic acid regulates organic acids metabolism in postharvest blueberry fruit

Bo Jiang[1,2,3,4,5†], Xiangjun Fang[2,3,4,5†], Daqi Fu[6], Weijie Wu[2,3,4,5], Yanchao Han[2,3,4,5], Hangjun Chen[2,3,4,5], Ruiling Liu[2,3,4,5*] and Haiyan Gao[1,2,3,4,5*]

[1]College of Food Science and Technology, Nanjing Agricultural University, Nanjing, China, [2]Food Science Institute, Zhejiang Academy of Agricultural Sciences, Hangzhou, China, [3]Key Laboratory of Post-Harvest Handling of Fruits, Ministry of Agriculture and Rural Affairs, Hangzhou, China, [4]Key Laboratory of Fruits and Vegetables Postharvest and Processing Technology Research of Zhejiang Province, Hangzhou, China, [5]Key Laboratory of Postharvest Preservation and Processing of Fruits and Vegetables, China National Light Industry, Hangzhou, China, [6]College of Food Science and Nutritional Engineering, China Agricultural University, Beijing, China

Fruit acidity is an essential factor affecting blueberry organoleptic quality. The organic acid content in blueberry fruit mainly contributes to fruit acidity. This study aims to evaluate the effect of exogenous salicylic acid (SA), the principal metabolite of aspirin, on the organoleptic quality and organic acid metabolism in rabbiteye blueberry (*Vaccinium virgatum* Ait, 'Powderblue') during cold storage (4 °C). Results showed that SA-treated fruit reduced fruit decay and weight loss delayed fruit softening, and decline of total soluble solids (TSS). TA and total organic acid amounts stayed the same during the late storage period in SA-treated fruit. Four kinds of organic acid components, malic acid, quinic acid, citric acid, and succinic acid, were at higher levels in fruit treated by SA as compared to control. SA enhanced the activities of PEPC, NAD-MDH, and CS to promote the synthesis of malic acid and citric acid. Meanwhile, the activities of NADP-ME, ACL, and ACO, which participated in the degradation of malic acid and citric acid, were inhibited by SA. qPCR results also showed that the expression of *VcPEPC*, *VcNAD-MDH*, and *VcCS* genes were upregulated. In contrast, SA downregulated the expression of *VcNADP-ME*, *VcACL*, and *VcACO* genes. In conclusion, SA could regulate the key genes and enzymes that participated in organic acids metabolism to maintain the freshness of blueberry during cold storage, therefore minimizing the economic loss.

KEYWORDS

salicylic acid, organic acid metabolism, blueberry fruit, postharvest storage, organoleptic quality

Introduction

Blueberry, the *Vaccinium* genus, is popular with consumers because of its high nutritional and healthy benefits. Fruit acidity is an essential component affecting fruit quality and edible flavor (Etienne et al., 2013). Fruit acidity is mainly affected by the accumulation of organic acids (Giné Bordonaba and Terry, 2010). The type and proportion of main organic acids in fruit differ from species and cultivars (Mark et al., 1994). For instance, citric acid is the primary organic acid in ponkan (Gao et al., 2018) and tomato (Yan et al., 2021) fruit. Malic acid is dominant in apples (Zhu et al., 2022), pears (Wu et al., 2022), and peach (Yang et al., 2020) fruit. The content of organic acids varied during fruit development and storage (Das et al., 2022; Dragišić Maksimović et al., 2022). In the three maturation stages of blueberry fruit (green, red, and blue), the total acid decrease with the fruit ripening (Li et al., 2020). Five kinds of organic acid identified from O' Neal blueberry fruit (*V. corymbosum*) all dropped from green to blue stage. The levels of various organic acids in blueberry also showed the different trend during the storage (Nguyen et al., 2021; Smrke et al., 2021).

The change of organic acids in fruit is attributed to acid balance between acid synthesis and degradation (Zheng et al., 2021). The tricarboxylic acid (TCA) cycle is the main pathway to synthesizing organic acids, such as malic acid and citric acid (Huang et al., 2021). Malic acid accumulation and degradation were regulated by the activities of NAD-dependent malate dehydrogenase (NAD-MDH, EC 1.1.1.37), cytosolic NADP-dependent malic enzyme (NADP-ME, EC1.1.1.40), and phosphoenolpyruvate carboxylase (PEPC, EC4.1.1.31) (Liao et al., 2022). NAD-MDH and PEPC activities are responsible for the malic acid biosynthesis, while NADP-ME relates to malic acid degradation (Liu et al., 2016). As for the citric acid, citrate synthase (CS, EC, 2.3.3.1), aconitate hydratase (ACO, EC 4.2.1.3), and ATP-citrate synthase (ACL, EC 4.1.3.8) participated in the citrus metabolism. One of citrate degradation is a γ-Aminobutyric acid (GABA) shunt that citric acid is catalyzed to form succinic acid (Li et al., 2020). Another pathway is to join in the transformation of malic acid by forming OAA and acetyl-CoA under the action of ACL (Guo et al., 2020).

Salicylic acid (SA), the principal metabolite of aspirin, crucial endogenous hormone, participated in fruit quality formation and disease resistance against the pathogen (Rachappanavar et al., 2022). In recent years, exogenous SA treatment has been shown to maintain postharvest fruit quality and delay fruit decay and disease incidence (Yang et al., 2020; Yang et al., 2022). Moreover, SA treatment promoted the accumulation of organic acid in citrus fruit (Wang et al., 2020) and jujube fruit (Yang et al., 2022). However, another study indicated that organic acids were no significant difference in peach fruit between SA treated and control fruit (Yang et al., 2020). Therefore, the effect of exogenous SA on organic acid metabolism needs to be further studied. In addition, our previous study found that SA affected the titratable acidity (TA) level in blueberry fruit during ambient temperature storage (25 °C) (Jiang et al., 2022). However, the change regularity and metabolism mechanism of organic acid under SA treatment in postharvest blueberry fruit was still less reported. This paper studied the change of organic acids and their metabolism related enzymes and genes expression levels in postharvest blueberry treated by exogenous SA. These results may provide some evidence for revealing the regulation of SA on organic acid mechanism in blueberry stored in cold condition (4°C).

Materials and methods

Experimental materials

The mature rabbiteye blueberries (*Vaccinium virgatum* Ait, 'Powderblue') were harvested from a commercial orchard located in Xinchang, Zhejiang Province, on July 15, 2021. The same maturity, uniform size, no disease, and no mechanical damage, blueberry was selected to slip back to the laboratory for subsequent experiments.

Treatment and sampling

All berries were divided randomly into two groups (SA group and control group). SA group was soaked in 1.0 mmol L^{-1} SA solution for 5 min (SA group). Control group was soaked with sterile water for 5 min. Each group was performed in triplicate. The treated berries were air-dried and packed in a plastic box with polyethylene terephthalate. Each box of 125 g berries was stored at 4 °C for 30 days.

Fruit quality was analyzed at six days intervals during cold storage. Forty-five berries were taken from each replication at random for measurement of fruit decay and weight loss every six days, respectively. ten berries were selected for the determination of fruit firmness. Ten berries were sampled for total soluble solids (TSS) and TA. The remaining berries per replicate were cut into small pieces with a scalpel and frozen quickly in liquid nitrogen. The sample pieces were stored in -80 °C for assays of organic acids metabolism.

Analysis of fruit quality

The decay incidence was evaluated according to the number of berries with rot, lesion, or visible pathogen growth among all berries. The result was presented as the percentage (%) of decay berries with respect to the total number of berries. The weight loss was calculated by weighing berries before and after storage.

The result was evaluated as the percentage (%) of weight reduction relative to the original weight. The fruit firmness was measured by a texture analyzer (TA-XT Plus, Stable Micro Systems Ltd, Surrey, U.K.) equipped with a probe of 6 mm diameter. The experimental parameters were as follows. Compression position: fruit equator; compression distance: 5 mm; measuring speed: 1.0 mm s^{-1}. The firmness was presented as the maximum pressing force (N). TSS content in berries was recorded by a digital refractometer (PAL-1, Atago, Tokyo, Japan), and the result was expressed as a percentage (%). TA in berries was measured by an automatic titrator (877 Titrino plus, Metrohm, Herisau, Switzerland), and the result was expressed as a percentage of malic acid (%).

Determination of organic acids

Determination of organic acids was conducted following the method of Li et al. (2020). Approximately 2 g frozen sample (ground powder) was added into 2mL ultrapure water and then extracted by ultrasonic irradiation for 30 min. The mixture was centrifuged at 8000 ×g for 10 min (4 °C). The supernatant was collected into a centrifuge tube of 10 mL, and the residue was extracted again with ultrapure water of 1 mL. The second extract was centrifuged at 8000 ×g for 10 min (4 °C). The supernatant centrifuged twice were mixed and filtered through a 0.22 μm microporous membrane filter. The filtrate was used for the analysis of organic acids.

The composition and content of organic acids was analyzed by HPLC. The HPLC analysis was performed by Waters Alliance 2995 system (Waters Corporation, Milford, USA) with an RP-HPLC XDB-C18 column (5 μm,250 mm×4.6 mm, Agilent, CA, USA). The mobile phase was 0.01 M KH_2PO_4 buffer (pH=2.7) with 4% (v: v) methanol. The flow rate was 0.6 mL/min. The temperature of the column was set at 25°C. The wavelength of the ultraviolet detector (2998, Waters Corporation, Milford, USA) was set at 210 nm. The injection volume was 10 μL. Organic acid was quantified by different external standards purchased from Sigma-Aldrich (St. Louis, MO, USA). The retention time, calibration curves and correlation coefficients of external standards were showed in Supplementary Table S1.

Extraction and assay of enzyme activities.

Crude enzymes of PEPC, NAD-MDH, NADP-ME, and CS were extracted according to the method of Millaleo et al. (2019). PEPC, NAD-MDH, NADP-ME, and CS activity were measured according to Chen et al. (2009). ACL and ACO were extracted and assayed following the method of Guo et al. (2020). All enzyme activities were described as Unit (U) kg^{-1} fresh weight (FW).

Extraction of RNA and synthesis of cDNA

Total RNA was extracted from 150 mg frozen samples (ground powder in liquid nitrogen) using an RNAprep Pure Plant Kit (Polysaccharides & Polyphenolics-rich) (Tiangen, Beijing, China). The concentration and purity of total RNA were assayed using a BioSpec-nano spectrophotometer (Shimadzu Corporation, Tokyo, Japan). The first-strand cDNA was synthesized using a StarScript II First-strand cDNA synthesis kit with gDNA Remover (GeneStar, Beijing, China)

Quantitative real-time PCR analysis

The qRT-PCR primers were designed using Primer Premier 5.0 software (Premier Biosoft International, San Francisco, USA) and synthesized by Youkang Biotech (Hangzhou, China). The specific primers sequences of organic acid metabolism-related genes were shown in Table 1. The qRT-PCR analysis was operated by using 2×RealStar Green Fast Mixture with ROX (GeneStar, Beijing, China) and a quantitative fluorescence analyzer (StepOne Plus, ABI, Waltham, USA). The qPCR procedure was as follows: predenaturation at 95°C for 2 min, followed by a cycle reaction (40 cycles) of 95 °C for 15s, 55 °C for 30 s. Melting curve was preformed from 55 to 95 °C at an increasing speed of 0.5°C per second. The relative gene expression levels were evaluated using the ABI's Stepone 2.3 software and the $2^{-\Delta\Delta Ct}$ method (Livak and Schmittgen, 2001). The GAPDH gene (gene accession number: AY123769) was served as the internal reference gene to normalize the expression data. All qRT-PCR reactions were performed in triplicate.

TABLE 1 The sequences of primers used for qPCR.

Gene	GeneID	Forward primer sequence (5'-3')	Reverse primer sequence (5'-3')
VcPEPC	KT995478	CCGCCTTCGTGACTCCTACAT	TGCTATCGCCTATGAAGTCC
VcNAD-MDH	Vadar_g11215	ACGATCTGTTCAACATCAATGC	GCTCCCAGTACTTTGATTTTGG
VcNADP-ME	Vadar_g15676	CTGATGGCGAGCGGATTTTG	TATGGGCAGGCACGAAGAAG
VcCS	DR067095	GTAGACACGGTGCCCAAATC	TCATGGTGGAGCAAATGAAG
VcACL	MH048701	GGCTCAACTCTTTCGGACCA	CAGGGCTTCCACAAGGGAAT
VcACO	Vadar_g34681	TGGCAAGAGGAACTTTCGCA	CTGCTCCGGCCAAGACAATA
VcGAPDH	AY123769	GCTGTACCACAAACTGTCTTGC	ATGAAGCAGCTCTTCCACCTCT

Statistical analysis

Statistical analysis was conducted using SPSS 19.0 statistical software package (IBM Corporation, Chicago, USA). The significant difference was carried out using One-way analysis of variance (ANOVA) combined with Duncan's multiple-range test ($P < 0.05$), Figures were plotted with Origin 9.4 (OriginLab, Northampton, USA). Online Hiplot software (Shanghai Tengyun Biotech, Shanghai, China) (https://hiplot-academic.com/basic/corrplot) was applied to illustrate the correlation. All data are presented as mean ± standard deviation.

Results

Effect of SA treatment on fruit quality

The weight loss of fruit showed an increasing trend during cold storage. Compared to the control fruit, SA-treated fruit had lower weight loss (Figure 1A). The decayed fruit began to appear after 12 days of storage, and the decay incidence in the control fruit reached 20.0% at 30 d, while decay incidence in SA-treated fruit was only 12.5% (Figure 1B). The change in firmness was opposite to the change in weight loss. The fruit becomes softer after storage. SA treatment could delay the decrease of fruit firmness (Figure 1C). The content of TSS exhibited a downward trend, and the differences between SA-treated and control fruit appeared after 12 days and 18 days of storage, respectively (Figure 1D).

Effect of SA treatment on TA and organic acids

As shown in Figure 2, TA level in fruit displayed a declining trend during cold storage. Compared with control, the TA in SA-treated fruit was higher during the late stage (After 18 days) (Figure 2A). The change of total organic acids, not completely consistent with the change of TA, showed a tendency to decrease first and then remain unchanged (Figure 2B). In comparison, SA treatment maintained the total organic acid to some degree. Malic acid was the highest organic acid content in 'Powderblue' blueberry, followed by quinic acid, citric acid, and succinic acid. Malic acid content in control fruit decreased from 8.66 g kg^{-1} at 0 d to 6.70 g kg^{-1} at 18 d, and then slightly decreased to 7.34 g kg^{-1} at 30 d. While malic acid in SA-treated fruit showed no obvious change during storage (Figure 2C). Compared with the control fruit, quinic acid in SA-treated fruit great declined after 6 days, but after 12 days, quinic acid content increased first and then decreased (Figure 2D). Although the content of citric acid in the control fruit decreased during storage, there was a high peak

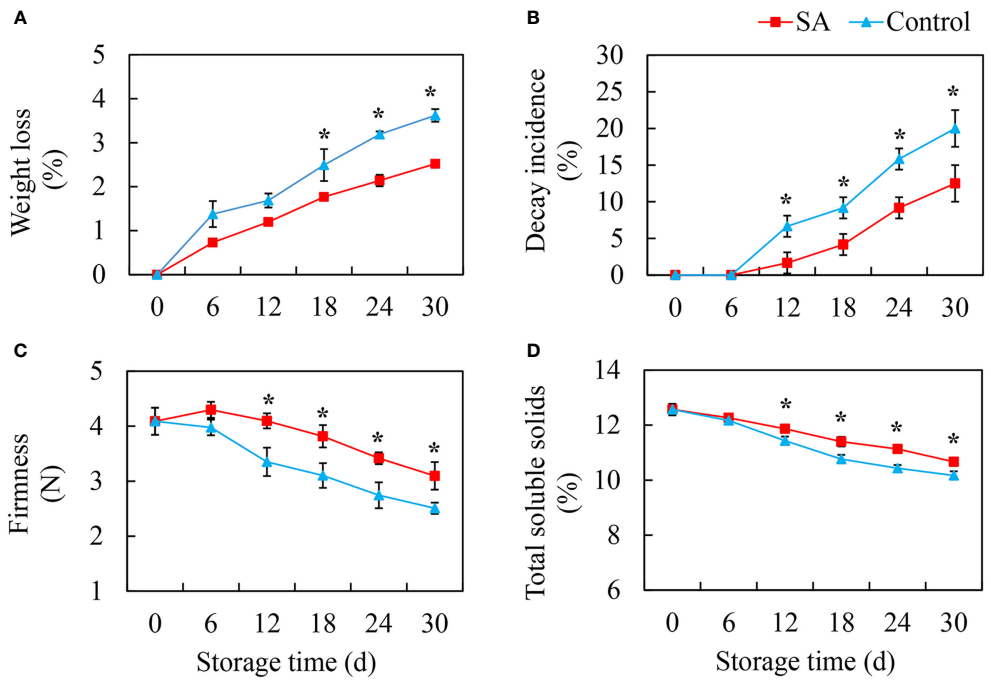

FIGURE 1
Effects of Salicylic acid treatment on fruit quality of blueberry during cold storage. **(A)**, Weight loss; **(B)**, Decay incidence; **(C)**, Firmness; **(D)**, Total soluble solids (TSS). Error bars represent the standard deviations of the means (n=3). The asterisks show a significant difference between SA-treated and control fruit ($P < 0.05$).

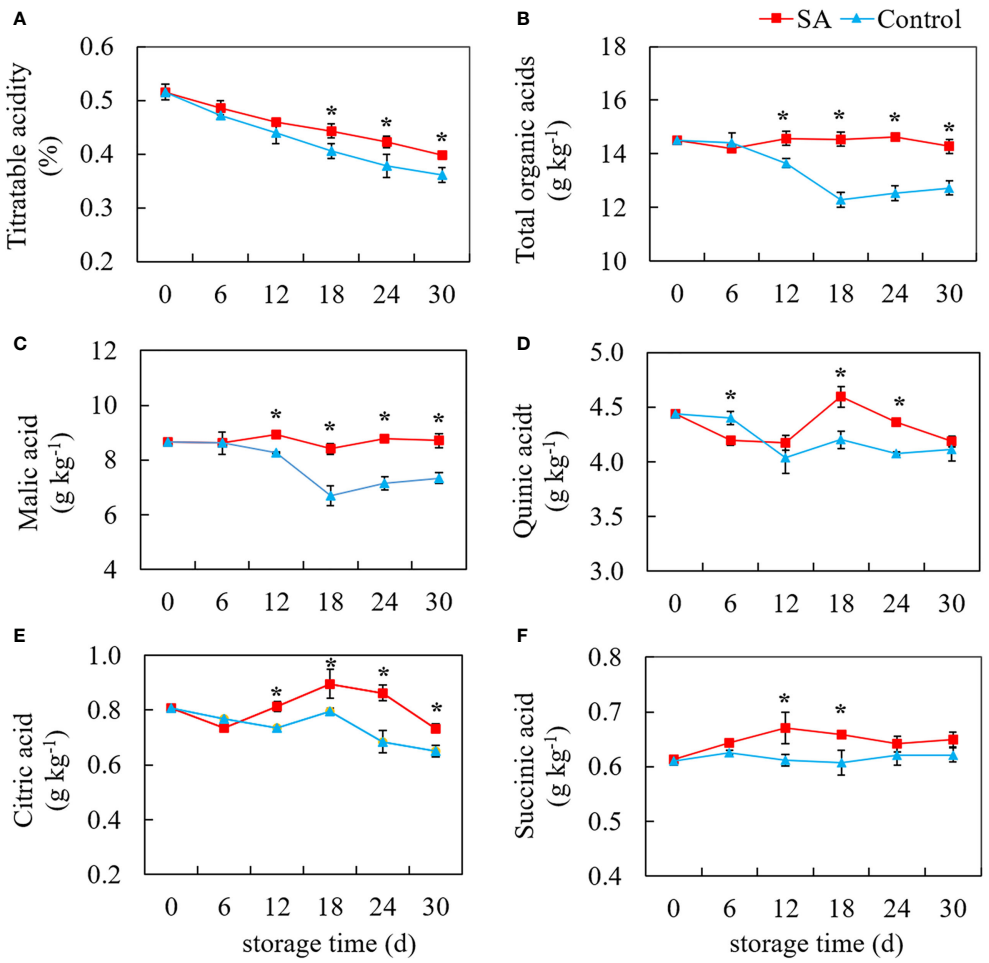

FIGURE 2
Effects of Salicylic acid treatment on organic acid of blueberry during cold storage. **(A)**, Titratable acidity (TA); **(B)**, total organic acid; **(C)**, Malic acid; **(D)**, Quinic acid; **(E)**, Citric acid; **(F)**, Succinic acid. Error bars represent the standard deviations of the means (n=3). The asterisks show a significant difference between SA-treated fruit and control fruit ($P < 0.05$).

value at 18 d (Figure 2E). SA treatment increased the content of citric acid during the mid and late periods. Succinic acid was the lowest of the four organic acids, accounting for 4.22% of total organic acid. There was no significant change in the succinic acid content of control during storage, but succinic acid in SA-treated fruit was an obvious increasing trend before 18 days (Figure 2F). These results showed SA treatment might mediate blueberry's organic acid metabolism after harvest.

Effect of SA treatment on enzymes activities participating in organic acids metabolism

Figure 3 shows the change patterns of three malic acid metabolism-related enzymes (PEPC, NAD-MDH, and NADP-ME) and three citric acid metabolism-related enzymes (CS, ACO, and ACL) in SA treated and control fruit during cold storage. PEPC activity in the control fruit was no significant change with the extension of storage time (Figure 3A). But SA-treated fruit maintained higher PEPC activity as compared to control. The activity of NAD-MDH declined from 0.31 U kg^{-1} at 0 d to 0.24 U kg^{-1} and 0.22 U kg^{-1} at 6 d in SA-treated and control fruit, respectively (Figure 3B). But an increase in NAD-MDH activity in control fruit was observed at the -mid-stage (from 12 to 18 days) and then decreased to 0.19 U kg^{-1} at 30 d. Although the change of enzyme activity was similar to that in control, NAD-MDH activity in SA-treated showed higher levels during the late period (24 days and 30 days). Considering the level of NADP-ME activity, a drop of activity was observed in the first six days, and activity climbed to the highest peak at 18 d (Figure 3C). While during the late storage, the fruit showed a

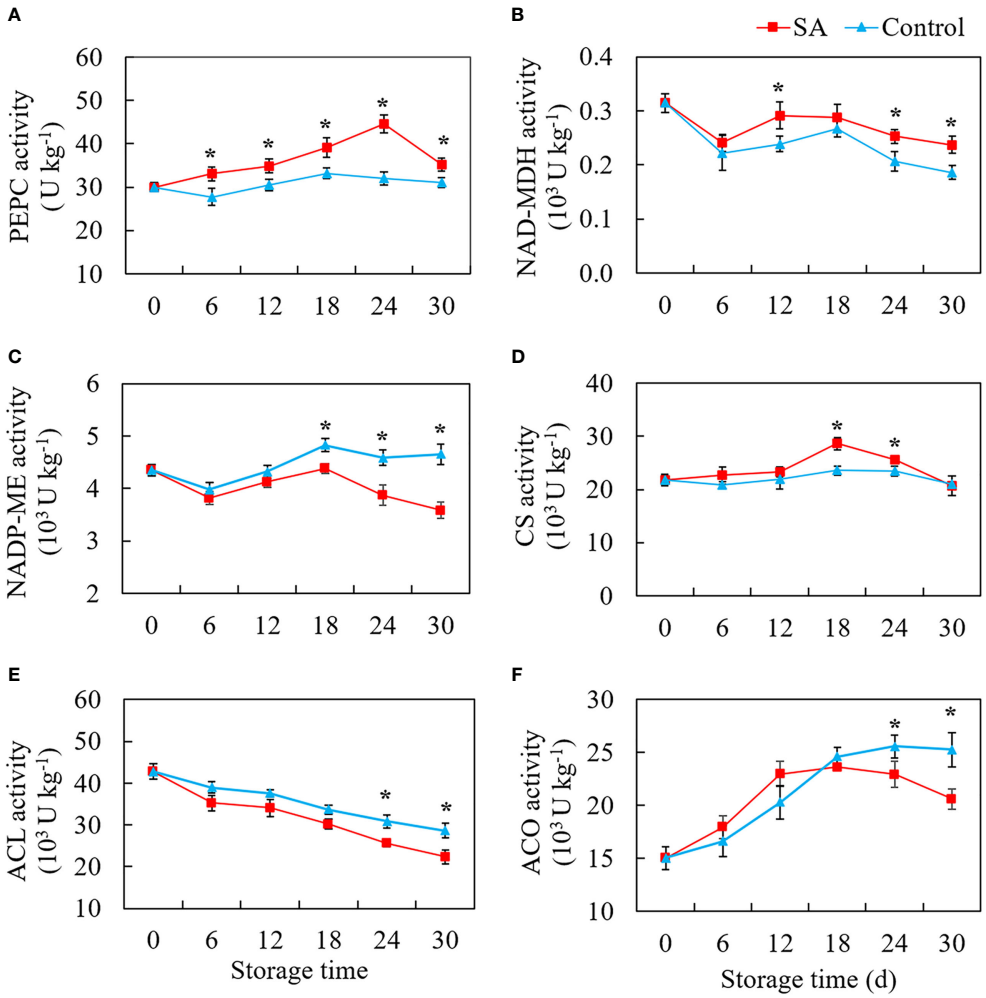

FIGURE 3
Effects of salicylic acid treatment on enzyme activities participated in organic acid metabolism of blueberry during cold storage. **(A)**, phosphoenolpyruvate carboxylase (PEPC); **(B)**, NAD-dependent malate dehydrogenase (NAD-MDH); **(C)**, NADP-dependent malic enzyme (NADP-ME); **(D)**, Citrate synthase (CS); **(E)**, ATP-citrate synthase (ACL); **(F)**, cytoplasm aconitase (ACO). Error bars represent the standard deviations of the means (n=3). The asterisks show a significant difference between SA-treated fruit and control fruit ($P < 0.05$).

significant decline in NADP-ME activity, and the fruit treated by SA had a higher NADP-ME activity than the control fruit. As for three enzymes that participated in citric acid accumulation, control fruit had no obvious fluctuation in CS activity during whole storage, while the CS activity in SA-treated fruit showed an increasing trend after 12 days and then declined to the same level in control at 30 d (Figure 3D). The ACL activity decreased overall during storage both in SA-treated and control fruit. The higher enzyme activities happened in fruit with SA treatment at 6 d and 30 d as compared with control (Figure 3E). The activity level of ACO in fruit reached a higher level from 15.01 U kg^{-1} at 0 d to 24.58 U kg^{-1} at 18 d during the early storage and then remained stable for 30 days (Figure 3F). SA treatment reduced ACO activity during the late storage.

Effect of SA treatment on genes expression involved in organic acids metabolism

VcPEPC gene expression increased from 0 d to 18 d then declined to 30 d in control fruit during storage (Figure 4A). Even if similar to the changing trend of control, the SA-treated fruit showed a more extended increasing period from 0 d to 24 d. SA treatment promoted the *VcPEPC* expression during whole storage, except at 18 d. Fluctuation of the gene expression level of *VcNAD-MDH* in SA-treated and control fruit was consistent with storage time (Figure 4B). SA-treated fruit was higher in *VcNAD-MDH* expression at 12 d and 30 d compared to control. regarding the transcript level of

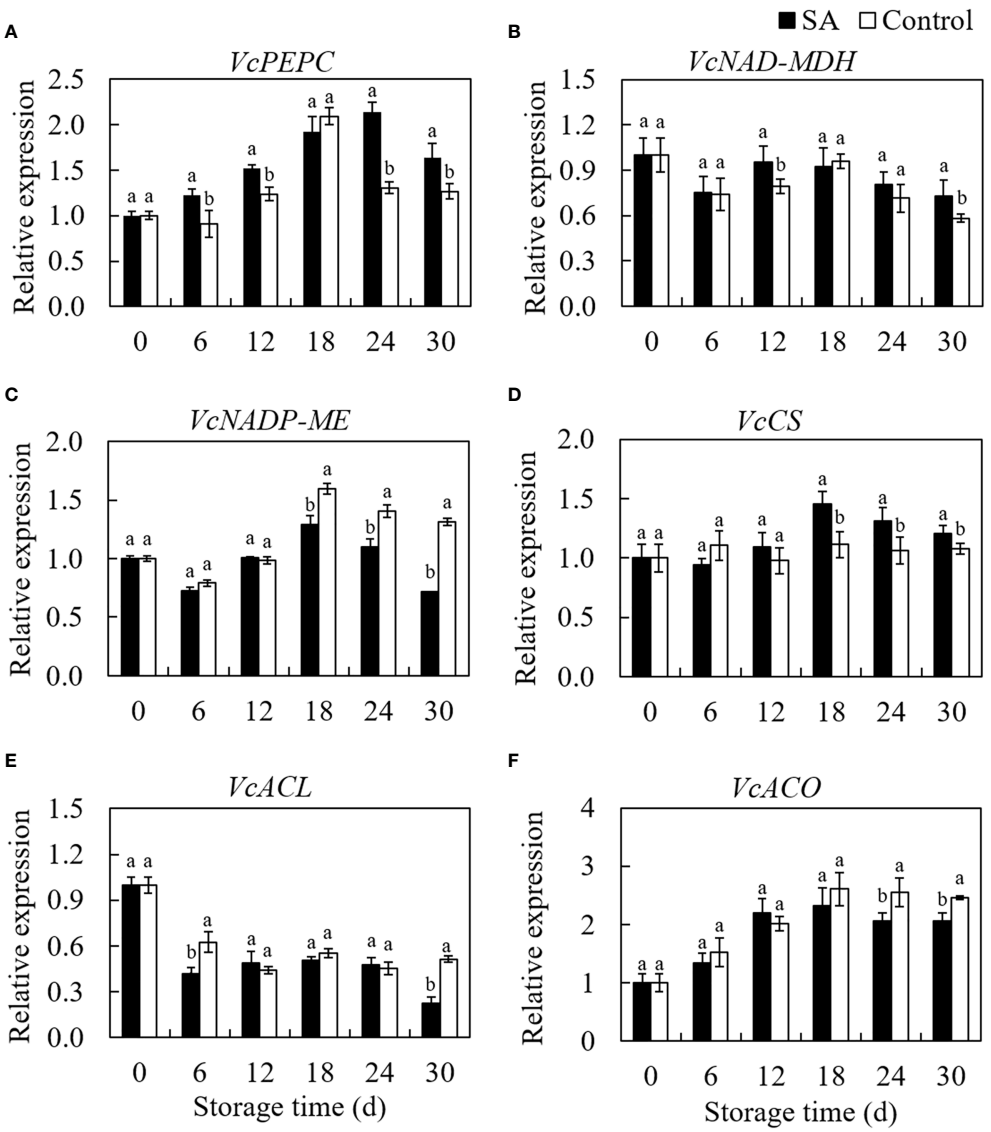

FIGURE 4
Effects of Salicylic acid treatment on genes expressions involved in organic acid metabolism of blueberry during cold storage. **(A)**, *VcPEPC*; **(B)**, *VcNAD-MDH*; **(C)**, *VcNADP-ME*; **(D)**, *VcCS*; **(E)** *VcACL*; **(F)**, *VcACO*. Error bars represent the standard deviations of the means (n=3). The different lowercase letters indicate the significant differences between SA-treated and control fruit at each sampling time (P<0.05).

VcNADP-ME in blueberry, a higher expression in SA-treated fruit was observed than that in control during the end of storage (from day 18 to day 30) (Figure 4C). The transcription of *VcCS* was no significantly changed in control during storage, while SA treatment upregulated the expression of *VcCS* in blueberry after 12 days of storage (Figure 4D). *VcACL* expression in control showed a decreasing trend at the early stage (before 12 days) and remain stableto 24 d (Figure 4E). It is noteworthy that *VcACL* expression considerably rose from 24 d to 30 d (about 1.80 times). Fruit treated by SA still was in a lower level of *VcACL* at 30 d. The *VcACO* expression increased by 2.61 times from 0 d to 18 d in control and then declined slightly to 30 days (Figure 4F). The change trend in SA-treated fruit was similar to the change in control, but lower expression levels were observed than that in control during the late storage. These results indicated that SA treatment could regulate the expression of key genes involved in the organic acid metabolism of blueberry.

Correlation analysis of indicators involved in organic acid metabolism

Correlation analysis in all indicators involved in organic acid metabolism was conducted by the Pearson correlation coefficient. From the results in Figure 5, we found that the coefficient between TA and total organic acid was 0.66, suggesting that fruit acidity was closely positively related to blueberry's organic acid content during storage. Three kinds of enzymes, NAD-MDH, PEPC, and NADP-ME, participated in the accumulation and degradation of malic acid was highly related to *VcNAD-MDH*, *VcPEPC*, and *VcNADP-ME* genes, respectively. These results implicated that these genes may regulate relevant enzyme activities to affect malic acid metabolism. The correlation between three enzymes (CS, ACO, and ACL) and three genes (*VcCS*, *Vc*ACO, and *VcACL*) involved in citric acid biosynthesis and transfer showed a similar feature. In addition, the correlation difference between total organic acids and four organic acids indicated that the contribution of four acids to total acids was not equal. Interestingly, although citric acid and malic acid could transform each other by various pathways, the correlation between them was not high (0.44). This result may indicate that malic acid content did not depend entirely on the level of citric acid. In addition, organic acid, the decay incidence and weight loss of fruit were negatively correlated with total organic acids and malic acid. The firm firmness showed positively correlation with malic acids (0.72) and citric acid (0.56).

Discussion

The weight loss, softening, and decay of 'Powderblue' blueberry occurred during cold storage, and these changes also existed in the postharvest period of other blueberry cultivars (Abeli et al., 2021; Xu et al., 2021). We found that SA treatment

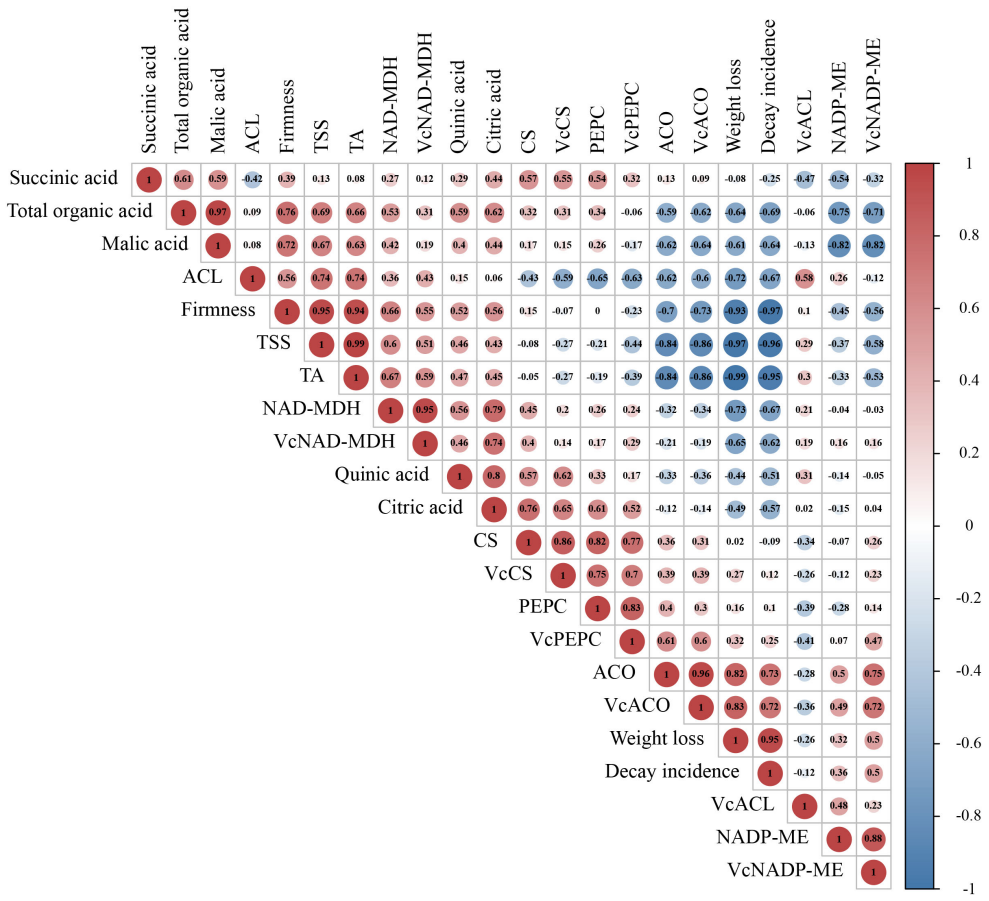

FIGURE 5
Correlation analysis of indicators involved in organic acid metabolism. The Correlation in all indicators was conducted by Pearson Correlation Analysis. The value in the circle represents the Pearson correlation coefficient between the heading of the column and the row. The closer the value is near to 1 or -1, the greater the correlation. Red color represents positive correlation; blue represents negative correlation.

delayed the decline of weight loss and firmness, and slowed fruit decay incidence. These results were similar to other fruits such as strawberries (Zhang et al., 2022), peach (Yang et al., 2020), and litchi (Kumari et al., 2015) treated by SA. The possible reason for maintenance of fruit quality was that exogenous salicylic acid treatment induced the increase of endogenous salicylic acid content, thereby reducing the respiratory metabolism and delaying fruit senescence, which was confirmed in jujube fruit (Yang et al., 2022).

Acidity and sweetness play essential roles in the flavor quality of fruit (Yang et al., 2020). Our results showed SA treatment effectively inhibited the decline of TSS and TA, therefore maintained the taste and quality of blueberry during storage. More importantly, organic acid, the main responsible for acidity, is also closely related to the aging process and storage performance (Etienne et al., 2013). Some citrus cultivars with high-content organic acids or organic acid degradation slowly have better storage performance. The consumption of organic acid during storage after harvest was the main reason for fruit flavor and quality decline, which brings severe economic loss to fruit production (Wang et al., 2014). The total organic acids in 'Powderblue' fruit gradually decreased during storage. SA treatment significantly delayed the fall down of total organic acids. The higher level of organic acid in fruit provided abundant substrates for maintaining the postharvest quality of fruit. Some studies showed that the changes of organic acids affect fruit senescence and storage characteristics (Sheng et al., 2017; Habibi et al., 2020). Moreover, malic acid and citric acid, also as the intermediate products of plant cell respiration metabolism, play an important role in plant material metabolism and energy metabolism (Etienne et al., 2013). The reduced fruit decay in the treated blueberry fruit could be ascribed to SA inhibited the degradation of organic acids, which helped to suppress respiration and resulted in lower energy consumption Meanwhile, the reduction of organic acids consumption maintained an acidic environment, which slowed down fruit senescence (Angioni and Schirra, 2011). Among four kinds of organic acids, malic acid was the predominant acid, followed by quinic and citric acid. The types and distribution of organic acids in blueberry were different in cultivars. Citric acid was the primary acid in lowbush (*Vaccinium angustifolium*) (Kalt and McDonald, 1996) and highbush blueberry (*V. corymbosum*) (Zhang et al., 2020). But the interesting thing is that quinic acid was the highest in some clones of lowbush blueberry (Gibson et al., 2013). The distribution discrepancy of organic acids may be due to diversity in blueberry genotypes and growth environment.

Although the total amount of organic acids decreased in blueberry during storage, the changes were not consistent between the four kinds of acids. These change differences in organic acids were also reported in other highbush blueberry cultivars during storage (Smrke et al., 2021; Dragišić Maksimović et al., 2022). Dragišić Maksimović et al. (2022) found that the total acids, citric acid, malic acid, and shikimic acid in 'Bluecrop' and 'Liberty' blueberry showed the decline in varying degrees with the elongation of the storage period, while quinic acid content was no significant change. In our study, SA treatment slowed the descent of malic acid in the mid and late storage period. Malic acid is the key intermediate in the TCA cycle, and synthesis and degradation of malic acid are closely related to the TCA cycle pathway (Fernie and Martinoia, 2009). Malic acid accumulation was reported to be negatively related to NADP-ME and positively related to NAD-MDH and PEPC activity in fruit (Liu et al., 2016). SA treatment was found to inhibit the NADP-ME activity and maintain the higher activity of NAD-MDH, suggesting that SA kept the balance of malic acid biosynthesis and degradation *via* regulating these enzyme activities. NAD-MDH catalyzes the reversible reactions from OAA to malic acid (Li et al., 2020). In addition, malic acid and OAA also participated in gluconeogenesis metabolism during the fruit ripening process (Etienne et al., 2013). In the gluconeogenesis pathway, OAA was formed from phosphoenolpyruvic acid under the catalysis of PEPC (Perotti et al., 2010). The higher level of OAA accumulation also increases the possibility of malate synthesis. PEPC was also positively correlated with malic acid accumulation in apples (Yao et al., 2009). The higher activity of PEPC in SA-treated blueberry suggested that the result was consistent with higher malic acid content than that in the control fruit. CS, ACL, and ACO are involved in citric acid biosynthesis and degradation. SA treatment enhanced the CS activity and inhibited ACO and ACL activity in the late period, which explained the increase of citric acid content. But the changing trend of ACL and ACO activities levels, two citrate degrading enzymes, presented the inverse trend during whole storage. These indicated that citric acid accumulation and degradation were co-regulated by several enzymes. The coregulation phenomenon often occurs in the acid metabolism of other fruits, such as apples (Liu et al., 2016) and peach (Liao et al., 2022).

The catalytic function of enzymes in organic acid metabolism requires transcription regulation by related genes. The results of qRT-PCR suggest that SA treatment upregulated the expression of the *VcPEPC* gene and downregulated *VcNADP-ME* during storage, consistent with changes in PEPC and NADP-ME activity. Similarly, a higher level in *VcNADP-MDH* gene expression and NADP-MDH activity in SA-treated fruit also demonstrated that SA maintained malic acid in blueberry after harvest by regulating the malic acid biosynthesis/degradation enzymes and related genes expression. Yang et al. (2022) also found that malic acid content in stored Jujube fruit was higher after being treated by exogenous SA. In addition, the study on citrus fruit also indicated that SA-induced differential expression of proteins participated in the TCA cycle and acid metabolism (Wang et al., 2020). Regarding citric acid metabolism, SA partially inhibited the transcript expression of *VcACL* and *VcACO genes*, leading to

the lower activities of citric acid degrading enzyme activities as compared to control. Meanwhile, the upregulation of *VcCS* expression in SA-treated fruit also promoted the *CS* activity to accumulate citric acid. In addition to promoting citric acid synthesis, SA treatment affected succinic acid content in mid-storage time. citric acid degradation and succinic acid synthesis were also regulated by the GABA shunt (Fait et al., 2008). We speculated that the increase of citric acid and succinic acid in SA-treated fruit might be regulated by GABA pathway. However, how SA would affect citric acid and succinic acid in postharvest blueberry through regulating key enzymes and genes involved in the GABA pathway remains to be further studied.

Conclusion

In our study, postharvest SA treatment reduced weight loss and decay incidence of blueberry fruit and delayed the decline of firmness and TSS, which maintained fruit sensory quality during cold storage. Exogenous SA was also effective in maintaining fruit acidity and organic acids of harvested blueberry. The decrease of four kinds of organic acid (malic acid, quinic acid, citric acid, and succinic acid) in 'Powderblue' fruit was inhibited by SA treatment to a different degree. SA upregulated the malic acid and citric acid biosynthesis-related enzymes (PEPC, NAD-MDH, and CS) and genes (*VcPEPC*, *VcNAD-MDH*, and *VcCS*) expression. Meanwhile, the activities of three enzymes (NADP-ME, ACL, and ACO) and expression levels of genes (*VcNADP-ME*, *VcACL*, and *VcACO*) participated in malic acid and citric acid degradation was downregulated by SA during storage. Under the co-regulation of enzymes and genes, the decline of organic acid content in SA-treated blueberry after harvest was delayed.

Data availability statement

The original contributions presented in the study are included in the article/Supplementary Material. Further inquiries can be directed to the corresponding authors.

Author contributions

BJ: Investigation, Formal analysis, Writing - Original Draft. XF: Investigation, Formal analysis, Writing - Review and Editing. DF: Methodology, Writing - Review and Editing. WW: Methodology, Writing - Review and Editing. YH: Writing - Review and Editing. HC: Writing - Review and Editing. RL: Supervision, Methodology, Writing - Review and Editing. HG: Conceptualization, Supervision, Project administration, Writing - Review.and Editing. All authors contributed to the article and approved the submitted version.

Funding

This work was supported by the National Natural Science Foundation of China (Grant No. 31772042) and the Key Research & Development Program of Zhejiang Province (2021C02015).

Conflict of interest

The authors declare that the research was conducted in the absence of any commercial or financial relationships that could be construed as a potential conflict of interest.

Publisher's note

Supplementary material

The Supplementary Material for this article can be found online at: https://www.frontiersin.org/articles/10.3389/fpls.2022.1024909/full#supplementary-material

References

Abeli, P. J., Fanning, P. D., Isaacs, R., and Beaudry, R. M. (2021). Blueberry fruit quality and control of blueberry maggot (*Rhagoletis mendax* Curran) larvae after fumigation with sulfur dioxide. *Postharvest. Biol. Technol.* 179, 111568. doi: 10.1016/j.postharvbio.2021.111568

Angioni, A., and Schirra, M. (2011). Long-term frozen storage impact on the antioxidant capacity and chemical composition of sardinianmyrtle (*Myrtus communis* l.) berries. *J. Agric. Sci. Technol. B.* 1, 1168–1175.

Chen, F., Liu, X., and Chen, L. (2009). Developmental changes in pulp organic acid concentration and activities of acid-metabolising enzymes during the fruit development of two loquat (*Eriobotrya japonica* lindl.) cultivars differing in fruit acidity. *Food Chem.* 114 (2), 657–664. doi: 10.1016/j.foodchem.2008.10.003

Das, P. R., Darwish, A. G., Ismail, A., Haikal, A. M., Gajjar, P., Balasubramani, S. P., et al. (2022). Diversity in blueberry genotypes and developmental stages enables discrepancy in the bioactive compounds, metabolites, and cytotoxicity. *Food Chem.* 374, 131632. doi: 10.1016/j.foodchem.2021.131632

Dragišić Maksimović, J., Milivojević, J., Djekić, I., Radivojević, D., Veberič, R., and Mikulič Petkovšek, M. (2022). Changes in quality characteristics of fresh blueberries: Combined effect of cultivar and storage conditions. *J. Food Compos. Anal.* 111, 104597. doi: 10.1016/j.jfca.2022.104597

Etienne, A., Genard, M., Lobit, P., Mbeguie, A. M. D., and Bugaud, C. (2013). What controls fleshy fruit acidity? a review of malate and citrate accumulation in fruit cells. *J. Exp. Bot.* 64 (6), 1451–1469. doi: 10.1093/jxb/ert035

Fait, A., Fromm, H., Walter, D., Galili, G., and Fernie, A. R. (2008). Highway or byway: the metabolic role of the GABA shunt in plants. *Trends Plant Sci.* 13 (1), 14–19. doi: 10.1016/j.tplants.2007.10.005

Fernie, A. R., and Martinoia, E. (2009). Malate. jack of all trades or master of a few? *Phytochemistry* 70 (7), 828–832. doi: 10.1016/j.phytochem.2009.04.023

Gao, Y., Kan, C., Wan, C., Chen, C., Chen, M., and Chen, J. (2018). Effects of hot air treatment and chitosan coating on citric acid metabolism in ponkan fruit during cold storage. *PloS One* 13 (11), e0206585. doi: 10.1371/journal.pone.0206585

Gibson, L., Rupasinghe, H. P., Forney, C. F., and Eaton, L. (2013). Characterization of changes in polyphenols, antioxidant capacity and physico-chemical parameters during lowbush blueberry fruit ripening. *Antioxid. (Basel).* 2 (4), 216–229. doi: 10.3390/antiox2040216

Giné Bordonaba, J., and Terry, L. A. (2010). Manipulating the taste-related composition of strawberry fruits (*Fragaria×ananassa*) from different cultivars using deficit irrigation. *Food Chem.* 122 (4), 1020–1026. doi: 10.1016/j.foodchem.2010.03.060

Guo, L., Liu, Y., Luo, L., Hussain, S. B., Bai, Y., and Alam, S. M. (2020). Comparative metabolites and citrate-degrading enzymes activities in citrus fruits reveal the role of balance between ACL and cyt-ACO in metabolite conversions. *Plants (Basel).* 9 (3), 350. doi: 10.3390/plants9030350

Habibi, F., Ramezanian, A., Guillén, F., Serrano, M., and Valero, D. (2020). Blood oranges maintain bioactive compounds and nutritional quality by postharvest treatments with γ-aminobutyric acid, methyl jasmonate or methyl salicylate during cold storage. *Food Chem.* 306, 125634. doi: 10.1016/j.foodchem.2019.125634

Huang, X. Y., Wang, C. K., Zhao, Y. W., Sun, C. H., and Hu, D. G. (2021). Mechanisms and regulation of organic acid accumulation in plant vacuoles. *Hortic. Res.* 8 (1), 227. doi: 10.1038/s41438-021-00702-z

Jiang, B., Liu, R., Fang, X., Tong, C., Chen, H., and Gao, H. (2022). Effects of salicylic acid treatment on fruit quality and wax composition of blueberry (*Vaccinium virgatum* ait). *Food Chem.* 368, 130757. doi: 10.1016/j.foodchem.2021.130757

Kalt, W., and McDonald, J. E. (1996). Chemical composition of lowbush blueberry cultivars. *J. Am. Soc. Hortic. Sci.* 121 (1), 142–146. doi: 10.21273/jashs.121.1.142

Kumari, P., Barman, K., Patel, V. B., Siddiqui, M. W., and Kole, B. (2015). Reducing postharvest pericarp browning and preserving health promoting compounds of litchi fruit by combination treatment of salicylic acid and chitosan. *Sci. Hortic.* 197, 555–563. doi: 10.1016/j.scienta.2015.10.017

Liao, H., LIN, X., Du, J., Peng, J., and Zhou, K. (2022). Transcriptomic analysis reveals key genes regulating organic acid synthesis and accumulation in the pulp of *Litchi chinensis* sonn. cv. feizixiao. *Sci. Hortic.* 303, 111220. doi: 10.1016/j.scienta.2022.111220

Li, X., Li, C., Sun, J., and Jackson, A. (2020). Dynamic changes of enzymes involved in sugar and organic acid level modification during blueberry fruit maturation. *Food Chem.* 309, 125617. doi: 10.1016/j.foodchem.2019.125617

Liu, R., Wang, Y., Qin, G., and Tian, S. (2016). Molecular basis of 1-methylcyclopropene regulating organic acid metabolism in apple fruit during storage. *Postharvest. Biol. Technol.* 117, 57–63. doi: 10.1016/j.postharvbio.2016.02.001

Livak, K. J., and Schmittgen, T. D. (2001). Analysis of relative gene expression data using real-time quantitative PCR and the $2^{-\Delta\Delta CT}$ method. *Methods* 25 (4), 402–408. doi: 10.1006/meth.2001.1262

Mark, K. E., Filmore, I. M., and James, R. B. (1994). Unique organic acid profile of rabbiteye vs. highbush blueberries. *Hortscience.* 29 (4), 321–323. doi: 10.21273/hortsci.29.4.321

Millaleo, R., Alvear, M., Aguilera, P., González-Villagra, J., de la Luz Mora, M., Alberdi, M., et al. (2019). Mn Toxicity differentially affects physiological and biochemical features in highbush blueberry (*Vaccinium corymbosum* l.) cultivars. *J. Soil Sci. Plant Nutr.* 20 (3), 795–805. doi: 10.1007/s42729-019-00166-0

Nguyen, C. T. T., Lee, J. H., and Tran, P.-T. (2021). Accumulation of sugars and associated gene expression in highbush blueberries differ by cultivar, ripening stage, and storage temperature. *J. Berry. Res.* 11 (3), 511–527. doi: 10.3233/jbr-210748

Perotti, V. E., Figueroa, C. M., Andreo, C. S., Iglesias, A. A., and Podesta, F. E. (2010). Cloning, expression, purification and physical and kinetic characterization of the phosphoenolpyruvate carboxylase from orange (*Citrus sinensis osbeck* var. Valencia) fruit juice sacs. *Plant Sci.* 179 (5), 527–535. doi: 10.1016/j.plantsci.2010.08.003

Rachappanavar, V., Padiyal, A., Sharma, J. K., and Gupta, S. K. (2022). Plant hormone-mediated stress regulation responses in fruit crops- a review. *Sci. Hortic.* 304, 111302. doi: 10.1016/j.scienta.2022.111302

Sheng, L., Shen, D., Luo, Y., Sun, X., Wang, J., Luo, T., et al. (2017). Exogenous γ-aminobutyric acid treatment affects citrate and amino acid accumulation to improve fruit quality and storage performance of postharvest citrus fruit. *Food Chem.* 216, 138–145. doi: 10.1016/j.foodchem.2016.08.024

Smrke, T., Cvelbar Weber, N., Veberic, R., Hudina, M., and Jakopic, J. (2021). Modified atmospheric CO_2 levels for maintenance of fruit weight and nutritional quality upon long-term storage in blueberry (*Vaccinium corymbosum* l.) 'Liberty'. *Horticulturae* 7 (11), 478. doi: 10.3390/horticulturae7110478

Wang, X. Y., Wang, P., Qi, Y. P., Zhou, C. P., Yang, L. T., Liao, X. Y., et al. (2014). Effects of granulation on organic acid metabolism and its relation to mineral elements in *Citrus grandis* juice sacs. *Food Chem.* 145, 984–990. doi: 10.1016/j.foodchem.2013.09.021

Wang, S., Zhou, Y., Luo, W., Deng, L., Yao, S., and Zeng, K. (2020). Primary metabolites analysis of induced citrus fruit disease resistance upon treatment with oligochitosan, salicylic acid and *Pichia membranaefaciens*. *Biol. Control.* 148, 104289. doi: 10.1016/j.biocontrol.2020.104289

Wu, J., Fan, J., Li, Q., Jia, L., Xu, L., Wu, X., et al. (2022). Variation of organic acids in mature fruits of 193 pear (*Pyrus* spp.) cultivars. *J. Food Compos. Anal.* 109, 104483. doi: 10.1016/j.jfca.2022.104483

Xu, F., Liu, S., Liu, Y., and Wang, S. (2021). Effect of mechanical vibration on postharvest quality and volatile compounds of blueberry fruit. *Food Chem.* 349, 129216. doi: 10.1016/j.foodchem.2021.129216

Yang, C., Duan, W., Xie, K., Ren, C., Zhu, C., Chen, K., et al. (2020). Effect of salicylic acid treatment on sensory quality, flavor-related chemicals and gene expression in peach fruit after cold storage. *Postharvest. Biol. Technol.* 161, 111089. doi: 10.1016/j.postharvbio.2019.111089

Yang, W., Kang, J., Liu, Y., Guo, M., and Chen, G. (2022). Effect of salicylic acid treatment on antioxidant capacity and endogenous hormones in winter jujube during shelf life. *Food Chem.* 397, 133788. doi: 10.1016/j.foodchem.2022.133788

Yan, L., Zheng, H., Liu, W., Liu, C., Jin, T., Liu, S., et al. (2021). UV-C treatment enhances organic acids and GABA accumulation in tomato fruits during storage. *Food Chem.* 338, 128126. doi: 10.1016/j.foodchem.2020.128126

Yao, Y., Li, M., Liu, Z., You, C., Wang, D., Zhai, H., et al. (2009). Molecular cloning of three malic acid related genes *MdPEPC*, *MdVHA-a*, *MdcyME* and their expression analysis in apple fruits. *Sci. Hortic.* 122 (3), 404–408. doi: 10.1016/j.scienta.2009.05.033

Zhang, Y., Li, S., Deng, M., Gui, R., Liu, Y., Chen, X., et al. (2022). Blue light combined with salicylic acid treatment maintained the postharvest quality of strawberry fruit during refrigerated storage. *Food Chem.: X.* 15, 100384. doi: 10.1016/j.fochx.2022.100384

Zhang, J., Nie, J.-y., Li, J., Zhang, H., Li, Y., Farooq, S., et al. (2020). Evaluation of sugar and organic acid composition and their levels in highbush blueberries from two regions of China. *J. Integr. Agric.* 19 (9), 2352–2361. doi: 10.1016/s2095-3119(20)63236-1

Zheng, B., Zhao, L., Jiang, X., Cherono, S., Liu, J., Ogutu, C., et al. (2021). Assessment of organic acid accumulation and its related genes in peach. *Food Chem.* 334, 127567. doi: 10.1016/j.foodchem.2020.127567

Zhu, J., Li, C., Fan, Y., Qu, L., Huang, R., Liu, J., et al. (2022). γ-aminobutyric acid regulates mitochondrial energy metabolism and organic acids metabolism in apples during postharvest ripening. *Postharvest. Biol. Technol.* 186, 111846. doi: 10.1016/j.postharvbio.2022.111846

frontiers | Frontiers in Plant Science

TYPE Original Research
PUBLISHED 25 October 2022
DOI 10.3389/fpls.2022.1014532

OPEN ACCESS

EDITED BY
Zhenfeng Yang,
Zhejiang Wanli University, China

REVIEWED BY
Zhengke Zhang,
Hainan University, China
Jemaa Essemine,
Partner Institute for Computational Biology, China

*CORRESPONDENCE
António Teixeira
antonio.teixeira@bio.uminho.pt
Henrique Noronha
henriquenoronha@bio.uminho.pt

SPECIALTY SECTION
This article was submitted to Crop and Product Physiology, a section of the journal Frontiers in Plant Science

RECEIVED 08 August 2022
ACCEPTED 21 September 2022
PUBLISHED 25 October 2022

CITATION
Teixeira A, Noronha H, Sebastiana M, Fortes AM and Gerós H (2022) A proteomic analysis shows the stimulation of light reactions and inhibition of the Calvin cycle in the skin chloroplasts of ripe red grape berries.
Front. Plant Sci. 13:1014532.
doi: 10.3389/fpls.2022.1014532

A proteomic analysis shows the stimulation of light reactions and inhibition of the Calvin cycle in the skin chloroplasts of ripe red grape berries

António Teixeira[1]*, Henrique Noronha[1]*, Mónica Sebastiana[2], Ana Margarida Fortes[2] and Hernâni Gerós[1]

[1]Centre of Molecular and Environmental Biology (CBMA), Department of Biology, University of Minho, Braga, Portugal, [2]BioISI – Instituto de Biosistemas e Ciências Integrativas, Faculdade de Ciências, Universidade de Lisboa, Lisbon, Portugal

The role of photosynthesis in fruits still challenges scientists. This is especially true in the case of mature grape berries of red varieties lined by an anthocyanin-enriched exocarp (skin) almost impermeable to gases. Although chlorophylls are degraded and replaced by carotenoids in several fruits, available evidence suggests that they may persist in red grapes at maturity. In the present study, chloroplasts were isolated from the skin of red grape berries (cv. Vinhão) to measure chlorophyll levels and the organelle proteome. The results showed that chloroplasts (and chlorophylls) are maintained in ripe berries masked by anthocyanin accumulation and that the proteome of chloroplasts from green and mature berries is distinct. Several proteins of the light reactions significantly accumulated in chloroplasts at the mature stage including those of light-harvesting complexes of photosystems I (PSI) and II (PSII), redox chain, and ATP synthase, while chloroplasts at the green stage accumulated more proteins involved in the Calvin cycle and the biosynthesis of amino acids, including precursors of secondary metabolism. Taken together, results suggest that although chloroplasts are more involved in biosynthetic reactions in green berries, at the mature stage, they may provide ATP for cell maintenance and metabolism or even O2 to feed the respiratory demand of inner tissues.

KEYWORDS

grape berry skin, chloroplasts, proteomics, photosynthesis, *Vitis vinifera*

Introduction

In higher plants, whether photosynthesis can occur in sink organs is still a matter of debate. Fruit photosynthesis has been studied in coffee, peas, soybeans, avocados, oranges, apples, and grape berries (Quebedeaux and Chollet, 1975; Atkins et al., 1977; Blanke and Lenz, 1989; Lopez et al., 2000; Aschan and Pfanz, 2003; Breia et al., 2013; Garrido et al., 2018), where it may contribute additional organic carbon to plant growth (Aschan and Pfanz, 2003), O_2 for respiration, and secondary metabolites biosynthesis (Rolletschek et al., 2003; Breia et al., 2013; Garrido et al., 2018). It could even refix CO_2 produced during mitochondrial respiration (Blanke and Lenz, 1989). Nonetheless, the role of photosynthesis in fruits is far from being completely understood.

Grape berries are composed of different tissues and cell layers with distinct anatomical characteristics and biochemical profiles that play distinct roles during development and ripening. The exocarp (or skin) is formed by an epidermis covered with an outer waxy cuticle and a hypodermis that has up to 17 layers of collenchymatous cells (Considine and Knox, 1979; Hardie et al., 1996; Breia et al., 2013). Early observations suggested that ripe berries have no stomata (Pratt, 1971), but recent scanning electron microscopy showed very few yet functional stomata in young berries and wax-filled stomata in older berries (Rogiers et al., 2004). Nonetheless, depending on the cultivar, the abundance of stomata in young berries may be 100-fold less than in the abaxial epidermis of a typical leaf (Blanke and Leyhe, 1988; Blanke and Lenz, 1989; Rogiers et al., 2011). In young fruits, stomata are as sensitive in leaves and regulate the rate of CO_2 exchange to a certain extent, while in the ripening fruit, the cuticular component and mostly unregulated lenticels dominate the diffusive resistance to CO_2 (Aschan and Pfanz, 2003). The gradual disappearance of stomata and/or the development of an impermeable waxy cuticle during development results in an internal environment characterized by high CO_2 and low O_2 levels (Blanke and Leyhe, 1987; Blanke and Leyhe, 1988).

In contrast to the planar morphology of leaves, the large volumetry of fruits, especially fleshy fruits, imposes physical constraints on light penetration into the inner tissues and restricts the photic zone to the outermost layers (Breia et al., 2013). Light transmission through the skin of *Vitis* berries was reported to reach 47% of the incident photon flux density and only up to 2% reaches the innermost regions (Aschan and Pfanz, 2003). A clear tissue-specific distribution pattern of photosynthetic competence was observed in the white grape berries from cv. Alvarinho (Breia et al., 2013). The exocarp revealed the highest photosynthetic capacity and the lowest susceptibility to photoinhibition. Meanwhile, low fluorescence signals and photochemical competence were found in the mesocarp. Recent studies of the same variety have shown that the photosynthetic activity of the exocarp was responsive to low and high light microclimate intensity differences in the canopy (Garrido et al., 2019). Because chlorophyll pigments are kept during the transition to the mature stage, although in lower amounts than in green berries (Giovanelli and Brenna, 2007; Kamffer et al., 2010), the accumulation of anthocyanins accounts for the change in color in red varieties. This is the case for Merlot, where the amount of photosynthetic chlorophyll pigments decreases from 19 to 10 μg/berry fresh weight (FW). Contrarily, chlorophylls are replaced by carotenoids during the ripening of tomatoes (Bean et al., 1963; Stiles, 1982; Blanke and Lenz, 1989), thus, fruit metabolism changes from partially photosynthetic (12 to 39 μg *chl* g FW^{-1} chlorophyll) at the green stage to truly heterotrophic at the mature stage (Lytovchenko et al., 2011). This transition appears to be coupled with a decline in the expression and enzymatic activities associated with carbon assimilation (Lytovchenko et al., 2011).

Hints at the grape berries' photosynthetic competence during development and ripening have been provided at the gene and protein levels in whole berries, berry pulp, and skin. In general, transcripts encoding proteins associated with photosynthesis-related functions are strongly expressed during phase I of berry development (Terrier et al., 2005; Waters et al., 2005; Deluc et al., 2007; Grimplet et al., 2007; Dal Santo et al., 2013; Ghan et al., 2017), while genes encoding Calvin cycle enzymes such as glyceraldehyde-3-phosphate dehydrogenase (GAPDH), phosphoribulokinase (PRK), transketolase (TK), and small subunits of ribulose biphosphate carboxylase/oxygenase (RuBisCO) are highly expressed during phase I and then decline during phase III of berry development (Waters et al., 2005; Deluc et al., 2007). Analysis of gene expression in detached skins (Grimplet et al., 2007; Ghan et al., 2017) reveals a higher proportion of transcripts encoding proteins with functions related to photosynthesis and carbon assimilation compared to pulp (Grimplet et al., 2007), but this proportion decreases in late-ripening berries (Ghan et al., 2017).

Compared to gene expression studies, literature addressing photosynthesis in grape berries through proteomic approaches is much less abundant. In the skin of Cabernet Sauvignon berries, proteins involved in photosynthesis and carbohydrate metabolism were found overly accumulated at the beginning of color change, while those involved in energy and general metabolism decreased from the onset of ripening to the end of color change (Deytieux et al., 2007). Interestingly, pivotal proteins involved in photosynthesis were detected in the skin in higher amounts than in the pulp of ripe berries of Cabernet Sauvignon (Grimplet et al., 2009), including several light-harvesting components (chlorophyll *a*/*b*-binding proteins, photosystem II (PSII) components, oxygen-evolving enhancer protein 1) and enzymes involved in carbon fixation like the large subunit of RuBisCO.

In the present study, we wanted to clarify whether chloroplasts are kept in the anthocyanin-rich skin of mature

red grape berries, where they may contribute to fruit metabolism by providing organic carbon, energy, or reducing power, as well as act as precursors for ripening-related pathways that start in that organelle. To address this hypothesis, plastids from green and mature grape exocarp were purified from cv. Vinhão (an important Portuguese red variety) for proteomic analysis. From a total of 4,852 proteins identified in the skin of chloroplastidial fractions, 1,053 entries were assigned to the chloroplast by bioinformatic tools, and 268 chloroplastic proteins were differentially accumulated between the green and mature phases. The results revealed that several proteins of the light reactions significantly accumulated in the skin chloroplasts at the mature stage, in parallel with a strong decrease in proteins involved in the reduction of $NADP^+$ to NADPH and in the biosynthetic reactions of the Calvin cycle.

Materials and methods

Plant material

Grape berries from the red cv. 'Vinhão' were collected in 2019 in a Portuguese ampelographic collection (Estaçaço Vitivinícola Amândio Galhano, N41°48′55.55′′/W8°24′38.07′′), located in the controlled appellation (DOC - Denominação de Origem Controlada) region of Vinhos Verdes in the northwest region of Portugal. Thirty-three-year-old vines were trained and spur-pruned on an ascendant simple cordon system. The soil was Cambic Umbrisol and acidic with low levels of phosphorous and potassium, rich in nitrogen, with low mineral colloids and high fertility at the first layer. Grape berries were sampled over four consecutive days at the late green (E-L 34) and mature (E-L 38) stages (Coombe, 1995) from 48 grapevines (12 grapevines per biological replicate) and transported to the laboratory in cooled containers. The exocarp of the berries was carefully separated from the mesocarp and used for plastid purification (Figure 1). From each vine, the seventh leaf from the apex was collected to ensure that measurements conducted on different dates correspond to leaves at a similar development stage.

Plastid purification from the skin of grape berries

Exocarp tissues from 120 berries per replicate were homogenized in 200 ml of ice-cold extraction buffer (150

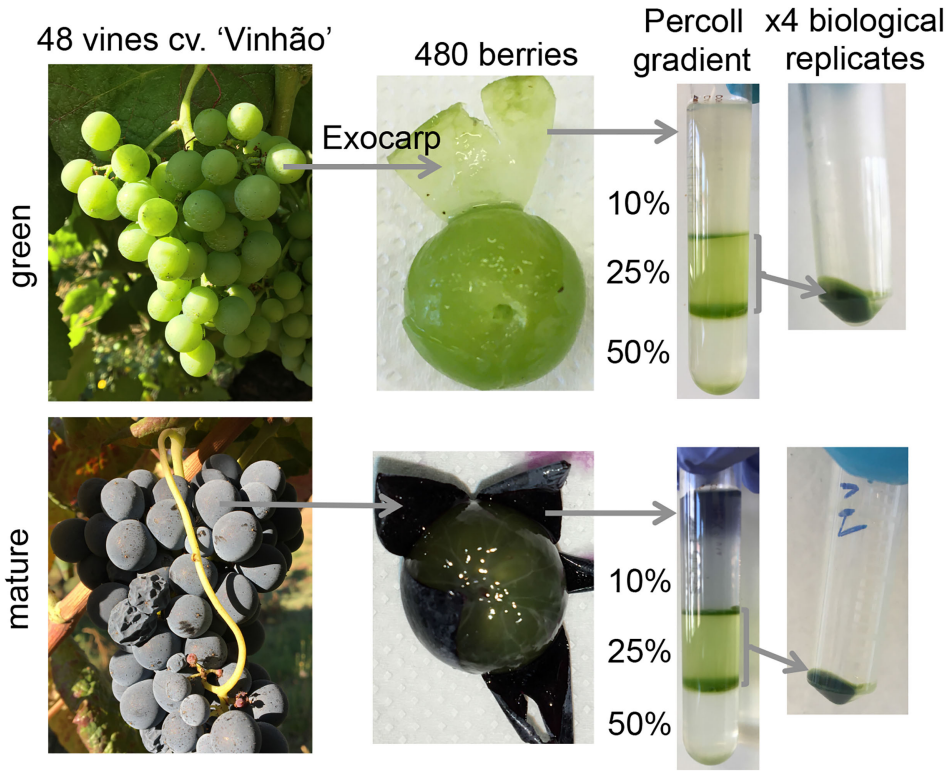

FIGURE 1
Plastid purification from the exocarp of Vitis vinifera cv. Vinhão at green (E-L 34) and mature (E-L 38) developmental stages.

mMof Tris-HC1, pH 8.2, 5 mM of $MgCl_2$, 5 mM of Ethylenediaminetetraacetic acid (EDTA), 500 mM of sorbitol, 2 mM of DL-Dithiothreitol (DTT), 0.5% of bovine serum albumin, and 2 mm of Phenylmethylsulfonyl fluoride (PMSF) in a Waring Blender (type 7012G) Waring Commercial Laboratory Blender (Waring Laboratories, Torrington, Conn., U.S.A. 2 × 7 s, maximum speed) (Figure 1). The homogenate was filtered through two layers of a 100-μm nylon mesh, transferred to 50-ml Falcon tubes, and centrifuged at 1,620×*g* for 10 min at 4°C (Eppendorf 5804R). The resulting crude organelle fraction was resuspended in 20 ml of the purification buffer (50 mM of Tris-HC1, pH 8.0, 1 mM of $MgCl_2$, 1 mM of EDTA, 330 mM of sorbitol, 2 mM of DTT, 0.1% of Bovine Serum Albumin (BSA), and 2 mM of PMSF) and centrifuged at 150×*g* for 5 min at 4°C. The supernatant was recovered and centrifuged at 3,000×*g* for 10 min at 4°C; the pellet was resuspended in 5 ml of the purification buffer and layered to the top of 12 ml of discontinuous Percoll gradients (4 ml of 50%, 4 ml of 25%, 4 ml of 10% Percoll, dissolved in a purification buffer without BSA). The gradients were centrifuged at 4,500×*g* at 4°C for 10 min (A-4-44 rotor, Eppendorf 5804R centrifuge with medium acceleration and low deacceleration). The two middle bands (50%–25% and 25%–10% interfaces) that contained intact plastids were collected and washed twice in a purification buffer without BSA and centrifuged at 4,500×*g* at 4°C for 5 min to remove the Percoll gradients. The plastid pellet was finally resuspended in 1 ml of the purification buffer lacking BSA and centrifuged at 4,500×*g* at 4°C for 10 min, and the sediment was flash frozen in liquid nitrogen for proteomic analysis and chlorophyll quantification.

Chlorophyll quantification

Chlorophyll quantification was performed accordingly with minor modifications (Lichtenthaler and Wellburn, 1983). Briefly, the above-described frozen pellets of the plastidial fraction were freeze-dried (Christ Alpha 2-4 LD Plus lyophilizer) and dissolved in 0.4 ml of acetone. Grapevine leaves and green berry skin were pulverized in liquid N_2, and ±50 mg of each tissue was extracted in 1 ml of acetone. The samples were centrifuged at 14,000×*g*, and the absorbance of the supernatants was measured at 661 and 644 nm. Chlorophylls *a* and *b* and *a* + *b* were quantified using the following equations: $Ca = 11.24A_{661} - 2.04A_{644}$; $Cb = 20.13A_{644} - 4.19A_{661}$, $Ca + b = 7.05A_{644} + 18.09A_{644}$, where the different values correspond to the absorption coefficients of acetone-specific pigments and A corresponds to the absorbance obtained in each wavelength. Values were normalized by the total protein amount that was determined spectrophotometrically by Bradford assay (Bradford, 1976).

Sample preparation for proteomic analysis

Proteins were extracted from purified plastid preparations according to the procedure described by Tamburino et al. (2017). In brief, isolated plastid pellets were resuspended in a buffer containing 100 mM of Tris-HCl (pH 7.5), 100 mM of EDTA, 50 mM of Borax, 50 mM of ascorbic acid, 2% (w/v) of 2-mercaptoethanol, 30% (w/v) of sucrose, and 1 mM of PMSF. Samples were vortexed for 5 min, and then an equal volume of Tris-saturated phenol (pH 8.0) was added before vortexing again for 10 min. Samples were centrifuged at 15,000×*g* for 15 min at 4°C, and the upper phenolic phase was transferred to a new tube. Five Volumes of ammonium sulfate-saturated methanol were added to precipitate proteins, and samples were incubated at -20°C for 48 h. Samples were centrifuged at 15,000×*g* for 30 min at 4°C, and the protein pellets were washed once in methanol (ice-cold) and three times with acetone (ice-cold). In each washing step, protein pellets were centrifuged at 15,000×*g* for 15 min at 4°C. The final pellets were air-dried at room temperature, resuspended in a buffer containing 0.1 M of Tris-HCl (pH 8.5) and 1% of Sodium dodecyl sulfate (SDS), and stored at -20°C. The protein concentration was determined in subsamples again resuspended in 0.1 M of Tris-HCl (pH 8.5) and 0.1% of SDS, using the Bradford reagent (Bradford, 1976) and BSA as the standard.

The samples (10 μg) were reduced with dithiothreitol (100 mM for 60 min at 37°C) and alkylated in the dark with iodoacetamide (5 μmol for 20 min at 25°C). The resulting protein extract was washed with 2 M of urea with 100 mM of Tris-HCl and then with 50 mM of ammonium bicarbonate for digestion with endoproteinase Lys-C (1:10 w:w at 37°C, o/n, Wako, cat # 129-02541) and then for trypsin digestion (1:10 w:w for 8 h at 37°C, Promega cat # V5113) following (Wiśniewski and Mann, 2009) using the FASP Protein Digestion Kit procedure. After digestion, the peptide mix was acidified with formic acid and desalted with a MicroSpin C18 column (The Nest Group,Inc. Ipswich, USA) prior to LC-MS/MS analysis.

Chromatographic and mass spectrometric analysis

Samples were analyzed using an Orbitrap Eclipse mass spectrometer (Thermo Fisher Scientific, San Jose, CA, USA) coupled with an EASY-nLC 1200 (Thermo Fisher Scientific, Proxeon, Odense, Denmark). Peptides were loaded directly onto the analytical column and were separated by reversed-phase chromatography using a 50-cm column with an inner diameter of 75 μm and a spectrometer packed with 2 μm of C18 particles (Thermo Scientific, San Jose, CA, USA).

Chromatographic gradients started at 95% of buffer A and 5% of buffer B, with a flow rate of 300 nl/min for 5 min, and gradually increased to 25% of buffer B and 75% of buffer A in 79 min and then to 40% of buffer B and 60% of buffer A in 11 min. After each analysis, the column was washed for 10 min with 10% of buffer A and 90% of buffer B. Buffer A was 0.1% formic acid in water. Buffer B was 0.1% formic acid in 80% acetonitrile.

The mass spectrometer was operated in a positive ionization mode with the nanospray voltage set at 2.4 kV and the source temperature at 305°C. The acquisition was performed in data-dependent acquisition (DDA) mode. Full MS scans with one micro scan at a resolution of 120,000 were used over a mass range of 350–1,400 m/z in the Orbitrap mass analyzer. Auto gain control (AGC) was set to 'auto' and charge state filtering disqualifying singly charged peptides was activated. In each cycle of data-dependent acquisition analysis, following each survey scan, the most intense ions above a threshold ion count of 10,000 were selected for fragmentation. The number of selected precursor ions for fragmentation was determined by the "Top Speed" acquisition algorithm and a dynamic exclusion of 60 s. Fragment ion spectra were produced *via* high-energy collision dissociation (HCD) at a normalized collision energy of 28%, and they were acquired in the ion trap mass analyzer. AGC was set to 2E4, and an isolation window of 0.7 m/z and a maximum injection time of 12 ms were used.

Digested bovine serum albumin (New England Biolabs cat # P8108S) was analyzed between each sample to avoid sample carryover and to assure the stability of the instrument, and QCloud (Chiva et al., 2018) was used to control the instrument's longitudinal performance during the project.

Data analysis

Acquired spectra were analyzed using the Proteome Discoverer software suite (v. 2.4, Thermo Fisher Scientific) and the Mascot search engine (v. 2.6, Matrix Science) (Perkins et al., 1999). The data were sought against a *Vitis vinifera* database (Canaguier et al., 2017), a list of common contaminants, and all the corresponding decoy entries (Beer et al., 2017). For peptide identification, a precursor ion mass tolerance of 7 ppm was used for MS1 level, trypsin was chosen as the enzyme, and up to three missed cleavages were allowed. The fragment ion's mass tolerance was set to 0.5 Da for the MS2 spectra. Oxidation of methionine and N-terminal protein acetylation were used as variable modifications whereas carbamidomethylation on cysteines was set as a fixed modification. The false discovery rate (FDR) in peptide identification was set to a maximum of 5%.

Peptide quantification data were retrieved from the precursor ion area detector node of the Proteome Discoverer (v. 2.4) using 2 ppm mass tolerance for the peptide extracted ion current (XIC). The values normalized by total peptide amount were used to calculate the protein fold change *p*-values and the adjusted *p*-values of mature berry vs. green berry (Figure S1).

Subcellular localization of proteins from their amino acid sequences

From the normalized data set, proteins present in at least three of the four replicates for each condition were retrieved and filtered using the *Vitis vinifera* proteome database universe (Canaguier et al., 2017) with the Qiime tool (v. 1.9.1, from the Galaxy project) (Afgan et al., 2018). The retrieved sequences were analyzed with three online bioinformatic tools (DeepLoc 1.0, Predotar, and TargetP 2.0), to recognize sorting signals and predict the subcellular localization of proteins from their amino acid sequences (Small et al., 2004; Almagro Armenteros et al., 2017; Salvatore et al., 2019). Principal component analysis (PCA) was performed in R software (v. 4.1.0) using the mixOmics package (v. 6.16.3) (Rohart et al., 2017).

The differentially accumulated proteins (DAP) that had been sorted into plastid/chloroplast by the three tools were retrieved for further analysis.

Gene Ontology term, Kyoto Encyclopedia of Genes and Genomes pathway enrichment, MapMan analysis, and protein interaction network

To perform a Gene Ontology (GO) term enrichment and KEGG (Kyoto Encyclopedia of Genes and Genomes) pathway enrichment analysis on the predicted chloroplastidial DAPs, the *Vitis vinifera* ENSEMBL annotations of DAPs were converted to ENTREZID *via* the "bitr" function from ClusterProfiler package (v. 4.0) (Yu et al., 2012). The ID was used as a reference for the search of the GO terms. To match the ID to the GO terms in a fast and reliable way, an SQLite annotation data package was created using a modified version of the popular AnnotationForge R package, adapted to work with plant genomes (Carlson and Pagès, 2019), according to the R script published by (Santos et al., 2020).

The biological process (BP), molecular function (MF), and cellular component (CC) of the GO-term enrichment analysis of chloroplastidial proteins were performed separately for both the less and more accumulated proteins with the "enrichGO" function from the R package clusterProfiler, with the DAPs as the universe, Benjamini-Hochberg for the pAdjustMethod, pvalueCutoff = 0.05, qvalueCutoff = 0.05, and the above-described annotation-created data package as OrgDb. Due to the hierarchical nature of gene ontologies, a semantic reduction of GO terms using the "rrvgo" R package (v. 1.4.0) was performed, grouping similar terms based on their semantic similarity. For both the less and more accumulated proteins, the similarity matrices of the biological process, molecular

function, and cellular component's GO terms were created using the "Rel" (Relevance) as the method and "org.At.tair.db" (*Arabidopsis thaliana*) as a reference database. Similarity matrices were reduced using a threshold of 0.7. KEGG pathway enrichment was performed with the "enrichKEGG" function from the clusterProfiler, using the same conditions of GO enrichment with *Vitis vinifera* (vvi) as an organism.

The chloroplastidial DAPs were categorized with MapMan standalone software (v. 3.5.1) (Thimm et al., 2004), and the results were visualized in MapMan pathways.

To construct a protein–protein interaction (PPI) network for a protein module, we used the open-source database of known and predicted protein interactions STRING (v. 11.5, http://string-db.org) (Szklarczyk et al., 2019). The function protein query was used under the criteria for linkage with experiments, co-expression, databases, experiments, and textmining, with the default settings (medium confidence score: 0.400, network depth: 0 interactions). The resulting network and protein description files were used to produce the networks in Cytoscape 3.8.2 (http://www.cytoscape.org). Additionally, we used clusterMaker2 (v. 1.2.1) to perform Markov clustering (MCL) (Enright et al., 2002) of the protein network to obtain the subnetworks.

Results

Chloroplasts and chlorophylls in the skin of green and mature berries

The chlorophyll content in the skin tissues of green berries was three- and two-fold lower than in leaves sampled at the green and mature stages of berry development, respectively (Figure 2A). Purified plastids from the skin tissues of green and mature berries were observed under a fluorescence microscope (Figure 2B), and the corresponding chlorophyll content is depicted in Figure 2A. Unlike the tomato fruit that undergoes a physiological transition during ripening on the differentiation of photosynthetically active chloroplasts into chromoplasts, Figure 2 shows that in the mature berries of red grapes, the transition in color is not associated with a loss of chloroplasts in the skin, and the plastid content in total chlorophylls also did not decrease (Figure 2A). In green berries, the amount of total chlorophyll per mg^{-1} of protein increased from 28 in skin tissues to 200 in purified plastids, which shows a good degree of chloroplast enrichment during purification.

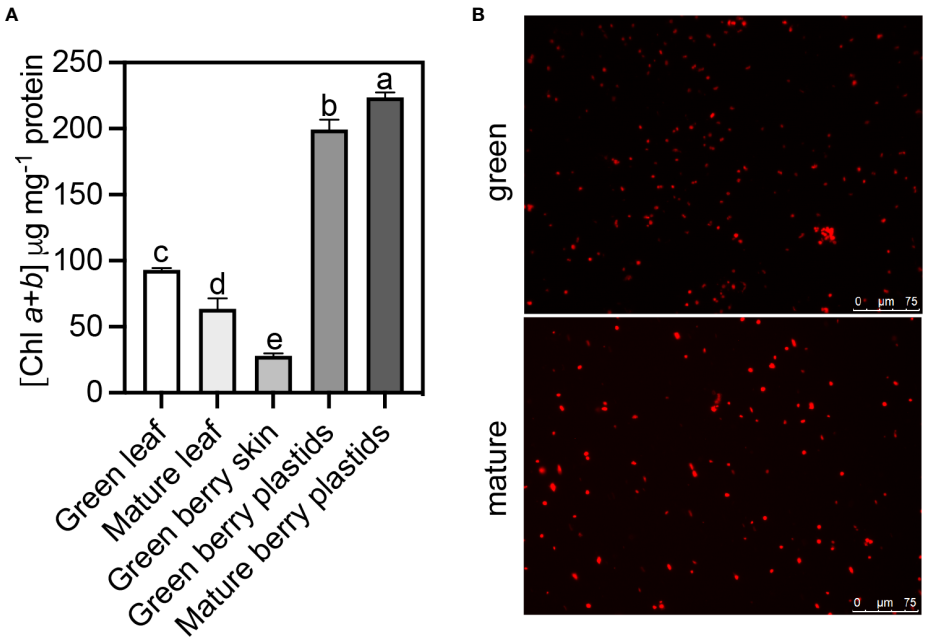

FIGURE 2
Plastid purification from the exocarp of Vitis vinifera cv. Vinhão at green (E-L 34) and mature (E-L 38) developmental stages. **(A)** Total chlorophyll content (a + b) present in grapevine leaves at the green and mature stages, in berry skin at the green stage, and in the purified plastids of grape berry skin at the green and mature stages of development and **(B)** visualized by fluorescence microscopy. One-way ANOVA with Tukey's post-hoc test; different letters denote statistical differences between bars.

Gene Ontology annotation of differentially accumulated proteins identified in the skin chloroplasts

A total of 4,852 proteins present in at least three of four replicates were identified in the chloroplastidial fractions from the skins of both green and mature berries (Supplementary Table 1). The prediction of their subcellular localization was analyzed with three different algorithm tools. These tools revealed that a large part of the identified proteins localizes unequivocally in the chloroplast (Supplementary Figure 2). The concatenated results from the three sub-cellular bioinformatic tools showed 1,053 entries of chloroplastidial proteins (Supplementary Figure 2A–C; Supplementary Table 2), of which 268 were differentially accumulated ($|\log2FC| > 1.0$; adjusted p-value ≤ 0.05) in the skin of both green and mature berries (Supplementary Table 3). The principal component analysis of the differentially accumulated chloroplastidial proteins showed a clear separation indicating that the proteome of this organelle is distinct between the green and mature developmental stages (Supplementary Figure 2D).

The Gene Ontology enrichment analysis of chloroplastidial differentially accumulated proteins was conducted to assess which biological processes of the three sub-ontologies (biological process, BP; molecular function, MF; and cellular component, CC) incurred significant changes in the transition between the green and mature stages (Figure 3). The GO terms enriched in chloroplastidial proteins from the skins of green berries (negative LogFC values) were the BP sub-ontology for photosynthesis, with the highest number of enriched terms, followed by the "generation of precursor metabolites and energy." The MF sub-ontology also showed more enriched terms at the green stage. Regarding CC, chloroplastidial proteins revealed similar enriched GO terms at both developmental stages. In the chloroplasts from the skins of mature berries, the photosynthesis, generation of precursor metabolites and energy, and organophosphate biosynthetic process were the most enriched terms for the BP sub-ontology;

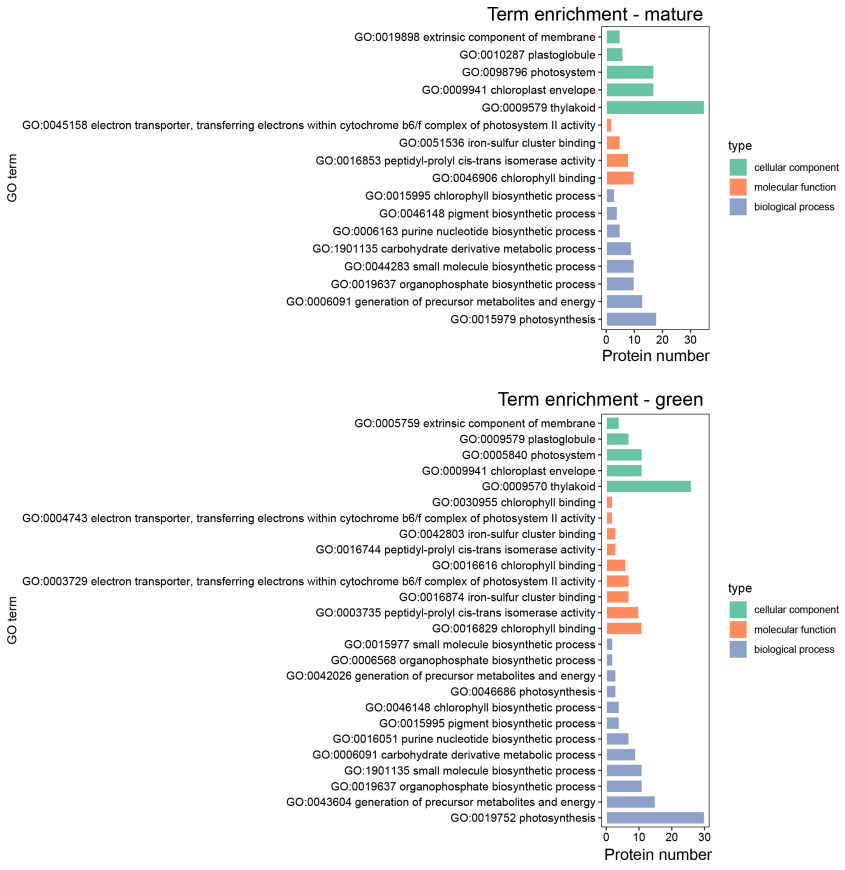

FIGURE 3
Gene Ontology (GO) term enrichment of differentially accumulated proteins (DAPs) in the chloroplasts of Vitis vinifera cv. Vinhão exocarp at the mature stage (E-L 38) vs. the green stage (E-L 34).

chlorophyll-binding was the most enriched term for the MF sub-ontology; lastly, the thylakoid and chloroplast envelope or photosystem were the most enriched terms for the CC sub-ontology.

Kyoto Encyclopedia of Genes and Genomes and MapMan annotation of differentially accumulated proteins identified in the skin chloroplasts

Five enriched KEGG pathways were assigned to proteins more accumulated in the skin chloroplasts at the mature stage, including photosynthesis and photosynthesis-antenna pathways. The proteins contributing to the enrichment of the photosynthesis pathway are involved in photosystem repair, synthesis of ATP, or electron transfer between the photosystems, while the proteins contributing to the enrichment of the photosynthesis-antenna pathway are involved in light-harvesting and delivery of excitation energy to photosystems (Supplementary Table 4).

In the skin chloroplasts at the green stage, the biosynthesis of amino acids was the most enriched pathway (28 proteins) with proteins such as ribulose-phosphate 3-epimerase, involved in the initial steps of amino acid biosynthesis, or chorismate mutase and tryptophan synthase, involved in the biosynthesis of the aromatic amino acids phenylalanine, tyrosine, and tryptophan. Only two of the seven DAPs found as involved in the aromatic amino acid biosynthetic pathway were more accumulated at the mature stage. The carbon metabolism biosynthetic pathway was the second most-enriched pathway in the green stage with proteins such as malate dehydrogenase, involved in the tricarboxylic acid biosynthesis; GAPDH, involved in the glycolysis; or transaldolase, involved in the biosynthesis of pentose phosphate (Figure 4).

MapMan analysis (Figure 5A) showed that several proteins of the light reactions significantly accumulated in the skin

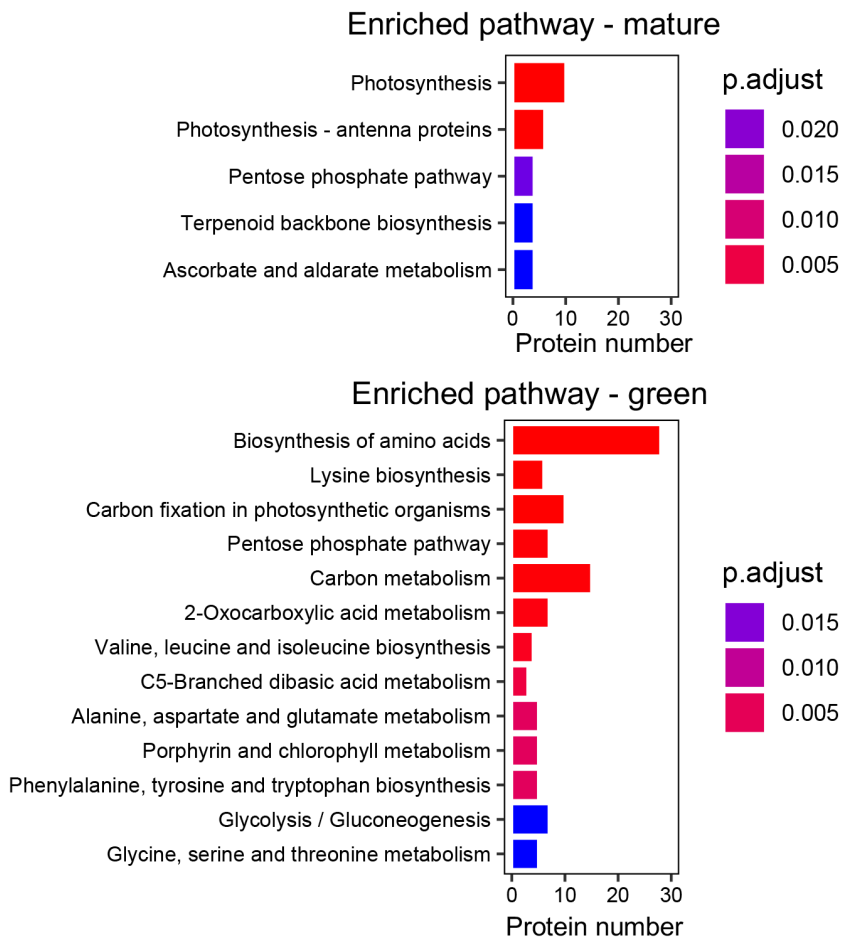

FIGURE 4
Kyoto Encyclopedia of Genes and Genomes (KEGG) pathway enrichment of differentially accumulated proteins (DAPs) in the chloroplasts of Vitis vinifera cv. Vinhão exocarp at the mature stage (E-L 38) vs. the green stage (E-L 34).

chloroplasts at the mature stage (up to 11-fold): six proteins from the photosystem II light-harvesting complex (LHC) (bin 1.1.1.1); nine PSII polypeptide subunits (bin 1.1.1.2); five proteins from the redox chain, including two from cytochrome *b6/f* (bin 1.1.3); and two polypeptide subunit proteins of photosystem I (PSI). ATP synthase beta and delta subunits (bins 1.1.4.2 and 1.1.4.7) also accumulated at the mature stage, suggesting that energy production is stimulated. Conversely, two ferredoxin-$NADP^+$ reductase proteins (bin 1.1.5.2) were less abundant (up to a 21-fold change decrease from the green to mature stage), suggesting that the production of NADPH that feeds the Calvin cycle is downregulated at this stage. Correspondingly, proteins involved in biosynthetic reactions in the chloroplast, such as ribulose phosphate carboxylases (bin 1.3.1), RuBisCO-interacting proteins (bins 1.2.13 and 1.3.2), glyceraldehyde-3-phosphate dehydrogenases (bin 1.3.4), fructose-biphosphate aldolases (bin. 1.3.6), sedoheptulase-1,7-biphosphatase (bin 1.3.9), ribulose-5-phosphate-3-epimerase (bin 1.3.11), and PRK (bin 1.3.12) also decreased from the green to the mature stage up to 19-fold (Figure 5B). Remarkably, transketolase (bin 1.3.8), decreased 600-fold. Some chloroplastidial proteins like phosphoglycolate phosphatase (bin 1.2.1), glycolate oxidase (bin 1.2.2), glycine cleavage (1.2.4.2/.4), and hydroxypyruvate reductase (bin 1.2.6) (Supplementary Table 5) related to photorespiration also accumulated more at the green stage.

Protein–protein interaction network of mapped chloroplastidial differentially expressed proteins

String network analysis was performed to reveal the PPI network of 40 significant DAPs assigned to the chloroplast (Figure 6A, Supplementary Table 6). The PPI network (default score filter of 0.4) of 40 nodes and 374 edges revealed

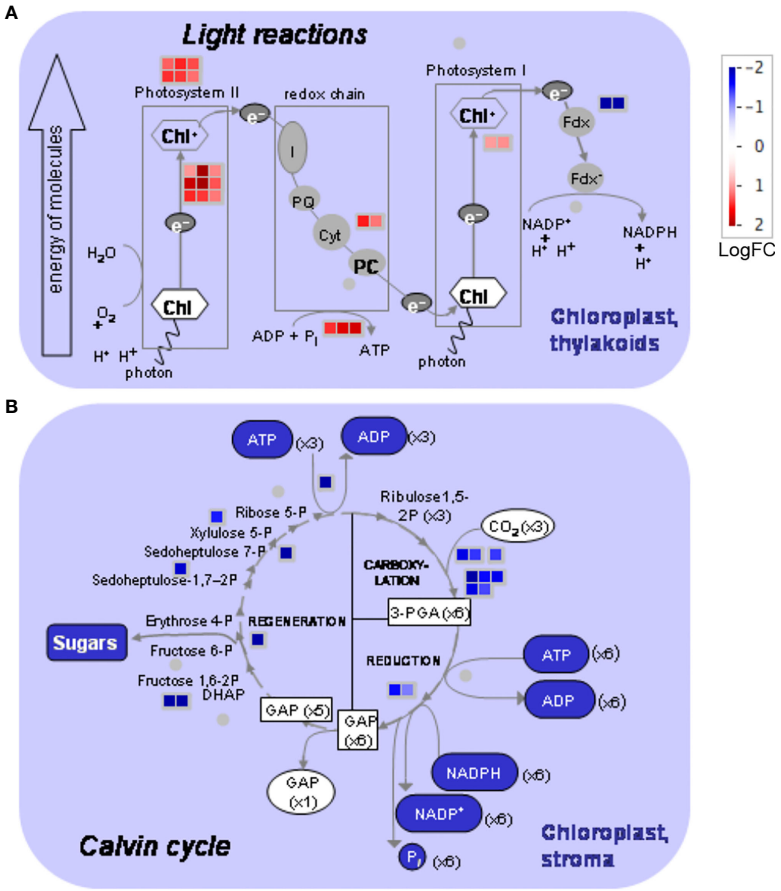

FIGURE 5
MapMan photosynthesis overview obtained from differentially accumulated proteins (DAPs) in the chloroplasts of Vitis vinifera cv. Vinhão exocarp at the mature stage (E-L 38) vs. the green stage (E-L 34). **(A)** Light reactions and **(B)** Calvin cycle. In red, proteins more accumulated in mature berries; in blue, proteins more accumulated in green berries. The MapMan figure was made by MapMan Version 3.6.0rc1 (https://mapman.gabipd.org/).

significantly more interactions than expected (expected number of edges = 21, p-value <1.0e-^{16}), indicating that the proteins are at least partially biologically connected as a group. The network showed a functional association tight cluster of co-expressed proteins assigned to light reaction photosystems and the Calvin cycle (Figure 6A). The proteins highly accumulated at the mature stage (red circles) and were involved in light reaction photosystems (green nodes) co-expressed with the ones involved in the Calvin cycle reactions (gray nodes) and more accumulated at the green stage (blue circles). Several of these co-expression interactions were experimentally obtained (pink edges) (Figure 6A). The network subset limited to "physical interaction" revealed three modules where proteins with the same expression pattern correlated (Figure 6B). Photosystem II LHC-II proteins correlated with PSII polypeptide subunits, while PSI polypeptide subunits correlated with the light reaction ATP synthases. The proteins involved in the Calvin cycle were classified into two clusters: fructose biphosphate aldolases that correlated with GAPDH and PRK in one cluster (light gray nodes) and RuBisCO subunits that correlated with another cluster (dark gray nodes). These clusters reveal a strong physical interaction among proteins with similar expression patterns.

Discussion

The skin of the green and mature grape berries is rich in chloroplasts

A continuous decrease in chlorophyll content during ripening has been observed in different grape berries of red varieties (Giovanelli and Brenna, 2007; Kamffer et al., 2010). In whole cv. Merlot berries, the amount of chlorophyll pigments decreased from 19 to 10 µg/berry fresh weight, but in our study that targeted the skin of the red cv. Vinhão grapes, the number of chloroplasts and their relative content in chlorophylls remained high at the mature stage (Figures 2A, B). Conversely, a decrease in chlorophyll content was observed in the leaves of cv. Vinhão, in agreement with previous results (Bertamini and Nedunchezhian, 2002; Casanova-Gascón et al., 2018). The degradation of chlorophyll in leaves can result from a

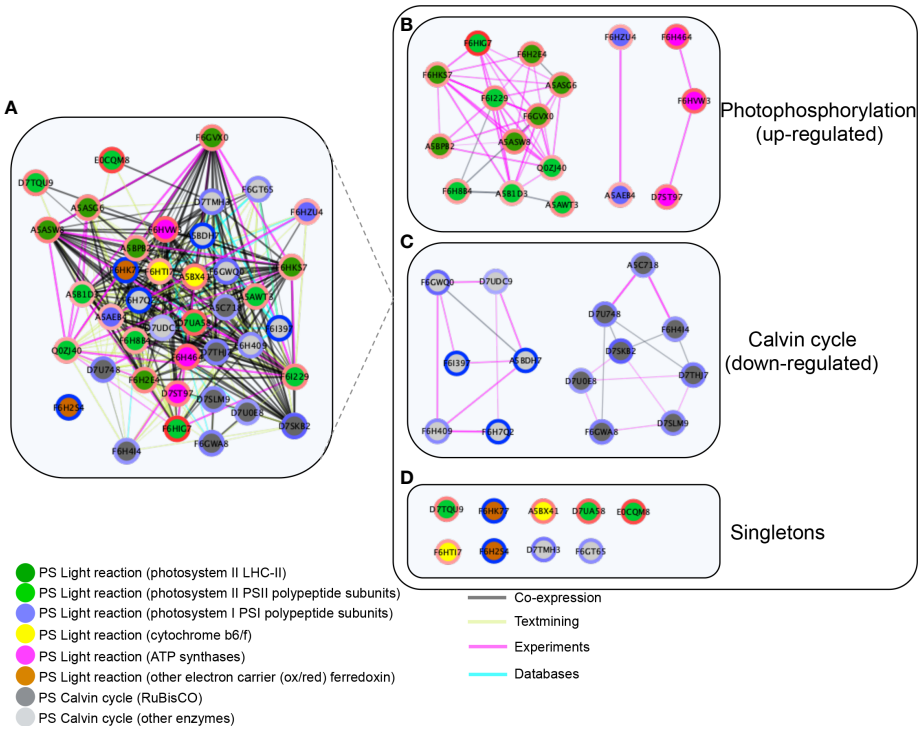

FIGURE 6
Network protein–protein interactions of differentially accumulated proteins (DAPs) in the chloroplasts of Vitis vinifera cv. Vinhão exocarp at the mature stage (E-L 38) vs. the green stage (E-L 34). **(A)** Functional association cluster network. Network limited to "physical interaction" clusters. **(B)** Photophosphorylation-involved proteins; **(C)** Calvin cycle involved proteins, and **(D)** Singletons. LogFC ratios of protein abundance between the green and mature stages were mapped around the nodes using a blue (negative) and red (positive) color gradient. The inner nodes were colored according to the MapMan bins. The edge scores are visualized by co-expression (black), co-occurrence (blue), experiments (pink), and textmining (light green). The network clusters were obtained using Markov clustering on the STRING network of proteins from panel **(A)**. Proteins were named according to their canonical name.

genetically programmed senescence process and in response to environmental factors such as temperature and low humidity (Casanova-Gascón et al., 2018). Our results thus strongly suggest that the skin of mature berries of cv. Vinhão is rich in chloroplasts and anthocyanins, which are known to accumulate after veraison. Supporting histological studies showed a clear colocalization of chlorophylls and anthocyanins in the skin of ripe berries of cv. Pinot Noir (Agati et al., 2007). Because anthocyanins protect the photosynthetic machinery in leaves (Gould, 2004; Lo Piccolo et al., 2018) and may retard leaf senescence (Lo Piccolo et al., 2018), one cannot discard that they may have similar protective roles in the berry skin of red cultivars. Hence, unlike tomatoes, where chlorophylls are replaced by carotenoids upon maturation, grape skins are likely to be kept photosynthetically competent until maturity. It is worth noting that chloroplast proteomes are different between the green and mature berries, further suggesting that photosynthesis in the skins of mature berries from cv. Vinhão may have relevant physiological roles, as discussed below (Figures 3, 4).

Light reactions are stimulated and the Calvin cycle is inhibited in the skin of mature grape berries

The observation that several proteins of the light reactions were significantly accumulated in the skin chloroplasts at the mature stage, and that the transition from the green to mature stage was accompanied by a strong decrease in proteins involved in the biosynthetic reactions of the Calvin cycle, suggested that the skin of mature red berries has a major role in ATP production through the stimulation of cyclic electron flow. Among the 22 highly accumulated proteins in the skin of mature berries, we cite those from the antenna complex, PSII, PSI, cytochrome *b6/f*, and ATP synthase. It is worth noting that two ferredoxin-NADP$^+$ reductase proteins were underrepresented up to 20.5-fold at the mature stage, suggesting that the reducing power of ferredoxin is being used to produce ATP through ATP synthase rather than NADPH for the Calvin cycle (Figures 5, 7). The STRING network subset limited to 'physical interaction', evidenced well-defined modules were proteins with the same accumulation pattern, like (Figure 6). Conversely, among the 17 impoverished proteins from the Calvin cycle are those from RuBisCO and other key enzymes: ribulose-5-phosphate-3-epimerase, PRK, glyceraldehyde 3-phosphate, fructose 1,6-bisphosphate aldolase, sedoheptulose 1,7-bisphosphatase, and transketolase (600-fold). This strongly suggests that the synthesis of organic C compounds is switched off during the transition from the green to mature stage in the skin of the mature berries.

As reported in the Introduction, few studies have addressed the proteome of the grape berry as it relates to photosynthesis, energy, and C metabolism (Deytieux et al., 2007; Grimplet et al., 2009). To the best of our knowledge, we report here the first proteomics study on isolated chloroplast in the grape berry skin. In a proteomics approach conducted in detached skins of Cabernet Sauvignon, proteins involved in photosynthesis and carbohydrate metabolism, including RuBisCO and TK (found as impoverished at the mature stage in the present study), were

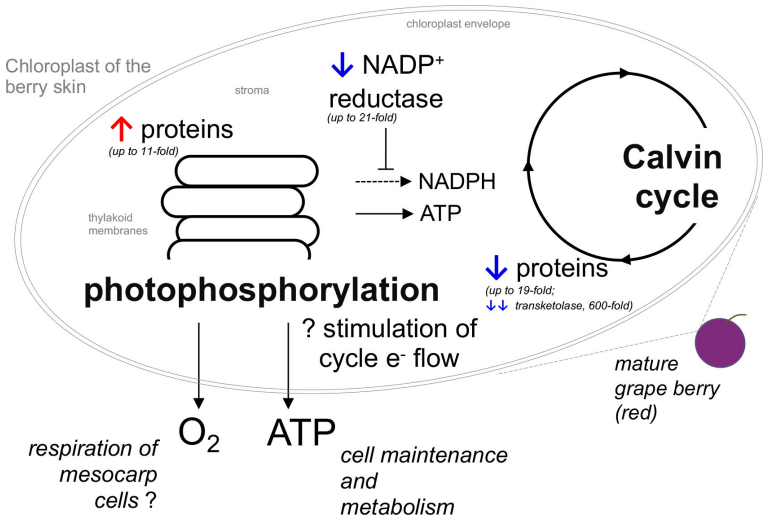

FIGURE 7
Illustration of the proposed changes in photosynthesis occurring in the chloroplasts of the skin of red grape berries during the transition from the green (E-L 34) to the mature stage (E-L 38). Blue and red arrows denote that the proteins are overrepresented (↑) or underrepresented (↓) at the mature stage when compared to the green stage.

identified as being overrepresented at the beginning of color change, while the end of color change was characterized by an overrepresentation of proteins involved in anthocyanin synthesis (Deytieux et al., 2007). In the present study, the proteins detected in the isolated chloroplasts of the skin, including chlorophyll *a*/*b* proteins, plastidic fructose-bis-phosphate aldolase (upregulated at the mature stage in the present study), and RuBisCO subunits or TK (found as impoverished at the mature stage in the present study), were also found to be more abundant in the skin than in the pulp of mature Cabernet Sauvignon berries (Grimplet et al., 2009), but their results are more difficult to compare with those of the present study. Specific changes in protein amounts throughout the berry formation and ripening processes were described in Muscat Hamburg (Martínez-Esteso et al., 2013), but that study was performed on berry mesocarp and thus, is not directly comparable to our study. Nonetheless, and in agreement with our results, a decrease in the abundance profiles up to the mature stage of several Calvin cycle proteins, including PRK and RuBisCO, was observed (in the mesocarp), with a sharper decrease observed from the green stage to the onset of veraison. This may suggest that the impoverishment of C-fixing proteins from the green to the mature stage occurs both in the pulp and in the skin of berries. However, contrary to the observations reported here, light reaction proteins, which displayed a moderate increase in abundance during the grape berry's first growth period (EL-31 to EL-33), were impoverished during fruit ripening (Martínez-Esteso et al., 2013).

Previous transcriptomics approaches performed on berries of Corvina, Shiraz, Cabernet Sauvignon, Cabernet Franc, Merlot, Pinot Noir, Chardonnay, Sauvignon Blanc, and Semillon (in whole berries and skins) during development and ripening (Terrier et al., 2005; Waters et al., 2005; Deluc et al., 2007; Grimplet et al., 2007; Sweetman et al., 2012; Dal Santo et al., 2013; Ghan et al., 2017) showed that transcript-encoding proteins associated with photosynthesis-related functions, including photoreaction centers I (PCI) and II (PCII), chlorophyll *a*/*b*-binding proteins, photosystem II core complex proteins (enriched in the skin of mature berries in the present study) were strongly expressed during the phase I of berry development. On the other hand, genes encoding Calvin cycle enzymes such as glyceraldehyde-3-phosphate dehydrogenase, PRK, TK as well as RuBisCO small subunit (impoverished in the skin of mature berries in the present study) were highly expressed during phase I and then declined during phase III of berry development. In accordance with the present study, a strong decrease in proteins involved in biosynthetic reactions of the Calvin cycle was observed (Figure 5). Results from transcriptomic analysis in the detached skins of mature berries showed that this tissue is particularly rich in several light-harvesting and photosystem components, including cytochrome C6A and light-harvesting complex II type I, and that transcript abundance decreased in late ripening stages (Grimplet et al., 2007; Ghan et al., 2017).

Amino acid metabolism is tightly linked to energy and carbohydrate metabolism, protein synthesis, and secondary metabolism. In grapevines, the amino acids isoleucine, leucine, phenylalanine, and valine are precursors of higher alcohols and esters, which contribute to the desirable aromas in wines, while phenylalanine is the main substrate in the phenylpropanoid pathway that leads to the synthesis of important organoleptic compounds such as anthocyanins and stilbenes (Garde-Cerdán and Ancín-Azpilicueta, 2008). The present study showed that 28 proteins of the amino acid biosynthetic pathways were strongly impoverished from the green to the mature stage. A study on cv. Nebbiolo Lampia also showed a decrease in three enzymes of amino acid metabolism from the green to the mature stages (Giribaldi et al., 2007), while a proteome study on cv. Barbera grape skins showed an increase in the expression of seven proteins (10% of the functional categories) of the amino acid metabolism from veraison to the mature stage, from which five decreased until they reached full maturity (Negri et al., 2008).

The high respiratory demand of the berry tissues, particularly at the mature stage, entrains O_2 deficiency that was recently reported to be associated with cell death in cv. Shiraz (Tilbrook and Tyerman, 2008; Xiao et al., 2019). This is particularly relevant in the context of ongoing climate warming because higher temperatures increase the respiratory rate of tissues. In this regard, the light reactions of chloroplasts on the skin are likely an important source of O_2 for berry tissues when gas exchange is very limited at the mature stage, but they may also provide ATP and/or reduce power to other physiological processes, including anthocyanin synthesis, which is an energy-demanding process (Figure 7).

Conclusions

Chloroplasts are key plant cell organelles where pivotal biochemical reactions occur, but their role in fruit ripening in several species is still far from being fully understood. For the first time, the present subcellular proteomic study focused on the analysis of chloroplastic proteins from the skin of green and mature grape berries. Our data confirmed that chloroplasts are present in mature berries but are masked by anthocyanins that accumulate during fruit maturation. Skin chloroplasts from green and mature berries have distinct proteomes that suggest different physiological roles; while proteins of the Calvin cycle are upregulated at the green stage, proteins involved in energy-yielding reactions predominate in mature red berries.

Data availability statement

The mass spectrometry proteomics data have been deposited to the ProteomeXchange Consortium via the PRIDE partner repository with the dataset identifier PXD037346.

Author contributions

AT: methodology, investigation, formal analysis, writing of the original draft, and review and editing of the draft. HN: conceptualization, methodology, investigation, formal analysis, and review and editing of the draft. MS: methodology, investigation, and review and editing of the draft. AF: conceptualization, methodology, review and editing of the draft. HG: conceptualization, resources, funding acquisition, writing of the original draft, and review and editing of the draft. All authors contributed to the article and approved the submitted version.

Funding

This work was supported by the "Contratos-Programa" UIDB/04046/2020 and UIDB/ BIA/04050/2020 and by the core research project BerryPlastid (PTDC/BIA-FBT/28165/ 2017 and POCI-01-0145 - FEDER-028165). AT was supported by a postdoctoral researcher contract/position within the project BerryPlastid. HN was supported by an FCT postdoctoral grant (SFRH/BPD/115518/ 2016). AF was supported by UIDB/04046/ 2020 and UIDP/ 04046/2020 (to BioISI) Centre Grants from FCT, Portugal. MS was supported by FCT in the context of Norma Transitória — DL57/2016/CP[12345/2018]/CT[2475]. This work benefited from networking activities within the CoLAB Vines & Wines.

Conflict of interest

The authors declare that the research was conducted in the absence of any commercial or financial relationships that could be construed as a potential conflict of interest.

Publisher's note

All claims expressed in this article are solely those of the authors and do not necessarily represent those of their affiliated organizations, or those of the publisher, the editors and the reviewers. Any product that may be evaluated in this article, or claim that may be made by its manufacturer, is not guaranteed or endorsed by the publisher.

Supplementary material

The Supplementary Material for this article can be found online at: https://www.frontiersin.org/articles/10.3389/fpls.2022.1014532/full#supplementary-material

References

Afgan, E., Baker, D., Batut, B., Van Den Beek, M., Bouvier, D., Čech, M., et al. (2018). The galaxy platform for accessible, reproducible and collaborative biomedical analyses: 2018 update. *Nucleic Acids Res.* 46, W537–W544. doi: 10.1093/nar/gky379

Agati, G., Meyer, S., Matteini, P., and Cerovic, Z. G. (2007). *Assessment of anthocyanins in grape (Vitis vinifera L.) berries using a noninvasive chloro*.

Almagro Armenteros, J. J., Sønderby, C. K., Sønderby, S. K., Nielsen, H., and Winther, O. (2017). DeepLoc: prediction of protein subcellular localization using deep learning. *Bioinformatics* 33, 3387–3395. doi: 10.1093/bioinformatics/btx431

Aschan, G., and Pfanz, H. (2003). Non-foliar photosynthesis–a strategy of additional carbon acquisition. *Flora-Morphol Distribution Funct. Ecol. Plants* 198, 81–97. doi: 10.1078/0367-2530-00080

Atkins, C. A., Kuo, J., Pate, J. S., Flinn, A. M., and Steele, T. W. (1977). Photosynthetic pod wall of pea (Pisum sativum l.) distribution of carbon dioxide-fixing enzymes in relation to pod structure. *Plant Physiol.* 60, 779–786. doi: 10.1104/pp.60.5.779

Bean, R. C., Porter, G., and Barr, B. K. (1963). Photosynthesis & respiration in developing fruits. III. variations in photosynthetic capacities during color change in citrus. *Plant Physiol.* 38, 285. doi: 10.1104/pp.38.3.285

Beer, L. A., Liu, P., Ky, B., Barnhart, K. T., and Speicher, D. W. (2017). Efficient quantitative comparisons of plasma proteomes using label-free analysis with MaxQuant. In:D. Greening and R. Simpson. (eds) *Serum/Plasma Proteomics. Methods in Molecular Biology* vol 1619 (New York, NY: Humana Press), 1619 339–352. doi: 10.1007/978-1-4939-7057-5_23

Bertamini, M., and Nedunchezhian, N. (2002). Leaf age effects on chlorophyll, rubisco, photosynthetic electron transport activities and thylakoid membrane protein in field grown grapevine leaves. *J. Plant Physiol.* 159, 799–803. doi: 10.1078/0176-1617-0597

Blanke, M. M., and Lenz, F. (1989). Fruit photosynthesis. *Plant Cell Environ.* 12, 31–46. doi: 10.1111/j.1365-3040.1989.tb01914.x

Blanke, M. M., and Leyhe, A. (1987). Stomatal activity of the grape berry cv. Riesling, müller-thurgau and ehrenfelser. *J. Plant Physiol.* 127, 451–460. doi: 10.1016/S0176-1617(87)80253-5

Blanke, M. M., and Leyhe, A. (1988). Stomatal and cuticular transpiration of the cap and berry of grape. *J. Plant Physiol.* 132, 250–253. doi: 10.1016/S0176-1617(88)80170-6

Bradford, M. M. (1976). A rapid and sensitive method for the quantitation of microgram quantities of protein utilizing the principle of protein-dye binding. *Analytical Biochem.* 72, 248–254. doi: 10.1016/0003-2697(76)90527-3

Breia, R., Vieira, S., da Silva, J. M., Geros, H., and Cunha, A. (2013). Mapping grape berry photosynthesis by chlorophyll fluorescence imaging: the effect of saturating pulse intensity in different tissues. *Photochem. Photobiol.* 89, 579–585. doi: 10.1111/php.12046

Canaguier, A., Grimplet, J., Di Gaspero, G., Scalabrin, S., Duchêne, E., Choisne, N., et al. (2017). A new version of the grapevine reference genome assembly (12X. v2) and of its annotation (VCost. v3). *Genomics Data* 14, 56. doi: 10.1016/j.gdata.2017.09.002

Carlson, M., and Pagès, H. (2019). AnnotationForge: Tools for building SQLite-based annotation data packages. *R Package version* 1.

Casanova-Gascón, J., Martín-Ramos, P., Martí-Dalmau, C., and Badía-Villas, D. (2018). Nutrients assimilation and chlorophyll contents for different grapevine varieties in calcareous soils in the somontano DO (Spain). *Beverages* 4, 90. doi: 10.3390/beverages4040090

Chiva, C., Olivella, R., Borras, E., Espadas, G., Pastor, O., Sole, A., et al. (2018). QCloud: A cloud-based quality control system for mass spectrometry-based proteomics laboratories. *PloS One* 13, e0189209. doi: 10.1371/journal.pone.0189209

Considine, J., and Knox, R. (1979). Development and histochemistry of the cells, cell walls, and cuticle of the dermal system of fruit of the grape, *Vitis vinifera* l. *Protoplasma* 99, 347–365. doi: 10.1007/BF01275807

Coombe, B. G. (1995). Growth stages of the grapevine: adoption of a system for identifying grapevine growth stages. *Aust. J. Grape Wine Res.* 1, 104–110. doi: 10.1111/j.1755-0238.1995.tb00086.x

Dal Santo, S., Tornielli, G. B., Zenoni, S., Fasoli, M., Farina, L., Anesi, A., et al. (2013). The plasticity of the grapevine berry transcriptome. *Genome Biol.* 14, 1–18. doi: 10.1186/gb-2013-14-6-r54

Deluc, L. G., Grimplet, J., Wheatley, M. D., Tillett, R. L., Quilici, D. R., Osborne, C., et al. (2007). Transcriptomic and metabolite analyses of Cabernet sauvignon grape berry development. *BMC Genomics* 8, 1–42. doi: 10.1186/1471-2164-8-429

Deytieux, C., Geny, L., Lapaillerie, D., Claverol, S., Bonneu, M., and Doneche, B. (2007). Proteome analysis of grape skins during ripening. *J. Exp. Bot.* 58, 1851–1862. doi: 10.1093/jxb/erm049

Enright, A. J., Van Dongen, S., and Ouzounis, C. A. (2002). An efficient algorithm for large-scale detection of protein families. *Nucleic Acids Res.* 30, 1575–1584. doi: 10.1093/nar/30.7.1575

Garde-Cerdán, T., and Ancín-Azpilicueta, C. (2008). Effect of the addition of different quantities of amino acids to nitrogen-deficient must on the formation of esters, alcohols, and acids during wine alcoholic fermentation. *LWT-Food Sci. Technol.* 41, 501–510. doi: 10.1016/j.lwt.2007.03.018

Garrido, A., Breia, R., Serôdio, J., and Cunha, A. (2018). Impact of the light microclimate on photosynthetic activity of grape berry (*Vitis vinifera*): Insights for radiation absorption mitigations' measures. In: F. Alves, W. Leal Filho and U. Azeiteiro. (eds) *Theory and practice of climate adaptation. Climate Change Management*. (Cham: Springer), 419–441. doi: 10.1007/978-3-319-72874-2_24

Garrido, A., Serôdio, J., De Vos, R., Conde, A., and Cunha, A. (2019). Influence of foliar kaolin application and irrigation on photosynthetic activity of grape berries. *Agronomy* 9, 685. doi: 10.3390/agronomy9110685

Ghan, R., Petereit, J., Tillett, R. L., Schlauch, K. A., Toubiana, D., Fait, A., et al. (2017). The common transcriptional subnetworks of the grape berry skin in the late stages of ripening. *BMC Plant Biol.* 17, 1–21. doi: 10.1186/s12870-017-1043-1

Giovanelli, G., and Brenna, O. V. (2007). Evolution of some phenolic components, carotenoids and chlorophylls during ripening of three Italian grape varieties. *Eur. Food Res. Technol.* 225, 145–150. doi: 10.1007/s00217-006-0436-4

Giribaldi, M., Perugini, I., Sauvage, F., and Schubert, A. (2007). Analysis of protein changes during grape berry ripening by 2-DE and MALDI-TOF. *Proteomics* 7, 3154–3170. doi: 10.1002/pmic.200600974

Gould, K. S. (2004). Nature's Swiss army knife: the diverse protective roles of anthocyanins in leaves. *J. Biomed Biotechnol.* 2004, 314. doi: 10.1155/S1110724304406147

Grimplet, J., Deluc, L. G., Tillett, R. L., Wheatley, M. D., Schlauch, K. A., Cramer, G. R., et al. (2007). Tissue-specific mRNA expression profiling in grape berry tissues. *BMC Genomics* 8, 1–23. doi: 10.1186/1471-2164-8-187

Grimplet, J., Wheatley, M. D., Jouira, H. B., Deluc, L. G., Cramer, G. R., and Cushman, J. (2009). Proteomic and selected metabolite analysis of grape berry tissues under well-watered and water-deficit stress conditions. *C. Proteomics* 9, 2503–2528. doi: 10.1002/pmic.200800158

Hardie, W. J., O'brien, T., and Jaudzems, V. (1996). Morphology, anatomy and development of the pericarp after anthesis in grape, *Vitis vinifera* l. *Aust. J. Grape Wine Res.* 2, 97–142. doi: 10.1111/j.1755-0238.1996.tb00101.x

Kamffer, Z., Bindon, K. A., and Oberholster, A. (2010). Optimization of a method for the extraction and quantification of carotenoids and chlorophylls during ripening in grape berries (*Vitis vinifera* cv. merlot). *J. Agric. Food Chem.* 58, 6578–6586. doi: 10.1021/jf1004308

Lichtenthaler, H. K., and Wellburn, A. R. (1983). Determinations of total carotenoids and chlorophylls a and b of leaf extracts in different solvents. *Biochem Soc Trans* 11:591–592. doi: 10.1042/bst0110591

Lopez, Y., Riano, N., Mosquera, P., Cadavid, A., and Arcila, J. (2000). Activities of phosphoenolpyruvate carboxylase and ribulose-1, 5-bisphosphate carboxylase/oxygenase in leaves and fruit pericarp tissue of different coffee (Coffea sp.) genotypes. *Photosynthetica* 38, 215–220. doi: 10.1023/A:1007265715108

Lo Piccolo, E., Landi, M., Pellegrini, E., Agati, G., Giordano, C., Giordani, T., et al. (2018). Multiple consequences induced by epidermally-located anthocyanins in young, mature and senescent leaves of prunus. *Front. Plant Sci.* 9, 917. doi: 10.3389/fpls.2018.00917

Lytovchenko, A., Eickmeier, I., Pons, C., Osorio, S., Szecowka, M., Lehmberg, K., et al. (2011). Tomato fruit photosynthesis is seemingly unimportant in primary metabolism and ripening but plays a considerable role in seed development. *Plant Physiol.* 157, 1650–1663. doi: 10.1104/pp.111.186874

Martínez-Esteso, M. J., Vilella-Antón, M. T., Pedreño, M.Á., Valero, M. L., and Bru-Martínez, R. (2013). iTRAQ-based protein profiling provides insights into the central metabolism changes driving grape berry development and ripening. *BMC Plant Biol.* 13, 1–20. doi: 10.1186/1471-2229-13-167

Negri, A. S., Prinsi, B., Scienza, A., Morgutti, S., Cocucci, M., and Espen, L. (2008). Analysis of grape berry cell wall proteome: A comparative evaluation of extraction methods. *J. Plant Physiol.* 165, 1379–1389. doi: 10.1016/j.jplph.2007.10.011

Perkins, D. N., Pappin, D. J., Creasy, D. M., and Cottrell, J. S. (1999). Probability-based protein identification by searching sequence databases using mass spectrometry data. *ELECTROPHORESIS: Int. J.* 20, 3551–3567. doi: 10.1002/(SICI)1522-2683(19991201)20:18<3551::AID-ELPS3551>3.0.CO;2-2

Pratt, C. (1971). Reproductive anatomy in cultivated grapes-a review. *Am. J. Enol Viticult* 22, 92–109.

Quebedeaux, B., and Chollet, R. (1975). Growth and development of soybean (Glycine max [L.] merr.) pods: CO2 exchange and enzyme studies. *Plant Physiol.* 55, 745–748. doi: 10.1104/pp.55.4.745

Rogiers, S. Y., Hardie, W. J., and Smith, J. P. (2011). Stomatal density of grapevine leaves (*Vitis vinifera* l.) responds to soil temperature and atmospheric carbon dioxide. *Aust. J. Grape Wine Res.* 17, 147–152. doi: 10.1111/j.1755-0238.2011.00124.x

Rogiers, S. Y., Hatfield, J. M., Jaudzems, V. G., White, R. G., and Keller, M. (2004). Grape berry cv. Shiraz epicuticular wax and transpiration during ripening and preharvest weight loss. *Am. J. Enol Viticult* 55, 121–127. doi: 10.1111/j.1755-0238.2011.00124.x

Rohart, F., Gautier, B., Singh, A., and Lê Cao, K.-A. (2017). mixOmics: An r package for 'omics feature selection and multiple data integration. *PloS Comput. Biol.* 13, e1005752. doi: 10.1371/journal.pcbi.1005752

Rolletschek, H., Weber, H., and Borisjuk, L. (2003). Energy status and its control on embryogenesis of legumes. embryo photosynthesis contributes to oxygen supply and is coupled to biosynthetic fluxes. *Plant Physiol.* 132, 1196–1206. doi: 10.1104/pp.102.017376

Salvatore, M., Emanuelsson, O., Winther, O., von Heijne, G., Elofsson, A., and Nielsen, H. (2019). Detecting novel sequence signals in targeting peptides using deep learning. *bioRxiv*. 2019. doi: 10.1101/639203

Santos, B., Nascimento, R., Coelho, A. V., and Figueiredo, A. (2020). Grapevine–downy mildew rendezvous: Proteome analysis of the first hours of an incompatible interaction. *Plants* 9, 1498. doi: 10.3390/plants9111498

Small, I., Peeters, N., Legeai, F., and Lurin, C. (2004). Predotar: a tool for rapidly screening proteomes for n-terminal targeting sequences. *Proteomics* 4, 1581–1590. doi: 10.1002/pmic.200300776

Stiles, E. W. (1982). Fruit flags: two hypotheses. *Am. Nat.* 120, 500–509. doi: 10.1086/284007

Sweetman, C., Wong, D. C., Ford, C. M., and Drew, D. P. (2012). Transcriptome analysis at four developmental stages of grape berry (*Vitis vinifera* cv. Shiraz) provides insights into regulated and coordinated gene expression. *BMC Genomics* 13, 1–25. doi: 10.1186/1471-2164-13-691

Szklarczyk, D., Gable, A. L., Lyon, D., Junge, A., Wyder, S., Huerta-Cepas, J., et al. (2019). STRING v11: protein–protein association networks with increased coverage, supporting functional discovery in genome-wide experimental datasets. *Nucleic Acids Res.* 47, D607–D613. doi: 10.1093/nar/gky1131

Tamburino, R., Vitale, M., Ruggiero, A., Sassi, M., Sannino, L., Arena, S., et al. (2017). Chloroplast proteome response to drought stress and recovery in tomato (Solanum lycopersicum l.). *BMC Plant Biol.* 17, 1–14. doi: 10.1186/s12870-017-0971-0

Terrier, N., Glissant, D., Grimplet, J., Barrieu, F., Abbal, P., Couture, C., et al. (2005). Isogene specific oligo arrays reveal multifaceted changes in gene expression during grape berry (*Vitis vinifera* l.) development. *Planta* 222, 832–847. doi: 10.1007/s00425-005-0017-y

Thimm, O., Bläsing, O., Gibon, Y., Nagel, A., Meyer, S., Krüger, P., et al. (2004). MAPMAN: a user-driven tool to display genomics data sets onto diagrams of metabolic pathways and other biological processes. *Plant J.* 37, 914–939. doi: 10.1111/j.1365-313X.2004.02016.x

Tilbrook, J., and Tyerman, S. D. (2008). Cell death in grape berries: varietal differences linked to xylem pressure and berry weight loss. *Funct. Plant Biol.* 35, 173–184. doi: 10.1071/FP07278

Waters, D. L., Holton, T. A., Ablett, E. M., Lee, L. S., and Henry, R. J. (2005). cDNA microarray analysis of developing grape (*Vitis vinifera* cv. Shiraz) berry skin. *Funct. Integr. Genomics* 5, 40–58. doi: 10.1007/s10142-004-0124-z

Wiśniewski, J. R., and Mann, M. (2009). Reply to "Spin filter–based sample preparation for shotgun proteomics". *Nat. Methods* 6, 785–786. doi: 10.1038/nmeth1109-785b

Xiao, Z., Liao, S., Rogiers, S. Y., Sadras, V. O., and Tyerman, S, (2019). Are berries suffocating to death under high temperature and water stress? *D. Wine viticult J.*, 42–45.

Yu, G., Wang, L.-G., Han, Y., and He, Q.-Y. (2012). clusterProfiler: an r package for comparing biological themes among gene clusters. *Omics: J. Integr. Biol.* 16, 284–287. doi: 10.1089/omi.2011.0118

frontiers | Frontiers in Plant Science

TYPE Original Research
PUBLISHED 07 December 2022
DOI 10.3389/fpls.2022.1059979

OPEN ACCESS

EDITED BY
María Serrano,
Miguel Hernández University of Elche, Spain

REVIEWED BY
Gholamreza Gohari,
University of Maragheh, Iran
Mesbah Babalar,
University of Tehran, Iran

*CORRESPONDENCE
Zhenfeng Yang
yangzf@zwu.edu.cn

SPECIALTY SECTION
This article was submitted to Crop and Product Physiology, a section of the journal Frontiers in Plant Science

RECEIVED 02 October 2022
ACCEPTED 21 November 2022
PUBLISHED 07 December 2022

CITATION
Zhou C, Dong W, Jin S, Liu Q, Shi L, Cao S, Li S, Chen W and Yang Z (2022) γ-Aminobutyric acid treatment induced chilling tolerance in postharvest peach fruit by upregulating ascorbic acid and glutathione contents at the molecular level.
Front. Plant Sci. 13:1059979.
doi: 10.3389/fpls.2022.1059979

γ-Aminobutyric acid treatment induced chilling tolerance in postharvest peach fruit by upregulating ascorbic acid and glutathione contents at the molecular level

Chujiang Zhou[1,2], Wanqi Dong[2], Shuwan Jin[2], Qingli Liu[2], Liyu Shi[2], Shifeng Cao[2], Saisai Li[2], Wei Chen[2] and Zhenfeng Yang[2]*

[1]College of Food Science and Technology, Shanghai Ocean University, Shanghai, China, [2]College of Biological and Environmental Sciences, Zhejiang Wanli University, Ningbo, China

Peach fruit was treated with 5 mM γ-aminobutyric acid (GABA) to further investigate the mechanism by which GABA induced chilling tolerance. Here, we found that GABA not only inhibited the occurrence of chilling injury in peach fruit during cold storage but also maintained fruit quality. Most of the ascorbic acid (AsA) and glutathione (GSH) biosynthetic genes were up-regulated by GABA treatment, and their levels were increased accordingly, thus reducing chilling damage in treated peaches. Meanwhile, the increased transcript of genes in the AsA-GSH cycle by GABA treatment was also related to the induced tolerance against chilling. GABA treatment also increased the expression levels of several candidate ERF transcription factors involved in AsA and GSH biosynthesis. In conclusion, our study found that GABA reduced chilling injury in peach fruit during cold storage due to the higher AsA and GSH contents by positively regulating their modifying genes and candidate transcription factors.

KEYWORDS

γ-aminobutyric acid, ascorbic acid, glutathione, chilling injury, peach

Introduction

Peach (*Prunus persica* (L.) Batsch) is a typical climacteric fruit. Low-temperature storage can inhibit its respiratory and endogenous ethylene peak during postharvest storage, which slows the process of postharvest ripening and senescence (Mahmud et al., 2017). However, when exposed to unsuitable cold temperatures, peach fruit is highly

susceptible to chilling damage. Chilling symptoms such as fruit flocculation, flesh browning, and juice reduction can occur under low-temperature storage, resulting in loss of fruit flavor and texture, seriously affecting its edible quality and market economic value.

γ-Aminobutyric acid (GABA) is a naturally occurring amino acid in plants and animals (Nicolas and Hillel, 2004). In plants, GABA plays a role under stress conditions by regulating the activities of related enzymes or the synthesis of metabolites (Bao et al., 2015; Ramesh et al., 2017; Li et al., 2021). For instance, exogenous GABA inhibited chilling injury in tomatoes by scavenging reactive oxygen species (ROS) and increasing antioxidant enzyme activity (Malekzadeh, 2015). Wang et al. (2014a) found that exogenous GABA treatment induced resistance against chilling in melon by promoting polyamine synthesis Additionally, exogenous GABA treatment induced the synthesis of endogenous GABA in bananas (Wang et al., 2014c), persimmon (Niazi et al., 2021) and cucumber (Malekzadeh et al., 2017), thereby increasing the cold resistance and prolonging their low-temperature storage time. There are also many studies on GABA in peach fruit. For example, Aghdam et al. (2016) found that GABA can effectively maintain the content of ascorbic acid, total phenol, flavonoids, and other substances in peach fruit and the ability to eliminate free radicals. Recently, a study found that GABA can improve the cold resistance of peach fruits by promoting the methionine sulfoxide reductase thioredoxin reductase system (Jiao, 2022).

When plants are subjected to stress, ROS are produced rapidly, resulting in tissue damage (Baxte et al., 2014). A complete antioxidant system in plants can rapidly reduce the level of ROS to the average level. AsA and GSH are important antioxidants that can scavenge excess ROS and reduce damage caused by different stresses (Alscher et al., 1997; Song et al., 2016; Hasanuzzaman et al., 2019; Ma et al., 2019). Therefore, investigating the formation and regulation of AsA and GSH is of great significance in improving fruit quality and enhancing stress resistance in postharvest fruit.

Significant progress has been made in investigating the AsA biosynthetic pathway in plants. Four possible pathways of AsA biosynthesis in plants have been proposed. Among these pathways, the L-galactose pathway plays a leading role in plant AsA synthesis (Wheeler et al., 1998), while other pathways such as D-galacturonate, L- gluose and Myo-inositol supplement it (Agius et al., 2003; Lorence et al., 2004; Wolucka et al., 2005). All the genes encoding the enzymes involved in this pathway have been identified, including phosphomannomutase (PMM), GDP-D-mannose pyrophorylase (GMP), GDP-D-mannose-3',5'-heteroisomerase (GME), GDP-L-galactose phophorylase (GGP), L-galactose-1-phosphate phophoratase (GPP) and L-galactose dehydrogenase (GalDH). PMM and GMP catalyze the synthesis of GDP-D-mannose, providing a substrate for AsA synthesis. GME catalyzes the conversion of GDP-D-mannose to GDP-L-galactose, which is the first step of AsA biosynthesis at the glycoside level. GGP catalyzes GDP-L-galactose to produce GDP-L- galactose -1- phosphate (Wheeler et al., 1998), which is one of the vital catalytic enzymes in the L-galactose pathway. GalDH catalyzes L- galactose to produce L- galactose -1,4-lactone, one of the rate-limiting enzymes in the L-galactose pathway. The specific catalytic steps of the other three AsA synthetic pathways in plants are still at the stage of speculation because the enzyme genes in these pathways have not been fully identified except for inositol oxygenase (MXIO) and D-galactonic acid dehydrogenase (GalUR) (Wolucka and Van Montagu, 2003; Lorence et al., 2004).

GSH biosynthesis is mainly catalyzed by γ-glutamylcysteine ligase (GCS) and glutathione synthase (GS). First, L-glutamic acid and cysteine are catalyzed by GCS to synthesize γ-glutathione cysteine. Then, under the catalysis of glutathione synthase (GS), glycine is added to the C-terminus of γ-glutathione cysteine to produce glutathione.

Our previous study showed that GABA could inhibit chilling injury of peach fruit during cold storage (Shang et al., 2011; Yang et al., 2011). However, the transcriptional activity of genes involved in the metabolism of AsA and GSH remained unstudied. Therefore, this study further investigated the mechanism by which GABA induced cold tolerance in chilled peach fruit by influencing AsA and GSH levels at the molecular level. In addition, we also analyzed the expression of three ERF transcription factors that may be related to ASA-GSH metabolism.

Materials and methods

GABA treatment

Peach fruit (*Prunus. Persica* Batsch cv. Hujing) were harvested at commercial maturity (120 days after flowering) from experimental farm of Fenghua Peach Fruit Research Institute (Ningbo, China). The peaches were picked and transported to laboratory quickly and then selected in uniform size and randomly divided into two groups with sixty-six fruit in each group. The conforming and undamaged fruit were selected and randomly divided into two groups According to our previous study (Yang et al., 2011), the fruit in first group were immersed in a solution of 5 mM GABA for 20 min, while the other was immersed in water for 20 min as control. Afterwards, both groups of fruit was air-dried for approximately two hours and transfer to 4 °C stored for thirty-five days. Eight peaches from each sampling site in each group were frozen in liquid nitrogen and stored in an ultra-low temperature refrigerator after fruit firmness, total soluble solid (TSS) and relative electrical conductivity were determined. From three weeks of cold storage, another six peaches were taken at each sampling

point and transferred from 4 °C to 20 °C for three days to simulate the shelf environment and evaluated the chilling injury index. The whole experiment was repeated three times.

Determination of chilling injury index, fruit firmness, total soluble solid and relative electrical conductivity

The degree of chilling was visually assessed on the mesocarp surface, following a double cut parallel to the axial diameter. The extent of flesh browning was divided into four classes: 0, no browning; 1, browning covering <25% of the cut surface; 2, browning covering ≥25% but <50% of cut surface; 3, browning covering ≥50%. CI index was calculated using the following formula: Chilling injury index = Σ [(browning level) × (number of fruit at the browning level)]/(total number of fruit in the treatment).

A texture analyzer (TMS-Touch, US) with a 7.5 mm diameter probe at a rate of 10 mm s^{-1} was used to measure the firmness of both sides of peeled peaches. TSS was measured using a handheld refractometer (G-won, GMK-701AC, Korea).

Electrolyte leakage was evaluated according to Zhao et al. (2019). Cylinders of peach tissue were excised with a 5 mm diameter stainless steel cork borer from the equatorial region. After rinsing three times (2 min to 3 min) with deionized water, 12 small discs (0.1 cm thick, 0.5. cm diameter) were incubated in 25 mL of deionized water at 20°C, followed by shaking for 30 min. Electrolyte leakage of the solution was measured using a conductivity meter (DDS-11A; Shanghai, China). The solution was then heated to 100°C for 15 min and quickly cooled. The total electrolytes of the solution were then measured again. Relative leakage was expressed as a percentage of the total electrolyte leakage.

Determination of levels of AsA, GSH and GSSG

A method of Hu et al. (2016) was used to measure AsA content. Approximately 0.1 g of frozen sample were ground in liquid nitrogen. The homogenates were then extracted with 5 mL of 5% (w/v) trichloroacetic acid (TCA) and centrifuged at 12,000 g at 4° for 15 min to obtain supernatant for AsA determination. Took 1 ml of supernatant after centrifugation at 4°C and added 0.5 ml of 0.4% phosphoric acid ethanol solution, 1.0 ml of 0.5% phenanthroline ethanol solution, 0.5 ml of 0.03% $FeCl_3$ ethanol solution. After mixing, put the solution at 30°C and reacted for 60 min, then measured the absorbance at 534 nm. Two grams of peach fruit was grounded in liquid nitrogen with 2 mL of extraction solution and then centrifuged at 12000 g for 10 min at 4°C. The supernatant was collected for GSH and GSSG determination with a glutathione kit (Beijing Solabao Technology Co., Ltd., Ningbo, China).

Gene expression analysis

Extraction and reverse transcription of total RNA were performed according to the method of Zhang et al. (2021). Gene expression analysis was performed on a StepOnePlus™ real-time PCR instrument (BIO-RAD, Hercules, California, USA) using SYBR Green I Master Mix (Vazyme, Nanjing, Jiangsu, China) and specific primers (Supplementary Table 1). The real-time fluorescence quantitative PCR reaction system is 6.25 μL GreenMaster Mix, 0.5 μL upstream primer, 0.5 μL downstream primer, 5.25 μL template DNA. Reaction range Sequence: 95 °C pre denaturation for 5 min; deformation at 95 °C for 10 s, annealing at 60 °C for the 30 s, and cycling for 40 times. Gene expression was calculated using the $2^{-\Delta Ct}$ method.

Statistical analysis

Experimental data were analyzed using GraphPad Prism 9 software. Differences between control and treatment were tested using multiple t tests (* $P < 0.05$, ** $P < 0.01$, and *** $P < 0.001$).

Results

Effect of GABA treatment on CI index in peaches

CI of the non-treated peach fruit increased sharply after three weeks of cold storage. GABA treatment reduced the occurrence of Cl, and the index was considerably lower than that of untreated peach after 28 d of storage (Figures 1A, B). In the 35 d, CI of peach treated with GABA was 44.2% lower than the untreated group.

Effect of GABA treatment on fruit firmness, TSS and relative electrical conductivity in peaches

Both GABA-treated and non-treated peaches exhibited a decline in fruit firmness with storage time. Compared to the control group, fruit treated with GABA maintained a greater level of firmness over the whole storage (Figure 2A). TSS contents of peach fruit gradually decreased along with storage time, GABA-treated fruit experienced higher TSS levels than the controls (Figure 2B). Relative electrical conductivity increased

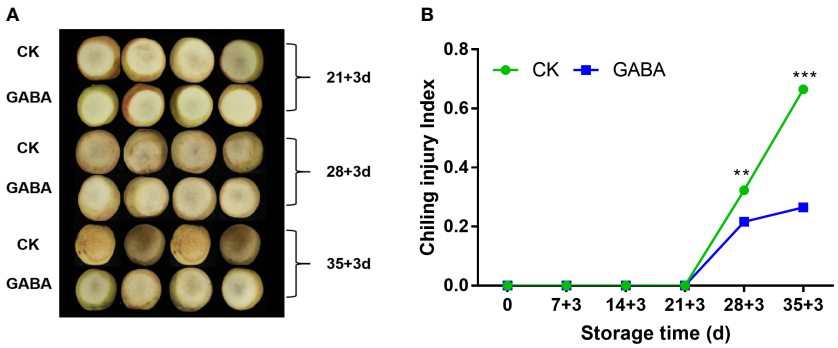

FIGURE 1
Effect of GABA treatment on the appearance **(A)** and chilling injury index **(B)** of peach stored at 4°C. Asterisks indicate significant differences between CK and GABA treatment (*p < 0.05, **p < 0.01, and ***p < 0.001).

rapidly in control peaches during the cold storage, which was inhibited with GABA treatment (Figure 2C).

Effect of GABA treatment on levels of AsA, GSH and GSSG in peaches

At the beginning of cold storage, AsA levels increased, but then decreased until the end (Figure 3A). On day 7, the contents of AsA content in both control and GABA treated peaches reached the maximum values. After that, the content in the untreated group decreased rapidly, while the GABA-treated group maintained a higher level. Overall, the AsA content in the GABA-treated peach were higher than those of the controls throughout the whole storage. The levels of GSH and GSSG in the non-treated peach decreased gradually within the storage. The results showed that GABA treatment up-regulated peach fruit's GSH and GSSG contents throughout storage (Figures 3B, C).

Effect of GABA treatment on expression of genes involved in AsA biosynthesis in peaches

During storage, the expression of *PpPMM* gradually decreased, GABA treatment induced its expression on day 7, 21 and 35 (Figure 4A). The transcripts of *PpGMP* and *PpGME1* increased firstly and then declined thereafter. GABA upregulated *PpGMP* after fourteen days of storage but *PpGME1* during the whole storage (Figures 4B, C). The expression of *PpGME2* declined dramatically during the first seven days of storage and then remained unchanged. A higher level of its expression was observed on day 7 in GABA-treated peaches (Figure 4D). The transcript abundance of *PpGGP* and *PpGPP* increased during first 21 d of storage followed by a decline during the remaining storage time. Higher transcripts of *PpGGP* were observed on day 14 and 28 of storage after GABA treatment (Figure 4E). The treatment also upregulated *PpGPP* expression on day 14 and 21 as compared to the controls (Figure 4F).

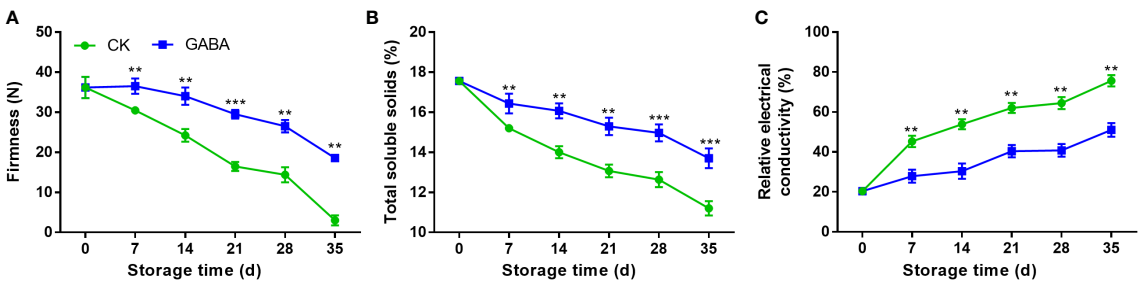

FIGURE 2
Effect of GABA treatment on fruit firmness **(A)**, total soluble solids **(B)** and relative electrical conductivity **(C)** of peach stored at 4°C. Asterisks indicate significant differences between CK and GABA treatment (*p < 0.05, **p < 0.01, and ***p < 0.001).

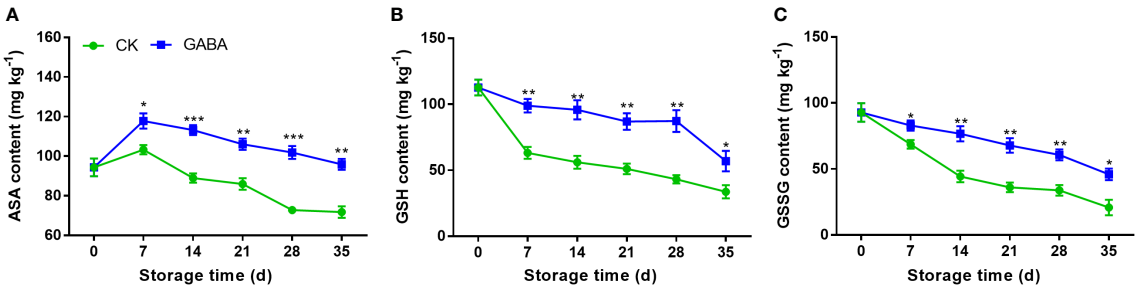

FIGURE 3
Effect of GABA treatment on AsA **(A)**, GSH **(B)** and GSSG **(C)** contents of peach stored at 4°. Asterisks indicate significant differences between CK and GABA treatment (*p < 0.05, **p < 0.01, and ***p < 0.001).

A decrease of *PpGALDH* expression was observed in non-treated peaches, GABA treatment induced it after 28 d of storage (Figure 4G). GABA treatment also upregulated the expression of *PpMXIO4* during the first 14 d of storage but inhibited it after 28 d (Figure 4H). Regarding to the gene *PpGALUR* in D-galacturonate pathway and gene *PpAO2* in AsA degradation, both of their expression increased within the storage in peaches, GABA induced *PpGALUR* after 28 d of storage, however, no difference was observed in *PpAO2* expression between the control and treated peaches (Figures 4I, J).

Effect of GABA treatment on expression of genes involved in GSH biosynthesis in peaches

As shown in Figure 5, the transcripts of all three genes such as *PpGCS1*, *PpGCS2* and *PpGS* increased firstly and declined gradually thereafter. GABA treatment induced *PpGCS1* expression in peach during the whole storage (Figure 5A). Higher transcripts of *PpGCS2* were observed on day 14 and 28 of storage after GABA treatment (Figure 5B). The treatment also upregulated *PpGS* expression on day 7 and 21 as compared with the control (Figure 5C).

Effect of GABA treatment on expression of genes involved in AsA-GSH recycling in peaches

Expression of *PpGR2* increased initially and then began to decrease while the expression of *PpDHAR2* decreased gradually during storage. GABA promoted the transcription level of both genes over the storage (Figure 6A, B). During the first 21 d of storage, *PpMDHAR* and *PpGPX2* transcript abundance increased but then decreased quickly. Up-regulations of *PpMDHAR* was observed on day 7 and 28 in GABA-treated peaches (Figure 6C) and GABA also induced *PpGPX2* expression on day 21 and 28 (Figure 6D). Compared with the control peach, there was no difference in the levels of *PpAPX* expression between the treated and control fruit in the early storage stage. However, GABA treatment increased the abundance of *PpAPX* transcripts after 28 d of cold storage (Figure 6E).

Effect of GABA treatment on expression of ERF transcription factors in peaches

The transcript levels of all the three candidate ERF transcription factors exhibited a sharp increase and subsequent decrease during the cold storage in both treated and non-treated peach. GABA treatment increased *PpERF4* expression during the whole storage (Figure 7A). Higher transcripts of *PpERF106* were observed on day 7 and 14 of storage after GABA treatment (Figure 7B). The treatment also upregulated *PpERF115* expression on day 21 and 28 as compared to the controls (Figure 7C).

Discussion

GABA is a non-protein amino acid that accumulates rapidly in plants when stressed (Ramos-Ruiz et al., 2019). It plays a crucial role in regulating pH in the cytosol, controlling carbon and nitrogen metabolism, and protecting cells from biotic and abiotic stresses (Hijaz et al., 2018). In recent years, there have also been many related researches on GABA-inducing chilling tolerance in post-harvest in fruit and vegetables (Ali et al., 2022; Fan et al., 2022; Jiao, 2022). Same as our previous studies (Yang et al., 2011), here we also found GABA could effectively reduce chilling incidence and maintain fruit quality during postharvest storage.

AsA plays a critical role in oxidative stress defense and membrane degradation in plants. Increased plant resistance against cold stress due to enhanced hydrogen peroxide scavenging system by AsA, is widely reported in postharvest

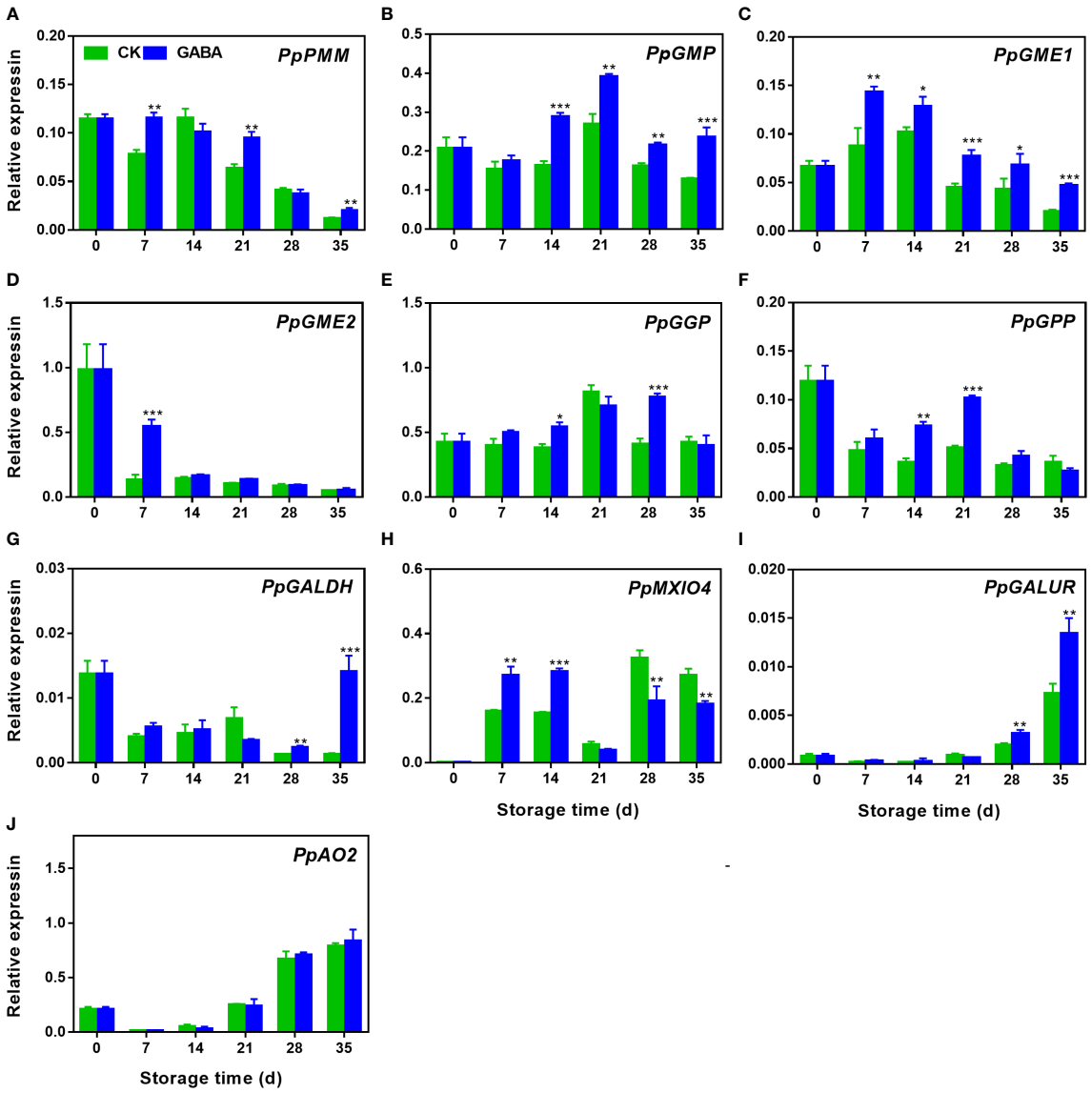

FIGURE 4
Effect of GABA treatment on expression of genes involved in AsA biosynthesis of peach stored at 4°C. Expression levels of *PpPMM* **(A)**, *PpGMP* **(B)**, PpGME1 **(C)**, PpGME2 **(D)**, PpGGP **(E)**, PpGPP **(F)**, PpGALDR **(G)**, PpGALUR **(H)**, PpMXIO4 **(I)** and PpAO2 **(J)** were analysed. Asterisks indicate significant differences between CK and GABA treatment (*p < 0.05, **p < 0.01, and ***p < 0.001).

bananas, kiwifruit and peach (Wang et al., 2014b; Yang et al., 2016; Lo'Ay and El-Khateeb, 2018). Here, our research found the AsA levels in GABA-treated peach increased during storage which was crucial to relieve oxidative stress and reduce the chilling injury in peach fruit.

The biosynthesis of AsA in plant is mainly divided into four pathways, namely L-galactose (Wheeler et al., 1998), D-galacturonate (Agius et al., 2003), L-glucose (Wolucka et al., 2005) and myo-inositol (Lorence et al., 2004). Among them, the L-galactose pathway has been officially recognized as the leading synthetic pathway of AsA biosynthesis (Zhang et al., 2015). Gómez-García and Ochoa-Alejo (2016) found that it was the primary mechanism for AsA biosynthesis in fruit and leaves of peppers. Li et al. (2011) revealed that the expression of four L-galactose genes such as *MdGME*, *MdGPP* and *MdGaLDH*) in young apple fruit was correlated well with the AsA content. In our current study, most genes of the L-galactose pathway were up-regulated by GABA treatment, consequently responsible for the corresponding increase in AsA levels to some extent.

Besides the L-galactose pathway, the D-galacturonate pathway is also reported to be the major pathway for AsA biosynthesis in plants, in which *GALUR* is a crucial enzyme

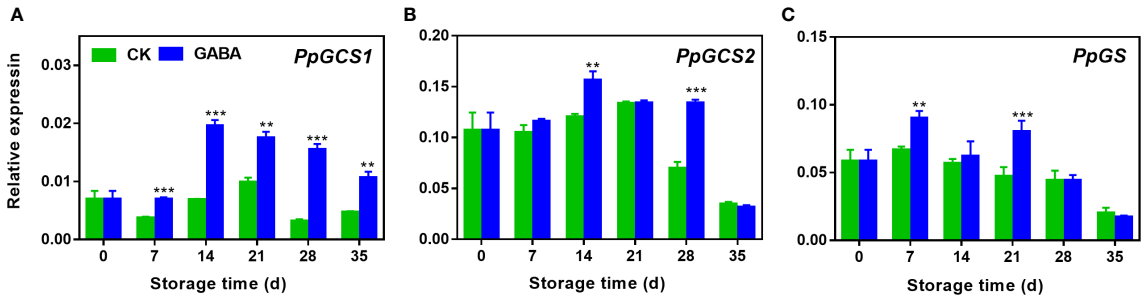

FIGURE 5
Effect of GABA treatment on expression of genes involved in GSH biosynthesis of peach stored at 4°C. Expression levels of *PpGCS1* **(A)**>, *PpGCS2* **(B)** and *PpGS* **(C)** were analysed. Asterisks indicate significant differences between CK and GABA treatment (*p < 0.05, **p < 0.01, and ***p < 0.001).

(Agius et al., 2003), converting D-galacturonate into L-galactose acid (Badejo et al., 2012). In Arabidopsis overexpressed with strawberry *FaGALUR* gene ectopically, AsA content was increased (Wolucka and Van Montagu, 2003). However, there was no apparent relationship between AsA content and *AdGALUR* expression in kiwifruit (Bulley et al., 2009). Our experiment here showed that GABA treatment did not enhance the transcription level of *PpGALUR* in the early stage of storage but considerably increased expression was observed at the end of storage. Therefore, we speculated that *PpGALUR* in GABA-treated peach might play a role in inducing AsA accumulation during the late period of storage.

In addition to the two AsA biosynthetic pathways described above, we also studied the transcriptional abundance of some genes in the myo-inositol and degradation pathways. As a key enzyme in the myo-inositol pathway, the role of *MIOX* in the plant AsA biosynthesis pathway is still unclear (Munir et al., 2020). Previous studies have suggested that overexpression of *AtMIOX* in Arabidopsis increased the AsA level by 2-to-3 fold (Lorence et al., 2004). A study has shown, however, that

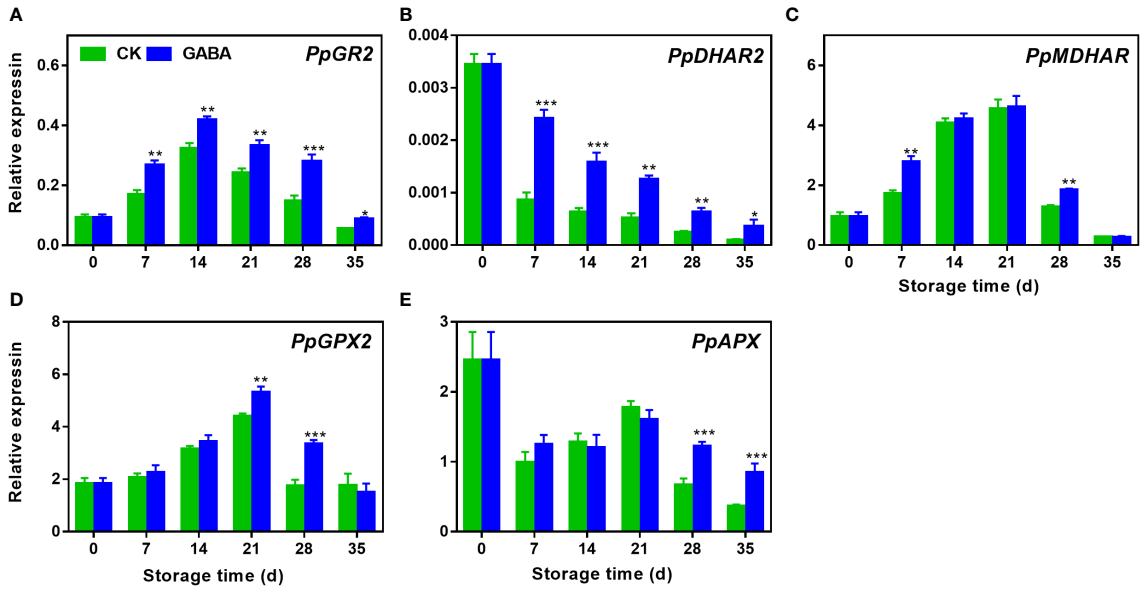

FIGURE 6
Effect of GABA treatment on expression of genes involved in ASA-GSH cycle of peach stored at 4°C. Expression levels of PpGR2 **(A)**, PpDHAR2 **(B)**, PpMDHAR **(C)**, PpGPX2 **(D)** and PpAPX **(E)** were analysed. Asterisks indicate significant differences between CK and GABA treatment (*p < 0.05, **p < 0.01, and ***p < 0.001).

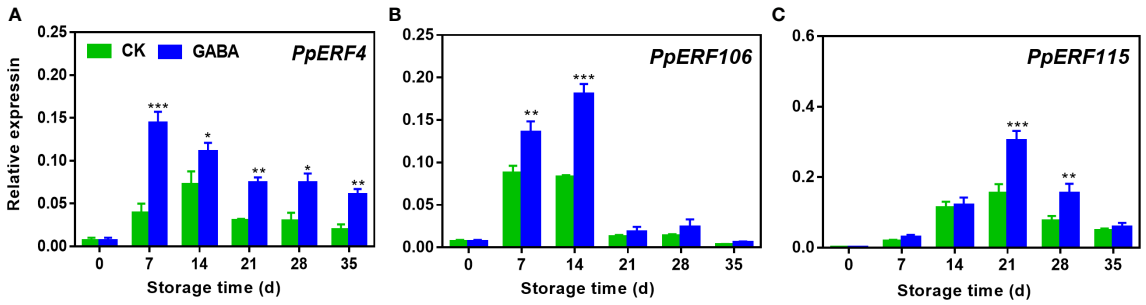

FIGURE 7
Effect of GABA treatment on expression of *ERF* transcription factors of peach stored at 4°C. Expression levels of PpERF4 **(A)**, PpERF106 **(B)** and PpERF115 **(C)** were analysed. Asterisks indicate significant differences between CK and GABA treatment (*p < 0.05, **p < 0.01, and ***p < 0.001).

AtMIOX regulated the Myo-inositol level without increasing AsA content (Endres and Tenhaken, 2009). In our present study, the different responses of *PpMIOX4* transcripts in response to GABA treatment were observed indicating the precise mechanism of *PpMIOX4* in AsA biosynthesis in peach fruit needs to be further explored. In respect to the AsA degradation, no differential expression of *PpAO2* was found in peaches treated with GABA. Therefore, we believed that the GABA signal was not involved in the regulation of AsA degradation.

GSH is another well-known antioxidant in plants that can reduce the accumulation of ROS produced in various adversity stresses (Chen and Yang, 2020). It was found that increasing GSH content could reduce chilling injury in postharvest fruit such as iwifruit, pears and bell pepper (Wei et al., 2019; Yao et al., 2021; Jiao et al., 2022). Similarly, in GABA-treated peach treatment, higher GSH content was observed, which was also related to the induced chilling tolerance in peach treated with GABA.

It is well documented that GSH biosynthesis is mainly a free amino acid-dependent enzymatic synthesis of ATP and Mg^{2+}. γ-Glutamylcysteine ligase (GCS) is a key rate-limiting enzyme in GSH biosynthesis catalyzing γ-COOH and cysteine to glutamate -NH-binding acid while consuming ATP to generate glutamylcysteine (γ-EC) (Noctor et al., 2012). Then, glutathione synthase (GS) catalyzes γ-EC to generate GSH (Jobbagy et al., 2019). In our experiments, GABA treatment increased the expression of all of the three GSH biosynthetic genes in peach, thus inducing GSH accumulation.

The AsA-GSH cycle is an essential H_2O_2 scavenging system in plants (Hasanuzzaman et al., 2019). AsA and GSH are important non-enzymatic antioxidants in this cycle, and their redox states can represent the redox states in the cellular environment (Wang et al., 2013). GPX, MDHAR, DHAR, GR and APX are critical enzymes in the metabolism of the AsA-GSH cycle. GPX has a defensive role against oxidative damage in plant cells (Lushchak, 2012). MDHAR and DHAR can reduce MDHA and DHA respectively to form AsA, ensuring the efficient regeneration of AsA, while GSH is oxidized to GSSG (Aravind and Prasad, 2005; Ma et al., 2019). GR can use NAD (P) H as an electron donor to regenerate GSSG into GSH and maintain the reduced state of GSH. APX can use AsA as an electron donor to reduce H_2O_2 to H_2O, and remove excess H_2O_2 in cells (Yin et al., 2010). Studies have shown that Glycine betaine treatment reduced oxidative stress damage and improved cold resistance by regulating the metabolism of the AsA-GSH cycle in plants (Einset and Connolly, 2009). In peach, we found that GABA treatment up-regulated the expression of *PpGR2, PpDHAR2, PpMDHAR, PpGPX2* and *PpAPX* genes in the AsA-GSH cycle during cold storage, which was similar to the results obtained by Wang et al. (Wang et al., 2016), who reported that Glycine betaine treatment also induced associated genes in the AsA-GSH cycle, thus improving cold resistance in pepper fruit. Our results showed that GABA treatment up-regulated the expression of related genes in the AsA-GSH cycle, thereby maintaining higher AsA and GSH levels during cold storage and inhibiting the occurrence of chilling injury in peach fruit.

Many studies have found transcription factors such as ERFs have been identified to be involved in AsA metabolic pathway in Arabidopsis, tomato and citrus fruit (Zhang et al., 2009; Hu et al., 2016; Ye et al., 2019). *AtERF98* triggers the expression of genes involved in the D-Man/L-Gal synthesis pathway and the *MIOX4* gene in the myo-inositol pathway (Yuan et al., 2020). The function of *AtERF98*-regulated AsA synthesis was severely impaired in vtc1-1 mutants, suggesting that *AtERF98* is involved in the D-Man/L-Gal synthesis pathway and plays a vital role in regulating the synthesis of AsA (Zhang et al., 2012). In this study, we found that the expression of three *PpERF* genes was up-regulated in the peach GABA-treated group when compared with the untreated group, showing that ERFs might also participate in the metabolic regulation of AsA and GSH contents.

Conclusion

In conclusion, after GABA treatment, the chilling injury of peach fruit was decreased. GABA increased AsA and GSH levels by regulating the expression of AsA and GSH-related genes in cold-stored peach. Therefore, we believed that GABA treatment could enhance chilling tolerance due to the increased levels of AsA and GSH. Furthermore, our results also suggested three candidate ERF transcription factors might be involved in AsA and GSH biosynthesis. However, more evidence is needed to determine the relationship of ERF transcription factors and their networks to hormone signalling and hormone-mediated stress responses, which may help provide insight into the transcriptional regulation of AsA-GSH metabolic processes in postharvest peach.

Data availability statement

The original contributions presented in the study are included in the article/Supplementary Material. Further inquiries can be directed to the corresponding author.

Author contributions

CZ, ZY and SC contributed to conception and design of the study. SJ organized the database. QL performed the statistical analysis. CZ wrote the first draft of the manuscript. LS, SL, WC and WD wrote sections of the manuscript. All authors contributed to manuscript revision, read, and approved the submitted version.

Funding

The work was supported by the National Natural Science Foundation of China (32172646), the Key Projects of Natural Science Foundation of Zhejiang Province (LZ21C200002) and the Natural Science Foundation of Zhejiang Province (LQ20C200006).

Conflict of interest

The authors declare that the research was conducted in the absence of any commercial or financial relationships that could be construed as a potential conflict of interest.

Publisher's note

All claims expressed in this article are solely those of the authors and do not necessarily represent those of their affiliated organizations, or those of the publisher, the editors and the reviewers. Any product that may be evaluated in this article, or claim that may be made by its manufacturer, is not guaranteed or endorsed by the publisher.

Supplementary material

The Supplementary Material for this article can be found online at: https://www.frontiersin.org/articles/10.3389/fpls.2022.1059979/full#supplementary-material

References

Aghdam, M. S., Razavi, F., and Karamneghad, F. (2016). Maintaining the postharvest nutritional quality of peach fruits by γ-aminobutyric acid. *Plant Physiol.* 5 (4), 1457–1463. doi: 10.30495/IJPP.2015.539673

Agius, F., Gonzalez-Lamothe, R., Caballero, J. L., Munoz-Blanco, J., Botella, M. A., and Valpuesta, V. (2003). Engineering increased vitamin c levels in plants by overexpression of a d-galacturonic acid reductase. *Nat. Biotechnol.* 21 (2), 177–181. doi: 10.1038/nbt777

Ali, S., Anjum, M. A., Nawaz, A., Ejaz, S., Anwar, R., Khaliq, G., et al. (2022). Postharvest gamma-aminobutyric acid application mitigates chilling injury of aonla (*Emblica officinalis gaertn.*) fruit during low temperature storage. *Postharvest Biol. Technol.* 185, 111803. doi: 10.1016/j.postharvbio.2021.111803

Alscher, R. G., Donahue, J. L., and Cramer, C. L. (1997). Reactive oxygen species and antioxidants: Relationships in green cells. *Physiol. Plant* 100, 224–233. doi: 10.1111/j.1399-3054.1997.tb04778.x

Aravind, P., and Prasad, M. N. V. (2005). Modulation of cadmium-induced oxidative stress in *Ceratophyllum demersum* by zinc involves ascorbate–glutathione cycle and glutathione metabolism. *Postharvest Biol. Technol.* 43 (2), 107–116. doi: 10.1016/j.plaphy.2005.01.002

Badejo, A. A., Wada, K., Gao, Y., Maruta, T., Sawa, Y., Shigeoka, S., et al. (2012). Translocation and the alternative d-galacturonate pathway contribute to increasing the ascorbate level in ripening tomato fruits together with the d-mannose/L-galactose pathway. *J. Exp. Bot.* 63 (1), 229–239. doi: 10.1093/jxb/err275

Bao, H., Chen, X., Lv, S., Jiang, P., Feng, J., Fan, P., et al. (2015). Virus-induced gene silencing reveals control of reactive oxygen species accumulation and salt tolerance in tomato by gamma-aminobutyric acid metabolic pathway. *Plant Cell Environ.* 38 (3), 600–613. doi: 10.1111/pce.12419

Baxte, A., Mittler, R., and Suzuki, N. (2014). ROS as key players in plant stress signaling. *J. Exp. Bot.* 65, 1229–1240. doi: 10.1093/jxb/ert375

Bulley, S. M., Rassam, M., Hoser, D., Otto, W., Schünemann, N., Wright, M., et al. (2009). Gene expression studies in kiwifruit and gene over-expression in *Arabidopsis* indicates that GDP-l-galactose guanyltransferase is a major control point of vitamin c biosynthesis. *J. Exp. Bot.* 60 (3), 765–778. doi: 10.1093/jxb/ern327

Chen, Q., and Yang, G. (2020). Signal function studies of ROS, especially RBOH-dependent ROS, in plant growth, development and environmental stress. *J. Plant Growth Regul.* 39 (1), 157–171. doi: 10.1007/s00344-019-09971-4

Einset, J., and Connolly, E. L. (2009). Glycine betaine enhances extracellular processes blocking ROS signaling during stress. *Plant Signal. Behav.* 4 (3), 197–199. doi: 10.4161/psb.4.3.7725

Endres, S., and Tenhaken, R. (2009). Myoinositol oxygenase controls the level of myoinositol in arabidopsis, but does not increase ascorbic acid. *Plant Physiol.* 149 (2), 1042–1049. doi: 10.1104/pp.108.130948

Fan, Z., Lin, B., Lin, H., Lin, M., Chen, J., and Lin, Y. (2022). γ-aminobutyric acid treatment reduces chilling injury and improves quality maintenance of cold-stored Chinese olive fruit. *Food Chem. X* 13, 100208. doi: 10.1016/j.fochx.2022.100208

Gómez-García, M., and Ochoa-Alejo, N. (2016). Predominant role of the l-galactose pathway in l-ascorbic acid biosynthesis in fruits and leaves of the

Capsicum annuum l. chili pepper. *Braz. J. Bot.* 39 (1), 157–168. doi: 10.1007/s40415-015-0232-0

Hasanuzzaman, M., Bhuyan, M. B., Anee, T. I., Parvin, K., Nahar, K., Mahmud, J. A., et al. (2019). Regulation of ascorbate-glutathione pathway in mitigating oxidative damage in plants under abiotic stress. *Antioxidants* 8 (9), 384. doi: 10.3390/antiox8090384

Hijaz, F., Nehela, Y., and Killiny, N. (2018). Application of gamma-aminobutyric acid increased the level of phytohormones in citrus sinensis. *Planta* 248 (4), 909–918. doi: 10.1007/s00425-018-2947-1

Hu, T., Ye, J., Tao, P., Li, H., Zhang, J., Zhang, Y., et al. (2016). The tomato HD-zip I transcription factor SlHZ24 modulates ascorbate accumulation through positive regulation of the d-mannose/L-galactose pathway. *Plant J.* 85 (1), 16–29. doi: 10.1111/tpj.13085

Jiao, C. (2022). γ-aminobutyric acid boosts chilling tolerance by promoting the methionine sulfoxide reductase-thioredoxin reductase system in peach fruit. *Hortic. Environ. Biotechnol.* 63, 353–361. doi: 10.1007/s13580-021-00408-0

Jiao, J., Jin, M., Liu, H., Suo, J., Yin, X., Zhu, Q., et al. (2022). Application of melatonin in kiwifruit (*Actinidia chinensis*) alleviated chilling injury during cold storage. *Sci. Hortic.* 296 (5), 110876. doi: 10.1016/j.scienta.2022.110876

Jobbagy, S., Vitturi, D. A., Salvatore, S. R., Turell, L., Pires, M. F., Kansanen, E., et al. (2019). Electrophiles modulate glutathione reductase activity *via* alkylation and upregulation of glutathione biosynthesis. *Redox Biol.* 21, 101050. doi: 10.1016/j.redox.2018.11.008

Li, M. J., Chen, X. S., Wang, P. P., and Ma, F. W. (2011). Ascorbic acid accumulation and expression of genes involved in its biosynthesis and recycling in developing apple fruit. *J. Am. Soc Hortic. Sci.* 136 (4), 231–238. doi: 10.21273/JASHS.136.4.231

Li, L., Dou, N., Zhang, H., and Wu, C. (2021). The versatile GABA in plants. *Plant Signal. Behav.* 16 (3), 1862565. doi: 10.1080/15592324.2020.1862565

Lo'Ay, A., and El-Khateeb, A. (2018). Antioxidant enzyme activities and exogenous ascorbic acid treatment of 'Williams' banana during long-term cold storage stress. *Sci. Hortic.* 234 (14), 210–219. doi: 10.1016/j.scienta.2018.02.038

Lorence, A., Chevone, B. I., Mendes, P., and Nessler, C. L. (2004). Myo-inositol oxygenase offers a possible entry point into plant ascorbate biosynthesis. *Plant Physiol.* 134 (3), 1200–1205. doi: 10.1104/pp.103.033936

Lushchak, V. I. (2012). Glutathione homeostasis and functions: potential targets for medical interventions. *Amino Acids* 2012, 1–26. doi: 10.1155/2012/736837

Mahmud, J. A., Hasanuzzaman, M., Nahar, K., Rahman, A., Hossain, M., and Fujita, M. (2017). γ-aminobutyric acid (GABA) confers chromium stress tolerance in *Brassica juncea* l. by modulating the antioxidant defense and glyoxalase systems. *Ecotoxicology* 26 (5), 675–690. doi: 10.1007/s10646-017-1800-9

Ma, Y., Huang, D., Chen, C., Zhu, S., and Gao, J. (2019). Regulation of ascorbate-glutathione cycle in peaches *via* nitric oxide treatment during cold storage. *Sci. Hortic.* 247 (15), 400–406. doi: 10.1016/j.scienta.2018.12.039

Malekzadeh, P. (2015). Influence of exogenous application of glycinebetaine on antioxidative system and growth of salt-stressed soybean seedlings (*Glycine max* l.). *Physiol. Mol. Biol. Plants* 21 (2), 225–232. doi: 10.1007/s12298-015-0292-4

Malekzadeh, P., Khosravi-Nejad, F., Hatamnia, A. A., and Sheikhakbari Mehr, R. (2017). Impact of postharvest exogenous γ-aminobutyric acid treatment on cucumber fruit in response to chilling tolerance. *Physiol. Mol. Biol. Plants* 23 (4), 827–836. doi: 10.1007/s12298-017-0475-2

Munir, S., Mumtaz, M. A., Ahiakpa, J. K., Liu, G., Chen, W., Zhou, G., et al. (2020). Genome-wide analysis of myo-inositol oxygenase gene family in tomato reveals their involvement in ascorbic acid accumulation. *BMC Genom.* 21 (1), 1–15. doi: 10.1186/s12864-020-6708-8

Niazi, Z., Razavi, F., Khademi, O., and Aghdam, M. S. (2021). Exogenous application of hydrogen sulfide and γ-aminobutyric acid alleviates chilling injury and preserves quality of persimmon fruit (*Diospyros kaki*, cv. karaj) during cold storage. *Sci. Hortic.* 285 (27), 110198. doi: 10.1016/j.scienta.2021.110198

Nicolas, B., and Hillel, F. (2004). GABA in plants: just a metabolite. *Trends Plant Sci.* 9 (3), 110–115. doi: 10.1016/j.tplants.2004.01.006

Noctor, G., Mhamdi, A., Chaouch, S., Han, Y., Neukermans, J., Marquez-Garcia, B., et al. (2012). Glutathione in plants: an integrated overview. *Plant Cell Environ.* 35 (2), 454–484. doi: 10.1111/j.1365-3040.2011.02400.x

Ramesh, S. A., Tyerman, S. D., Gilliham, M., and Xu, B. (2017). γ-aminobutyric acid(GABA) signalling in plants. *Cell. Mol. Life Sci.* 74 (9), 1577–1603. doi: 10.1007/s00018-016-2415-7

Ramos-Ruiz, R., Martinez, F., and Knauf-Beiter, G. (2019). The effects of GABA in plants. *Cogent. Food Agr.* 5 (1), 1670553. doi: 10.1080/23311932.2019.1670553

Shang, H. T., Cao, S. F., Yang, Z. F., Cai, Y. T., and Zheng, Y. H. (2011). Effect of exogenous gamma-aminobutyric acid treatment on proline accumulation and chilling injury in peach fruit after long-term cold storage. *J. Agric. Food Chem.* 59 (4), 1264–1268. doi: 10.1021/jf104424z

Song, L., Wang, J., Shafi, M., Liu, Y., Wang, J., Wu, J., et al. (2016). Hypobaric treatment effects on chilling injury, mitochondrial dysfunction, and the ascorbate-glutathione (AsA-GSH) cycle in postharvest peach fruit. *J. Agric. Food Chem.* 64 (22), 4665–4674. doi: 10.1021/acs.jafc.6b00623

Wang, Q., Ding, T., Zuo, J., Gao, L., and Fan, L. (2016). Amelioration of postharvest chilling injury in sweet pepper by glycine betaine. *Postharvest Biol. Technol.* 112, 114–120. doi: 10.1016/j.postharvbio.2015.07.008

Wang, C., Fan, L., Gao, H., Wu, X., Li, J., Lv, G., et al. (2014a). Polyamine biosynthesis and degradation are modulated by exogenous gamma-aminobutyric acid in root-zone hypoxia-stressed melon roots. *Plant Physiol. Biochem.* 82, 17–26. doi: 10.1016/j.plaphy.2014.04.018

Wang, Y., Luo, Z., Huang, X., Yang, K., Gao, S., and Du, R. (2014c). Effect of exogenous γ-aminobutyric acid (GABA) treatment on chilling injury and antioxidant capacity in banana peel. *Sci. Hortic.* 168 (26), 132–137. doi: 10.1016/j.scienta.2014.01.022

Wang, K., Shao, X., Gong, Y., Xu, F., and Wang, H. (2014b). Effects of postharvest hot air treatment on gene expression associated with ascorbic acid metabolism in peach fruit. *Plant Mol. Biol. Rep.* 32 (4), 881–887. doi: 10.1007/s11105-014-0699-z

Wang, J., Zeng, Q., Zhu, J., Liu, G., and Tang, H. (2013). Dissimilarity of ascorbate-glutathione (AsA–GSH) cycle mechanism in two rice (*Oryza sativa* l.) cultivars under experimental free-air ozone exposure. *Agric. Ecosyst. Environ.* 165 (15), 39–49. doi: 10.1016/j.agee.2012.12.006

Wei, C., Ma, L., Cheng, Y., Guan, Y., and Guan, J. (2019). Exogenous ethylene alleviates chilling injury of 'Huangguan' pear by enhancing the proline content and antioxidant activity. *Sci. Hortic.* 257 (17), 108671. doi: 10.1016/j.scienta.2019.108671

Wheeler, G. L., Jones, M. A., and Smirnoff, N. (1998). The biosynthetic pathway of vitamin c in higher plants. *Nature* 393, 365–369. doi: 10.1038/30728

Wolucka, B. A., Goossens, A., and Inzé, D. (2005). Methyl jasmonate stimulates the *de novo* biosynthesis of vitamin c in plant cell suspensions. *J. Exp. Bot.* 56, 2527–2538. doi: 10.1093/jxb/eri246

Wolucka, B. A., and Van Montagu, M. (2003). GDP-Mannose 3', 5'-epimerase forms GDP-l-gulose, a putative intermediate for the *de novo* biosynthesis of vitamin c in plants. *J. Biol. Chem.* 278 (48), 47483–47490. doi: 10.1074/jbc.M309135200

Yang, A., Cao, S., Yang, Z., Cai, Y., and Zheng, Y. (2011). γ-aminobutyric acid treatment reduces chilling injury and activates the defence response of peach fruit. *Food Chem.* 129 (4), 1619–1622. doi: 10.1016/j.foodchem.2011.06.018

Yang, Q., Wang, F., and Rao, J. (2016). Effect of putrescine treatment on chilling injury, fatty acid composition and antioxidant system in kiwifruit. *PloS One* 11 (9), e0162159. doi: 10.1371/journal.pone.0162159

Yao, M., Ge, W., Zhou, Q., Zhou, X., Luo, M., Zhao, Y., et al. (2021). Exogenous glutathione alleviates chilling injury in postharvest bell pepper by modulating the ascorbate-glutathione (AsA-GSH) cycle. *Food Chem.* 352 (1), 129458. doi: 10.1016/j.foodchem.2021.129458

Ye, J., Li, W., Ai, G., Li, C., Liu, G., Chen, W., et al. (2019). Genome-wide association analysis identifies a natural variation in basic helix-loop-helix transcription factor regulating ascorbate biosynthesis *via* d-mannose/L-galactose pathway in tomato. *PloS Genet.* 15 (5), e1008149. doi: 10.1371/journal.pgen.1008149

Yin, L., Wang, S., Eltayeb, A. E., Uddin, M., Yamamoto, Y., Tsuji, W., et al. (2010). Overexpression of dehydroascorbate reductase, but not monodehydroascorbate reductase, confers tolerance to aluminum stress in transgenic tobacco. *Planta* 231 (3), 609–621. doi: 10.1007/s00425-009-1075-3

Yuan, J., Yu, Z., Lin, T., Wang, L., Chen, X., Liu, T., et al. (2020). BcERF070, a novel ERF (ethylene-response factor) transcription factor from non-heading Chinese cabbage, affects the accumulation of ascorbic acid by regulating ascorbic acid-related genes. *Mol. Breed.* 40 (1), 1–18. doi: 10.1007/s11032-019-1065-5

Zhang, G.-Y., Liu, R.-R., Zhang, C.-Q., Tang, K.-X., Sun, M.-F., Yan, G.-H., et al. (2015). Manipulation of the rice l-galactose pathway: evaluation of the effects of transgene overexpression on ascorbate accumulation and abiotic stress tolerance. *PloS One* 10 (5), e0125870. doi: 10.1371/journal.pone.0125870

Zhang, W. Y., Lorence, A., Gruszewski, H. A., Chevone, B. I., and Nessler, C. L. (2009). AMR1, an arabidopsis gene that coordinately and negatively regulates the mannose/L-galactose ascorbic acid biosynthetic pathway. *Plant Physiol.* 150 (1), 942–950. doi: 10.1104/pp.108.134767

Zhang, Y., Wang, K., Xiao, X., Cao, S., Chen, W., Yang, Z., et al. (2021). Effect of 1-MCP on the regulation processes involved in ascorbate metabolism in kiwifruit. *Postharvest Biol. Technol.* 179, 111563. doi: 10.1016/j.postharvbio.2021.111563

Zhang, Z. J., Wang, J., Zhang, R. X., and Huang, R. F. (2012). The ethylene response factor AtERF98 enhances tolerance to salt through the transcriptional activation of ascorbic acid synthesis in arabidopsis. *Plant J.* 71 (2), 273–287. doi: 10.1111/j.1365-313X.2012.04996.x

Zhao, Y., Zhu, X., Hou, Y., Wang, X., and Li, X. (2019). Effects of nitric oxide fumigation treatment on retarding cell wall degradation and delaying softening of winter jujube (*Ziziphus jujuba mill.* cv. dongzao) fruit during storage. *Postharvest Biol. Technol.* 156, 110954. doi: 10.1016/j.postharvbio.2019.110954

frontiers | Frontiers in Plant Science

TYPE Original Research
PUBLISHED 15 December 2022
DOI 10.3389/fpls.2022.1087452

OPEN ACCESS

EDITED BY
Shifeng Cao,
Zhejiang Wanli University, China

REVIEWED BY
Feng Xu,
Ningbo University, China
Jianqing Chen,
Fujian Agriculture and Forestry University, China

*CORRESPONDENCE
Haoru Tang
htang@sicau.edu.cn
Yong Zhang
Zhyong@sicau.edu.cn

†These authors have contributed equally to this work

SPECIALTY SECTION
This article was submitted to Crop and Product Physiology, a section of the journal Frontiers in Plant Science

RECEIVED 02 November 2022
ACCEPTED 28 November 2022
PUBLISHED 15 December 2022

CITATION
Lin Y, Tang H, Zhao B, Lei D, Zhou X, Yao W, Fan J, Zhang Y, Chen Q, Wang Y, Li M, He W, Luo Y, Wang X, Tang H and Zhang Y (2022) Comparative changes of health-promoting phytochemicals and sugar metabolism of two hardy kiwifruit (*Actinidia arguta*) cultivars during fruit development and maturity. *Front. Plant Sci.* 13:1087452. doi: 10.3389/fpls.2022.1087452

Comparative changes of health-promoting phytochemicals and sugar metabolism of two hardy kiwifruit (*Actinidia arguta*) cultivars during fruit development and maturity

Yuanxiu Lin[1,2†], Honglan Tang[1†], Bing Zhao[1], Diya Lei[1], Xuan Zhou[1], Wantian Yao[1], Jinming Fan[3], Yunting Zhang[1,2], Qing Chen[1], Yan Wang[1,2], Mengyao Li[1], Wen He[1,2], Ya Luo[1], Xiaorong Wang[1,2], Haoru Tang[1,2*] and Yong Zhang[1*]

[1]College of Horticulture, Sichuan Agricultural University, Chengdu, China, [2]Institute of Pomology and Olericulture, Sichuan Agricultural University, Chengdu, China, [3]General Manager's Office, Sichuan Innofresh Agricultural Science and Technology Co., Ltd., Ya'an, China

Introduction: Hardy kiwifruit (*Actinidia arguta*) has an extensive range of nutritional and bioactive compounds and has been valued as a great resource for kiwifruit breeding. A better understanding of the dynamic changes of the composition and accumulation of nutritional compounds during fruit development and ripening is required before genetic or cultural improvements can be targeted.

Methods: In the present study, the phytochemical analysis of two *A. arguta* cultivars 'Yilv' and 'Lvmi-1' showed that they comprised different morphology, with a higher fruit diameter while a lower vertical fruit diameter of 'Lvmi-1' compared with 'Yilv'. The antioxidant capacity of both cultivars decreased during the maturity time and showed no significant difference between them. Furthermore, although glucose gradually increased during the maturity time, the predominant sugar composition was speculated to be fructose in 'Lvmi-1' fruit while sucrose in 'Yilv' fruit at the early fruit developmental stages. Moreover, the predominant acids in 'Yilv' and 'Lvmi-1' were citric acid followed by quinic acid, malic acid, and oxalic acid. The expression of sugar- and starch-related genes encoding the crucial enzymes suggested different changes in 'Yilv' and 'Lvmi-1'. Notably, a subsequent correlation analysis showed a significant positive correlation between sucrose phosphate synthase (SPS) expression and glucose in 'Yilv', fructokinase (FK) expression, and starch

content in 'Lvmi-1', implying their vital roles in sugar and starch accumulation. By contrast, a significant negative correlation between FK expression and fructose in 'Lvmi-1' fruit was observed.

Results and Discussion: In summary, our results provide supplementary information for the dynamic changes of nutritional compounds and antioxidant capacity during hardy kiwifruit maturity time and give a clue for exploring the mechanism of sugar and starch accumulation in hardy kiwifruit.

KEYWORDS

***actinidia arguta*, antioxidant capacity, nutritional compounds, organic acids, sugars**

Introduction

Kiwifruit (*Actinidia*, Actinidiaceae), a worldwide commercially domesticated and cultivated perennial fruit tree, is a sought-after fresh fruit in the marketplace due to its delicious taste and multiple health-promoting nutritional components (Wang et al., 2021). Although there are 15 out of over 50 *Actinidia* species producing edible fruits, only three of them are now commercially available (Silva et al., 2019). Among them, *A. chinensis* and *A. deliciosa* have been suggested as the most commercially significant species (Follett et al., 2019), whereas increasing evidence has appeared to indicate that *A. arguta*, also known as hardy kiwifruit, kiwiberry, baby kiwi, or grape kiwi has a lot of horticultural advantages over kiwifruit, such as high frost hardiness (down to -30°C in the dormant period), richer bioactive compounds, stronger antioxidant activities, and edible skin (Latocha et al., 2015; Latocha, 2017; Wojdyło et al., 2017; Zhang et al., 2021).

Hardy kiwifruit (*A. arguta*) grew up first outside Asia but is native from northeast Asian countries. It is worldwide consumed and appreciated mainly due to its high phenolic, ascorbic acid (AsA, also known as vitamin C), and mineral contents (Latocha et al., 2015; Wojdyło and Nowicka, 2019). Moreover, hardy kiwifruit has been recognized as one of the most nutritionally rich fruits and an excellent source of health-promoting phytochemicals, such as sugars, organic acids, minerals, dietary fiber, vitamins (especially vitamin C), and antioxidants (mainly polyphenols) (Pinto et al., 2020). In addition, it has been shown that the antioxidative activity of hardy kiwifruit is strongly correlated with the content of AsA and polyphenols (Latocha et al., 2015). The much higher polyphenols and AsA in hardy kiwifruit compared with common kiwifruit (Leontowicz et al., 2016) has made hardy kiwifruit as a promising natural antioxidant. Due to these attractive health-promoting traits, hardy kiwifruit is of great interest to researchers, being a potential candidate to be included in a healthy and sustainable diet, and becoming popular to consumers.

In recent years, an increasing number of studies have been reported with subjects on the nutritional value and health benefits in hardy kiwifruit, most of which point to and confirm a rich composition of health-promoting ingredients, such as AsA, phenolics, anthocyanins, and sugars (Latocha, 2017; Wojdyło et al., 2017). However, even though the metabolite levels in hardy kiwifruit are generally higher than those in common kiwifruit, they vary in different hardy kiwifruit cultivars. Nowadays, there are various varieties of hardy kiwifruit on the market, the most representative and well-known are 'Ananasnaya', 'Geneva', 'Weiki', 'Issai', 'Jumbo', 'Ken's Red', and 'Maki' (Pinto et al., 2020). It was found that the cultivar 'Ananasnaya' contains a higher AsA content compared with 'Geneva' (Latocha et al., 2013), whereas the AsA content found in one of the hardy kiwifruits *A. kolomikta* is over 1,000 mg/100 g of fresh weight (FW) (Latocha et al., 2010). The total sugar content ranges from 6.2 to 9.6 g/100 g FW in different hardy kiwifruit cultivars (Wojdyło et al., 2017). Cultivar 'HR' and 'CJ-1' comprise around two times higher total phenolic content than 'LD-121' (Zhang et al., 2021).

According to the authors, changes in biochemical, phenolic, and antioxidant properties in fruit considerably differ not only among cultivar types and growing regions but also in the degree of fruit maturity at harvest (Lee et al., 2015; Park et al., 2022). However, as far as we know, most recent studies focus on comparing the phytochemical and antioxidant properties of selected fruit cultivars at commercial harvest, but there is little information on the changes that occur in nutritional composition of hardy kiwifruit during maturation (Boldingh et al., 2000; Han et al., 2019; Li et al., 2021). In order to better understand the nutritional value offered by hardy kiwifruit during the maturity stages of the fruit, it is imperative to study the changes in the nutritional contents of commercially grown

hardy kiwifruit cultivars. The objective of this study was to quantify the accumulation of nutritional compounds and antioxidant capacity in two hardy kiwifruit cultivars 'Yilv' and 'Lvmi-1' grown in Sichuan Province, China, at different fruit maturity stages. We first determined the dynamic phenotypic changes of these two cultivars during fruit maturity. Subsequently, the composition of sugars and organic acids was assessed to give more detailed information about the physiochemical changes. Finally, the antioxidant capacity was also measured during fruit maturity. These findings would be beneficial for providing critical information on selecting the best harvest stage of these varieties, which would facilitate the extension of cultivation of these two cultivars and the improvement of other kiwifruit varieties.

Materials and methods

Plant materials and sample preparation

The fruit samples were the same with those in our previous study (Lin et al., 2022). Fruits of 'Yilv' and 'Lvmi-1' were collected from Sichuan Innofresh Agricultural Science and Technology Co., Ltd. A total of about 1,000 flowers from at least 150 plants (4 years old) were tagged. Fruits at 30 days post anthesis (DPA), 40 DPA, 50 DPA, 60 DPA, 70 DPA, and 80 DPA were collected for measurement. For each cultivar, 90 fruits were harvested without physical injuries in total, 60 of which were used for biological trait determination in three biological replicates with 20 fruits each. The other 30 fruits were frozen in liquid nitrogen and stored at −80°C and were used for RNA extraction and real-time quantitative PCR (qPCR) analysis. Each 10 fruits were randomly selected as one biological replicate.

Measurement of fruit phenotypic characteristics

Fruit length and width referring to the vertical diameter and fruit diameter, respectively, were measured using a vernier caliper. The fruit firmness was measured using a penetrometer (model SMTT50; Toyo Baldwin, Tokyo, Japan) fitted with a 5-mm plunger.

Determination of titratable acidity and total soluble solids

Titratable acidity (TA) was determined by titration aliquots of homogenate of fresh fruits by 0.1 N NaOH to an end point of pH 8.1 using an automatic pH titration system (pH meter type IQ 150; Warsaw, Polska) and expressed as citric acid equivalents. Total soluble solids (SSC) were determined in fresh juices with a refractometer (Atago RX-5000, Atago Co., Ltd., Japan) and expressed as °Brix.

Quantification of starch and sugar content

Soluble sugars, including glucose, fructose, and sucrose, were extracted and analyzed as previously described with some modification (Li et al., 2019). Fresh samples (100 mg) were added to 5 ml of distilled water and homogenized for 1 min. The mixture was then extracted in a water bath at 80°C for 30 min. The supernatant was collected after centrifugation at 8,000g at room temperature for 5 min, filtered through a 0.45-μm cellulose acetate filter, and then analyzed by HPLC using an Agilent 1260 instrument equipped with a refractive index detector (Agilent Technologies, Inc., Palo Alto, USA). Samples (10 μl) were separated at 35°C on an Agilent ZORBAX carbohydrate column (250 × 4.6 mm i.d.; 5 μm particle size) using 80% acetonitrile at a flow rate of 1.0 ml per min. Contents of individual soluble sugars (glucose, fructose, and sucrose) were determined using the standard calibration curves for each sugar (Sangon Biotech Co., Ltd., Shanghai, China).

Starch content was measured as previously described (Li et al., 2021). The precipitation obtained when extracting sugars was autoclaved for 1 h and then incubated in 55°C with amyloglucosidase in 0.25 M acetate buffer (pH 4.5) for 1 h. The sample was then centrifuged for 10 min at 7,000 rpm, and the supernatant was used to determine the starch concentration using a colorimetric measurement.

Extraction, identification, and quantification of organic acid compounds

Organic acid compound extraction was conducted according to the previous method (Wojdyło et al., 2017), with slight modifications. Fresh sampled fruits (0.5 g) were mixed with 20 ml of H_2O, boiled at 100°C for 20 min, sonicated for 15 min, and centrifuged at 10,000 g for 15 min. The supernatant was filtered through a 0.45-μm cellulose acetate filter and then analyzed by HPLC using an Agilent 1260 instrument equipped with a refractive index detector (Agilent Technologies, Inc., Palo Alto, USA). The elution system consisted of 40 mM KH_2PO4–H_3PO4 buffer (pH 2.4) with a flow rate of 0.6 ml min^{-1}. Organic acids were separated on an ODS C18 column (250 × 4.6 mm i.d.; 5 μm particle size) and detected using a diode-array detector set up at 210 nm. Standard curves for pure standards of organic acids (oxalic, citric, malic, and quinic acids) (Sigma, Poole, Dorset, UK) were used for quantification.

Determination of total phenolic content and total flavonoid content

Total phenolic content (TPC) of the hardy kiwifruit was measured using the Folin–Ciocalteu method with minor modification (Lee et al., 2019). The fruit extract (300 µl) was mixed with Folin–Ciocalteu's phenol reagent (400 µl); after 5 min in darkness, 2 ml of 5% Na_2CO_3 was added, and the final volume was adjusted to 10 ml with distilled water. After incubating for 60 min at room temperature, the absorbance value was read at 765 nm using a spectrophotometer. TPC was expressed in mg gallic acid equivalents (GAE)/100 g FW.

Total flavonoid content (TFC) was measured using a modified colorimetric method described by Kim (Kim et al., 2003). The fruit extract (150 µl) was mixed with deionized water (3.2 ml) and 5% (w/v) $NaNO_2$ solution (150 µl) and incubated at room temperature for 5 min. A volume of 150 ml of 10% (w/v) $Al(NO_3)_3$ solution was added to the mixture and further incubated at room temperature for 1 min. The mixture was mixed with 1 M NaOH (1 ml) and measured immediately at 510 nm using the spectrophotometer. TFC of hardy kiwifruit was expressed in mg rutin equivalents (RE)/100 g FW.

Antioxidant capacity assays

2,2-Azino-bis(3-ethylbenzothia-zoline-6-sulfonic acid) (ABTS), 2,2-diphenyl-1-picrylhydrazyl radical (DPPH), and ferric reducing antioxidant power (FRAP) assays were conducted by the previous method (Barreca et al., 2011). For ABTS assay, 5 ml aqueous ABTS solution (7 mM) was added to 88 µl of 140 mM of a potassium per sulfate solution, which was heated in a water bath at 70°C for 30 min to create ABTS radicals. The solution of ABTS radicals was adjusted to an absorbance of around 0.650 at 734 nm. The reaction between the ABTS radical solution (980 ml) and the appropriately diluted extracts (20 ml) was conducted at 37°C for 10 min. Absorbance at 734 nm was measured using the spectrophotometer immediately. DPPH was determined as described. The absorbance of fresh DPPH radicals in 80% (v/v) aqueous methanol was set to 0.650 at 517 nm. The reaction between DPPH radical solution (2.95 ml) and the appropriately diluted extracts (50 ml) took place at 23°C for 30 min. The reduction of absorbance at 517 nm was measured immediately. FRAP reagent was prepared by mixing 200 ml acetate buffer (300 mM, pH 3.60), 20 ml TPTZ solution (10 mM in 40 mM HCl), and 20 ml of $FeCl_3{\cdot}6H_2O$ solution (20 mM). FRAP reagent (3.80 ml) was added to 200 µl of fruit extract. After 30 min at ambient temperature, the absorbance was detected at a wavelength of 593 nm. The results of ABTS, DPPH, and FRAP were represented as µmol of Trolox equivalent (TE) per gram dry wight (µmol TE/g DW) for fruits.

Real-time qPCR reactions

Total RNA was isolated by using the improved CTAB method (Lin et al., 2022) and subsequently quantified by electrophoresis and using a NanoDrop nucleic acid protein analyzer. First-strand cDNA was synthesized referring to the instructions of the reverse transcription kit of Beijing Quanshijin Biotechnology Co., Ltd. qPCR reactions were carried out with SYBR qPCR Mix using a Bio-Rad CFX96 Real-Time System. *AaActin* was used as the internal control to normalize gene expression. The relative expression levels of genes were calculated based on the $2^{-\Delta\Delta CT}$ method. The primer sequences were designed using Primer Premier 5.0 software, and the sequence information is listed in Table S1 (Supplementary Table 1). The expression of six key enzymes involved in sugar and starch metabolism were detected, including neutral invertase (NI), soluble acid invertase (SAI), sucrose synthase (SS), sucrose phosphate synthase (SPS), hexokinase (HK), and fructokinase (FK).

Data analysis

Statistical analysis was performed using SPSS 19.0 software (SPSS Inc., Chicago, IL, USA), and significant differences among the samples were calculated using one-way ANOVA followed by Duncan's multiple-range test at the 5% level ($p < 0.05$). Data were expressed as the means ± SD (standard deviation), and each sample has three independent repeats. Principal component analysis (PCA) and Pearson correlation matrix were performed using Origin 2017 and the statistical program R (version 3.5.0), respectively. Correlation analysis was also conducted by SPSS 19.0 software using Pearson's method.

Results

Morphological characteristics of fruit

As shown in Figure 1A, a visual inspection of six different representative stages during fruit development and maturity of 'Yilv' and 'Lvmi-1' appeared with different morphology, which was supported by the following equatorial diameter (Figure 1B), vertical fruit diameter (Figure 1C), and shape index of fruit (Figure 1D) measurement during the development. The results (Figure 1) showed that 'Yilv' and 'Lvmi-1' are both in small size

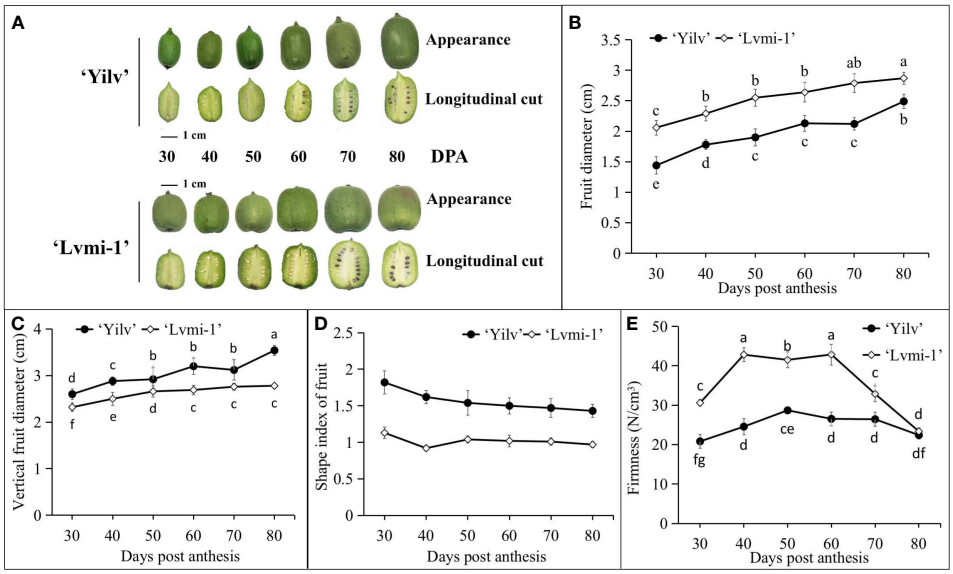

FIGURE 1
Morphological characteristics of the 'Yilv' and 'Lvmi-1' fruits. **(A)** Fruit phenotypes during development and maturity. **(B)** Diameter of fruit changes during fruit development. **(C)** Changes of vertical diameter of fruit in different developmental stages. **(D)** Shape index of fruit during development. **(E)** Firmness changes in different developmental stages of 'Lvmi-1' and 'Yilv' fruit. Data were represented by the mean values ± standard deviation. Different letters indicated significant difference at the $p \leq 0.05$ level.

with fruit diameter below 3 cm at 80 DPA. Moreover, the fruit diameter of 'Lvmi-1' was significantly higher than that of 'Yilv', whereas the vertical fruit diameter of these two cultivars showed no significant difference. Thus, the shape index of fruit (ratio of vertical diameter and equatorial diameter) of 'Lvmi-1' was significantly lower than 'Yilv'. Furthermore, the seeds of the 'Yilv' fruit appeared to turn to black at 60 DPA, whereas the seeds of the 'Lvmi-1' fruit turned to black around 10 days later at 70 DPA. This result of firmness determination showed that the firmness of the 'Lvmi-1' and 'Yilv' fruits decreased at 70 and 60 DPA, respectively, and 'Lvmi-1' comprised a significant higher firmness level than 'Yilv' at the early stages, whereas no significant difference of firmness in 'Yilv' and 'Lvmi-1' at the mature stage (80 DPA) was observed, indicating that the decrease of 'Lvmi-1' firmness was more rapid than that of 'Yilv' during development and maturity (Figure 1E). It was also found that there were two rapid growth periods (50–60 and 70–80 DPA) of 'Yilv' fruit, during which the fruit length and diameter increased rapidly, while the fruit of 'Lvmi-1' appeared a steady increase during the whole development process (Figure 1).

Conventional nutrient content during fruit development

According to the results, a general increase of TA (Figure 2A) and SSC (Figure 2B) in 'Yilv' and 'Lvmi-1' was observed. A significant higher TA level while a lower SSC level was shown in 'Yilv' than 'Lvmi-1' at the mature stage (80 DPA) (Figure 2B). No significant difference of SSC between 'Yilv' and 'Lvmi-1' was observed during the fruit development and maturity (30–70 DPA). In addition, the antioxidants including total phenolic and flavonoid were also estimated. As a result, the TPC and TFC showed a gradual decrease during fruit development and maturity (Figures 2C, D). There was no significant difference of TPC in 'Yilv' and 'Lvmi-1' during fruit development, except for that at 30 and 80 DPA, in which 'Yilv' exhibited a comparatively higher level of TPC than 'Lvmi-1'. By contrast, the fruit of 'Yilv' contained a lower level of TFC than the 'Lvmi-1' fruit during the fruit development until 80 DPA.

Antioxidative characterization during fruit development

Since the fruit maturity is recognized as an oxidative process, the antioxidative activity during the fruit development and maturity was measured to characterize the differences between two cultivars. Generally, as detected by FRAP (Figure 3A), ABTS (Figure 3B), and DPPH scavenging activity (Figure 3C), the antioxidative activity gradually decreased during fruit development and ripening. There was no significant difference between 'Yilv' and 'Lvmi-1' with ABTS level. For the FRAP level,

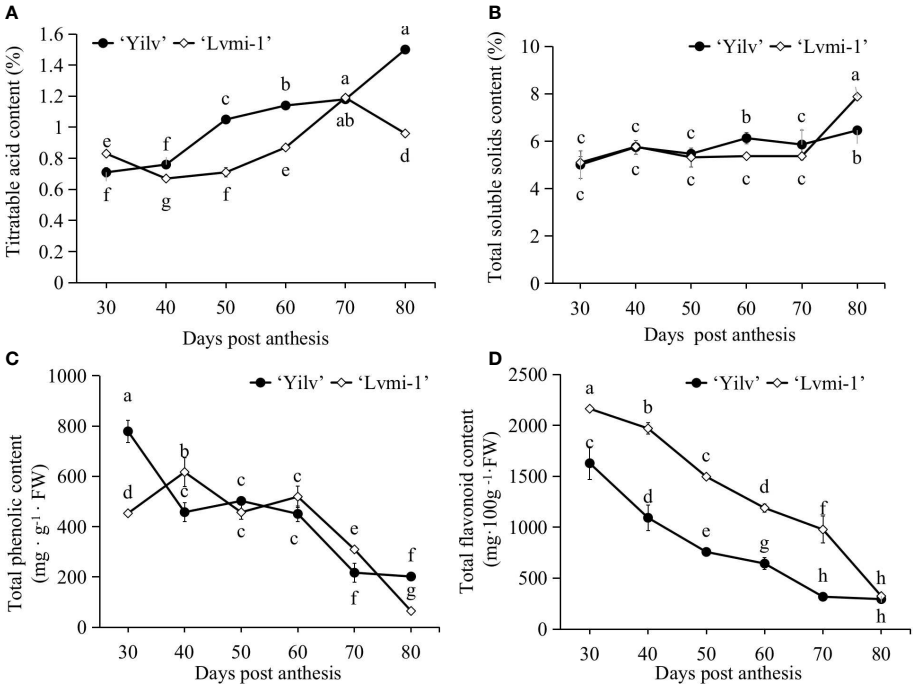

FIGURE 2
Changes of conventional nutrient contents in 'Yilv' and 'Lvmi-1' fruits during fruit development and maturity. **(A)** Titratable acid content changes during fruit development. **(B)** Total soluble solid content changes during fruit development. **(C)** Total phenolic content changes during fruit development. **(D)** Total flavonoid content changes during fruit development. Data were represented by the mean values ± standard deviation. Different letters indicated significant difference at $p \leq 0.05$ level. The titratable acid content was expressed as citric acid equivalents.

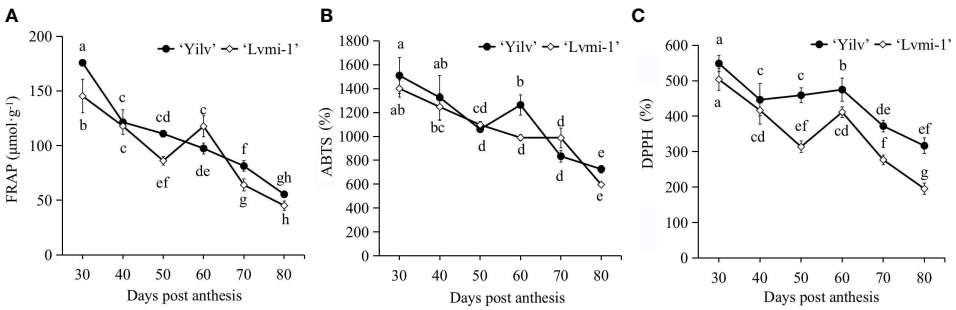

FIGURE 3
Changes of antioxidant activity of 'Yilv' and 'Lvmi-1' fruits during fruit development and maturity. **(A)** Ferric reducing antioxidant power, FRAP. **(B)** 2,2'-Azino-bis (2-ethylbenzothizoline-6-sulfonic acid), ABTS. **(C)** 2,2-Diphenyl-1-picrylhydrazyl radical, DPPH. Data were represented by the mean values ± standard deviation. Different letters indicated significant difference at the $p \leq 0.05$ level.

a significant difference was only observed at 30, 50, and 60 DPA. However, except for the level at 30 and 40 DPA, the DPPH level was higher in 'Yilv' fruit than in 'Lvmi-1'. Moreover, the highest antioxidative activity was detected by ABTS (Figure 3B), followed by DPPH (Figure 3C), and the lowest was detected by FRAP (Figure 3A), but the general change pattern during fruit development detected by these three different methods was the same.

Changes of organic acids in 'Lvmi-1' and 'Yilv'

The accumulation of organic acid is one of the most important traits of fruit development and maturity; to elucidate more differences between hardy kiwifruit cultivar 'Yilv' and 'Lvmi-1' during the fruit ripening, the dynamic changes of organic acid components were determined by HPLC methods. Based on the results, oxalic acid (Figure 4A) showed no obvious increase or decrease patterns in both cultivars. It remained at a relatively stable level during the development of 'Lvmi-1'. The content of quinic acid (Figure 4B) gradually increased during fruit development, and a higher level in 'Yilv' at 30 and 80 DPA was observed compared with 'Lvmi-1', whereas citric acid (Figure 4C) gradually increased from 30 to 80 DPA in both cultivars and a higher level in 'Yilv' fruit was found. Furthermore, malic acid (Figure 4D) did not show a regular change pattern in both cultivars, and it did not show significant change during fruit development of 'Lvmi-1'. In addition, the oxalic acid content was the lowest compared with other three acids, the highest content proved to be quinic acid at the early developmental stages while citric acid at the late maturity stages in both 'Yilv' and 'Lvmi-1'.

Changes of starch and sugar during the fruit development

As shown in Figure 5A, it was evident that the starch level increased from 30 to 60 and 70 DPA, respectively, in 'Yilv' and 'Lvmi-1' fruits, and it was sharply decreased thereafter until 80 DPA. A significantly higher level of starch was observed in 'Yilv' from 40 to 70 DPA compared with 'Lvmi-1'. In terms of sugar content, the fructose content accumulated at a high level at 30 and 40 DPA; thereafter, it decreased until 60 DPA and increased again at 70 and 80 DPA (Figure 5B). The sucrose content increased and reached a peak at 50 DPA and decreased during the later maturity stages in 'Lvmi-1', whereas it decreased from 30 to 40 DPA and then increased to 60 DPA and finally decreased at 70 DPA and increased at 80 DAP (Figure 5C). Although the glucose content showed a gradual increase during the whole fruit development and maturity, the accumulation level of glucose was the lowest compared with the fructose and sucrose content in the 'Lvmi-1' fruit (Figure 5D). Similar change patterns were also observed in 'Yilv' fruit (Figure 5). Interestingly, the predominant sugar was speculated to be fructose in the 'Lvmi-1' fruit while sucrose in the 'Yilv' fruit

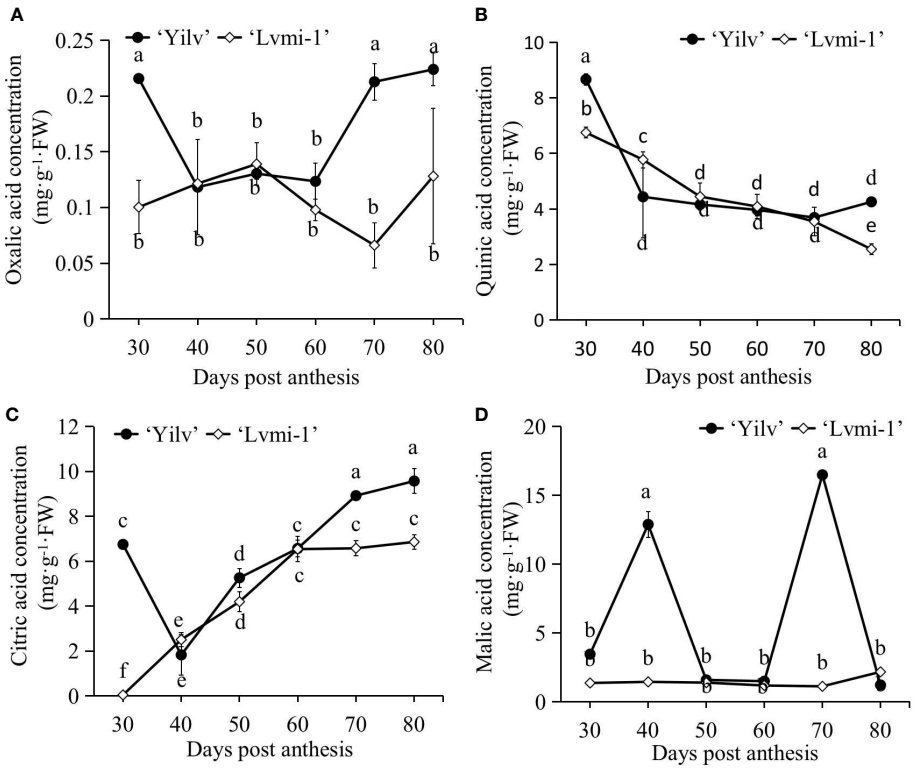

FIGURE 4
Changes of organic acid composition and content of 'Yilv' and 'Lvmi-1' fruits during fruit development and maturity. **(A)** Oxalic acid content. **(B)** Quinic acid content. **(C)** Citric acid content. **(D)** Malic acid content. FW, fresh weight. Data were represented by the mean values ± standard deviation. Different letters indicated significant difference at the $p \leq 0.05$ level.

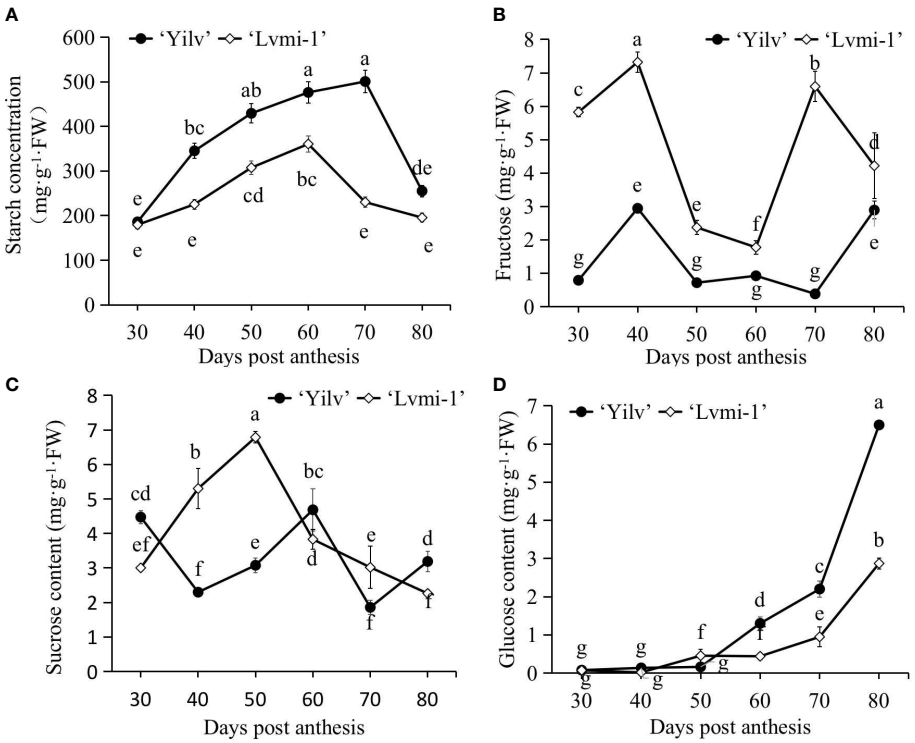

FIGURE 5
Changes in sugar and starch content of 'Yilv' and 'Lvmi-1' fruit during fruit development and maturity. **(A)** Starch content. **(B)** Fructose content. **(C)** Sucrose content. **(D)** Glucose content. FW, fresh weight. Data were represented by the mean values ± standard deviation. Different letters indicated significant difference at the $p \leq 0.05$ level.

according to the highest level of the three determined sugar components.

Principal component analysis and correlation analysis

In order to identify the necessary components explaining the greater part of variances, all of the physiological changes in the two cultivars were subjected to PCA. As a result (Figure 6A), the first and second principal components (PC1 and PC2) accounted for 45.5% and 25.0% of the total variation, respectively. The points of different developmental stages were obviously separated along PC1, whereas the points of different cultivars were mainly separated along PC2, revealing the variance between cultivars and developmental stages. In addition, the content of quinic acid, total phenolic, and antioxidant capacity was positively related to the early (DPA 30–60) developmental stages of 'Yilv'. Meanwhile, the organic acid content was positively related to the late stages in 'Yilv'. By contrast, in 'Lvmi-1', a performance of sugar (sucrose and fructose), total flavonoid, and firmness was observed in the early developmental stages, and a preference of fruit weight, diameter, and TSS in the late stages of 'Lvmi-1' occurred.

Correlation analysis suggested that FRAP, ABTS, and DPPH were positively correlated in both 'Yilv' and 'Lvmi-1' cultivars (Figures 6B, C), implying the consistency and accuracy of antioxidant capacity using different detection methods. Moreover, TPC and TFC were significantly and positively correlated with each other, indicating their similar change trend. Specifically, in the 'Lvmi-1' fruit, only TFC was significantly positively correlated with FRAP, ABTS, and DPPH (Figure 6B), suggesting it might contribute more to the total antioxidant capacity than TPC in this cultivar. Furthermore, a strong negative correlation between fruit morphology and antioxidant capacity was observed, indicating a decrease trend for antioxidant capacity during fruit development. Citric acid and quinic acid were shown to be highly positively and negatively related to fruit morphology, respectively. However, in the 'Yilv' fruit, TPC and TFC showed a high positive correlation with FRAP, ABTS, and DPPH during development (Figure 6C), revealing their significant contribution on the antioxidant capacity. Glucose content and TSS were suggested to be positively correlated with fruit

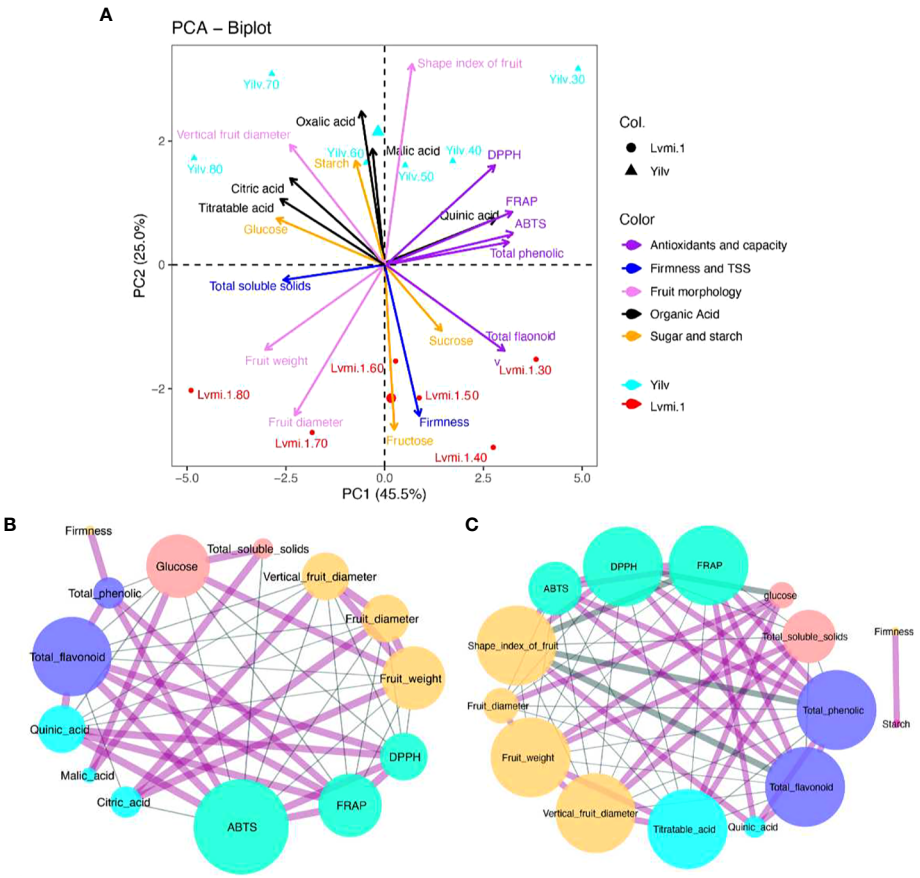

FIGURE 6
PCA biplot and correlation analysis. **(A)** PCA biplot. **(B)** Correlation analysis in 'Lvmi-1'. **(C)** Correlation analysis in 'Yilv'. Correlation pairs with |r| >0.8 are shown; the edge indicates coefficient r values. The red line indicates a positive correlation; the blue line indicates a negative correlation. Different colors of node circles present different types of compounds: purple indicates the antioxidants, yellow represents fruit morphological characteristics, pink and blue indicate sugar and organic acids, respectively, and the green circles indicate the antioxidant capacity. Size of nodes indicates the correlated node numbers.

morphology. A strong correlation between starch and firmness was also found in 'Yilv' fruit.

Expression analysis of the starch and sugar metabolism-related genes during fruit development

To deeply explore the molecular mechanism of starch and sugar changes during fruit development in these two cultivars, the expression of related key genes was detected by qPCR. It was shown (Figure 7) that the highest level of *SS* gene expression appeared at 30 DPA in both cultivars, then it gradually decreased from 40 to 80 DPA. A higher level of *SS* expression was observed in the early developmental stages (30 to 60 DPA), whereas no significant difference was found on 60, 70, and 80 DPA. On the contrary, the expression of the *SPS* gene displayed the opposite trend. The expression of *SPS* steadily increased from the early stage to the late mature stage, and a significantly higher level occurred in 'Lvmi-1' from 50 to 80 DPA. The expression of *SAI* and *NI* exhibited similar decrease change patterns in both cultivars. They both peaked at 30 DPA and gradually decreased with fruit maturity in 'Yilv', whereas they increased first from 30 to 60 DPA and decreased subsequently in 'Lvmi-1'. The highest *HK* expression was detected at 50 DPA in both 'Lvmi-1' and 'Yilv', whereas the expression at other developmental stages was low and no obvious change was observed. For the expression of *FK*, it decreased from 30 to 50 DPA and thereafter remained at a relatively stable level in 'Yilv'. In 'Lvmi-1', it increased from 30 to 50 DPA and showed a slight decrease then. These results indicated different expression patterns of the key related genes in two cultivars.

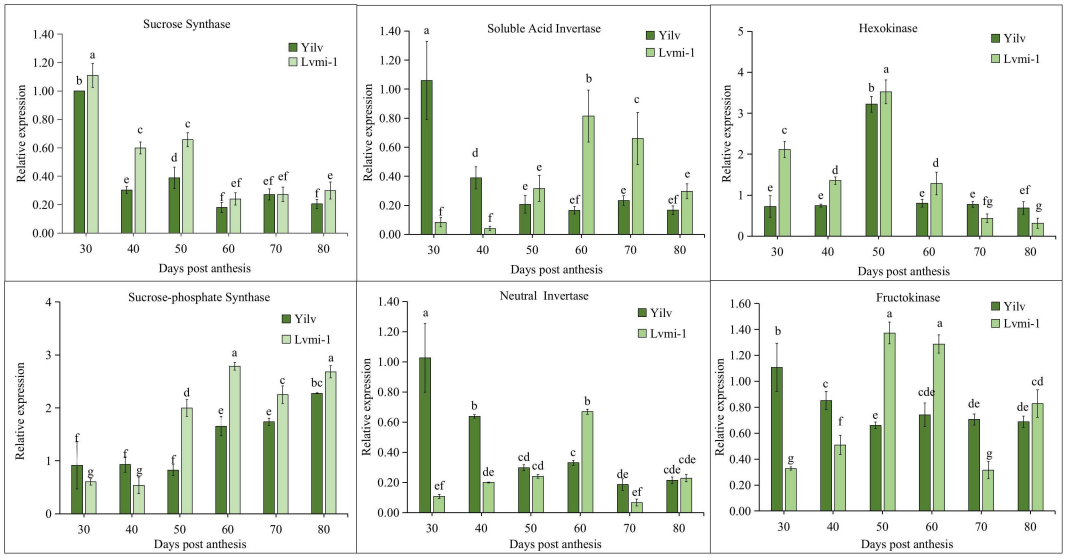

FIGURE 7
Expression profiling of genes related to sugar and starch metabolism during fruit development in 'Yilv' and 'Lvmi-1'. Relative expression was normalized against the value in the 'Yilv' fruit at 30 DPA. Error bars indicated the standard deviation of three biological replicates. Different letters indicated significant difference at the $p \leq 0.05$ level.

Correlation analysis of the starch and sugar content and related gene expression

To investigate the relationship between gene expression and the content of sugar and starch, Pearson correlation analysis was conducted. As shown in Table 1, most of the gene expressions were negatively correlated with sugar and starch in the 'Yilv' fruit during development. An exception was observed in *HK* and *SPS* expressions, which exhibited a positive correlation with sucrose, fructose, and starch content, although only *SPS* expression and glucose were correlated at a significant level (Table 1). Interestingly, in the 'Lvmi-1' fruit, the gene expression of *FK* was significantly negatively correlated with fructose content but positively correlated with the content of starch. Similarly, *NI* expression also showed a highly positive correlation with starch, indicating they had important roles in the accumulation of starch during fruit development (Table 2). Moreover, the expression of *SS* was positively correlated with sucrose and fructose but negatively correlated with glucose and starch, whereas a totally opposite correlation was found in *SPS* and *SAI* expressions. The expressions of *HK* and *NI* displayed a positive correlation with sucrose and starch but a negative correlation with glucose and fructose. Overall, these results indicated the different accumulation of sugar and starch and corresponding potential molecular mechanism in 'Yilv' and 'Lvmi-1'.

TABLE 1 Correlation coefficient between expression of related key genes with sugar and starch content in 'Yilv'.

	Expression level						Sucrose	Glucose	Fructose	Starch
	SS	HK	NI	SPS	SAI	FK				
Sucrose	-0.099	0.801	-0.027	-0.728	-0.200	-0.240	1			
Glucose	-0.420	-0.178	-0.570	0.853*	-0.446	-0.485	-0.544	1		
Fructose	-0.314	-0.330	0.011	0.233	-0.170	-0.060	-0.082	0.418	1	
Starch	-0.658	0.282	-0.686	0.101	-0.702	-0.681	0.346	-0.184	-0.439	1

*Significant differences at the 0.05 level.

TABLE 2 Correlation coefficient between expression of related key genes with sugar and starch content in 'Lvmi-1'.

	Expression level						Sucrose	Glucose	Fructose	Starch
	SS	HK	NI	SPS	SAI	FK				
Sucrose	0.203	0.790	0.102	-0.238	-0.195	0.508	1			
Glucose	-0.521	-0.561	-0.065	0.621	0.116	0.074	-0.544	1		
Fructose	0.262	-0.387	-0.745	-0.665	-0.502	-0.932**	-0.244	-0.142	1	
Starch	-0.422	0.334	0.819*	0.513	0.670	0.822*	0.494	-0.280	-0.769	1

*Significant differences at the 0.05 level.
**Significant differences at the 0.01 level.

Discussion

The general morphological characterization and nutritional content of hardy kiwifruit

In China, hardy kiwifruit is considered as an underutilized fruit; the varieties are only cultivated and consumed in certain provinces. The two cultivars in the present study are cultivated in Ya'an, Sichuan; little information about their physicochemical changes during maturity is available until now. Morphological appearances and physicochemical features including TSS, firmness, AsA content, and TA are fruit quality traits which could be used to indicate the maturation, harvest time, and shelf life (Wang et al., 2021). Fruit maturity is depicted by a decrease in firmness, TA reduction, and TSS increase (Krupa et al., 2011; Mitalo et al., 2019). Therefore, it could be speculated that 'Lvmi-1' starts to mature earlier at 60 DPA, whereas 'Yilv' might be later at 70 DPA according to our results obtained in this study. From 60 DPA, the 'Lvmi-1' fruit showed a slow increase in fruit size, a significant decrease in fruit firmness, a rapid increase in fructose content, and a peak of starch content, whereas these changes started from 70 DPA in the 'Yilv' fruit. Moreover, TSS and TA can reflect the taste of fruit. The TSS increased rapidly from 70 to 80 DPA (Figure 2), which were similar among the two cultivars. This was similar with other studies on TSS in *A. deliciosa*, *A. chinensis*, and *A. arguta* (Boldingh et al., 2000; Ainalidou et al., 2016; Li et al., 2021). Correspondingly, the TA started to decrease in 'Lvmi-1' at 70 DPA, indicating that the fruit of this cultivar might start to form a good taste. Overall, the seasonal fruit quality and physiological characteristics reported here could provide basic data for evaluating the harvest time of hardy kiwifruit cultivars 'Yilv' and 'Lvmi-1'.

The antioxidant capacity in hardy kiwifruit

The TPC and TFC were among the most important antioxidant compounds contributing to total antioxidant capacity. Various studies have revealed a positive correlation between the phenolic content and antioxidant activity (Wojdyło and Nowicka, 2019). Consistent with this, the correlation analysis in the present study showed that the TPC and TFC were significantly positively correlated with the antioxidant capacity in 'Yilv' fruit (Figure 6C), indicating their important contributions on antioxidant capacity. This is consistent with a previous study (Jeong et al., 2020), in which a high correlation between TPC, TFC, and antioxidant capacity during the cold storage of hardy kiwifruits was proposed, whereas in the 'Lvmi-1' fruit, only a correlation between TFC and antioxidant capacity was observed (Figure 6B), suggesting that their contribution may vary with cultivars in hardy kiwifruit. It has also been suggested that TPC and TFC are significantly different among the hardy kiwifruit genotypes at the maturity stage (Wang et al., 2018). Similarly, our results showed that 'Yilv' contained significantly higher TPC than the 'Lvmi-1' fruit (Figure 2C), indicating a probable higher antioxidant capacity of the 'Yilv' fruit than that of 'Lvmi-1'. This was also supported by the subsequent antioxidant capacity assays, which showed a slightly higher level of antioxidant capacity (ABTS, DPPH, and FRAP) in 'Yilv' than in 'Lvmi-1' (Figure 2). Moreover, the antioxidant capacity determined by three different methods in this study have shown similar patterns during the maturity time, indicating the reliability of the determination.

The organic acid, starch, and sugar changes in hardy kiwifruit

Generally, most hardy kiwifruits have citric and quinic acids as their predominant organic acids, followed by malic acid (Latocha, 2017; Wojdyło et al., 2017). Consistent with this, our results have found that the predominant acids in 'Yilv' and 'Lvmi-1' were citric acid followed by quinic acid, malic acid, and oxalic acid (Figure 4). The citric acid level gradually increased during the maturity time and was determined to be 5–10 g/100 g FW in the mature 'Yilv' and 'Lvmi-1' fruits (Figure 4C), which is consistent with a previous report (Wojdyło et al., 2017). However, the content of hardy kiwifruit was only 0.5–1.5 g/100 g FW in

Japan (Nishiyama et al., 2008), which might be due to the different growth areas of plants. Moreover, quinic acid was prevalent in the young fruit and decreased thereafter (Figure 4B), whereas the amount of malic acid and oxalic acid was little affected by fruit maturity in 'Lvmi-1', which is the same with previous results (Kim et al., 2012). The two abnormal-like peaks of malic acid at 40 and 70 DPA in the 'Yilv' fruit might be caused by the measured sample specificity. The balance between sugars and organic acids strongly influences the sensory properties and fruit palatability (Jaeger et al., 2003). It has been suggested that the main soluble sugars in kiwifruit (*A. deliciosa*) are glucose and fructose, with a smaller amount of sucrose present, whereas sucrose is the predominant sugar in hardy kiwifruit (*A. arguta*) followed by glucose and fructose (Park et al., 2006; Kim et al., 2012). At the mature stage, the highest level of sugar was proven to be glucose in 'Yilv' and sucrose in 'Lvmi-1'; our results (Figure 5) show similar results. The hardy kiwifruit also accumulates a high level of starch. The two cultivars detected in this study showed similar changes in starch content over the fruit development period. For 'Yilv', starch accumulation occurred between 40 and 70 DPA, which is longer than that of 'Lvmi-1' between 40 and 60 DPA (Figure 5A). This difference probably resulted from dilution caused by cultivar difference in growth (Moscatello et al., 2011); the larger growth of 'Lvmi-1' than 'Yilv' fruit might cause the decrease and continuous increase in starch content in corresponding cultivar. A decrease in starch level was observed for both cultivars (Figure 5A) in the late developmental stages, which is similar with other studies (Li et al., 2021). This decrease might be caused by the conversion of starch to total sugar content (Ghasemnezhad et al., 2013).

Key genes involved in sugar metabolism in hardy kiwifruit

Sweetness is one of the most important quality traits for kiwifruit cultivation and breeding. Sugars including sucrose, fructose, and glucose are important molecules in plants and function in many processes (Smeekens et al., 2010). However, there was limited information about the expression analysis of key genes involved in sugar metabolism in hardy kiwifruit. Here, the expression analysis of key genes encoding the crucial enzymes related to sugar metabolism showed that *SS* was highly expressed in immature fruit and gradually decreased in subsequent stages of fruit development, whereas *SPS* exhibited a low expression in immature fruit and a higher expression level in mature stages (Figure 7). This result is in consistent with that of *A. chinensis* as previously suggested (Tang et al., 2016). Moreover, *SPS* expression significantly positively correlated with glucose content in the 'Yilv' fruit (Table 1), which indicated the important role of *SPS* in glucose accumulation. Fructose, another one of the most important sugars in kiwifruit, can be phosphorylated to fructose-6-phosphate by *FK* (Granot, 2007). It was suggested by our results that in the 'Lvmi-1' fruit, *FK* expression negatively correlated with fructose but positively correlated with starch (Table 2), implying the conversion from fructose to starch content.

Conclusions

In summary, the phenotypes and metabolites vary with fruit development and ripening in cultivars of hardy kiwifruit. Specifically, the 'Yilv' fruit contains higher TFC and starch and glucose content than 'Lvmi-1', whereas the 'Lvmi-1' fruit might start to mature around 10 days earlier than the 'Yilv' fruit under the growth condition in Ya'an, Sichuan. Moreover, *SPS* and *FK* could be developed as candidates to regulate the sugar and starch content in hardy kiwifruit. The findings reported here contribute to a better understanding of the changes of nutritional compounds and antioxidants during fruit development and maturity in hardy kiwifruit.

Data availability statement

The original contributions presented in the study are included in the article/Supplementary Material. Further inquiries can be directed to the corresponding authors.

Author contributions

Authors' contributions: Conceived and designed the experiments: HT and YZ. Performed the experiments: YXL, HLT, BZ, XZ. Analyzed the data: YXL, DL and WY. Wrote the paper: YXL. Revised the paper: JF, YTZ, QC, YW, ML, YL, WH and XW. All authors contributed to the article and approved the submitted version.

Funding

This work was supported by the Double Support Project of Discipline Construction of Sichuan Agricultural University (03573134). The funding body had no role in the design of the study, collection, analysis and interpretation of data, and writing of the manuscript.

Acknowledgments

We thank College of Horticulture for providing the HPLC test system for sugar and organic acid content measurement in this study. We thank Sichuan Innofresh Agricultural Science and Technology Co., Ltd., for providing part of materials in this study.

Conflict of interest

Author JF was employed by Sichuan Innofresh Agricultural Science and Technology Co., Ltd.

The remaining authors declare that the research was conducted in the absence of any commercial or financial relationships that could be construed as a potential conflict of interest.

Publisher's note

Supplementary material

The Supplementary Material for this article can be found online at: https://www.frontiersin.org/articles/10.3389/fpls.2022.1087452/full#supplementary-material

References

Ainalidou, A., Tanou, G., Belghazi, M., Samiotaki, M., Diamantidis, G., Molassiotis, A., et al. (2016). Integrated analysis of metabolites and proteins reveal aspects of the tissue-specific function of synthetic cytokinin in kiwifruit development and ripening. *J. Proteomics* 143, 318–333. doi: 10.1016/j.jprot.2016.02.013

Barreca, D., Bellocco, E., Caristi, C., Leuzzi, U., and Gattuso, G. (2011). Elucidation of the flavonoid and furocoumarin composition and radical-scavenging activity of green and ripe chinotto (Citrus myrtifolia raf.) fruit tissues, leaves and seeds. *Food Chem.* 129, 1504–1512. doi: 10.1016/j.foodchem.2011.05.130

Boldingh, H., Smith, G. S., and Klages, K. (2000). Seasonal concentrations of non-structural carbohydrates of five actinidia species in fruit, leaf and fine root tissue. *Ann. Bot.* 85, 469–476. doi: 10.1006/anbo.1999.1094

Follett, P. A., Jamieson, L., Hamilton, L., and Wall, M. (2019). New associations and host status: Infestability of kiwifruit by the fruit fly species bactrocera dorsalis, zeugodacus cucurbitae, and ceratitis capitata (Diptera: Tephritidae). *Crop Prot.* 115, 113–121. doi: 10.1016/j.cropro.2018.09.007

Ghasemnezhad, M., Ghorbanalipour, R., and Shiri, M. A. (2013). Changes in physiological characteristics of kiwifruit harvested at different maturity stages after cold storage. *Agric. Conspec Sci.* 78, 41–47.

Granot, D. (2007). Role of tomato hexose kinases. *Funct. Plant Biol.* 34, 564–570. doi: 10.1071/FP06207

Han, N., Park, H., Kim, C.-W., Kim, M.-S., and Lee, U. (2019). Physicochemical quality of hardy kiwifruit (Actinidia arguta l. cv. cheongsan) during ripening is influenced by harvest maturity. *For. Sci. Technol.* 15, 187–191. doi: 10.1080/21580103.2019.1658646

Jaeger, S. R., Rossiter, K. L., Wismer, W. V., and Harker, F. R. (2003). Consumer-driven product development in the kiwifruit industry. *Food Qual Prefer* 14, 187–198. doi: 10.1016/S0950-3293(02)00053-8

Jeong, H. R., Cho, H. S., Cho, Y. S., and Kim, D. O. (2020). Changes in phenolics, soluble solids, vitamin c, and antioxidant capacity of various cultivars of hardy kiwifruits during cold storage. *Food Sci. Biotechnol.* 29, 1763–1770. doi: 10.1007/s10068-020-00822-7

Kim, J. G., Beppu, K., and Kataoka, I. (2012). Physical and compositional characteristics of 'mitsuko' and local hardy kiwifruits in Japan. *Hortic. Environ. Biotechnol.* 53, 1–8. doi: 10.1007/s13580-012-0066-7

Kim, D.-O., Jeong, S. W., and Lee, C. Y. (2003). Antioxidant capacity of phenolic phytochemicals from various cultivars of plums. *Food Chem.* 81, 321–326. doi: 10.1016/S0308-8146(02)00423-5

Krupa, T., Latocha, P., and Liwińska, A. (2011). Changes of physicochemical quality, phenolics and vitamin c content in hardy kiwifruit (*Actinidia arguta* and its hybrid) during storage. *Sci. Hortic.* 130, 410–417. doi: 10.1016/j.scienta.2011.06.044

Latocha, P. (2017). The nutritional and health benefits of kiwiberry (*Actinidia arguta*) - a review. *Plant Foods Hum. Nutr.* 72, 325–334. doi: 10.1007/s11130-017-0637-y

Latocha, P., Krupa, T., Wołosiak, R., Worobiej, E., and Wilczak, J. (2010). Antioxidant activity and chemical difference in fruit of different *Actinidia* sp. *Int. J. Food Sci. Nutr.* 61, 381–394. doi: 10.3109/09637480903517788

Latocha, P., Łata, B., and Stasiak, A. (2015). Phenolics, ascorbate and the antioxidant potential of kiwiberry vs. common kiwifruit: The effect of cultivar and tissue type. *J. Func Foods* 19, 155–163. doi: 10.1016/j.jff.2015.09.024

Latocha, P., Wołosiak, R., Worobiej, E., and Krupa, T. (2013). Clonal differences in antioxidant activity and bioactive constituents of hardy kiwifruit (*Actinidia arguta*) and its year-to-year variability. *J. Sci. Food Agric.* 93, 1412–1419. doi: 10.1002/jsfa.5909

Lee, I., Im, S., Jin, C.-R., Heo, H. J., Cho, Y.-S., Baik, M.-Y., et al. (2015). Effect of maturity stage at harvest on antioxidant capacity and total phenolics in kiwifruits (*Actinidia* spp.) grown in Korea. *Hortic. Environ. Biotechnol.* 56, 841–848. doi: 10.1007/s13580-015-1085-y

Lee, B. H., Nam, T. G., Kim, S. Y., Chun, O. K., and Kim, D. O. (2019). Estimated daily per capita intakes of phenolics and antioxidants from coffee in the Korean diet. *Food Sci. Biotechnol.* 28, 269–279. doi: 10.1007/s10068-018-0447-5

Leontowicz, H., Leontowicz, M., Latocha, P., Jesion, I., Park, Y.-S., Katrich, E., et al. (2016). Bioactivity and nutritional properties of hardy kiwi fruit *Actinidia arguta* in comparison with actinidia deliciosa 'Hayward' and *Actinidia eriantha* 'Bidan'. *Food Chem.* 196, 281–291. doi: 10.1016/j.foodchem.2015.08.127

Li, Y. F., Jiang, W., Liu, C., Fu, Y., Wang, Z., Wang, M., et al. (2021). Comparison of fruit morphology and nutrition metabolism in different cultivars of kiwifruit across developmental stages. *PeerJ* 9, e11538. doi: 10.7717/peerj.11538

Lin, Y., Zhao, B., Tang, H., Cheng, L., Zhang, Y., Wang, Y., et al. (2022). L-ascorbic acid metabolism in two contrasting hardy kiwifruit (*Actinidia arguta*) cultivars during fruit development. *Sci. Hortic.* 297, 110940. doi: 10.1016/j.scienta.2022.110940

Li, D., Zhang, X., Xu, Y., Li, L., Aghdam, M. S., and Luo, Z. (2019). Effect of exogenous sucrose on anthocyanin synthesis in postharvest strawberry fruit. *Food Chem.* 289, 112–120. doi: 10.1016/j.foodchem.2019.03.042

Mitalo, O. W., Asiche, W. O., Kasahara, Y., Tosa, Y., Tokiwa, S., Ushijima, K., et al. (2019). Comparative analysis of fruit ripening and associated genes in two kiwifruit cultivars ('Sanuki gold' and 'Hayward') at various storage temperatures. *Postharvest Biol. Technol.* 147, 20–28. doi: 10.1016/j.postharvbio.2018.08.017

Moscatello, S., Famiani, F., Proietti, S., Farinelli, D., and Battistelli, A. (2011). Sucrose synthase dominates carbohydrate metabolism and relative growth rate in growing kiwifruit (*Actinidia deliciosa*, cv Hayward). *Sci. Hortic.* 128, 197–205. doi: 10.1016/j.scienta.2011.01.013

Nishiyama, I., Fukuda, T., Shimohashi, A., and Oota, T. (2008). Sugar and organic acid composition in the fruit juice of different *Actinidia* varieties. *Food Sci. Technol. Res.* 14, 67–73. doi: 10.3136/fstr.14.67

Park, Y. S., Jung, S. T., Kang, S. G., Drzewiecki, J., Namiesnik, J., Haruenkit, R., et al. (2006). *In vitro* studies of polyphenols, antioxidants and other dietary indices in kiwifruit (*Actinidia deliciosa*). *Int. J. Food Sci. Nutr.* 57, 107–122. doi: 10.1080/09637480600658385

Park, H., Kim, M. J., Kim, C. W., Han, N., and Lee, U. (2022). Harvest maturity highly affects fruit quality attributes of ethylene-treated 'autumn sense' hardy kiwifruit. *For. Sci. Technol.* 18, 1–6. doi: 10.1080/21580103.2022.2027275

Pinto, D., Delerue-Matos, C., and Rodrigues, F. (2020). Bioactivity, phytochemical profile and pro-healthy properties of *Actinidia arguta*: A review. *Food Res. Int.* 136, 109449. doi: 10.1016/j.foodres.2020.109449

Silva, A. M., Pinto, D., Fernandes, I., Gonçalves Albuquerque, T., Costa, H. S., Freitas, V., et al. (2019). Infusions and decoctions of dehydrated fruits of *Actinidia arguta* and *Actinidia deliciosa*: Bioactivity, radical scavenging activity and effects on cells viability. *Food Chem.* 289, 625–634. doi: 10.1016/j.foodchem.2019.03.105

Smeekens, S., Ma, J., Hanson, J., and Rolland, F. (2010). Sugar signals and molecular networks controlling plant growth. *Curr. Opin. Plant Biol.* 13, 273–278. doi: 10.1016/j.pbi.2009.12.002

Tang, W., Zheng, Y., Dong, J., Yu, J., Yue, J., Liu, F., et al. (2016). Comprehensive transcriptome profiling reveals long noncoding RNA expression and alternative splicing regulation during fruit development and ripening in kiwifruit (*Actinidia chinensis*). *Front. Plant Sci.* 7, 335. doi: 10.3389/fpls.2016.00335

Wang, S., Qiu, Y., and Zhu, F. (2021). Kiwifruit (*Actinidia* spp.): A review of chemical diversity and biological activities. *Food Chem.* 350, 128469. doi: 10.1016/j.foodchem.2020.128469

Wang, Y., Zhao, C.-L., Li, J.-Y., Liang, Y.-J., Yang, R.-Q., Liu, J.-Y., et al. (2018). Evaluation of biochemical components and antioxidant capacity of different kiwifruit (*Actinidia* spp.) genotypes grown in China. *Biotechnol. Biotechnol. Equip* 32, 558–565. doi: 10.1080/13102818.2018.1443400

Wojdyło, A., and Nowicka, P. (2019). Anticholinergic effects of actinidia arguta fruits and their polyphenol content determined by liquid chromatography-photodiode array detector-quadrupole/time of flight-mass spectrometry (LC-MS-PDA-Q/TOF). *Food Chem.* 271, 216–223. doi: 10.1016/j.foodchem.2018.07.084

Wojdyło, A., Nowicka, P., Oszmiański, J., and Golis, T. (2017). Phytochemical compounds and biological effects of *Actinidia* fruits. *J. Func Foods* 30, 194–202. doi: 10.1016/j.jff.2017.01.018

Zhang, J., Tian, J., Gao, N., Gong, E. S., Xin, G., Liu, C., et al. (2021). Assessment of the phytochemical profile and antioxidant activities of eight kiwi berry (*Actinidia arguta* (Siebold & zuccarini) miquel) varieties in China. *Food Sci. Nutr.* 9, 5616–5625. doi: 10.1002/fsn3.2525

frontiers | Frontiers in Plant Science

TYPE Original Research
PUBLISHED 23 December 2022
DOI 10.3389/fpls.2022.1107687

OPEN ACCESS

EDITED BY
Zhenfeng Yang,
Zhejiang Wanli University, China

REVIEWED BY
Zhengke Zhang,
Hainan University, China
Hetong Lin,
Fujian Agriculture and Forestry University, China

*CORRESPONDENCE
Zengyu Gan
ganzy@jxau.edu.cn

†These authors have contributed equally to this work

SPECIALTY SECTION
This article was submitted to Crop and Product Physiology, a section of the journal Frontiers in Plant Science

RECEIVED 25 November 2022
ACCEPTED 12 December 2022
PUBLISHED 23 December 2022

CITATION
Lin D, Yan R, Xing M, Liao S, Chen J and Gan Z (2022) Fucoidan treatment alleviates chilling injury in cucumber by regulating ROS homeostasis and energy metabolism.
Front. Plant Sci. 13:1107687.
doi: 10.3389/fpls.2022.1107687

Fucoidan treatment alleviates chilling injury in cucumber by regulating ROS homeostasis and energy metabolism

Duo Lin†, Ruyu Yan†, Mengying Xing, Shuyuan Liao, Jinyin Chen and Zengyu Gan*

Jiangxi Key Laboratory for Postharvest Technology and Nondestructive Testing of Fruits and Vegetables, Collaborative Innovation Center of Postharvest Key Technology and Quality Safety of Fruits and Vegetables, Jiangxi Agricultural University, Nanchang, China

Introduction: Chilling injury is a major hindrance to cucumber fruit quality during cold storage.

Methods and Results: In this study, we evaluated the effects of fucoidan on fruit quality, reactive oxygen species homeostasis, and energy metabolism in cucumbers during cold storage. The results showed that, compared with the control cucumber fruit, fucoidan-treated cucumber fruit exhibited a lower chilling injury index and less weight loss, as well as reduced electrolyte leakage and malondialdehyde content. The most pronounced effects were observed following treatment with fucoidan at 15 g/L, which resulted in increased 1,1-diphenyl-2-picrylhydrazyl and hydroxyl radical scavenging rates and reduced superoxide anion production rate and hydrogen peroxide content. The expression and activity levels of peroxidase, catalase, and superoxide dismutase were enhanced by fucoidan treatment. Further, fucoidan treatment maintained high levels of ascorbic acid and glutathione, and high ratios of ascorbic acid/dehydroascorbate and glutathione/oxidized glutathione. Moreover, fucoidan treatment increased the activities of ascorbate peroxidase, monodehydroascorbate reductase, dehydroascorbate reductase, and glutathione reductase and their gene expression. Fucoidan treatment significantly delayed the decrease in ATP and ADP, while preventing an increase in AMP content. Finally, fucoidan treatment delayed the decrease of energy charge and the activities and gene expression of H^+-ATPase, Ca^{2+}-ATPase, cytochrome c oxidase, and succinate dehydrogenase in cucumber fruits.

Conclusion: Altogether, our findings indicate that fucoidan can effectively enhance antioxidant capacity and maintain energy metabolism, thereby improving cucumber cold resistance during cold storage.

KEYWORDS

cucumber fruit, chilling injury, fucoidan, antioxidant capacity, energy metabolism

1 Introduction

Cold storage is a common method of preserving horticultural products after harvest. However, for cold-sensitive horticultural products, such as cucumber (Wang et al., 2018; Wang et al., 2020a), peach (Song et al., 2022), and kiwifruit (Liu et al., 2023), low temperatures can cause chilling injury (CI). CI damages the permeability of the fruit cell membrane, leading to cytoplasmic leakage. When cucumber fruit is transferred from cold storage to room temperature, the symptoms of CI appear quickly, manifested as watery spots on the fruit epidermis and an unpleasant odor, which are generally deemed unacceptable by consumers (Tsuchida et al., 2010; Wang et al., 2018).

Cold stress induces the accumulation of reactive oxygen species (ROS) in plant tissues, leading to a series of oxidative damage events, such as membrane lipid peroxidation, and eventually inducing cell death (You and Chan, 2015; Mittler et al., 2022). The plant ROS-scavenging system consists of an enzymatic defense system and a non-enzymatic antioxidant defense system (Gill and Tuteja, 2010). The former includes peroxidase (POD), catalase (CAT) and superoxide dismutase (SOD). SOD can remove excess superoxide anions (O_2^-) in plants and reduce the damage caused by O_2^- to the cell membrane. In turn, POD and CAT catalyze the decomposition of hydrogen peroxide (H_2O_2) to maintain H_2O_2 at a low level, minimize the production of hydroxyl radicals (-OH), and protect cell membrane structure (Yu et al., 2022). The ascorbic acid-glutathione (AsA-GSH) cycle is an important component of the non-enzymatic antioxidant system. The AsA-GSH cycle comprises ascorbate peroxidase (APX), monodehydroascorbate reductase (MDHAR), dehydroascorbate reductase (DHAR), and glutathione reductase (GR), which can directly remove H_2O_2 from plant tissues. The AsA-GSH cycle promotes the production of two non-enzymatic antioxidants (AsA and GSH) to maintain the balance of redox substances in plants (Peng et al., 2022). The ROS-scavenging system has been shown to be critical for the enhancement of cold resistance in many horticultural products, such as loquats (Cai et al., 2011), bell peppers (Endo et al., 2019), okra (Li et al., 2023), and bananas (Chen et al., 2021b). Therefore, improving antioxidant capacity is a promising approach for alleviating low temperature-induced oxidative damage in horticultural products.

Mitochondria are important sites for respiration and the production of ATP in living tissues, thus providing energy for all cellular activities (Chen et al., 2021a). H^+-ATPase, Ca^{2+}-ATPase, cytochrome c oxidase (CCO), and succinate dehydrogenase (SDH) are key enzymes involved in energy synthesis in the mitochondrial membrane (Li et al., 2021a). The decrease or loss of activity of these enzymes can lead to insufficient energy supply to cells, which in turn leads to cellular senescence and death. Numerous studies have shown that the occurrence of CI during the post-harvest cold storage of horticultural products, such as strawberries (Li et al., 2018), pears (Tao et al., 2019), and peaches (Jin et al., 2013), is related to energy metabolism. Energy loss leads to the accumulation of ROS, cell membrane damage, impaired metabolism, and a slow response to low temperature signals, thus accelerating the occurrence of CI.

Numerous preservation techniques, such as brief exposure to hot water (Nasef, 2018), pre-storage cold acclimation (Wang et al., 2018; Wang et al., 2021a), or treatment with hydrogen sulfide (Wang et al., 2022), melatonin (Madebo et al., 2021), or glycine betaine (Zhang et al., 2008), have been shown to extend the shelf life of cold-stored cucumber fruits. Polysaccharide coatings have also been used to improve cold resistance after harvest; for example, chitosan has been shown to improve cold resistance in cucumber fruit (Ru et al., 2020), and treatment with *Astragalus* polysaccharides inhibited the occurrence of CI in bananas (Tian et al., 2022). Fucoidan is a type of fucose-enriched and sulfated polysaccharide that extracted from different kinds of brown seaweed, which contains L-fucose and sulfate groups (Zhao et al., 2004). As a nontoxic natural heteropolysaccharide, fucoidan has multiple biological functions, such as anti-coagulation, anti-tumor, anti-thrombus, anti-virus, anti-oxidation and enhance the body's immune function (Senthilkumar et al., 2013; Wu et al., 2016). In addition, fucoidan can be used as a preservative for storing fruit and vegetables after harvest. Some studies have shown that fucoidan improves antioxidant capacity and maintains post-harvest fruit quality; indeed, fucoidan can extend the shelf life of some fruits, such as mangos (Xu and Wu, 2021), and strawberries (Duan et al., 2019; Luo et al., 2020). However, to date, the effect of fucoidan on CI in cucumber fruits has rarely been reported. Therefore, here, we investigated whether fucoidan treatment can improve cold resistance in cucumbers stored at low temperature, with a focus on ROS homeostasis and energy metabolism. Our findings support the use of fucoidan as a new preservative for cucumber cold storage.

2 Materials and methods

2.1 Plant materials and treatments

Cucumbers (*Cucumis sativus* cv. Sunstar) were collected during the commercial harvest period (approximately 10 d after flowering) from a farm in Nanchang, Jiangxi, China. Fruits were washed with distilled water and dried naturally. Fruits of uniform size and without any disease or defects were randomly separated into four groups and coated with 0 (control), 5, 10, or 15 g/L fucoidan (extract from brown algae, medium molecular weight, purity≥95%, Baichuan, Xi'an, China). Treatments were performed in triplicates comprising 300 fruits for each replicate. Treated fruits were packed in 0.01 mm thick polyethylene plastic bags and stored for 12 days at 4°C and 90% relative humidity. For each replicate, 20 fruits were collected every three days, 15 of which were placed at 20°C

for two days to observe CI, and the pulp (without peel tissue and internal seeds) of the remaining 5 fruits was collected at random and stored at -80°C after quick freezing under liquid nitrogen.

2.2 Measurement of CI, weight loss, electrolyte leakage, and malondialdehyde content

For CI: The degree of cucumber CI was divided into five levels. 0 = no CI, 1 = 0< CI area ≤ 25%, 2 = 25%< CI area ≤ 50%, 3 = 50%< CI area ≤ 75%, 4 = 75%< CI area ≤ 100%. CI inedx was calculated as follows:

$$\text{CI index} = \frac{\Sigma\,(\text{CI level} \times \text{number of fruit at that level})}{4 \times \text{total fruit}}$$

Ten tissue discs with uniform size (thickness: 1 mm, diameter: 8 mm) from five cucumber fruits were prepared for the measurement of electrolyte leakage. Electrolyte leakage, and malondialdehyde (MDA) content of the experimental cucumber fruits were measured as previously described (Wang et al., 2022).

For weight loss: five cucumber fruits were weighed using an electronic scale at a time, and the measurements were repeated three times. Weight loss was calculated as follows:

$$\text{Weight loss}\,(\,\% = \frac{\text{initial fruit weight} - \text{fruit weight at day 12}}{\text{initial fruit weight}} \times 100\,\%$$

2.3 Scavenging rates of free radicals, O_2 production rate, and H_2O_2 content

One gram of pulp from control and fucoidan-treated cucumber fruits was used for the measurement of 1,1-diphenyl-2-picrylhydrazyl (DPPH) scavenging rate, -OH scavenging rate, O_2^-production rate, and H_2O_2 content using a DPPH scavenging rate detection kit (BC4750, Solarbio, Beijing, China), -OH scavenging rate detection kit (BC1320, Solarbio, Beijing, China), O_2^- content detection kit (BC1290, Solarbio, Beijing, China), and H_2O_2 content detection kit (BC3595, Solarbio, Beijing, China), respectively. The unit percentage (%) represents the DPPH and -OH scavenging rates. The O_2^- production rate and H_2O_2 content are expressed as μmol s^{-1} kg^{-1} and mmol kg^{-1}, respectively.

2.4 Determination of antioxidant and ascorbic acid-glutathione cycle enzyme activities

To quantify POD, SOD, and CAT activities, 1.0 g of pulp from control and fucoidan-treated cucumber fruits was homogenized with 5 ml of 50 mM pre-cooled sodium phosphate buffer (pH 7.5) containing 5 mM dithiothreitol and 5% polyvinylpyrrolidone. The mixture was then centrifuged at 12,000 g for 15 min at 4°C and the supernatant was collected. POD, SOD, and CAT activities were determined as previously described (Chen et al., 2022), and expressed as U kg^{-1}. One U of POD and CAT activities represents an absorbance change of 0.01 per gram of sample per minute at 470 nm and 240 nm, respectively. In turn, 1 U of SOD activity represents the amount of SOD per gram of sample in 1 mL of reaction solution when SOD inhibition reached 50%.

The activities of APX, MDHAR, DHAR, and GR were determined using the appropriate test kits (BC0220 for APX activity, BC0650 for MDHAR activity, BC0660 for DHAR activity, and BC1160 for GR activity; Solarbio, Beijing, China) with absorbance measured at 290, 340, 412, and 340 nm, respectively. Enzyme activities are expressed as U kg^{-1}, where 1 U represents 1 μmol of enzyme oxidized per gram of sample per minute.

2.5 Determination of AsA, DHA, GSH, and GSSG content

One gram of homogenized cucumber fruit was mixed with 15 mL of pre-cooled 5% (w/v) trichloroacetic acid and centrifuged at 12,000 rpm for 20 min at 4°C. The supernatant was collected and AsA and DHA content (mg kg^{-1}) was determined as previously described (Zhang et al., 2021). DHA content was calculated as follows:

$$\text{DHA content} = \text{total AsA content} - \text{AsA content}$$

GSH and GSSG contents (mg kg^{-1}) were detected using the appropriate test kits (BC1170 for GSH content; BC1180 for GSSG content; Solarbio, Beijing, China) with absorbance measured at 412 nm.

2.6 Determination of ATP, ADP, and AMP content and energy charge

One gram of cucumber pulp tissue was ground under liquid nitrogen. Then, 6 mL pre-cooled 0.6 mol·L^{-1} perchloric acid solution was added and the sample was fully homogenized. The homogenate was placed on ice for 10 min and then centrifuged at 8000 rpm at 4°C for 15 min. After collecting the supernatant, the pH was adjusted to 6.8 with 1.0 mol·L^{-1} KOH. The neutralized sample was placed on ice for 30 min and then centrifuged at 8000 g at 4°C for 15 min. The supernatant was filtered through a 0.45 μm microporous membrane for use. ATP, ADP, and AMP contents (mg kg^{-1}) were determined by high-performance liquid chromatography (LC-2030 Plus, Shimadzu, Kyoto, Japan) using a C18 column (250 mm × 4.6 mm, 5 μm,

Waters) as previously described (Chen et al., 2021a). Energy charge was calculated as follows:

$$\text{Energy charge}\ (\%) = \frac{\text{ATP} + 0.5 \times \text{ADP}}{\text{ATP} + \text{ADP} + \text{AMP}} \times 100$$

2.7 Determination of H^+-ATPase, Ca^{2+}-ATPase, CCO, and SDH activities

One gram of pulp from control and fucoidan-treated cucumber fruits was used for measurement of H^+-ATPase and Ca^{2+}-ATPase activities using an ATPase activity test kit (A016-1-2, Jiancheng Bioengineering Institute, Nanjing, China) with absorbance measured at 660 nm. One gram of pulp from control and fucoidan-treated cucumber fruits was used for measurement of CCO and SDH activities as previously described (Chen et al., 2022). All results were expressed as U kg^{-1}.

2.8 Gene expression assays

0.5 g of pulp from control and fucoidan-treated cucumber fruits was used for RNA extraction and gene expression analysis as previously described (Gan et al., 2021). The 2X M5 HiPer Realtime PCR Super mix kit (Mei5bio, Beijing, China) was used to perform quantitative real-time polymerase chain reaction (qRT-PCR) using gene-specific primers (Supplementary Table S1). Relative gene expression levels were calculated using the $2^{-\Delta\Delta}$Ct method.

2.9 Statistical analysis

Each experiment was repeated in triplicate. Excel software was used to sort the data, and the results are expressed as the mean ± standard deviation (SD). Pairwise comparisons were made using the single factor method in SPSS26.0, and significant differences were analyzed using the least significant difference test and Duncan's method ($P< 0.05$ or $P< 0.01$). Graphs were drawn using GraphPad Prism 8.0.

3 Results

3.1 Fucoidan treatment alleviates chilling injury in cucumber fruits

Water-soaked depressions of the epidermis are the most obvious symptom of CI in cucumbers. After 12 days of storage at 4°C, the CI index was 0.65. Compared with controls, coating with 5, 10, or 15 g/L fucoidan decreased the CI index of cold-stored cucumbers (Figures 1A, B). Furthermore, weight loss, electrolyte leakage, and MDA content were all reduced following fucoidan treatment (Figures 1C–E), reflecting the protective effect of fucoidan against CI. Although all fucoidan treatments reduced CI, treatment with 15 g/L fucoidan achieved the best results; thus, 15 g/L fucoidan was used for subsequent experiments.

3.2 ROS scavenging capacity after fucoidan treatment

The DPPH and -OH scavenging rates in cucumbers initially increased and then decreased during cold storage. The DPPH scavenging rate peaked on day 6 of storage, while the -OH scavenging rate peaked on day 9. The DPPH and -OH scavenging rates of fucoidan-treated cucumber fruits were higher than those of control cucumbers (Figures 2A, B).

The rate of O_2^- production increased steadily throughout storage in both control and fucoidan-treated cucumbers. However, the O_2^- production rate remained lower in the fucoidan-treated group than in the control group throughout the storage period. Control cucumbers exhibited a gradual increase in H_2O_2 content, which peaked on day 6 of storage and subsequently declined slightly. In contrast, fucoidan treatment significantly reduced the accumulation of H_2O_2 in cold-stored cucumber fruits (Figures 2C, D).

3.3 Enzyme activity and gene expression of POD, CAT, and SOD after fucoidan treatment

The activities of the POD and CAT enzymes initially increased in control cucumbers upon cold storage, reaching a maximum on day 6 of storage, and gradually declining thereafter. Conversely, POD and CAT activities increased by 65% and 39%, respectively, following fucoidan treatment, compared to the control group on day 6 of cold storage, and the subsequent decline in these activities was considerably less pronounced than that in the controls (Figures 3A, C). In turn, SOD activity in cucumber fruits steadily decreased throughout the storage period, and fucoidan-treated cucumbers maintained higher SOD activity than control cucumbers (Figures 3E). Consistent with these results, fucoidan treatment induced the expression of *CsPOD*, *CsCAT2*, and *CsSOD* (Figures 3B, D, F).

3.4 Changes in AsA-GSH cycle components after fucoidan treatment

The AsA content of cucumber fruits decreased gradually during cold storage in both treated and control fruit groups, but remained higher in the fucoidan-treated group than in the control group on day 6. On day 12, the AsA content of

10.3389/fpls.2022.1107687

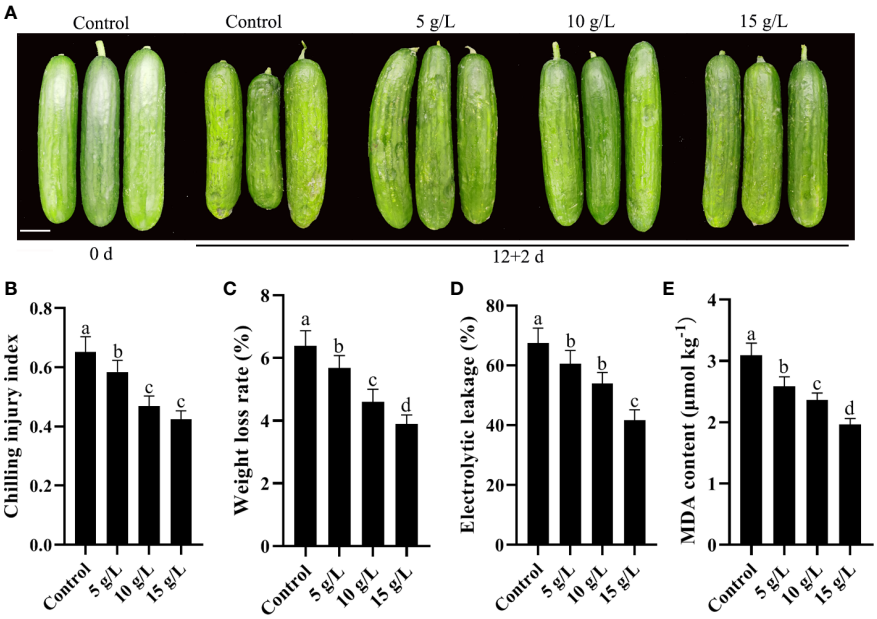

FIGURE 1
(A) Photograph comparing cucumbers treated with 0 (control), 5, 10, or 15 g L^{-1} fucoidan after 12 d of storage at 4°C. **(B-E)** Chilling injury index **(B)**, weight loss rate **(C)**, electrolytic leakage **(D)**, and MDA content **(E)** in cucumber fruit treated with 0, 5, 10, and 15 g L^{-1} fucoidan after 12 d of storage at 4°C. Values are presented as means ± SD of at least three replicates. Bars with different letters are significantly different at P< 0.05, as determined using Duncan's multiple range tests.

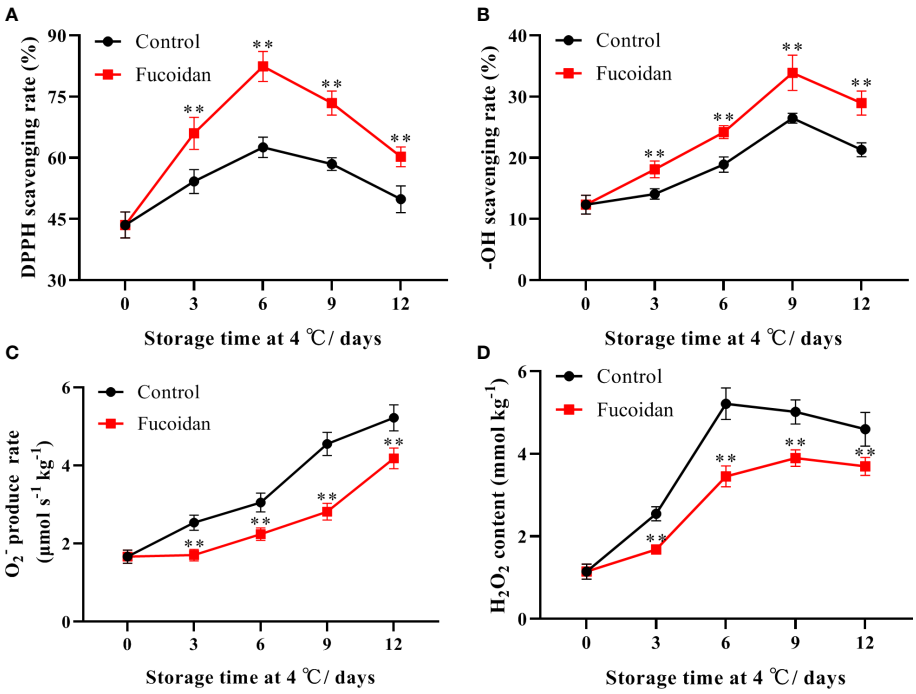

FIGURE 2
(A-D) The DPPH scavenging rate **(A)**, -OH scavenging rate **(B)**, O_2^- production rate **(C)**, and H_2O_2 content **(D)** in fucoidan-treated (15 g L^{-1}) and control cucumbers during storage at 4°C. Values are presented as means ± SD of at least three replicates. **P< 0.01.

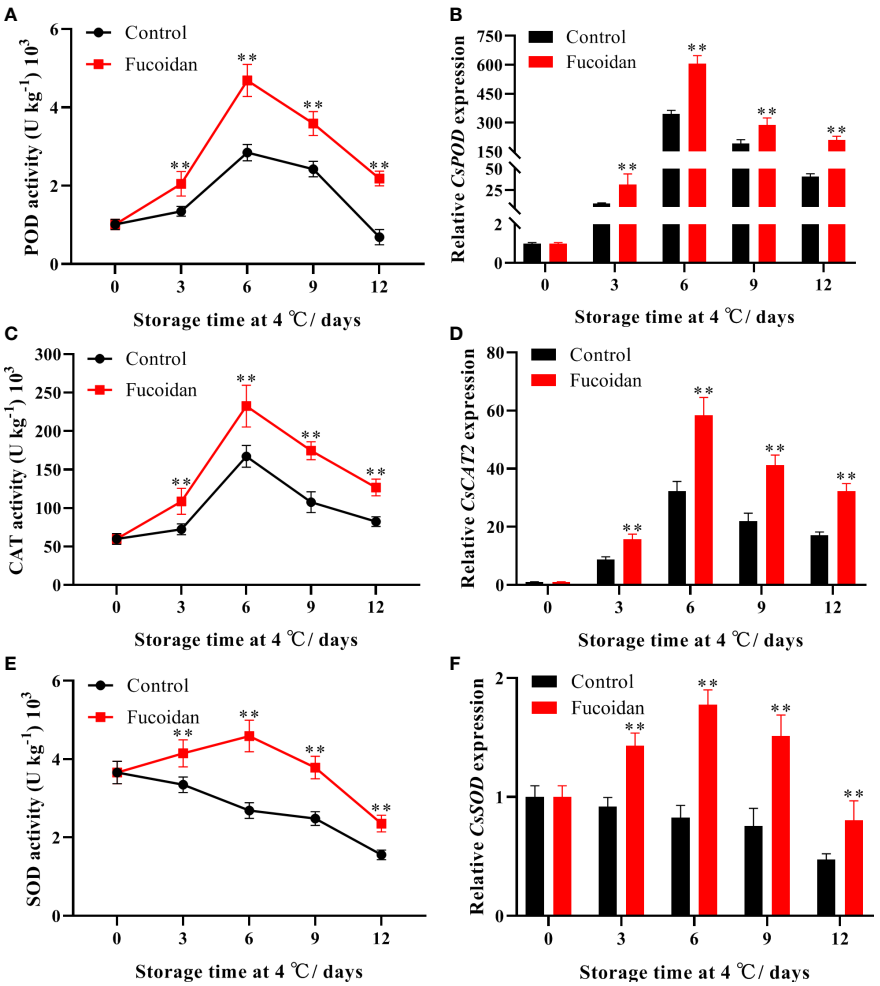

FIGURE 3
(A-F) The enzyme activities and gene expression of POD **(A, B)**, CAT **(C, D)**, and SOD **(E, F)** in fucoidan-treated (15 g L^{-1}) and control cucumbers during storage at 4°C. Values are presented as means ± SD of at least three replicates. **P< 0.01.

fucoidan-treated fruit was 12% higher than that in control group (Figure 4A). In contrast, DHA content in cucumber fruits was not affected by cold storage but was significantly lower in the fucoidan-treated group than in the control group on days 6 and 9 (Figure 4B). Although the AsA/DHA ratio decreased gradually during storage, the fucoidan-treated group maintained a higher AsA/DHA ratio than the control group (Figure 4C). The GSH content increased with increasing refrigeration time and was higher in fucoidan-treated cucumbers compared to controls throughout the entire storage period (Figure 4D). The GSSG content decreased gradually during cold storage, and was significantly higher in the fucoidan-treated group than in the control group from the 6th day of storage (Figure 4E). Finally, the GSH/GSSG ratio increased gradually during storage, and the fucoidan-treated group maintained a higher GSH/GSSG ratio than the control group did (Figure 4F).

3.5 Enzyme activity and gene expression of AsA-GSH cycle components after fucoidan treatment

APX activity initially increased and then decreased during cold storage, reaching a maximum on day 6. The APX activity of fruits in the fucoidan-treated group was significantly higher than that in the control group throughout the storage period (Figure 5A). Compared with the control group, MDHAR activity of fruits in the fucoidan-treated group was higher throughout the storage period, becoming 63% higher on day 6 of storage (Figure 5C). Similarly, DHAR and GR activities initially increased, reaching a maximum on day 3 before subsequently declining; the activities of both enzymes were significantly improved by fucoidan treatment (Figures 5E, G). The expression levels of *CsAPX*, *CsMDHAR*, and *CsDHAR* were

10.3389/fpls.2022.1107687

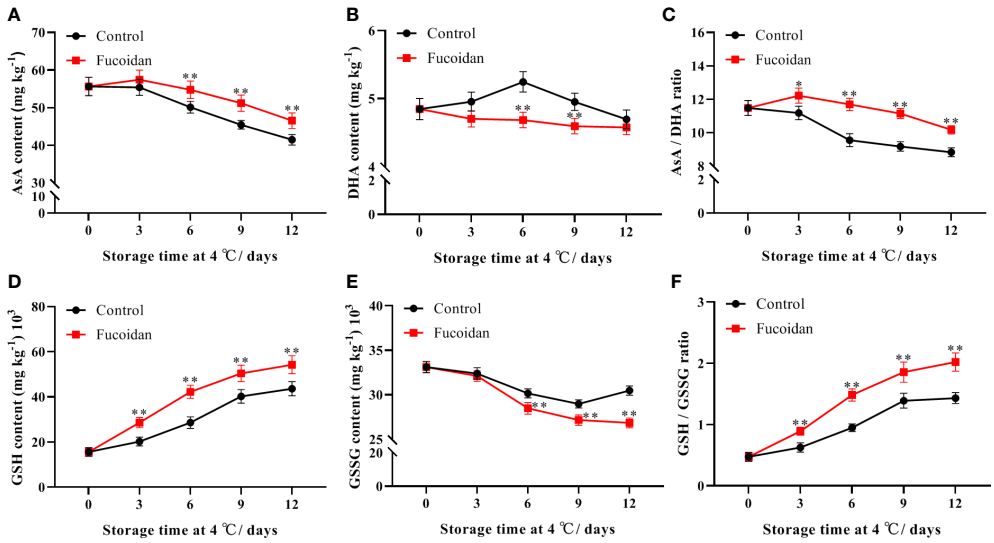

FIGURE 4
(A–F) AsA content **(A)**, DHA content **(B)**, AsA/DHA ratio **(C)**, GSH content **(D)**, GSSG content **(E)**, and GSH/GSSG **(F)** in fucoidan-treated (15 g L^{-1}) and control cucumbers during storage at 4°C. Values are presented as means ± SD of at least three replicates. *P< 0.05; **P< 0.01.

consistent with the trends described for enzyme activity, with fucoidan treatment inducing the expression of these genes. Finally, the expression level of *CsGR* in the fucoidan-treated group was significantly higher than that in the control group on days 3 and 6 (Figures 5B, D, F, H).

3.6 Change in energy levels after fucoidan treatment

The ATP and ADP contents of cucumber fruits declined continuously during cold storage. However, ATP and ADP were significantly higher in fucoidan-treated cucumbers than in control ones throughout the storage period. On day 12, ATP and ADP contents in the treatment group were 14% and 35% higher than those in the control group, respectively (Figures 6A, B). Conversely, AMP content in refrigerated cucumber fruits increased gradually during the storage period. Thus, after 6 days of storage, AMP content in fucoidan-treated fruits was significantly lower than that in the control group, decreasing to a level that was 25% lower on day 12 (Figure 6C). Consistently, energy charge declined slowly from day 1 to 8 and then declined sharply from the 9th day, with extension of storage time. Compared to control, fucoidan-treated cucumbers maintained a higher energy charge during cold storage (Figure 6D).

3.7 Enzyme activity and gene expression of energy metabolism-related enzymes after fucoidan treatment

Activity of H^+-ATPase initially increased and then decreased during cold storage. The activity of H^+-ATPase in fucoidan-treated cucumbers peaked on day 6 and was 33% higher than that of the control group on day 12 (Figure 7A). In contrast, Ca^{2+}-ATPase activity remained stable during cold storage, and fucoidan-treated fruit maintained a higher level of activity than control ones (Figure 7C). Similarly, CCO activity reached a maximum on day 6 of cold storage before declining. Fucoidan-treated cucumbers maintained a higher level of CCO activity after day 6, and it was 50% higher than that of the control group on day 12 (Figure 7E). Additionally, on day 3 of storage, SDH activity of both fucoidan-treated and control fruits peaked, with the former reaching a level 37% higher than that of the control group before beginning to decline (Figure 7G). The expression levels of *CsH*$^+$*-ATPase*, *CsCa*$^{2+}$*-ATPase*, *CsCCO*, and *CsSDH* corresponded with these trends in enzyme activity. Indeed, we found that fucoidan treatment significantly induced the expression of all four genes, thereby regulating the enhancement of their corresponding enzyme activities (Figures 7B, D, F, H) and maintaining metabolism in cucumber fruits to preserve normal physiological activities during cold storage.

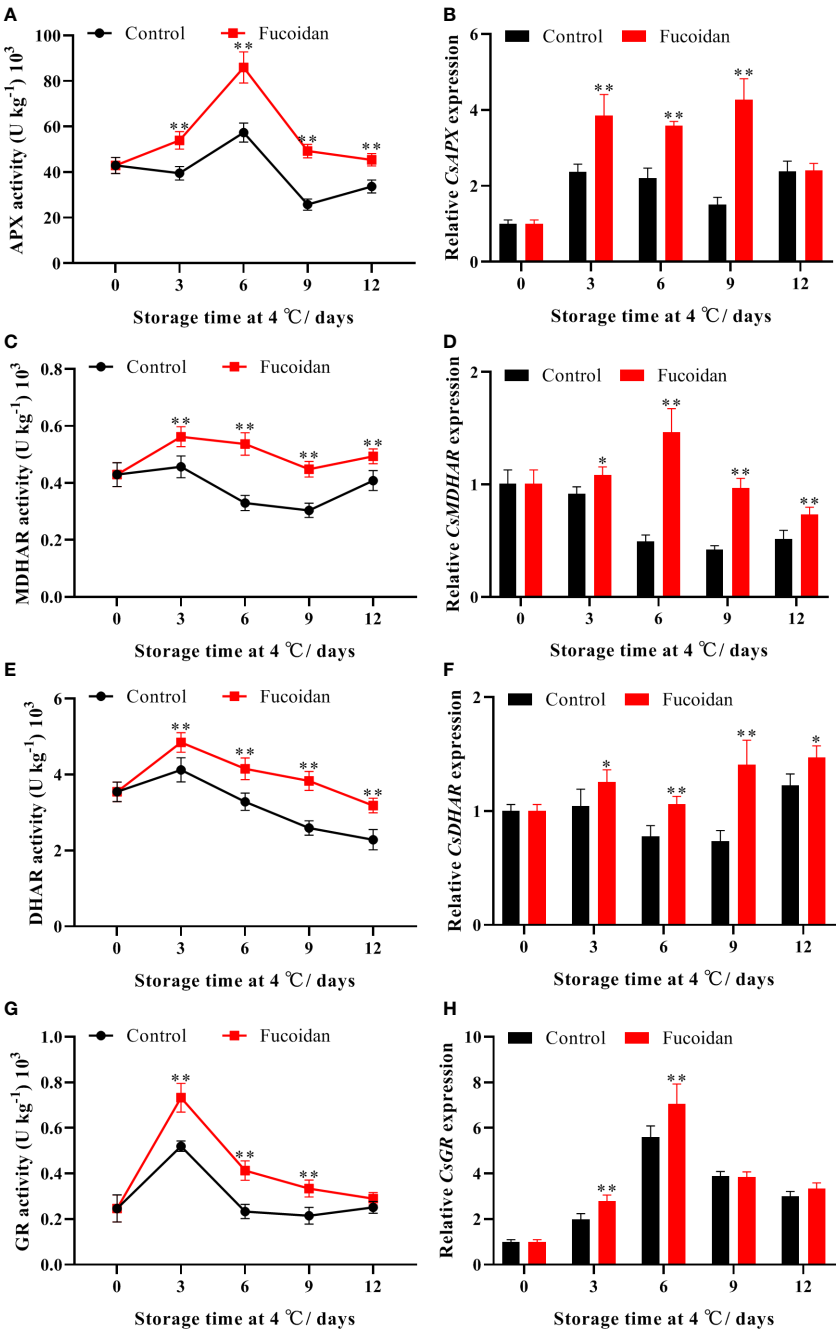

FIGURE 5
(A-H) The enzyme activities and gene expression of APX **(A, B)**, MDHAR **(C, D)**, DHAR **(E, F)**, and GR **(G, H)** in fucoidan-treated (15 g L^{-1}) and control cucumbers during storage at 4°C. Values are presented as means ± SD of at least three replicates. *P< 0.05; **P< 0.01.

4 Discussion

CI easily occurs in cold-stored cucumber fruits after harvest and leads to a decrease in fruit quality and commodity value (Wang et al., 2018; Madebo et al., 2021; Wang et al., 2022). Polysaccharide coatings are environment friendly materials for preservation and improving cold resistance of horticultural products. Carboxymethyl cellulose (CMC) coating help to reduce CI in pomegranate (Ehteshami et al., 2019) and mandarin fruit (Ali et al., 2021) during cold storage.

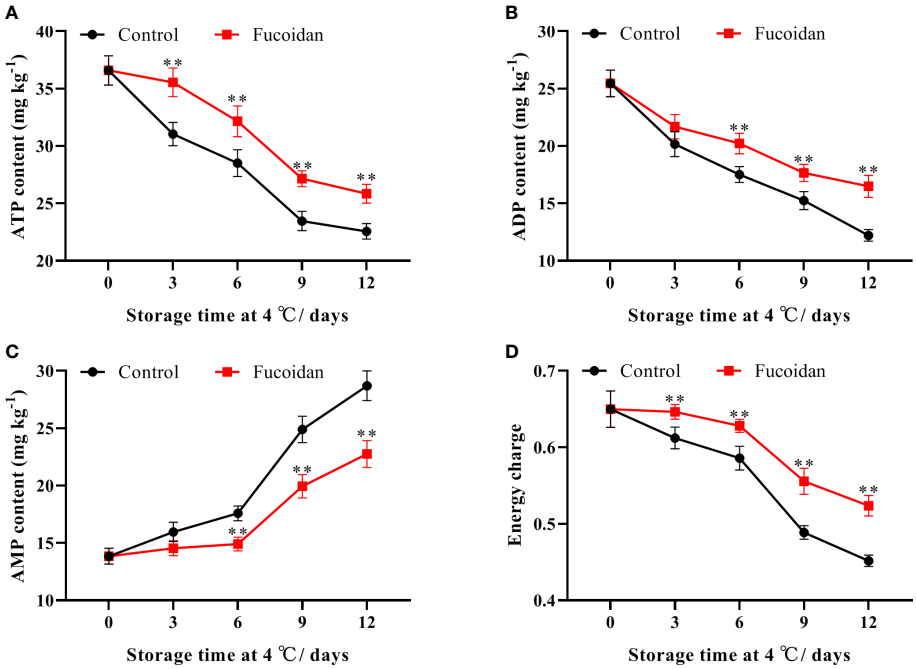

FIGURE 6
(A–D) ATP content **(A)**, ADP content **(B)**, AMP content **(C)**, and energy charge **(D)** in fucoidan-treated (15 g L^{-1}) and control cucumbers during storage at 4°C. Values are presented as means ± SD of at least three replicates. **P< 0.01.

Astragalus polysaccharides delayed the CI and attenuated postharvest peel browning of banana fruit (Tian et al., 2022). In vegetables, the coating of polysaccharide has a similar preservation effect to that of fruit. CMC-based water barrier coating is promising to control the water loss and further maintain the whole quality of pakchoi (Yu et al., 2022). Chitosan induced chilling resistance in cucumber fruit (Ru et al., 2020). Fucoidan has a wide range of biological activities (Zhao et al., 2004)., which has been used to maintain the quality of some fruits. Fucoidan treatment can effectively extend the shelf life of mangoes (Xu and Wu, 2021). Fucoidan treatment improved the cold resistance of strawberry fruit during cold storage (Duan et al., 2019; Luo et al., 2020). In this study, different concentrations of fucoidan (5, 10, and 15 g/L) effectively inhibited CI in cucumber fruits and delayed the appearance of CI symptoms. With the increase of fucoidan concentration, the CI index is lower, the treatment with 15 g/L fucoidan achieved the best results in this study. However, the best result of 15 g/L fucoidan is based on this work, may not the optimum concentration. Thus, the optimum concentration of fucoidan for reducing the CI in cucumber will be further explored.

Cold stress-induced plant damage typically involves an imbalance between ROS production and depletion (Duan et al., 2012); excessive accumulation of ROS, such as H_2O_2 and O_2^-, can irreversibly damage organelles, including chloroplasts and mitochondria. Protecting cells from oxidative damage under stress is considered a major mechanism of plant resistance to low temperatures, and this resistance may depend on the antioxidant system (Mittler et al., 2022). The enzymatic antioxidant system is the main mode of ROS scavenging, and SOD, CAT, and POD are the key antioxidant enzymes involved in this process (Tan et al., 2020). These three antioxidant enzymes work together to reduce the oxidative damage to the cell membrane caused by H_2O_2 and $O2^-$, thus maintaining its integrity and minimizing CI (Cao et al., 2018; Mirshekari et al., 2020). In this study, fucoidan treatment significantly enhanced the SOD activity of cucumber fruits, effectively reduced the $O2^-$ production rate, and maintained high CAT and POD activities, thereby inhibiting the accumulation of H_2O_2. Similarly, previous studies have reported that fucoidan treatment enhances antioxidant activity and improves the cold tolerance of strawberries (Duan et al., 2019; Luo et al., 2020). Thus, we conclude that fucoidan treatment is beneficial in regulating the redox state, and improves the antioxidant capacity of cold-stored cucumber fruits.

The AsA-GSH cycle is an important H_2O_2 scavenging system in plants. AsA and GSH are important non-enzymatic antioxidants in this cycle, which can scavenge excessive ROS produced by plant cells in response to low-temperature stress

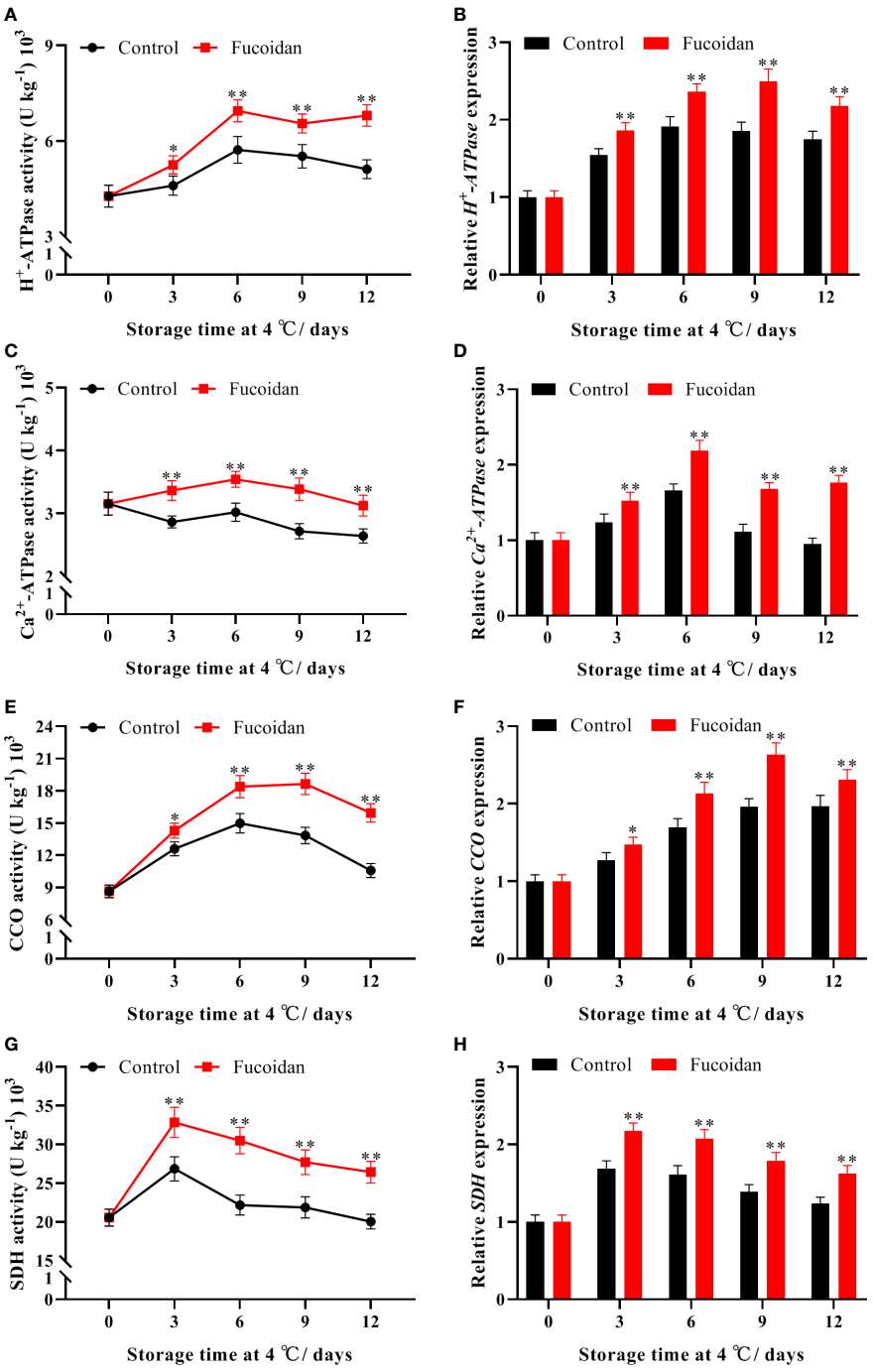

FIGURE 7
(A-H) The enzyme activities and gene expression of H^+-ATPase **(A, B)**, Ca^{2+}-ATPase **(C, D)**, CCO **(E, F)**, and SDH **(G, H)** in fucoidan-treated (15 g L^{-1}) and control cucumbers during storage at 4°C. Values are presented as means ± SD of at least three replicates. *P< 0.05; **P< 0.01.

injury (Li et al., 2010). The AsA/DHA and GSH/GSSG ratios reflect the redox capacity of plants. Generally, the higher the content of reducing substances, the stronger the stress tolerance of plants (Li et al., 2023). In this study, fucoidan treatment consistently maintained higher AsA and GSH contents and AsA/DHA and GSH/GSSG ratios in cucumber fruits, consistent with results from tomatoes (Li et al., 2019), and bell peppers (Endo et al., 2019). GSH/GSSG ratios play an important

role in cold tolerance of tomatoes (Li et al., 2019). Hot water treatment enhanced AsA-GSH cycle to alleviate CI in pepper fruit during postharvest cold storage (Endo et al., 2019). APX, MDHAR, DHAR, and GR are key enzymes involved in AsA-GSH metabolism that cooperate to scavenge excess H_2O_2 in cells and convert it into H_2O and O_2- (Li et al., 2010). Enhanced gene expression and activity of APX, MDHAR, DHAR, and GR has been shown to improve fruit cold tolerance and reduce the occurrence of CI in bell peppers (Wang et al., 2016; Endo et al., 2019), peaches (Song et al., 2016), okra (Li et al., 2023), and bananas (Chen et al., 2021b). These results support our findings that fucoidan treatment can regulate the activities of key enzymes and the expression of related genes in the AsA-GSH cycle of cucumber fruits during cold storage, thereby improving H_2O_2scavenging, reducing the degree of membrane lipid peroxidation, and delaying the occurrence of CI in cucumber fruits.

Energy molecules, such as ATP, play an important role in maintaining the integrity of cell membranes (Saquet et al., 2003). Energy deficits can impair the integrity of cell membranes and lead to a decline in the post-harvest quality of horticultural products (Wang et al., 2020c; Li et al., 2021a). ATP and ADP contents in loquats (Jin et al., 2015), kiwifruit (Wang et al., 2020b), and peaches (Hu et al., 2023), have been reported to drop rapidly and remain at low levels during cold storage. In this study, ATP, ADP, and energy charge declined rapidly in cucumber fruits during cold storage, and the symptoms of fruit CI were aggravated. Fucoidan treatment maintained higher levels of ATP, ADP, and energy charge in cucumber fruits, thereby reducing the ROS-induced membrane damage and alleviating CI. Mitochondria are responsible for energy synthesis; SDH, CCO, H^+-ATPase, and Ca^{2+}-ATPase are key respiratory enzymes located in the inner mitochondrial membrane, and their activities reflect the energy production status of mitochondria (Li et al., 2021b; Wang et al., 2021b). H^+-ATPase catalyzes ATP synthesis by establishing an H^+ electrochemical gradient on both sides of the cell membrane to generate transmembrane proton propulsion (Azevedo et al., 2008). Ca^{2+}-ATPase is a Ca^{2+} pump responsible for transporting Ca^{2+} into the mitochondria, and a decrease in Ca^{2+}-ATPase activity leads to the accumulation of Ca^{2+} in the cytoplasm, leading to the destruction of membrane structural integrity (Chung et al., 2000). SDH catalyzes the conversion of succinic acid to fumaric acid in the tricarboxylic acid cycle, leading to the production of H^+ and ATP (Ackrell et al., 1978). CCO provides energy to cells mainly through oxidative phosphorylation and is a key enzyme in the oxidative phosphorylation process in the mitochondrial respiratory chain (Millar et al., 1995). Cold stress affects the production of ATP by affecting mitochondrial structure and the activity of these enzymes, and the loss of ATP impairs metabolism and destroys cell structure; this further aggravates CI, resulting in a decline in the quality of horticultural products (Jin et al., 2015; Wang et al., 2020b; Hu et al., 2023). Altogether together, the results of this study demonstrate that fucoidan treatment can maintain mitochondrial function by improving the activities of relevant enzymes in cucumbers during cold storage, thereby ensuring continual energy synthesis and ultimately reducing the occurrence of CI.

5 Conclusion

Fucoidan treatment effectively reduced CI in cucumber fruits by modulating ROS scavenging and energy metabolism. Fucoidan treatment can reduce the accumulation of H_2O_2 and O_2^- and the degree of membrane lipid peroxidation by increasing the activity of antioxidant enzymes and the expression of key genes. Furthermore, fucoidan treatment helps maintain high energy levels by regulating the activities of enzymes related to mitochondrial metabolism, thus effectively improving the resistance of cold-stored cucumber fruits to low-temperature stress and reducing the symptoms of cold injury.

Data availability statement

The original contributions presented in the study are included in the article/Supplementary Material. Further inquiries can be directed to the corresponding author.

Author contributions

DL: Conceptualization, methodology, software, writing—original draft preparation. RY: validation, formal analysis, data curation, writing—original draft preparation. MX: investigation, resources. SL: visualization, data curation. JC: writing—review and editing, supervision. ZG: writing—review and editing, project administration, funding acquisition. All authors contributed to the article and approved the submitted version.

Funding

This work was supported by the National Natural Science Foundation of China (32060704), Natural Science Foundation of Jiangxi Province of China (20202BAB215005), and Jiangxi 2011 Col-laborative Innovation Center of Postharvest Key Technology and Quality Safety of Fruit and Vegetables, China (JXGS-05).

Conflict of interest

The authors declare that the research was conducted in the absence of any commercial or financial relationships that could be construed as a potential conflict of interest.

Publisher's note

All claims expressed in this article are solely those of the authors and do not necessarily represent those of their affiliated organizations, or those of the publisher, the editors and the reviewers. Any product that may be evaluated in this article, or claim that may be made by its manufacturer, is not guaranteed or endorsed by the publisher.

Supplementary material

The Supplementary Material for this article can be found online at: https://www.frontiersin.org/articles/10.3389/fpls.2022.1107687/full#supplementary-material

References

Ackrell, B. A., Kearney, E. B., and Singer, T. P. (1978). Mammalian succinate dehydrogenase. *Methods enzymol.* 53, 466–483. doi: 10.1016/s0076-6879(78)53050-4

Ali, S., Anjum, M. A., Ejaz, S., Hussain, S., Ercisli, S., Saleem, M. S., et al. (2021). Carboxymethyl cellulose coating delays chilling injury development and maintains eating quality of 'kinnow' mandarin fruits during low temperature storage. *Int. J. Biol. Macromol.* 168, 77–85. doi: 10.1016/j.ijbiomac.2020.12.028

Azevedo, I. G., Oliveira, J. G., da Silva, M. G., Pereira, T., Corrêa, S. F., Vargas, H., et al. (2008). P-type h^+-ATPases activity, membrane integrity, and apoplastic pH during papaya fruit ripening. *Postharvest Biol. Technol.* 48, 242–247. doi: 10.1016/j.postharvbio.2007.11.001

Cai, Y. T., Cao, S. F., Yang, Z. F., and Zheng, Y. H. (2011). MeJA regulates enzymes involved in ascorbic acid and glutathione metabolism and improves chilling tolerance in loquat fruit. *Postharvest Biol. Technol.* 59, 324–326. doi: 10.1016/j.postharvbio.2010.08.020

Cao, S. F., Shao, J. R., Shi, L. Y., Xu, L. W., Shen, Z. M., Chen, W., et al. (2018). Melatonin increases chilling tolerance in postharvest peach fruit by alleviating oxidative damage. *Sci. Rep.* 8, 806. doi: 10.1038/s41598-018-19363-5

Chen, C. Y., Cai, N., Wan, C. P., Kai, W. B., and Chen, J. Y. (2022). Carvacrol delays phomopsis stem-end rot development in pummelo fruit in relation to maintaining energy status and antioxidant system. *Food Chem.* 372, 131239. doi: 10.1016/j.foodchem.2021.131239

Chen, C. Y., Peng, X., Chen, J. Y., Gan, Z. Y., and Wan, C. P. (2021a). Mitigating effects of chitosan coating on postharvest senescence and energy depletion of harvested pummelo fruit response to granulation stress. *Food Chem.* 348, 129113. doi: 10.1016/j.foodchem.2021.129113

Chen, L. L., Shan, W., Cai, D. L., Chen, J. Y., Lu, W. J., Su, X. G., et al. (2021b). Postharvest application of glycine betaine ameliorates chilling injury in cold-stored banana fruit by enhancing antioxidant system. *Sci. Hortic.* 287, 110264. doi: 10.1016/j.scienta.2021.110264

Chung, W. S., Lee, S. H., Kim, J. C., Heo, W. D., Kim, M. C., Park, C. Y., et al. (2000). Identification of a calmodulin-regulated soybean $Ca^{(2+)}$-ATPase (SCA1) that is located in the plasma membrane. *Plant Cell* 12, 1393–1407. doi: 10.1105/tpc.12.8.1393

Duan, Z. H., Duan, W. W., Li, F. P., Li, Y. Q., Luo, P., and Liu, H. Z. (2019). Effect of carboxymethylation on properties of fucoidan from *Laminaria japonica*: Antioxidant activity and preservative effect on strawberry during cold storage. *Postharvest Biol. Technol.* 151, 127–133. doi: 10.1016/j.postharvbio.2019.02.008

Duan, M., Ma, N. N., Li, D., Deng, Y. S., Kong, F. Y., Lv, W., et al. (2012). Antisense-mediated suppression of tomato thylakoidal ascorbate peroxidase influences anti-oxidant network during chilling stress. *Plant Physiol. Biochem.* 58, 37–45. doi: 10.1016/j.plaphy.2012.06.007

Ehteshami, S., Abdollahi, F., Ramezanian, A., Dastjerdi, A. M., and Rahimzadeh, M. (2019). Enhanced chilling tolerance of pomegranate fruit by edible coatings combined with malic and oxalic acid treatments. *Sci. Hortic.* 250, 388–398. doi: 10.1016/j.scienta.2019.02.075

Endo, H., Miyazaki, K., Ose, K., and Imahori, Y. (2019). Hot water treatment to alleviate chilling injury and enhance ascorbate-glutathione cycle in sweet pepper fruit during postharvest cold storage. *Sci. Hortic.* 257, 108715. doi: 10.1016/j.scienta.2019.108715

Gan, Z. Y., Yuan, X., Shan, N., Wan, C. P., Chen, C. Y., Zhu, L. Q., et al. (2021). AcERF1b and AcERF073 positively regulate indole-3-acetic acid degradation by activating *AcGH3.1* transcription during postharvest kiwifruit ripening. *J. Agric. Food Chem.* 69, 13859–13870. doi: 10.1021/acs.jafc.1c03954

Gill, S. S., and Tuteja, N. (2010). Reactive oxygen species and antioxidant machinery in abiotic stress tolerance in crop plants. *Plant Physiol. Biochem.* 48, 909–930. doi: 10.1016/j.plaphy.2010.08.016

Hu, S. Q., Hou, Y. Y., Zhao, L. Y., Zheng, Y. H., and Jin, P. (2023). Exogenous 24-epibrassinolide alleviates chilling injury in peach fruit through modulating PpGATA12-mediated sucrose and energy metabolisms. *Food Chem.* 400, 133996. doi: 10.1016/j.foodchem.2022.133996

Jin, P., Zhang, Y., Shan, T. M., Huang, Y. P., Xu, J., and Zheng, Y. H. (2015). Low-temperature conditioning alleviates chilling injury in loquat fruit and regulates glycine betaine content and energy status. *J. Agric. Food Chem.* 63, 3654–3659. doi: 10.1021/acs.jafc.5b00605

Jin, P., Zhu, H., Wang, J., Chen, J. J., Wang, X. L., and Zheng, Y. H. (2013). Effect of methyl jasmonate on energy metabolism in peach fruit during chilling stress. *J. Sci. Food Agric.* 93, 1827–1832. doi: 10.1002/jsfa.5973

Li, X., Bao, Z. Y., Chen, Y. N., Lan, Q. Q., Song, C. B., Shi, L. Y., et al. (2023). Exogenous glutathione modulates redox homeostasis in okra (*Abelmoschus esculentus*) during storage. *Postharvest Biol. Technol.* 195, 112145. doi: 10.1016/j.postharvbio.2022.112145

Li, C. Y., Cheng, Y., Hou, J. B., Zhu, J., Sun, L., and Ge, Y. H. (2021a). Application of methyl jasmonate postharvest maintains the quality of nanguo pears by regulating mitochondrial energy metabolism. *J. Integr. Agric.* 20, 3075–3083. doi: 10.1016/S2095-3119(21)63611-0

Li, H. Z., Jiang, X. C., Lv, X. Z., Ahammed, G. J., Guo, Z. X., Qi, Z. Y., et al. (2019). Tomato GLR3.3 and GLR3.5 mediate cold acclimation-induced chilling tolerance by regulating apoplastic H_2O_2 production and redox homeostasis. *Plant Cell Environ.* 42, 3326–3339. doi: 10.1111/pce.13623

Li, Y. L., Liu, Y. F., and Zhang, J. G. (2010). Advances in the research on the AsA-GSH cycle in horticultural crops. *Front. Agric. China* 4, 84–90. doi: 10.1007/s11703-009-0089-8

Li, D., Li, L., Xiao, G., Limwachiranon, J., Xu, Y., Lu, H., et al. (2018). Effects of elevated CO2 on energy metabolism and gamma-aminobutyric acid shunt pathway in postharvest strawberry fruit. *Food Chem.* 265, 281–289. doi: 10.1016/j.foodchem.2018.05.106

Liu, Q. L., Li, X., Jin, B. S., Dong, W. Q., Zhang, Y., Chen, W., et al. (2023). γ-aminobutyric acid treatment induced chilling tolerance in postharvest kiwifruit (*Actinidia chinensis* cv. hongyang) *via* regulating ascorbic acid metabolism. *Food Chem.* 404, 134661. doi: 10.1016/j.foodchem.2022.134661

Li, D., Wang, D., Fang, Y. D., Li, L., Lin, X. Y., Xu, Y. Q., et al. (2021b). A novel phase change coolant promoted quality attributes and glutamate accumulation in postharvest shiitake mushrooms involved in energy metabolism. *Food Chem.* 351, 129227. doi: 10.1016/j.foodchem.2021.129227

Luo, P., Li, F. P., Liu, H. Z., Yang, X. M., and Duan, Z. H. (2020). Effect of fucoidan-based edible coating on antioxidant degradation kinetics in strawberry fruit during cold storage. *J. Food Process. Preserv.* 44, e14381. doi: 10.1111/jfpp.14381

Madebo, M. P., Luo, S. M., Wang, L., Zheng, Y. H., and Jin, P. (2021). Melatonin treatment induces chilling tolerance by regulating the contents of polyamine, γ-aminobutyric acid, and proline in cucumber fruit. *J. Integr. Agric.* 20, 3060–3074. doi: 10.1016/S2095-3119(20)63485-2

Millar, A. H., Atkin, O. K., Lambers, H., Wiskich, J. T., and Day, D. A. (1995). A critique of the use of inhibitors to estimate partitioning of electrons between mitochondrial respiratory pathways in plants. *Physiol. Plant.* 95, 523–532. doi: 10.1034/j.1399-3054.1995.950404.x

Mirshekari, A., Madani, B., Yahia, E. M., Golding, J. B., and Vand, S. H. (2020). Postharvest melatonin treatment reduces chilling injury in sapota fruit. *J. Sci. Food Agric.* 100, 1897–1903. doi: 10.1002/jsfa.10198

Mittler, R., Zandalinas, S. I., Fichman, Y., and Van Breusegem, F. (2022). Reactive oxygen species signalling in plant stress responses. *Nat. Rev. Mol. Cell Biol.* 23, 663–679. doi: 10.1038/s41580-022-00499-2

Nasef, I. N. (2018). Short hot water as safe treatment induces chilling tolerance and antioxidant enzymes, prevents decay and maintains quality of cold-stored cucumbers. *Postharvest Biol. Technol.* 138, 1–10. doi: 10.1016/j.postharvbio.2017.12.005

Peng, X., Zhang, Y. A., Wan, C. P., Gan, Z. Y., Chen, C. Y., and Chen, J. Y. (2022). Antofine triggers the resistance against penicillium italicum in ponkan fruit by driving AsA-GSH cycle and ROS-scavenging system. *Front. Microbiol.* 13. doi: 10.3389/fmicb.2022.874430

Ru, L., Jiang, L. F., Wills, R. B. H., Golding, J. B., Huo, Y. R., Yang, H. Q., et al. (2020). Chitosan oligosaccharides induced chilling resistance in cucumber fruit and associated stimulation of antioxidant and *HSP* gene expression. *Sci. Hortic.* 264, 109187. doi: 10.1016/j.scienta.2020.109187

Saquet, A. A., Streif, J., and Bangerth, F. (2003). Energy metabolism and membrane lipid alterations in relation to brown heart development in 'Conference' pears during delayed controlled atmosphere storage. *Postharvest Biol. Technol.* 30, 123–132. doi: 10.1016/s0925-5214(03)00099-1

Senthilkumar, K., Manivasagan, P., Venkatesan, J., and Kim, S. K. (2013). Brown seaweed fucoidan: biological activity and apoptosis, growth signaling mechanism in cancer. *Int. J. Biol. Macromol.* 60, 366–374. doi: 10.1016/j.ijbiomac.2013.06.030

Song, L. L., Wang, J. H., Shafi, M., Liu, Y., Wang, J., Wu, J. S., et al. (2016). Hypobaric treatment effects on chilling injury, mitochondrial dysfunction, and the ascorbate-glutathione (AsA-GSH) cycle in postharvest peach fruit. *J. Agric. Food Chem.* 64, 4665–4674. doi: 10.1021/acs.jafc.6b00623

Song, C. B., Wang, K., Xiao, X., Liu, Q. L., Yang, M. J., Li, X., et al. (2022). Membrane lipid metabolism influences chilling injury during cold storage of peach fruit. *Food Res. Int.* 157, 111249. doi: 10.1016/j.foodres.2022.111249

Tan, X. L., Zhao, Y. T., Shan, W., Kuang, J. F., Lu, W. J., Su, X. G., et al. (2020). Melatonin delays leaf senescence of postharvest Chinese flowering cabbage through ROS homeostasis. *Food Res. Int.* 138, 109790. doi: 10.1016/j.foodres.2020.109790

Tao, D., Wang, J., Zhang, L., Jiang, Y., and Lv, M. (2019). 1-methylcyclopropene alleviates peel browning of 'Nanguo' pears by regulating energy, antioxidant and lipid metabolisms after long term refrigeration. *Sci. Hortic.* 247, 254–263. doi: 10.1016/j.scienta.2018.12.025

Tian, J. X., Xie, S. Y., Zhang, P., Wang, Q., Li, J. K., and Xu, X. B. (2022). Attenuation of postharvest peel browning and chilling injury of banana fruit by *Astragalus polysaccharides*. *Postharvest Biol. Technol.* 184, 111783. doi: 10.1016/j.postharvbio.2021.111783

Tsuchida, H., Kozukue, N., Han, G. P., Choi, S. H., Levin, C. E., and Friedman, M. (2010). Low-temperature storage of cucumbers induces changes in the organic acid content and in citrate synthase activity. *Postharvest Biol. Technol.* 58, 129–134. doi: 10.1016/j.postharvbio.2010.06.006

Wang, H. B., Cheng, X., Wu, C. E., Fan, G. J., Li, T. T., and Dong, C. (2021b). Retardation of postharvest softening of blueberry fruit by methyl jasmonate is correlated with altered cell wall modification and energy metabolism. *Sci. Hortic.* 276, 109752. doi: 10.1016/j.scienta.2020.109752

Wang, Q., Ding, T., Zuo, J. H., Gao, L. P., and Fan, L. L. (2016). Amelioration of postharvest chilling injury in sweet pepper by glycine betaine. *Postharvest Biol. Technol.* 112, 114–120. doi: 10.1016/j.postharvbio.2015.07.008

Wang, T., Hu, M., Yuan, D., Yun, Z., Gao, Z., Su, Z., et al. (2020c). Melatonin alleviates pericarp browning in litchi fruit by regulating membrane lipid and energy metabolisms. *Postharvest Biol. Technol.* 160, 111066. doi: 10.1016/j.postharvbio.2019.111066

Wang, B., Shen, F., and Zhu, S. J. (2018). Proteomic analysis of differentially accumulated proteins in cucumber (*Cucumis sativus*) fruit peel in response to pre-storage cold acclimation. *Front. Plant Sci.* 8. doi: 10.3389/fpls.2017.02167

Wang, B., Wang, G., and Zhu, S. J. (2020a). DNA Damage inducible protein 1 is involved in cold adaption of harvested cucumber fruit. *Front. Plant Sci.* 10. doi: 10.3389/fpls.2019.01723

Wang, B., Wu, C. S., Wang, G., He, J. M., and Zhu, S. J. (2021a). Transcriptomic analysis reveals a role of phenylpropanoid pathway in the enhancement of chilling tolerance by pre-storage cold acclimation in cucumber fruit. *Sci. Hortic.* 288, 110282. doi: 10.1016/j.scienta.2021.110282

Wang, F., Yang, Q. Z., Zhao, Q. F., and Zhang, X. P. (2020b). Roles of antioxidant capacity and energy metabolism in the maturity-dependent chilling tolerance of postharvest kiwifruit. *Postharvest Biol. Technol.* 168, 111281. doi: 10.1016/j.postharvbio.2020.111281

Wang, J. D., Zhao, Y. Q., Ma, Z. Q., Zheng, Y. H., and Jin, P. (2022). Hydrogen sulfide treatment alleviates chilling injury in cucumber fruit by regulating antioxidant capacity, energy metabolism and proline metabolism. *Foods* 11, 2749. doi: 10.3390/foods11182749

Wu, L., Sun, J., Su, X., Yu, Q. L., Yu, Q. Y., and Zhang, P. (2016). A review about the development of fucoidan in antitumor activity: progress and challenges. *Carbohydr. Polymers* 154, 96–111. doi: 10.1016/j.carbpol.2016.08.005

Xu, B., and Wu, S. (2021). Preservation of mango fruit quality using fucoidan coatings. *LWT-Food Sci. Technol.* 143, 111150. doi: 10.1016/j.lwt.2021.111150

You, J., and Chan, Z. L. (2015). ROS regulation during abiotic stress responses in crop plants. *Front. Plant Sci.* 6. doi: 10.3389/fpls.2015.01092

Yu, K. B., Zhou, L., Xu, J., Jiang, F. H., Zhong, Z. W., Zou, L. Q., et al. (2022). Carboxymethyl cellulose-based water barrier coating regulated postharvest quality and ROS metabolism of pakchoi (*Brassica chinensis* l.). *Postharvest Biol. Technol.* 185, 111804. doi: 10.1016/j.postharvbio.2021.111804

Zhang, H. Y., Wang, Y. N., Han, T., Li, L. P., and Xu, L. (2008). Effect of exogenous glycine betaine on chilling injury and chilling-resistance parameters in cucumber fruits stored at low temperature. *Sci. Agricult. Sin.* 41, 2407–2412. doi: 10.3724/SP.J.1011.2008.00145

Zhang, Y., Wang, K., Xiao, X., Cao, S. F., Chen, W., Yang, Z. F., et al. (2021). Effect of 1-MCP on the regulation processes involved in ascorbate metabolism in kiwifruit. *Postharvest Biol. Technol.* 179, 111563. doi: 10.1016/j.postharvbio.2021.111563

Zhao, X., Xue, C. H., Li, Z. J., Cai, Y. P., Liu, H. Y., and Qi, H. T. (2004). Antioxidant and hepatoprotective activities of low molecular weight sulfated polysaccharide from *Laminaria japonica*. *J. Appl. Phycol.* 16, 111–115. doi: 10.1023/b:japh.0000044822.10744.59

frontiers | Frontiers in Plant Science

TYPE Original Research
PUBLISHED 05 January 2023
DOI 10.3389/fpls.2022.1084997

OPEN ACCESS

EDITED BY
Zhenfeng Yang,
Zhejiang Wanli University, China

REVIEWED BY
Jianfei Kuang,
South China Agricultural University, China
Daqi Fu,
China Agricultural University, China

*CORRESPONDENCE
Jeong-Ho Lim
jhlim@kfri.re.kr
Dong-Hwan Kim
dhkim92@cau.ac.kr

SPECIALTY SECTION
This article was submitted to Crop and Product Physiology, a section of the journal Frontiers in Plant Science

RECEIVED 31 October 2022
ACCEPTED 13 December 2022
PUBLISHED 05 January 2023

CITATION
Choi D, Choi JH, Park K-J, Kim C, Lim J-H and Kim D-H (2023) Transcriptomic analysis of effects of 1-methylcyclopropene (1-MCP) and ethylene treatment on kiwifruit (*Actinidia chinensis*) ripening. *Front. Plant Sci.* 13:1084997. doi: 10.3389/fpls.2022.1084997

Transcriptomic analysis of effects of 1-methylcyclopropene (1-MCP) and ethylene treatment on kiwifruit (*Actinidia chinensis*) ripening

Dasom Choi[1], Jeong Hee Choi[2], Kee-Jai Park[2], Changhyun Kim[3], Jeong-Ho Lim[2]* and Dong-Hwan Kim[1]*

[1]Department of Plant Science and Technology, Chung-Ang University, Anseong, Republic of Korea, [2]Food safety and Distribution Research Group, Korea Food Research Institute, Wanju, Republic of Korea, [3]Department of Systems Biotechnology, Chung-Ang University, Anseong, Republic of Korea

Ethylene (ET) is a gaseous phytohormone with a crucial role in the ripening of many fruits, including kiwifruit (*Actinidia* spp.). Meanwhile, treatment with 1-methylcyclopropene (1-MCP), an artificial ET inhibitor delays the ripening of kiwifruit. The objective of this study was to determine the effect of ET and 1-MCP application during time-course storage of kiwifruit. In addition, we aimed to elucidate the molecular details underlying ET-mediated ripening process in kiwifruit. For this purpose, we conducted a time-course transcriptomic analysis to determine target genes of the ET-mediated maturation process in kiwifruit during storage. Thousands of genes were identified to be dynamically changed during storage and clustered into 20 groups based on the similarity of their expression patterns. Gene ontology analysis using the list of differentially expressed genes (DEGs) in 1-MCP-treated kiwifruit revealed that the identified DEGs were significantly enriched in the processes of photosynthesis metabolism and cell wall composition throughout the ripening process. Meanwhile, ET treatment rapidly triggered secondary metabolisms related to the ripening process, phenylpropanoid (e.g. lignin) metabolism, and the biosynthesis of amino acids (e.g. Phe, Cys) in kiwifruit. It was demonstrated that ET biosynthesis and signaling genes were oppositely affected by ET and 1-MCP treatment during ripening. Furthermore, we identified a ET transcription factor, *AcEIL* (Acc32482) which is oppositely responsive by ET and 1-MCP treatment during early ripening, potentially one of key signaling factor of ET- or 1-MCP-mediated physiological changes. Therefore, this transcriptomic study unveiled the molecular targets of ET and its antagonist, 1-MCP, in kiwifruit during ripening. Our results provide a useful foundation for understanding the molecular details underlying the ripening process in kiwifruit.

KEYWORDS

ethylene, 1-MCP, kiwifruit, transcriptome, ripening

1 Introduction

Fruits undergo morphological and physiological changes during growth and maturation. Fruit ripening changes pigment accumulation, texture, softening, and the production of volatile compounds, as well as increases the production of ethylene (ET) by respiration. Fleshy fruits can be divided into two groups depending on their respiration patterns: climacteric and non-climacteric (Leliévre et al., 1997). Kiwifruit (*Actinidia* spp.) is categorized as a climacteric fruit; there is a rapid increase in the production of ET resulting from a 'climacteric' burst of respiration (Alexander and Grierson, 2002).

During ripening, fruit undergoes dynamic physiological and biochemical changes. Fruit ripening lead to the accumulation of sugars and changes in fruit texture. For example, fruit softening is accompanied during ripening, which is resulted from the degradation and secondary lignification of cell walls and the degradation of starch during storage (Li et al., 2010; Zhu et al., 2019). During ripening, various phenolic compounds such as anthocyanins and flavonoids are produced, which are derived from the phenylpropanoid pathway during ripening. As a result, fruit color is changed due to the degradation of chlorophyll and accumulation of phenolic compounds like carotenoids, flavonoids, and anthocyanins. Enzymes such as phenylalanine ammonia lyase (PAL), cinnamate 4-hydroxylase (C4H) and 4-coumarate:CoA ligae (4CL) constitutes general phenylpropanoids pathway and then subsequently branched into different biosynthesis pathways for a diversity of end products such as lignin, anthocyanins, flavonols, proanthocyanidins against adverse biotic and abiotic stress conditions (Singh et al., 2010).

These changes are caused by transcriptional reprogramming of genes related to fruit quality during ripening. RNA-sequencing (RNA-seq) technology facilitated a high-throughput transcriptomic analysis on ripening process of flesh fruits including apple (Nawaz et al., 2021), banana (Pathak et al., 2003), strawberry (Tian et al., 2000), and kiwifruit (Asiche et al., 2018; Salazar et al., 2021). These studies showed that many of differentially expressed genes along fruit ripening are involved in the photosynthesis, cysteine and methionine metabolism, phenylpropanoid biosynthesis, amino acid metabolism, starch and sucrose metabolism, and plant hormone signal transduction.

Among plant hormones, ET is the key player that regulates many aspects of fruit ripening (Liu et al., 2015). For example, softening of fruit is caused by modifications in the cell wall, such as reduction in intercellular adhesion, depolymerization of pectins and hemicellulose, and loss of pectic galactose side chains (Brummell and Harpster, 2001). ET induces the expression of several cellular metabolic enzymes, pectin methyl esterase, pectate lyase, polygalacturonase, xyloglucan transglucosylase/hydrolase, and expansin, which are involved in cell wall degradation (Iqbal et al., 2017; Brumos, 2021). For instance, pectin methylesterase (PME) is a hydrolytic enzyme of pectin, one of the most abundant macromolecules in the plant cell wall. Expression of *PME* genes was induced by ET treatment in tomatoes (Wen et al., 2020).

During the last decades, the ET biosynthesis and signaling pathways have been best revealed by intensive studies using the model plant, *Arabidopsis* (Klee, 2004; Kendrick and Chang, 2008). ET biosynthesis is regulated by two major enzymes, known as 1-aminocyclopropane-1-carboxylic acid (ACC) synthase (ACS) and ACC oxidase (ACO). In the ET biosynthesis pathway, S-adenosylmethionine (SAM) is transformed into ACC by the action of ACS, and the ACC is converted to ET *via* ACO (Yang and Hoffman, 1984; Giovannoni, 2004). During the ripening of climacteric fruit, the increased gene expression of ACS and ACO causes a transition to autocatalytic ET production.

In terms of ET signaling, ET receptors perceive the autocatalytic production of ET, and signals are transduced through the cascade to activate several transcription factors and hundreds of related target genes (Adams-Phillips et al., 2004). In *Arabidopsis*, the ET molecule is recognized by five different transmembrane receptors called ETHYLENE RESPONSE/RECEPTOR 1 (ETR1), ETHYLENE RESPONSE/RECEPTOR 2 (ETR2), ETHYLENE RESPONSE SENSOR 1 (ERS1), ETHYLENE RESPONSE SENSOR 2 (ERS2), and ETHYLENE INSENSITIVE 4 (EIN4). In the absence of ET, these ET receptors actively bind with the endoplasmic reticulum-associated Raf-like serine/threonine protein kinase CONSTITUTIVE TRIPLE RESPONSE 1 (CTR1) that constitutively phosphorylates a transmembrane protein named ETHYLENE INSENSITIVE 2 (EIN2). Thus, the ETR/ERS-CTR1 module is a negative regulator of ET signaling (Hua and Meyerowitz, 1998). By contrast, with ET binding to the ETR/ERS-CTR1 receptor module, the CTR1-mediated phosphorylation of EIN2 is not activated (Ju et al., 2012). Unphosphorylated EIN2 undergoes proteolytic cleavage into two fragments (N- and C-terminal fragments) by a yet-unidentified mechanism (Qiao et al., 2012). The N-terminal fragment, which contains multiple transmembrane domains, remains in the endoplasmic reticulum membrane, while the C-terminal fragment is released and translocated to the nucleus and the processing bodies (P-bodies). In the nucleus, the C-terminal EIN2 polypeptide activates transcription factors, such as ETHYLENE INSENSITIVE 3 (EIN3) and EIN3-LIKE 1 (EIL1), which, in turn, trigger expression of downstream ET-responsive genes (Guo and Ecker, 2004). This process leads to many changes to the fruit in addition to starch to sugar accumulation and cell wall degradation leading to softening (Payasi and Sanwal, 2010).

Inhibition of ET biosynthesis is an essential strategy for maintaining the quality of the climacteric fruit and extending the storage period. Application of a non-toxic inhibitor of ET, 1-methylcyclopropene (1-MCP), successfully delayed postharvest ripening of climacteric fruits, including apple (Fan and Mattheis,

1999; Lv et al., 2020), Chinese bayberry (Shi et al., 2018), mango (Reddy et al., 2017), papaya (Shen et al., 2017), and Asian pear (Wang et al., 2021). Similarly, the treatment of 1-MCP to kiwifruit markedly delayed ripening and maintained the fruit quality during storage (Park et al., 2014; Liu et al., 2021). In kiwifruit, ET biosynthetic genes like *AC-SAM1*, *AC-SAM2*, *AC-ACO1*, and *AC-ACO2* genes were shown to be required for the increase of ET production in propylene-treated kiwifruit (Mworia et al., 2010). Also, 1-MCP was shown to inhibit the expression of *KWACO1* and *KWACS1* genes which are related to ET production (Ilina et al., 2010). Furthermore, ET signaling factors in kiwifruit (*Actinidia deliciosa*) such as 4 AdEIN3-like (AdEILs) and 14 ethylene response factors (ERFs) were shown to be dynamically regulated during fruit ripening (Yin et al., 2010). Although the effect of ET and 1-MCP treatments on the physiological and metabolic changes in kiwifruit during ripening were previously examined, the molecular details underlying the postharvest effect of ET and 1-MCP in kiwifruit are still largely understood. Therefore, in this study, we aimed to perform a comparative transcriptomic analysis of kiwifruit before and after postharvest ET or 1-MCP treatment to capture the molecular mechanism involved in ripening and ET biosynthesis under various storage durations.

2 Materials and methods

2.1 Plant materials and treatment

One of the most popular kiwifruit varieties, the green kiwifruits 'Hayward' (dry matter was 15.5~17.5%) were harvested 160 days after full bloom from an orchard in Boseong, Joellanam-do, Korea. Fruit of uniform size and with no physical damage was used for this study. Before ET or 1-MCP treatment, kiwifruits were harvested and named as BT samples. Then, kiwifruit was exposed to 1-MCP (final concentration: 1.4 μL) or ET (final concentration: 1,000 μL) at 22°C in sealed plastic containers. After 24 h of treatment, the fruit was transferred to a storage chamber at 22°C. The fruit quality indexes (section 2.2) were measured at 0 days (0D, immediately after transfer to storage chamber), 3 days (3D, stored at storage chamber), 5 days (5D, stored at storage chamber), 7 days (7D, stored at storage chamber), 10 days (10D, stored at storage chamber), 12 days (12D, stored at storage chamber), and 14 days (14D, stored at storage chamber) of storage at storage chamber. For RNA-seq analysis, untreated control, ET-treated, and 1-MCP treated samples harvested at 0D, 3D, 5D, and 7D time points were frozen with liquid nitrogen and used for RNA extraction (section 2.3).

2.2 Measurement of fruit firmness, respiration, ET production, and color parameters

Fruit firmness was measured using a texture analyzer (Stable Micro Systems, Godalming, Surrey, UK) equipped with a 5 mm cylindrical probe. The puncture speed and depth were set at 0.5 mm/s and 7 mm, respectively. Puncture measurement was conducted after removing the skin from the central part of the samples, and the highest penetrating value was shown as the fruit firmness. For measuring ET production, fruit samples were located in plastic jars. A headspace sample was taken using a gas-tight syringe for 1 h after sealing the jars and injected into a gas-chromatograph (450-GC, Varian, Middelburg, Netherlands) equipped with a flame ionization detector (FID). CIE L^* (lightness), a^* (+ redness, – greenness), and b^* (+ yellowness, – blueness) values of the fruit surface were recorded with a chromameter (CR-700d, Konica Minolta Optics, Inc., Osaka, Japan).

2.3 Total RNA extraction and RNA-Sequencing

RNA-seq analysis was performed on control (untreated), ET- or 1-MCP-treated green kiwifruit 'Hayward' stored for 0D, 3D, 5D, and 7D. After an eight-section dissection of the kiwifruit, the middle discs of the fresh fruit were collected, directly frozen in liquid nitrogen, and stored at −80°C in a deep freezer. Frozen middle discs taken from five randomly selected fruit were pooled as a biological replicate. Three biological replicates were prepared for each time point. Total RNAs were extracted using the Spectrum™ Plant Total RNA Kit (Sigma, USA) according to the manufacturer's instructions. After treatment with DNase I (NEB, USA) to remove contaminated DNA, the quantity of total RNAs was calculated with a Nano-400A spectrophotometer (Allsheng, China). The quality of total RNAs extracted was assessed by electrophoresis on 1% agarose gels as well as with the RNA Nano 6000 Assay Kit in combination with an Agilent Bioanalyzer 2100 (Agilent Technologies, USA). Purified total RNAs were used for RNA-seq library construction using the TruSeq Stranded mRNA LT Sample Prep Kit according to the manufacturer's instruction (Illumina, USA). Prepared RNA-seq libraries were sequenced on an Illumina NovaSeq 6000 system to generate 101 bp paired-end reads (Macrogen Co., South Korea). In total, 36 RNA-seq libraries were constructed and named as GC-0D-1 (Green kiwifruit, Control, 0 day, replicate 1), GC-0D-2, GC-0D-3, GC-3D-1, GC-3D-2, GC-3D-3, GC-5D-1, GC-5D-2, GC-5D-3, GC-7D-1, GC-7D-2, GC-7D-3, GE-0D-1 (Green kiwifruit, ET-treated, 0 day, replicate 1), GE-0D-2, GE-0D-3, GE-3D-1, GE-

3D-2, GE-3D-3, GE-5D-1, GE-5D-2, GE-5D-3, GE-7D-1, GE-7D-2, GE-7D-3, GM-0D-1 (Green kiwifruit, 1-MCP-treated, 0 day, replicate 1), GM-0D-2, GM-0D-3, GM-3D-1, GM-3D-2, GM-3D-3, GM-5D-1, GM-5D-2, GM-5D-3, GM-7D-1, GM-7D-2, and GM-7D-3.

2.4 Alignment of RNA-Seq reads

The quality of raw reads was pre-checked using the FastQC software (http://www.bioinformatics.babraham.ac.uk/projects/fastqc). Low-quality reads and adaptor sequences were removed by using the Trimmomatic program (Bolger et al., 2014). Cleaned reads (percentage of reads exhibiting Q30 above 95%) were mapped to the kiwifruit genome (http://kiwifruitgenome.org/node/152174) using TopHat2 (2.0.12) with default parameters (Kim et al., 2013). Mapped reads were then converted to digital counts using featureCounts (Liao et al., 2014).

2.5 Identification of differentially expressed genes

The edgeR program was used to extract DEGs (Robinson et al., 2009). DEGs were identified based on an adjusted *P*-value <0.05 and an absolute $\log_2|\text{fold change}| \geq 1$. A multi-dimensional scaling (MDS) plot and correlation heatmap data were produced using R packages (ver. 3.6.0). Venn diagram analysis was performed using VENNY (ver. 2.1.0) (https://bioinfogp.cnb.csic.es/tools/venny/). Mapped reads were also converted to bigwig files for visualization using the Integrative Genomics Viewer (IGV) software of the Broad Institute (Thorvaldsdóttir et al., 2013). Gene Ontology (GO) enrichment analysis of DEGs was conducted using ShinyGO (ver. 0.76) (http://bioinformatics.sdstate.edu/go/). Heatmap analysis of DEGs was performed using the MeV program ver. 4.9.0 (Howe et al., 2010).

2.6 Quantitative RT-qPCR analysis

Total RNAs (5 μg) were used to synthesize complementary DNAs (cDNAs) using oligo-dT primer and M-MLV reverse transcriptase (Promega, USA). Gene-specific primers were designed by DNA Club software and synthesized by Bionics (South Korea). Primer sequences used in this study are listed in Supplementary Table S1. qRT-PCR analysis was performed using the BIOFACT™ 2X Real-Time PCR Master Mix (BioFact, South Korea) on a LineGene 9600 Plus Real-Time PCR system (BioER, China). The PCR reaction conditions were as follows: 12 min denaturation at 95°C, followed by 50 cycles at 95°C for 15 s for denaturation, 60°C for 25 s for annealing, and 72°C for 35 s for extension. *AcACTIN* (Acc08082.1) was used as a reference gene (Atkinson et al., 2009). The $2^{-\Delta\Delta CT}$ algorithm was employed to quantify the relative transcript level of genes (Livak and Schmittgen, 2001).

2.7 Statistical analysis

All statistical analyses in this study were performed using a statistical software package (SAS ver. 9.4; SAS Institute, Inc., Cary, NC, USA). Statistical differences were calculated through one-way analysis of variance (ANOVA) and *post-hoc* Tukey's test ($p < 0.05$), and the significance level was assessed at $P < 0.05$. All data results were expressed as mean ± standard deviation of three biological replicates.

3 Results

3.1 Effect of ET and 1-MCP treatment on fruit quality indexes during storage

Treatment with ET, a gaseous hormone, is well known to rapidly trigger the ripening of fruits, including kiwifruit, whereas 1-MCP, a non-toxic chemical inhibitor of ET, is demonstrated to prohibit ET-mediated ripening in climacteric fruits (Serek et al., 1995; Liu et al., 2015). To investigate the molecular details underlying ET or 1-MCP effects on kiwifruit ripening by analyzing the genome-wide transcriptional profile, we prepared three different sample groups: control (non-treated), ET-treated, and 1-MCP-treated samples. Each group was analyzed for fruit qualities, including fruit firmness, ET level, and color parameters (*L*a*b*), on eight different occasions: before treatment (BT), on 0 days (0D; immediately after 24 h-treatment), and post-treatment at 3, 5, 7, 10, 12, and 14 days of storage at 22°C (3D, 5D, 7D, 10D, 12D, and 14D; Figures 1A–E). Fruit firmness decreased significantly with storage time (Figure 1B). ET treatment accelerated the reduction in fruit firmness, whereas 1-MCP treatment dramatically maintained the fruit firmness throughout the entire time course (Figure 1B). Measurement of the endogenous amounts of ET revealed an increase at the 3D time point (8.817 μL/kg/h), but the level became similar to the control samples at later time points (5D, 7D, 10D, and 14D), although temporarily lower at the 12D time point than the control samples (Figure 1C). In contrast, the 1-MCP treatment had no significant effect on the ET levels at all tested time points (BT–14D), indicating that 1-MCP can strictly prohibit the biosynthesis of ET in kiwifruit.

Color parameters (*L*a*b**) of kiwifruit skin and flesh were measured from harvest (BT) to the end of storage (14D) in all

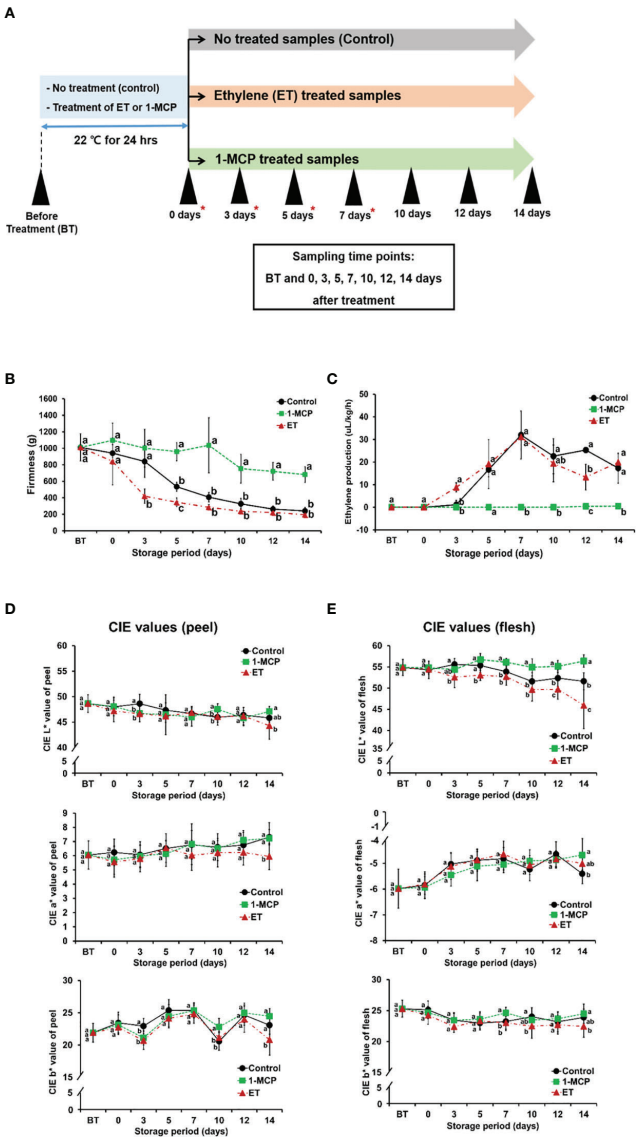

FIGURE 1
Characterization of firmness, ET amount, color (CIE *L**, *a**, and *b** values) of control, ET-treated, and 1-MCP-treated kiwifruit throughout ripening. **(A)** Schematic diagram showing kiwifruit sampling along ripening time course. Kiwifruit harvested immediately before each treatment was named BT, before treatment. Kiwifruit exposed to ET or 1-MCP, or non-treated (named as control) for 24 h in a chamber, then analyzed without further storage, were named 0D samples. Kiwifruit samples further stored for certain durations (3, 5, 7, 10, 12, and 14 days) were named 3D, 5D, 7D, 10D, 12D, and 14D, respectively. Red asterisks indicate the samples used for RNA-seq analysis. **(B)** Firmness of kiwifruit treated with ET or 1-MCP and non-treated control samples along ripening time course. **(C)** ET production of kiwifruit treated with ET or 1-MCP and non-treated control samples along ripening time course. **(D)** Peel color (*L*a*b**) of kiwifruit treated with ET or 1-MCP and non-treated control samples along ripening time course. **(E)** Flesh color (*L*a*b**) of kiwifruit treated with ET or 1-MCP and non-treated control samples along ripening time course. **(B–E)** Data were expressed as mean ± standard deviation. One-way analysis of variance (ANOVA) with Tukey's *post hoc* test was applied to calculate statistical differences. Different lowercase letters indicate significant differences (adjusted $P < 0.05$). ET, ethylene; 1-MCP, 1-methylcyclopropene.

three groups (Figures 1D, E). There was no obvious difference in the skin color parameters compared to the control samples at all time points, and the only significant difference in the color of kiwifruit flesh was the *L**-value of ET-treated samples, which decreased drastically compared to the control sample. Taken together, these results indicated that the experiments with control and ET- and 1-MCP-treated kiwifruit samples were successfully performed throughout ripening.

3.2 Transcriptional changes in kiwifruit during ripening

To dissect the transcriptomic changes in 'Hayward' kiwifruit during postharvest ripening, RNA-seq analysis was performed with kiwifruit stored for different durations (0, 3, 5, and 7 days after harvest) and termed GC-0D, GC-3D, GC-5D, and GC-7D, respectively. After filtering of poor-quality reads, paired reads with high-quality Q-values (>30) were aligned to the *Actinidia chinensis* 'Red5' reference genome, which was downloaded from the Kiwifruit Genome Database (KGD; https://kiwifruitgenome.org/) (Yue et al., 2020). The MDS plot of green kiwifruit samples across four time points showed group clustering between time point samples, indicating that the RNA-seq libraries were properly constructed and sequenced (Supplementary Figure S1A). The correlation heatmap analysis of control samples along the four different time points indicated that the GC-0D and GC-3D samples belonged to one group, and the GC-5D and GC-7D samples belonged to another group, indicating potentially similar transcriptomic profiles between the members of each group (Supplementary Figure S1B). This result suggested that dramatic changes in the transcriptome of kiwifruit might occur between 3D and 5D postharvest under our experimental condition.

A total of 2,706 (1,532 up- and 1,174 downregulated), 8,699 (3,655 up- and 5,044 downregulated) and 9,497 (4,178 up- and 5,319 downregulated DEGs were detected in pairwise comparisons ($\log_2$|fold change| > 1, *P*-value <0.05) of the 3D, 5D, and 7D samples with the non-stored sample, 0D (Figure 2A). In addition, the DEGs were grouped based on the expression profiles during storage, resulting in a total of 20 hierarchical clusters (Supplementary Figure S2). Genes belonging to each cluster might be useful as a resource for further investigation to understand the kiwifruit ripening process (Supplementary Table S2).

3.3 Transcriptomic dynamics of kiwifruit pretreated with ET and 1-MCP during ripening

As a plant hormone, ET plays a crucial role in kiwifruit ripening; thus, we aimed to capture the genome-wide transcriptional effects of ET and 1-MCP treatments on kiwifruit ripening at equivalent time points during storage. Sampling was performed at four different time points (0D, 3D, 5D, and 7D) post-treatment with ET or 1-MCP, and RNA-seq libraries were constructed. It should be emphasized that the 0D samples were those analyzed 24 h after the ET or 1-MCP treatment to examine the short-term effects of ET and 1-MCP. The MDS plot of the control, ET-treated, and 1-MCP-treated samples at each time point showed that samples exposed to the same treatment were closely clustered, indicating that the RNA-seq libraries were well constructed and sequenced (Supplementary Figure S3). After mapping to the 'Red5' reference genome, DEGs ($\log_2$|fold change| > 1 and *P*-value < 0.05) were isolated by comparison between control and ET-treated samples or between control and 1-MCP-treated samples (Figure 2B, Supplementary Figure S4). In ET-treated samples, 5,941, 5,780, 3,065, and 3,187 genes were differentially expressed at 0D, 3D, 5D, and 7D, respectively (Figure 2B). This pattern of a higher number of DEGs in the early time points (0D and 3D) than in later time points (5D and 7D) in ET-treated samples was opposite to the pattern displayed by 1-MCP-treated samples, in which the later time point samples (5D and 7D) exhibited substantially higher numbers of DEGs (10,389, and 10,396) compared to the early time point samples (0D and 3D with 2,746 and 2,793 DEGs, respectively) (Figure 2B). This contrasting pattern might imply that ET treatment strongly affects kiwifruit during early postharvest storage, whereas 1-MCP affects more sustainably on longer stored samples under our experimental condition.

3.4 DEGs upon ET or 1-MCP treatment during ripening

Considering the opposing roles of ET and 1-MCP in fruit ripening, we further analyzed the list of DEGs to extract genes oppositely affected by ET and 1-MCP treatment at individual time points. At 0D, 501 genes were upregulated by 1-MCP treatment and inversely downregulated by ET treatment. Meanwhile, 460 genes were downregulated in 1-MCP-treated samples but upregulated in ET-treated samples (Figure 2C). At the later time points of 3D, 5D, and 7D, we identified 755, 376, and 342 genes that were upregulated by 1-MCP and inversely downregulated by ET (Figures 2D–F). Meanwhile, 756, 475, and 413 genes were downregulated by 1-MCP and inversely upregulated by ET at 3D, 5D, and 7D, respectively. Information on the DEGs affected by ET and 1-MCP treatment at each time point is listed in Supplementary Table S3.

3.5 Cell wall genes are significantly affected by ET and 1-MCP treatment

It is well known that the amount of lignin (an end-product in the phenylpropanoids pathway) is increased during fruit ripening, whereas cellulose/hemicellulose is generally degraded; thus, fruit lignification is accelerated with fruit pigmentation (Zhang et al., 2021). Our results depicting the change in kiwifruit firmness during ripening (Figure 1B) are consistent with this pattern. To substantiate these observations, we identified the cell wall genes related to cellulose/hemicellulose degradation as well as cell wall lignification showing differential expression between ET- and 1-MCP-treated samples during the ripening phase. As a result, the expression patterns of a total of 131 genes were

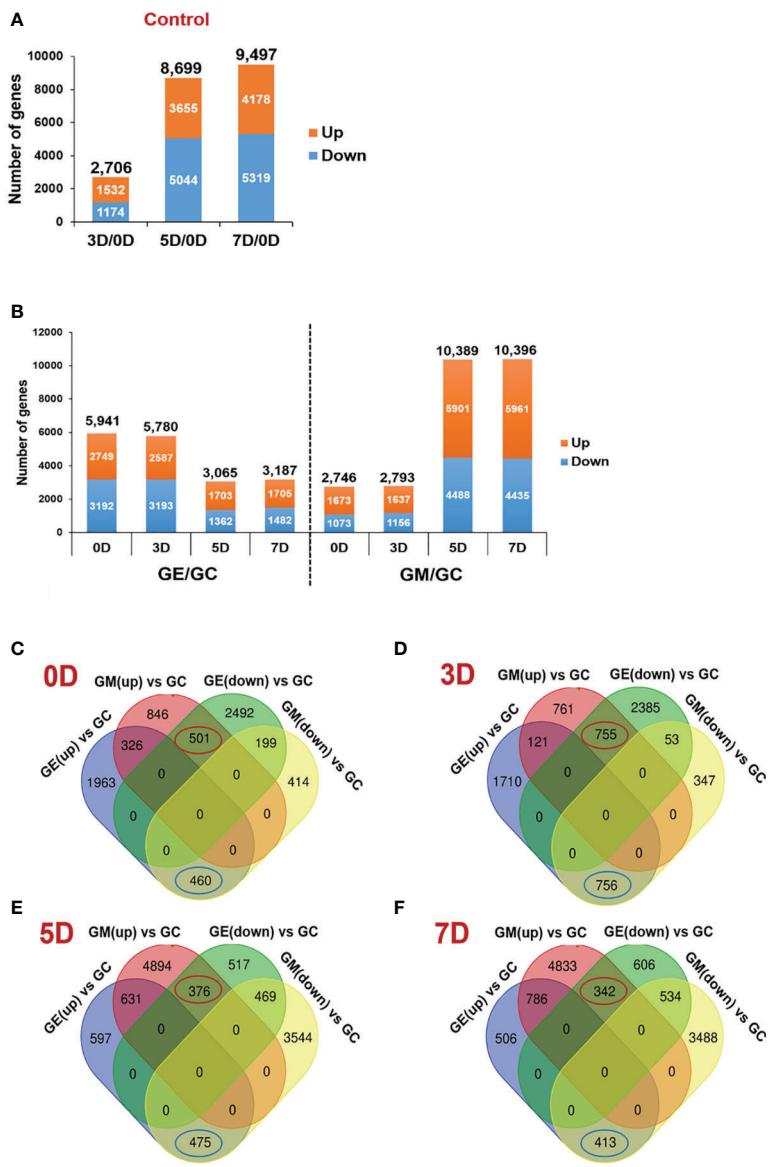

FIGURE 2
Identification of DEGs between ET-treated and control samples or between 1-MCP-treated samples and control samples. **(A)** Number of DEGs along the ripening time course of kiwifruit at 3, 5, and 7 days (3D, 5D, and 7D), respectively, compared to 0 days (0D) control. **(B)** Number of DEGs along the ripening course of kiwifruit at 0D, 3D, 5D, and 7D between ET-treated (GE) and control samples (GC) or 1-MCP-treated (GM) and control samples, respectively. **(C)** Venn diagram showing the overlapping and uniquely DEGs at 0D, compared between ET-treated sample and 1-MCP-treated sample. A total of 501 genes were upregulated by 1-MCP and downregulated by ET, whereas 460 genes were downregulated by 1-MCP and upregulated by ET. **(D)** Venn diagram showing the overlapping and uniquely DEGs at 3D, compared between ET-treated sample and 1-MCP-treated sample. A total of 755 genes were upregulated by 1-MCP and downregulated by ET, whereas 756 genes were downregulated by 1-MCP and upregulated by ET. **(E)** Venn diagram showing the overlapping and unique DEGs at 5D, compared between ET-treated sample and 1-MCP-treated sample. A total of 376 genes were upregulated by 1-MCP and downregulated by ET, whereas 475 genes were downregulated by 1-MCP and upregulated by ET. **(F)** Venn diagram showing the overlapping and uniquely DEGs at 7D, compared between ET-treated sample and 1-MCP-treated sample. A total of 342 genes were upregulated by 1-MCP and downregulated by ET, whereas 413 genes were downregulated by 1-MCP and upregulated by ET. DEG, differentially expressed gene; ET, ethylene; 1-MCP, 1-methylcyclopropene; GM, green kiwifruit with 1-MCP treatment; GC, green kiwifruit with no treatment (control); GE, green kiwifruit with ET treatment.

detected in ET- and 1-MCP-treated samples from 0D to 7D (Supplementary Table S4). Many genes, such as polygalacturonases and expansins, which are related to fruit ripening, were highly expressed in ET-treated samples but lowly expressed in 1-MCP-treated samples throughout the ripening process (Figures 3A, B). This result indicates that cell-wall-related genes are one of the targets of ET and 1-MCP during kiwifruit ripening. Consistent with the RNA-seq data, the qRT-

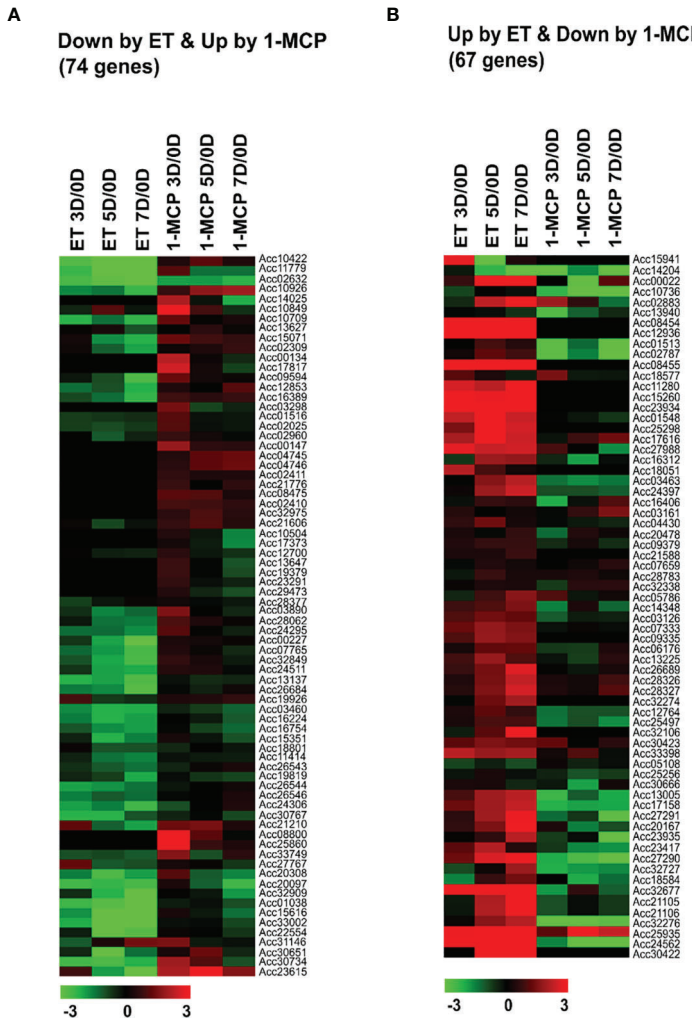

FIGURE 3
Normalized heatmaps showing expression levels of differentially expressed 'cell wall'-related genes inversely affected by ET and 1-MCP treatment along ripening time course. **(A)** Seventy-four cell-wall-related genes showed downregulated expression in ET treatment and upregulated expression in 1-MCP treatment. **(B)** Sixty-seven cell-wall-related genes showed upregulated expression in ET treatment and downregulated expression in 1-MCP treatment. Expression level of cell wall-related genes showing differential expression in treated samples stored for 3 vs. 0 days (3D/0D), 5 vs. 0 days (5D/0D), and 7 vs. 0 days (7D/0D). ET, ethylene; 1-MCP, 1-methylcyclopropene.

PCR analysis on *UDP-glucose pyrophosphorylase 3* (Acc01548), a cell-wall-related gene, showed that the expression level increased in ET-treated samples during storage, whereas it was repressed in 1-MCP-treated samples (Supplementary Figure S5A).

3.6 GO categories associated with photosynthesis and gene silencing were enriched in 1-MCP-treated samples

To grasp the biological categories affected by ET or 1-MCP treatment at individual time points, the GO analysis of the aforementioned DEGs was performed at individual time points (Figures 4A–D). First, DEGs downregulated by ET and inversely upregulated by 1-MCP were analyzed to identify the top 10 enriched GO terms at the 0D, 3D, 5D, and 7D time points, respectively. As a result, two biological processes related to photosynthesis and gene silencing were significantly enriched in the top 10 GO terms (Figures 4A–D). The result that the GO term related to photosynthesis was highly enriched in 1-MCP-treated samples at all time points reflected that one role of 1-MCP is to robustly block chlorophyll degradation and/or sustain photosynthetic light reactions and photosynthesis activity during fruit storage. Therefore, we collected the photosynthetic light reaction/photosynthesis-related genes from the KGD to examine their transcriptional patterns. A BLAST search using

10.3389/fpls.2022.1084997

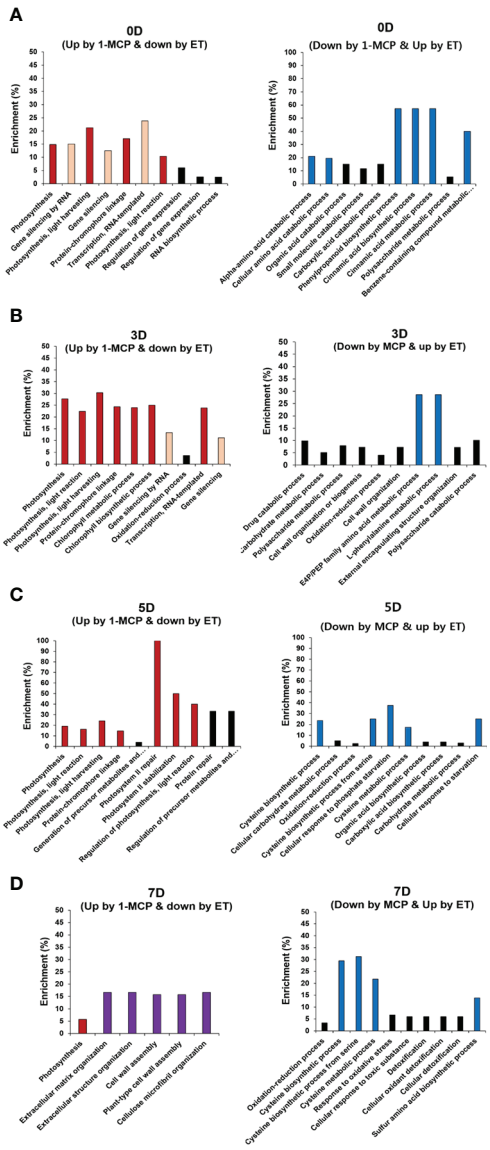

FIGURE 4
GO enrichment analysis of DEGs oppositely affected by ET and 1-MCP throughout ripening. Top 10 functional GO categories of DEGs showing inverse expression in kiwifruit exposed to ET and 1-MCP treatment and then stored for **(A)** 0 days (0D), **(B)** 3 days (3D), **(C)** 5 days (5D), and **(D)** 7 days (7D). A–D Left panels represent functional GO categories using genes showing upregulated expression by 1-MCP and downregulated expression by ET treatment, right panels represent functional GO categories using genes showing downregulated expression by 1-MCP and upregulated expression by ET. GO categories related to photosynthesis (red bars), gene silencing (yellow bars), the cell wall (purple bars), and cysteine biosynthesis (blue bars). GO, gene ontology; DEG, differentially expressed gene; ET, ethylene; 1-MCP, 1-methylcyclopropene.

sequence information of photosynthesis-related genes obtained from the model plant *Arabidopsis* identified 31 genes (Supplementary Table S5). As shown in Figure 5, most of the photosynthesis-related genes (27 out of 31) except four genes (Acc01594, Acc17809, Acc26523, and Acc09741) were highly upregulated upon 1-MCP treatment in at least one time point during ripening compared to those of ET-treated samples. It indicated that the photosynthetic light reaction/photosynthesis process is one of the main targets of 1-MCP in kiwifruit.

3.7 GO categories phenylpropanoids and amino acid biosynthesis are highly affected in ET-treated kiwifruit samples

Next, we also performed GO enrichment analysis with the list of DEGs showing upregulation by ET and downregulation by 1-MCP from 0D to 7D (Figures 4A–D). Phenylpropanoids (also referred to as cinnamic acid) biosynthesis and amino acid biosynthesis (cysteine and phenylalanine), both GO terms

10.3389/fpls.2022.1084997

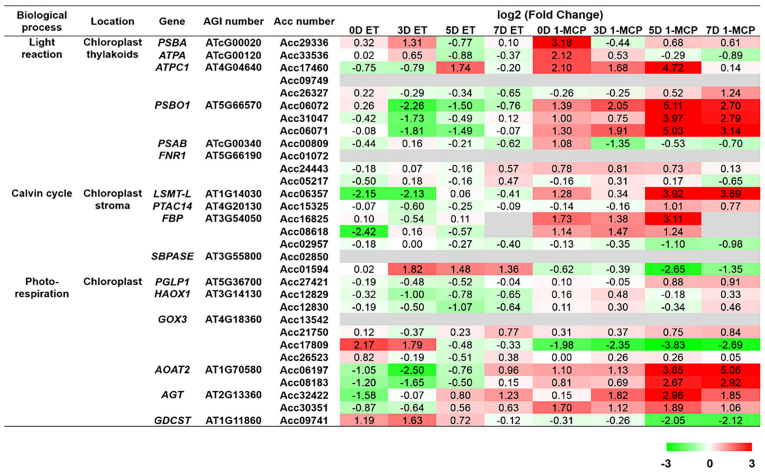

FIGURE 5
Normalized heatmap showing expression levels of photosynthesis-related genes upon ET and 1-MCP treatment along ripening time course. Thirty-one genes related to photosynthesis processes, like light reaction, Calvin cycle, and photorespiration, were found from the *Actinidia chinensis* genome database, and their expression levels were compared between ET-treated samples and 1-MCP-treated samples along ripening time course (0 days [0D], 3 days [3D], 5 days [5D], and 7 days [7D]). Twenty-seven of 31 total genes (87%) except four genes (Acc01594, Acc17809, Acc26523, and Acc09741) were highly upregulated upon 1-MCP treatment in at least one time point during ripening compared to those of ET-treated samples. ET, ethylene; 1-MCP, 1-methylcyclopropene; gene, *Arabidopsis* gene name; AGI, *Arabidopsis* gene index; Acc, *A. chinensis*.

related to secondary metabolisms, were substantially detected in the top 10 GO terms in the samples at all time points (Figures 4A–D). Phenylpropanoids are a group of secondary metabolites with diverse roles in plant development (i.e., cell wall formation) as well as fruit ripening (i.e., pigmentation) (Singh et al., 2010). Furthermore, they also play an important role in stress responses, such as the increased production of antioxidants in plants to counteract ultraviolet radiation-induced oxidative stress.

3.8 Expression of phenylpropanoid pathway genes was substantially affected by ET and 1-MCP treatment during ripening

Phenylpropanoids have a relatively simple structure and are synthesized by the shikimic acid pathway and the cinnamic acid pathway through sequential catalytic reactions starting from the condensation of 2-phosphoenolpyruvate and D-erythrose 4-phosphate. To check the expression pattern of the phenylpropanoid metabolic pathway genes, we first collected the phenylpropanoid metabolic pathway genes from the KGD. A total of 27 genes were identified as genes related to the phenylpropanoid pathway from the *Actinidia chinensis* genome (Supplementary Table S6). Many genes were upregulated in ET-treated samples compared to those in 1-MCP-treated samples over the entire time course. In particular, genes involved in the lignin biosynthesis pathway, an important branch of the general phenylpropanoids pathway, were significantly upregulated by the ET treatment in comparison to the 1-MCP treatment (Figure 6). For example, three *PAL* homologs, three *C4H* homologs, two *HCT* homologs, one *COMT* homolog, and three *CCR* homologs exhibited markedly higher expression in ET-treated samples than in 1-MCP-treated samples (Figure 6). To validate the RNA-seq result, we performed qRT-PCR analysis on a phenylalanine ammonia-lyase (named *AcPAL1)* in the phenylpropanoid pathway of *A. chinensis* (Supplementary S5B). Expression of *AcPAL1* (Acc08530) was substantially upregulated in ET-treated samples at all time points compared to levels in the control (GC). Meanwhile, 1-MCP-treated samples showed low expression of *AcPAL1* at all tested time points. Detailed information on the RNA-seq read count of each gene is listed in Supplementary Table S6. Taken together, these results indicate that phenylpropanoid pathway genes, particularly lignin biosynthesis pathway genes, are one target of the ET hormone during the ripening of kiwifruit.

3.9 Cysteine amino acid biosynthesis pathway was affected by ET and 1-MCP treatment during kiwifruit ripening

Another GO term was related to amino acid biosynthesis (phenylalanine and cysteine). As mentioned above,

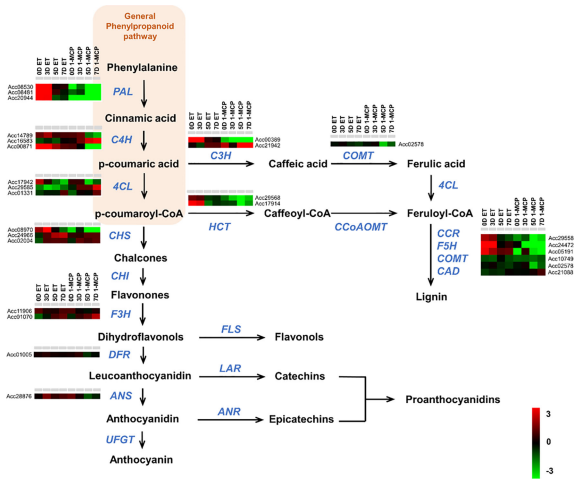

FIGURE 6
Expression profiles of phenylpropanoid pathway genes upon ET and 1-MCP treatment along ripening time course. Schematic diagram showing phenylpropanoid pathways beginning from general phenylpropanoid pathway constituting *PAL*, *C4H*, and *4CL* genes and then subsequently branched into different biosynthesis pathways for anthocyanins, proanthocyanidins, and lignin. Gene names responsible for each step of the phenylpropanoid pathway were indicated with italicized blue-colored letters. Expression levels of genes related to each step of the phenylpropanoid biosynthesis pathway were presented as a heatmap. Red cube represents upregulated gene expression, and green cube represents downregulated gene expression compared to the level of the control sample. ET, ethylene; 1-MCP, 1-methylcyclopropene.

phenylalanine is an amino acid derived from the shikimate pathway (Tohge et al., 2013) and is used as a precursor for the phenylpropanoid biosynthesis pathway, which synthesizes diverse metabolites like flavonols, dihydrochalcones, flavones, flavanones, and anthocyanins (Treutter, 2006). Another amino acid, cysteine, is one of the precursors for the synthesis of various sulfur-containing volatiles produced during fruit ripening (Panpetch and Sirikantaramas, 2021). For example, in ripening fruit, cysteine is used to generate defense-related compounds, such as glutathione, glucosinolates, camalexin, and ET hormone (Romero et al., 2014). The GO term related to cysteine biosynthesis was enriched at the later storage times (5D and 7D), whereas the GO term associated with phenylpropanoid (cinnamic acids) biosynthesis was observed at the relatively earlier time points (0D and 3D).

3.10 Transcriptional dynamics of cysteine biosynthetic pathway genes between ET- and 1-MCP-treated samples

Cysteine is a reduced donor compound involved in the biosynthesis of many essential secondary metabolites (Romero et al., 2014). Having established that the cysteine biosynthesis pathway was also a significantly enriched top 10 GO term using the list of DEGs (upregulated by ET and downregulated by 1-MCP), particularly at relatively late time points (5D and 7D) (Figures 4C, D), we examined the transcriptional profiles of genes related to cysteine biosynthesis in kiwifruit during ripening. Among a total of seven genes related to cysteine biosynthesis, six genes except Acc00356 were commonly upregulated by ET and downregulated by 1-MCP treatment during ripening (Figure 7; Supplementary Table S7). The RNA-seq data were validated by the qRT-PCR analysis performed on a cysteine biosynthesis pathway gene, *AcCAS-C1* (Acc20215) (Supplementary Figure S5C). It indicates that kiwifruit ripening is accompanied by cysteine biosynthesis.

3.11 Ripening of kiwifruit is accompanied by induction of ET biosynthetic genes and ET signaling

ET plays a pivotal role in the ripening of many fruits. In our study, treatment with ET and its inhibitor 1-MCP resulted in dynamic transcriptional changes in kiwifruit during ripening. Thus, we analyzed the expression profiles of the ET biosynthetic pathway genes as well as ET signaling genes in ET-treated and 1-MCP-treated samples over the ripening course. In total, 6 and 17 genes related to ET biosynthesis and ET signaling, respectively, were identified from the *A. chinensis* genome (Figure 8; Supplementary Table S8). Two *ACS* and five *ACO* homolog genes displayed markedly higher expression in ET-treated samples than in 1-MCP-treated samples over the ripening course. Among the ET signaling genes, five ET receptors and five CTR1 homologs commonly showed upregulated expression in ET-treated samples, particularly at early time points (0D and 3D), compared to the 1-MCP-treated samples (Figure 8A). Among the ET signaling transcription factor genes, such as *EIN2*, *EIN3*, and *EIN3-like*

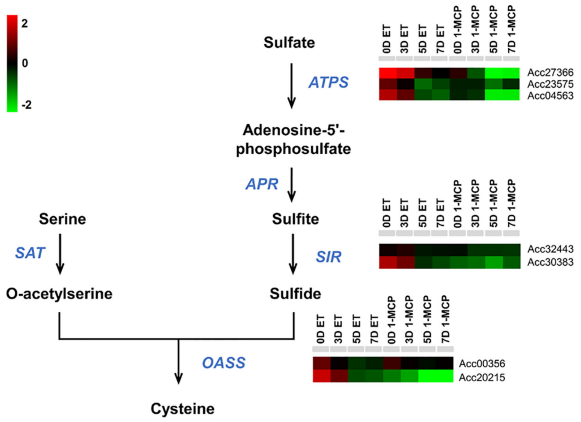

FIGURE 7
Expression profiles of cysteine biosynthesis pathway genes upon ET and 1-MCP treatment along ripening time course. Schematic diagram showing cysteine biosynthesis pathway from a precursor, sulfate. Gene names responsible for each step of the cysteine biosynthesis pathway were indicated with italicized blue-colored letters. Expression levels of genes related to each step of the cysteine biosynthesis pathway were presented as a heatmap. Red cube represents upregulated gene expression, and green cube represents downregulated gene expression compared to the level of the control sample. ET, ethylene; 1-MCP, 1-methylcyclopropene.

(EIL) homologs, five genes (Acc24758, Acc15132, Acc15131, Acc26185, and Acc32482) out of a total of seven genes showed differential expression in ET-treated and 1-MCP-treated samples, but the other two genes (Acc08532 and Acc26184) did not show a dramatic difference between the ET- and 1-MCP-treated samples (Figure 8A; Supplementary Table S8). To validate the RNA-seq result, we performed qRT-PCR analysis on an ET signaling gene (named *AcETR2*, Acc04179) and an ET biosynthesis gene (named *AcACS6*, Acc05955) (Supplementary Figure S5D). A similar pattern to the RNA-seq data was shown in the qRT-PCR result. Given the fact that EIN3 and EILs play an important role as transcription factors in ET-mediated signaling, *AcEIN3/AcEIL* homologs might play a crucial role as transcription factors in the ET-mediated ripening in kiwifruit. Among *AcEIN3/AcEIL* signaling transcription factors, most drastic expressional difference between ET- and 1-MCP-trreated samples was observed in the *AcEIL* (Acc32482), highly upregulated by ET and downregulated by 1-MCP treatment in the early storage time points (0D~3D) (Figure 8B). It suggested that *AcEIL* homolog (Acc32482) might play an important role in the ET signaling cascade in the early ripening stage of kiwifruit. Taken together, most ET signaling and ET biosynthesis pathway genes are positively regulated by ET treatment but negatively affected by 1-MCP treatment during ripening.

4 Discussion

To elucidate the molecular details underlying ET-mediated ripening of kiwifruit, we analyzed transcriptomic changes by the treatment of ethylene (ET) or 1-MCP, an artificial ethylene inhibitor along the different time course of storage. We found that ET and 1-MCP targets on metabolic pathway genes related to photosynthesis, the cell wall formation, phenylpropanoids, sugar and cysteine biosynthesis Furthermore, ET biosynthetic and signaling pathway genes oppositely affected by ET and 1-MCP treatment were identified in the course of kiwifruit ripening.

In the measurement of endogenous ET production in control, ET-treated, and 1-MCP treated kiwifruit samples, we unexpectedly observed that maximum peak level of ET in the ET-treated samples was similar to that of the control (Figure 1C). Regarding this observation, it is worthy to note that ET-treated samples exhibited the earlier ET production than the control sample and the softening rate was accelerated. It can be inferred that the ET production peak in the ET-treated samples might be around the 6th day, not the 7th day. Because measurement of ET was conducted every 2 days, it is likely that ET production peak time might be skipped. This data indicate that exogenous ET treatment might have a positive impact on kiwifruit ripening within 7 days in our tested condition. Meanwhile, 1-MCP treatment displayed constantly decreased ET production throughout all tested ripening period (BT~14 days), confirming that 1-MCP play a negative impact on the ET biosynthesis in kiwifruit ripening stage.

A recent paper performed transcriptomic analysis to dissect effects of ET and 1-MCP on kiwifruit fruit ripening (Salazar et al., 2021). This paper showed that ET greatly influences sugar metabolism and photosynthesis biosynthetic pathways which was also observed in our study. However, this research differs from our study in terms of sample time points. That is, RNA-seq analysis of the previous study was performed only at two time

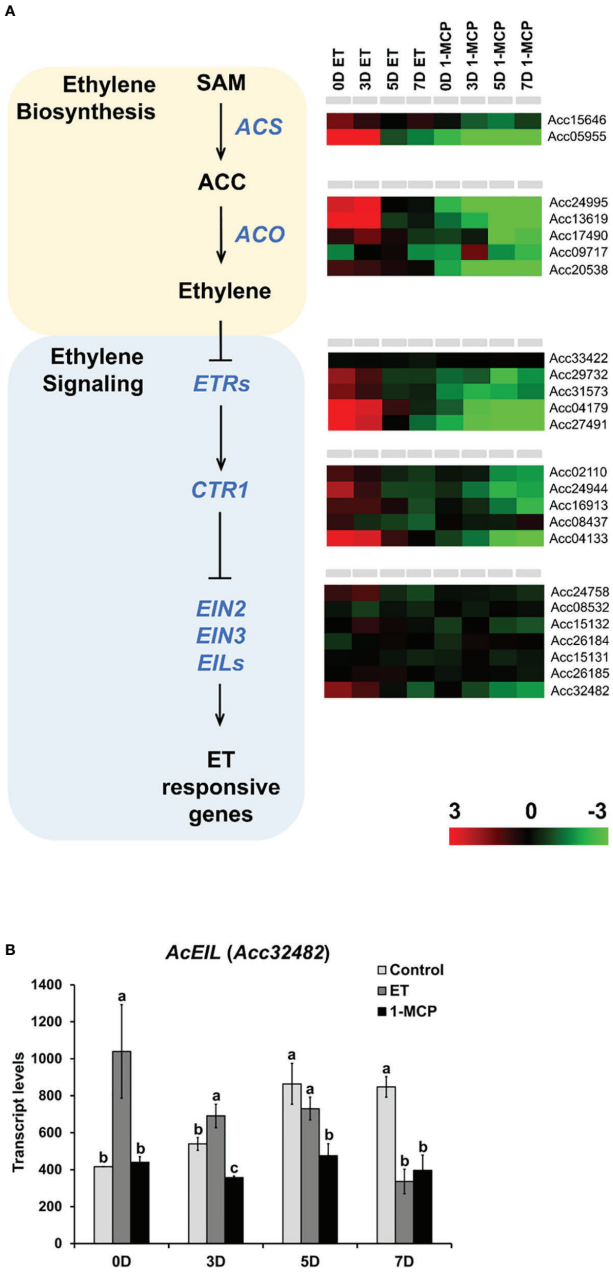

FIGURE 8
Expression profiles of ET signaling and biosynthesis pathway genes upon ET and 1-MCP treatment along ripening time course. **(A)** Schematic diagram showing ET biosynthesis (pink box) and ET signaling (blue box) beginning from a precursor, S-adenosyl methionine (SAM). Gene names responsible for each step of ET biosynthesis and signaling pathway were indicated with italicized blue-colored letters. Expression levels of genes related to each step of ET biosynthesis and signaling pathway were presented as a heatmap. Red cube represents upregulated gene expression, and green cube represents downregulated gene expression compared to the level of the control sample. ET, ethylene; 1-MCP, 1-methylcyclopropene. **(B)** Transcript levels of *AcEIL* (Acc32482) in the control, ET-treated, and 1-MCP-treated samples along four different time course (0D, 3D, 5D, and 7D). ET, ethylene; 1-MCP, 1-methylcyclopropene. Data represent the mean of the transcript values from three biological replicates with error bars showing standard deviation (n=3). One-way ANOVA and *post-hoc* Tukey's test ($p < 0.05$) was applied to calculate the statistical significance, and significant difference was indicated in the figures by different letters ($p < 0.05$).

points, 4 days and 13 days after treatment, whereas our transcriptome analysis was performed at four different time points (0, 3, 5, and 7 days after treatment). Through this delicate analysis, we tried to capture the comprehensive transcriptomic profiles spanning early stage of ripening (0 and 3 days) to later ripening (5 and 7 days). It was expected that our transcriptomic data might capture more molecular details than the previous paper, particularly on the dynamic transcriptional

events occurring during early stage of ripening. As a result, GO analysis using DEGs found in this study identified the target genes by ET and 1-MCP, which are related to diverse biological pathways such as photosynthesis, pigment change (e.g. chlorophyll), sugar metabolism, cell wall metabolism, cysteine biosynthesis, and phenylpropanoids (i.e. lignin) compared to the previous paper.

Interestingly, the GO term 'photosynthesis' was consistently detected at all (0D–7D) time points in our GO analysis. This result corroborates the previous reports that ET accelerates chlorophyll degradation, thus resulting in changes in fruit color (Iqbal et al., 2017; Salazar et al., 2021; Kapoor et al., 2022). Thus, it is likely that photosynthesis biosynthetic pathway might be the one of major target by ET-mediated ripening process. In a consistency, previous studies reported that ET signaling factors like APETALA2/ethylene responsive factor (AP2/ERF) family genes play an important role in the fruit ripening through regulation of genes related to photosynthesis, chlorophyll metabolism during fruit ripening (Zhai et al., 2022).

Another GO term related to gene silencing by RNA was also significantly found at the early time points (0D and 3D), suggesting that post-transcriptional gene silencing by non-coding RNAs (ncRNAs) like miRNAs might play an important role in the ET-mediated ripening process in kiwifruit. Involvement of ncRNAs-mediated gene silencing has been reported in many flesh fruit so far (Wang et al., 2022b). For example, a genetic study using cultivated and wild tomato species revealed that small interfering RNAs (siRNAs)-mediated gene silencing and DNA methylation contribute to heritable transgressive phenotypes (Shivaprasad et al., 2012). In case of kiwifruit, a high-throughput small RNA-seq analysis unveiled that differential expression and repression of *MYB* genes which are targeted by small RNAs like miR828 and its phased small RNA AcTAS4-D4(-) is responsible for variable accumulation of anthocyanin in kiwifruit (Wang et al., 2022a). In the last decade, advance of high-throughput sequencing technology facilitated genome-wide profiling of small RNAs in ripening fruits including tomato, grape, banana, and olive and suggested that small RNA-mediated gene silencing and DNA methylation/demethylation might contribute to the developmental transition in flesh fruits (Sato et al., 2012; Belli Kullan et al., 2015; Bi et al., 2015; Carbone et al., 2019; Wang et al., 2022b). Recent studies strongly suggest that ncRNAs play an important role in the regulation of fruit ripening process. Therefore, elucidation of ncRNAs involved in the kiwifruit ripening might broaden our understanding on the molecular mechanism underlying kiwifruit ripening.

Considering that exogenous ET treatment exhibited a positive effect on the expression of ET signaling and ET biosynthesis pathway genes, it is likely that exogenous ET treatment might further reinforce the biosynthesis of endogenous ET in ripening fruit. However, in our study, endogenous ET production was temporarily enhanced at an early time point (3D) in ET-treated samples but did not display a significant increase in later stages (5D and 7D) in ET-treated samples (Figure 1C). Hence, further clarification is needed to determine whether kiwifruit has a feedback regulation of ET production upon the treatment of exogenous ET. One plausible explanation would be that exogenous ET treatment triggered transcriptional activation of ET signaling and ET biosynthesis genes; negative feedback regulation might act at the translational or post-translational level to maintain homeostasis of endogenous ET in kiwifruit. Regarding this hypothesis, a study using the model plant *Arabidopsis* reported that ET signaling and biosynthesis are finely modulated at the protein level by EIN3-binding F-box proteins (EBF1 and EBF2), which interact with EIN3 and EIL1 and destabilize EIN3/EIL1 *via* ubiquitination-mediated protein degradation, thus providing negative feedback regulation (An et al., 2010). In addition to studying whether kiwifruit has EBF1/2-mediated feedback regulation in endogenous ET biosynthesis, it would also be worth studying whether different genotypes and storage conditions (i.e., temperature) influence the effect of exogenous ET and 1-MCP treatments on kiwifruit ripening.

Previous studies reported that some kiwifruit ET biosynthetic genes such as *AC-SAM1*, *AC-SAM2*, *AC-ACO1*, and *AC-ACO2* and ET signaling factor genes like *KWACO1* and *KWACS1* genes were activated and required for the ET biosynthesis (Ilina et al., 2010; Mworia et al., 2010). In addition, some ET signaling factors including AdEIN3-like (AdEILs) and ethylene response factors (ERFs) were reported to be dynamically regulated in ripening of kiwifruit (*Actinidia deliciosa*) (Yin et al., 2010). In our study, we also observed that 5 ET biosynthetic genes (2 *AcACS* and 3 *AcACO* homologs) and 7 ET signaling factor genes (4 *AcETRs*, 2 *AcCTRs*, and 1 *AcEIL* homolog) were up-regulated in ET-treated samples than control samples (Figure 8A). In contrast, 7 ET biosynthetic genes (2 *AcACS* and 5 *AcACO* homologs) and 9 ET signaling factor genes (4 *AcETRs*, 4 *AcCTRs*, and 1 *AcEIN3* homologs) were down-regulated in 1-MCP-treated samples along the ripening time course. It indicates that expression of both ET biosynthetic as well as ET signaling factors are dynamically modulated by ET and 1-MCP treatment during ripening. Particularly, this study found that *AcEIL* (Acc32482) was highly up-regulated by ET and down-regulated by 1-MCP at early ripening stage (0D~3D), suggesting that it might play an important role in ET-mediated ripening process of kiwifruit (Figure 8B). CRISPR-Cas9 Genome editing on key ET signaling factor genes like *AcEIN3/AcEIL* homologs (e.g. *AcEIL*) in kiwifruit might be helpful to unveil the molecular mechanism underlying ET-mediated ripening process in kiwifruit. Collectively, our transcriptomic study unveiled the molecular targets by ET and its antagonist, 1-MCP, such as ET-targeted metabolisms and ET-targeted metabolic genes in kiwifruit during ripening and might be valuable for further investigation on kiwifruit fruit ripening.

Data availability statement

The datasets presented in this study can be found in online repositories. The names of the repository/repositories and accession number(s) can be found below: https://www.ncbi.nlm.nih.gov/genbank/, GSE214748.

Author contributions

JL and D-HK designed the study. DC and JC prepared all materials. JC and K-JP analyzed firmness, ethylene, and sugar contents. DC and CK performed molecular experiments. DC and D-HK performed the transcriptome analysis. JL and D-HK supervised the experiments and wrote the manuscript. All authors contributed to the manuscript and approved the final version of the manuscript to be published.

Funding

This work was supported by a grant from the Main Research Program (E0211001) of the Korea Food Research Institute (KFRI) funded by the Ministry of Science and ICT to JL and in part by a research grant from the Chung-Ang University (2022) to D-HK.

Conflict of interest

The authors declare that the research was conducted in the absence of any commercial or financial relationships that could be construed as a potential conflict of interest.

Publisher's note

All claims expressed in this article are solely those of the authors and do not necessarily represent those of their affiliated organizations, or those of the publisher, the editors and the reviewers. Any product that may be evaluated in this article, or claim that may be made by its manufacturer, is not guaranteed or endorsed by the publisher.

Supplementary material

The Supplementary Material for this article can be found online at: https://www.frontiersin.org/articles/10.3389/fpls.2022.1084997/full#supplementary-material

References

Adams-Phillips, L., Barry, C., and Giovannoni, J. (2004). Signal transduction systems regulating fruit ripening. *Trends Plant Sci.* 9, 331–338. doi: 10.1016/j.tplants.2004.05.004

Alexander, L., and Grierson, D. (2002). Ethylene biosynthesis and action in tomato: a model for climacteric fruit ripening. *J. Exp. Bot.* 53, 2039–2055. doi: 10.1093/JXB/ERF072

An, F., Zhao, Q., Ji, Y., Li, W., Jiang, Z., Yu, X., et al. (2010). Ethylene-induced stabilization of ETHYLENE INSENSITIVE3 and EIN3-LIKE1 is mediated by proteasomal degradation of EIN3 binding f-box 1 and 2 that requires EIN2 in arabidopsis. *Plant Cell* 22, 2384–2401. doi: 10.1105/TPC.110.076588

Asiche, W. O., Mitalo, O. W., Kasahara, Y., Tosa, Y., Mworia, E. G., Owino, W. O., et al. (2018). Comparative transcriptome analysis reveals distinct ethylene-independent regulation of ripening in response to low temperature in kiwifruit. *BMC Plant Biol.* 18, 1–18. doi: 10.1186/S12870-018-1264-Y/FIGURES/10

Atkinson, R. G., Johnston, S. L., Yauk, Y. K., Sharma, N. N., and Schröder, R. (2009). Analysis of xyloglucan endotransglucosylase/hydrolase (XTH) gene families in kiwifruit and apple. *Postharvest Biol. Technol.* 51, 149–157. doi: 10.1016/j.postharvbio.2008.06.014

Belli Kullan, J., Lopes Paim Pinto, D., Bertolini, E., Fasoli, M., Zenoni, S., Tornielli, G. B., et al. (2015). miRVine: A microRNA expression atlas of grapevine based on small RNA sequencing. *BMC Genomics* 16, 1–23. doi: 10.1186/S12864-015-1610-5/FIGURES/2

Bi, F., Meng, X., Ma, C., and Yi, G. (2015). Identification of miRNAs involved in fruit ripening in Cavendish bananas by deep sequencing. *BMC Genomics* 16, 1–15. doi: 10.1186/S12864-015-1995-1/FIGURES/8

Bolger, A. M., Lohse, M., and Usadel, B. (2014). Trimmomatic: A flexible trimmer for illumina sequence data. *Bioinformatics* 30, 2114–2120. doi: 10.1093/bioinformatics/btu170

Brummell, D. A., and Harpster, M. H. (2001). Cell wall metabolism in fruit softening and quality and its manipulation in transgenic plants. *Plant Mol. Biol.* 47, 311–339. doi: 10.1023/A:1010656104304

Brumos, J. (2021). Gene regulation in climacteric fruit ripening. *Curr. Opin. Plant Biol.* 63, 102042. doi: 10.1016/j.pbi.2021.102042

Carbone, F., Bruno, L., Perrotta, G., Bitonti, M. B., Muzzalupo, I., and Chiappetta, A. (2019). Identification of miRNAs involved in fruit ripening by deep sequencing of olea europaea l. transcriptome. *PloS One* 14, e0221460. doi: 10.1371/JOURNAL.PONE.0221460

Fan, X., and Mattheis, J. P. (1999). Impact of 1-methylcyclopropene and methyl jasmonate on apple volatile production. *J. Agric. Food Chem.* 47, 2847–2853. doi: 10.1021/JF990221S

Giovannoni, J. J. (2004). Genetic regulation of fruit development and ripening. *Plant Cell* 16, 170–180. doi: 10.1105/tpc.019158

Guo, H., and Ecker, J. R. (2004). The ethylene signaling pathway: New insights. *Curr. Opin. Plant Biol.* 7, 40–49. doi: 10.1016/j.pbi.2003.11.011

Howe, E., Holton, K., Nair, S., Schlauch, D., Sinha, R., and Quackenbush, J. (2010). "Mev: multiexperiment viewer," in *Biomedical informatics for cancer research* (Boston, MA: Springer), 267–277. doi: 10.1007/978-1-4419-5714-6

Hua, J., and Meyerowitz, E. M. (1998). Ethylene responses are negatively regulated by a receptor gene family in arabidopsis thaliana. *Cell* 94, 261–271. doi: 10.1016/S0092-8674(00)81425-7

Ilina, N., Alem, H. J., Pagano, E. A., and Sozzi, G. O. (2010). Suppression of ethylene perception after exposure to cooling conditions delays the progress of softening in 'Hayward' kiwifruit. *Postharvest Biol. Technol.* 55, 160–168. doi: 10.1016/J.POSTHARVBIO.2009.11.005

Iqbal, N., Khan, N. A., Ferrante, A., Trivellini, A., Francini, A., and Khan, M. I. R. (2017). Ethylene role in plant growth, development and senescence: interaction with other phytohormones. *Front. Plant Sci.* 8. doi: 10.3389/fpls.2017.00475

Ju, C., Yoon, G. M., Shemansky, J. M., Lin, D. Y., Ying, Z. I., Chang, J., et al. (2012). CTR1 phosphorylates the central regulator EIN2 to control ethylene hormone signaling from the ER membrane to the nucleus in arabidopsis. *Proc. Natl. Acad. Sci. U. S. A.* 109, 19486–19491. doi: 10.1073/PNAS.1214848109

Kapoor, L., Simkin, A. J., George Priya Doss, C., and Siva, R. (2022). Fruit ripening: dynamics and integrated analysis of carotenoids and anthocyanins. *BMC Plant Biol.* 22, 1–22. doi: 10.1186/S12870-021-03411-W

Kendrick, M. D., and Chang, C. (2008). Ethylene signaling: new levels of complexity and regulation. *Curr. Opin. Plant Biol.* 11, 479–485. doi: 10.1016/J.PBI.2008.06.011

Kim, D., Pertea, G., Trapnell, C., Pimentel, H., Kelley, R., and Salzberg, S. L. (2013). TopHat2: accurate alignment of transcriptomes in the presence of insertions, deletions and gene fusions. *Genome Biol.* 14, 1–13. doi: 10.1186/gb-2013-14-4-r36

Klee, H. J. (2004). Ethylene signal transduction. moving beyond arabidopsis. *Plant Physiol.* 135, 660–667. doi: 10.1104/PP.104.040998

Leliévre, J.-M., Latché, A., Jones, B., Bouzayen, M., and Pech, J. C. (1997). Ethylene and fruit ripening. *Physiol. Plant* 101, 727–39. doi: 10.1002/9781118223086.ch11

Liao, Y., Smyth, G. K., and Shi, W. (2014). FeatureCounts: An efficient general purpose program for assigning sequence reads to genomic features. *Bioinformatics* 30, 923–930. doi: 10.1093/bioinformatics/btt656

Liu, Y., Lv, G., Chai, J., Yang, Y., Ma, F., and Liu, Z. (2021). The effect of 1-mcp on the expression of carotenoid, chlorophyll degradation, and ethylene response factors in 'qihong' kiwifruit. *Foods* 10, 3017. doi: 10.3390/FOODS10123017/S1

Liu, M., Pirrello, J., Chervin, C., Roustan, J. P., and Bouzayen, M. (2015). Ethylene control of fruit ripening: Revisiting the complex network of transcriptional regulation. *Plant Physiol.* 169, 2380–2390. doi: 10.1104/pp.15.01361

Livak, K. J., and Schmittgen, T. D. (2001). Analysis of relative gene expression data using real-time quantitative PCR and the 2(-delta delta C(T)) method. *Methods* 25, 402–408. doi: 10.1006/METH.2001.1262

Li, X., Xu, C., Korban, S. S., and Chen, K. (2010). Regulatory mechanisms of textural changes in ripening fruits. *Crit. Rev. Plant Sci.* 29, 222–243. doi: 10.1080/07352689.2010.487776

Lv, J., Zhang, M., Bai, L., Han, X., Ge, Y., Wang, W., et al. (2020). Effects of 1-methylcyclopropene (1-MCP) on the expression of genes involved in the chlorophyll degradation pathway of apple fruit during storage. *Food Chem.* 308, 125707. doi: 10.1016/J.FOODCHEM.2019.125707

Mworia, E. G., Yoshikawa, T., Yokotani, N., Fukuda, T., Suezawa, K., Ushijima, K., et al. (2010). Characterization of ethylene biosynthesis and its regulation during fruit ripening in kiwifruit, actinidia chinensis 'Sanuki gold.'. *Postharvest Biol. Technol.* 55, 108–113. doi: 10.1016/J.POSTHARVBIO.2009.08.007

Nawaz, I., Tariq, R., Nazir, T., Khan, I., Basit, A., Gul, H., et al. (2021). RNA-Seq profiling reveals the plant hormones and molecular mechanisms stimulating the early ripening in apple. *Genomics* 113, 493–502. doi: 10.1016/J.YGENO.2020.09.040

Panpetch, P., and Sirikantaramas, S. (2021). Fruit ripening-associated leucylaminopeptidase with cysteinylglycine dipeptidase activity from durian suggests its involvement in glutathione recycling. *BMC Plant Biol.* 21, 1–14. doi: 10.1186/S12870-021-02845-6/FIGURES/7

Park, Y. S., Im, M. H., and Gorinstein, S. (2014). Shelf life extension and antioxidant activity of 'Hayward' kiwi fruit as a result of prestorage conditioning and 1-methylcyclopropene treatment. *J. Food Sci. Technol. 2014 525* 52, 2711–2720. doi: 10.1007/S13197-014-1300-3

Pathak, N., Asif, M. H., Dhawan, P., Srivastava, M. K., and Nath, P. (2003). Expression and activities of ethylene biosynthesis enzymes during ripening of banana fruits and effect of 1-MCP treatment. *Plant Growth Regul.* 40, 11–19. doi: 10.1023/A:1023040812205

Payasi, A., and Sanwal, G. G. (2010). Ripening of climacteric fruits and their control. *J. Food Biochem.* 34, 679–710. doi: 10.1111/j.1745-4514.2009.00307.x

Qiao, H., Shen, Z., Huang, S. S. C., Schmitz, R. J., Urich, M. A., Briggs, S. P., et al. (2012). Processing and subcellular trafficking of ER-tethered EIN2 control response to ethylene gas. *Science* 338, 390–393. doi: 10.1126/SCIENCE.1225974

Reddy, S. V. R., Sharma, R. R., and Barthakur, S. (2017). Influence of 1-MCP on texture, related enzymes, quality and their relative gene expression in 'Amrapali' mango (Mangifera indica l.) fruits. *J. Food Sci. Technol.* 54, 4051–4059. doi: 10.1007/S13197-017-2874-3

Robinson, M. D., McCarthy, D. J., and Smyth, G. K. (2009). edgeR: A bioconductor package for differential expression analysis of digital gene expression data. *Bioinformatics* 26, 139–140. doi: 10.1093/bioinformatics/btp616

Romero, L. C., Aroca, M.Á., Laureano-Marín, A. M., Moreno, I., García, I., and Gotor, C. (2014). Cysteine and cysteine-related signaling pathways in arabidopsis thaliana. *Mol. Plant* 7, 264–276. doi: 10.1093/MP/SST168

Salazar, J., Zapata, P., Silva, C., González, M., Pacheco, I., Bastías, M., et al. (2021). Transcriptome analysis and postharvest behavior of the kiwifruit 'Actinidia deliciosa' reveal the role of ethylene-related phytohormones during fruit ripening. *Tree Genet. Genomes* 17, 1–19. doi: 10.1007/S11295-021-01493-Z

Sato, S., Tabata, S., Hirakawa, H., Asamizu, E., Shirasawa, K., Isobe, S., et al. (2012). The tomato genome sequence provides insights into fleshy fruit evolution. *Nat* 485, 635–641. doi: 10.1038/nature11119

Serek, M., Tamari, G., Sisler, E. C., and Borochov, A. (1995). Inhibition of ethylene-induced cellular senescence symptoms by 1-methylcyclopropene, a new inhibitor of ethylene action. *Physiol. Plant* 94, 229–232. doi: 10.1111/J.1399-3054.1995.TB05305.X

Shen, Y. H., Lu, B. G., Feng, L., Yang, F. Y., Geng, J. J., Ming, R., et al. (2017). Isolation of ripening-related genes from ethylene/1-MCP treated papaya through RNA-seq. *BMC Genomics* 18, 1–13. doi: 10.1186/S12864-017-4072-0/FIGURES/6

Shi, T., Sun, J., Wu, X., Weng, J., Wang, P., Qie, H., et al. (2018). Transcriptome analysis of Chinese bayberry (Myrica rubra sieb. et zucc.) fruit treated with heat and 1-MCP. *Plant Physiol. Biochem.* 133, 40–49. doi: 10.1016/J.PLAPHY.2018.10.022

Shivaprasad, P. V., Dunn, R. M., Santos, B. A. C. M., Bassett, A., and Baulcombe, D. C. (2012). Extraordinary transgressive phenotypes of hybrid tomato are influenced by epigenetics and small silencing RNAs. *EMBO J.* 31, 257–266. doi: 10.1038/EMBOJ.2011.458

Singh, R., Rastogi, S., and Dwivedi, U. N. (2010). Phenylpropanoid metabolism in ripening fruits. *Compr. Rev. Food Sci. Food Saf.* 9, 398–416. doi: 10.1111/J.1541-4337.2010.00116.X

Thorvaldsdóttir, H., Robinson, J. T., and Mesirov, J. P. (2013). Integrative genomics viewer (IGV): high-performance genomics data visualization and exploration. *Brief. Bioinform.* 14, 178–192. doi: 10.1093/BIB/BBS017

Tian, M. S., Prakash, S., Elgar, H. J., Young, H., Burmeister, D. M., and Ross, G. S. (2000). Responses of strawberry fruit to 1-methylcyclopropene (1-MCP) and ethylene. *Plant Growth Regul.* 32, 83–90. doi: 10.1023/A:1006409719333

Tohge, T., Watanabe, M., Hoefgen, R., and Fernie, A. R. (2013). Shikimate and phenylalanine biosynthesis in the green lineage. *Front. Plant Sci.* 4. doi: 10.3389/FPLS.2013.00062

Treutter, D. (2006). Significance of flavonoids in plant resistance: a review. *Environ. Chem. Lett. 2006 43* 4, 147–157. doi: 10.1007/S10311-006-0068-8

Wang, W., Moss, S. M. A., Zeng, L., Espley, R. V., Wang, T., Lin-Wang, K., et al. (2022a). The red flesh of kiwifruit is differentially controlled by specific activation–repression systems. *New Phytol.* 235, 630–645. doi: 10.1111/NPH.18122

Wang, W., Wang, Y., Chen, T., Qin, G., and Tian, S. (2022b). Current insights into posttranscriptional regulation of fleshy fruit ripening. *Plant Physiol.* kiac483. doi: 10.1093/PLPHYS/KIAC483

Wang, B., Wang, Y., Li, W., Zhou, J., Chang, H., and Golding, J. B. (2021). Effect of 1-MCP and ethylene absorbent on the development of lenticel disorder of 'Xinli No.7' pear and possible mechanisms. *J. Sci. Food Agric.* 101, 2525–2533. doi: 10.1002/JSFA.10879

Wen, B., Zhang, F., Wu, X., and Li, H. (2020). Characterization of the tomato (Solanum lycopersicum) pectin methylesterases: Evolution, activity of isoforms and expression during fruit ripening. *Front. Plant Sci.* 11. doi: 10.3389/fpls.2020.00238

Yang, S. F., and Hoffman, N. E. (1984). Ethylene biosynthesis and its regulation in higher plants. *Annu. Rev. Plant Physiol* 35, 155–189. doi: 10.1146/ANNUREV.PP.35.060184.001103

Yin, X. R., Allan, A. C., Chen, K. S., and Ferguson, I. B. (2010). Kiwifruit EIL and ERF genes involved in regulating fruit ripening. *Plant Physiol.* 153, 1280–1292. doi: 10.1104/PP.110.157081

Yue, J., Liu, J., Tang, W., Wu, Y. Q., Tang, X., Li, W., et al. (2020). Kiwifruit genome database (KGD): a comprehensive resource for kiwifruit genomics. *Hortic. Res.* 7, 1–8. doi: 10.1038/s41438-020-0338-9

Zhai, Y., Fan, Z., Cui, Y., Gu, X., Chen, S., and Ma, H. (2022). APETALA2/ethylene responsive factor in fruit ripening: Roles, interactions and expression regulation. *Front. Plant Sci.* 13. doi: 10.3389/FPLS.2022.979348/BIBTEX

Zhang, Q., Wang, L., Wang, Z., Zhang, R., Liu, P., Liu, M., et al. (2021). The regulation of cell wall lignification and lignin biosynthesis during pigmentation of winter jujube. *Hortic. Res.* 8, 238. doi: 10.1038/S41438-021-00670-4/42043609/41438_2021_ARTICLE_670.PDF

Zhu, X., Ye, L., Ding, X., Gao, Q., Xiao, S., Tan, Q., et al. (2019). Transcriptomic analysis reveals key factors in fruit ripening and rubbery texture caused by 1-MCP in papaya. *BMC Plant Biol.* 19, 1–22. doi: 10.1186/S12870-019-1904-X/FIGURES/10

frontiers | Frontiers in Plant Science

TYPE Original Research
PUBLISHED 11 January 2023
DOI 10.3389/fpls.2022.1086375

OPEN ACCESS

EDITED BY
Shifeng Cao,
Zhejiang Wanli University, China

REVIEWED BY
María Emma García Pastor,
Miguel Hernández University of Elche, Spain
Zhengke Zhang,
Hainan University, China

*CORRESPONDENCE
Jinyin Chen
jinyinchen@126.com
Chuying Chen
cy.chen@jxau.edu.cn

SPECIALTY SECTION
This article was submitted to Crop and Product Physiology, a section of the journal Frontiers in Plant Science

RECEIVED 01 November 2022
ACCEPTED 28 December 2022
PUBLISHED 11 January 2023

CITATION
Huang Q, Huang L, Chen J, Zhang Y, Kai W and Chen C (2023) Maintenance of postharvest storability and overall quality of 'Jinshayou' pummelo fruit by salicylic acid treatment.
Front. Plant Sci. 13:1086375.
doi: 10.3389/fpls.2022.1086375

Maintenance of postharvest storability and overall quality of 'Jinshayou' pummelo fruit by salicylic acid treatment

Qiang Huang, Lulu Huang, Jinyin Chen*, Yajie Zhang, Wenbin Kai and Chuying Chen*

Jiangxi Key Laboratory for Postharvest Preservation and Non-Destruction Testing of Fruits & Vegetables, College of Agriculture, Jiangxi Agricultural University, Nanchang, China

Introduction: The loss of postharvest storability of pummelo fruit reduces its commodity value for long run. To maintain its storability, the effects of postharvest dipping treatment by salicylic acid (SA) with different concentrations (0, 0.1, 0.2, or 0.3%) were investigated on pummelo fruit (*Citrus maxima* Merr. cv. Jinshayou) during the room temperature storage at 20 ± 2°C for 90 d.

Results and discussion: Among all treatments, pre-storage SA treatment at 0.3% demonstrated the most significant ability to reduce fruit decay incidence, decrease weight loss, delay peel color-turned process, and inhibit the declines in total soluble solids (TSS) as well as titratable acid (TA) content. The increases in electrolyte leakage, hydrogen peroxide (H_2O_2), and malondialdehyde (MDA) content of the 0.3% SA-treated pummelo fruit were reduced compared to the control (dipped in distilled water). Pummelo fruit treated with 0.3% SA exhibited the most outstanding ability to excess reactive oxygen species (ROS) accumulation, as evidenced by promoted the increases in glutathione (GSH), total phenolics and flavonoids contents, delayed the AsA decline, and enhanced the activities of antioxidant enzymes and their encoding genes expression.

Conclusion: Pre-storage treatment dipped with SA, particularly at 0.3%, can be used as a useful and safe preservation method to maintain higher postharvest storability and better overall quality of 'Jinshayou' pummelo fruit, and thus delaying postharvest senescence and extend the storage life up to 90 d at room temperature.

KEYWORDS

***Citrus maxima* Merr., salicylic acid, postharvest storablitiy, overall quality, ROS homeostasis**

1 Introduction

Pummelo (*Citrus maxima* Merr.) fruit, the largest known citrus fruit, is a non-climacteric subtropical fruit belonging to the *Citrus* family, and widely cultivated in Southeast China (e.g., Fujian, Jiangxi, Zhejiang, Guangdong, and other adjoining provinces) (Chen et al., 2021; Chen et al., 2022). Due to its rich nutrients (e.g., dietary fiber, organic acids, vitamins, pectins, flavonoids and minerals), full succulency, attractive appearance, pleasant flavor, and blessed moral, pummelo fruit is considered as a highly appreciated citrus fruit by consumers. Pummelo fruit has a huge shape and large weight, which is an enormous challenge during the postharvest periods, particularly during transportation and storage, leading into a remarkable restriction to the marketability and industrial development. Several preservation methods have been applied to maintain postharvest storability of harvested pummelo fruit, such as $CaCl_2$ (Chen et al., 2005), chitosan (Nie et al., 2020; Chen et al., 2021), gibberellic acid (Porat et al., 2001), and 1-methylcyclopropene (Lacerna et al., 2018). As the closest citrus fruit to pummelo fruit, grapefruit can be effectively preserved by using several postharvest approaches, including hot water, biocontrol agent GS-3, neem leaf extract, and pectic oligosaccharides (Porat et al., 2000; Vera-Guzmán et al., 2019; Deng et al., 2020; Khan et al., 2021). Due to the long-established application of postharvest methods for pummelo, and the dissimilarities between the above two citrus varieties, the development of effective postharvest technologies for pummelo preservation is of great importance and urgency.

Salicylic acid (SA), an important plant phenolic compound, acts as an important signaling molecule with a role in enhancing postharvest resistance to senescence stress and pathogen invasion in horticultural products during long-term storage and shipment (Belay and James Caleb, 2022). Recently, SA treatment applied for postharvest purposes to delay fruit senescence has attracted increasing attention. Numerous studies have demonstrated that pre-storage treatment with SA effectively alleviates firmness loss and quality deterioration in mandarin fruit (Haider et al., 2020), lemon fruit (Serna-Escolano et al., 2021), apricot fruit (Li et al., 2022), bell pepper (Ge et al., 2020), grapefruit (Shi et al., 2019), longan fruit (Chen et al., 2020), winter jujube (Sang et al., 2022), and pear fruit (Sinha et al., 2022). In these studies, the maintenance of postharvest storability in horticultural fruits was deemed to be related to phytochemicals and enzymes involved in cell wall metabolism, reactive active oxygen (ROS) metabolism, as well as energy metabolism. For example, Baswal et al. (2020) found that 2 μM SA could extend the cold-stored life of 'Kinnow' mandarin up to 75 d by reducing firmness loss, alleviating nutritional quality (ascorbic acid, carotenoids, soluble sugars and titratable acids) deterioration and delaying cell wall-softening enzymes activities. In addition, 2 mM SA treatment reduced postharvest decay and pulp browning of 'Patharnakh' pear by maintaining fruit firmness and nutritional quality, inhibiting fruit respiration, and enhancing the antioxidant system, whereas the high browning index correlated to the high PPO activity and the low total phenolics content (TPC) was observed in the control fruit (Adhikary et al., 2021). Furthermore, postharvest SA application is proved to be beneficial for enhancing nutritional quality and antioxidant potential of berry fruits (cornelian cherry, blueberry, and tomato) in the period of storage (Dokhanieh et al., 2013; Kumar et al., 2021; Jiang et al., 2022).

Although pre-storage SA treatment has been shown to be useful for the postharvest preservation of various fruits and vegetables, as far as we know, there is rarely information on the alleviatory effects of SA on pummelo postharvest senescence and the overall quality of 'Jinshayou' pummelo fruit during long-term storage. The aim of this study was to evaluate the preservative effect of SA on postharvest fruit quality, oxidative stress, antioxidant capacity, and ROS-scavenging system in 'Jinshayou' pummelo fruit during the room temperature storage, and provide theoretical evidence to develop SA as a green and efficacious preservative for postharvest pummelo fruit.

2 Material and methods

2.1 Chemicals

SA, sodium hydroxide (NaOH), thiobarbituric acid (TBA), hydrochloric acid (HCl), trichloroacetic acid (TCA), methanol, ethanol, aluminum chloride ($AlCl_3$), polyvinylpyrrolidone (PVP), and iron sulfate were purchased from Sinopharm Chemical Reagent Co. Ltd. (Shanghai, China). Folin–Ciocalteu reagent, gallic acid (GA), rutin, *L*-ascorbic acid (*L*-AsA), 2,2-diphenyl-1-picrylhydrazyl (DPPH), and dithiothreitol (DTT) were obtained from Sigma-Aldrich, Chemical Co. (Louis, MO, USA).

2.2 Fruit materials and SA treatment

Pummelo (*C. maxima* Merr. cv. 'Jinshayou') fruit, at mature-green stage (about 195 d after anthesis), were harvested from a commercial orchard in Ji'shui city (Jiangxi Province, China). Fruit with uniformity of weight, shape, color, maturity (firmness: 54.5–56.2 N; ripening index: 20.6–21.3), and without visible defects were selected, washed with sterile water, and randomly divided into four groups (n = 4, 240 fruit in total per treatment). Each group was dipped in 0 (control), 0.1%, 0.2%, 0.3% SA solution for 5 min. After being naturally air-dried, each fruit was individually film packaged, and stored at room temperature condition [20 ± 2°C, relative humidity (RH): 70 – 85%] for 90 d. Fruit color change, decay rate, weight loss, and other biochemical quality parameters were measured at 15 d intervals. For each sample, the tissues of juice sacs (n = 3, 10 fruit in total

per replicate) randomly taken from the control and three SA-treated groups were frozen in liquid nitrogen, ground into powder and then stored at -80°C.

2.3 Measurement of peel hue angle (h°) and color difference (ΔE)

The CIE parameters of L* (dark to light), a* (green to red) and b* (blue to yellow) on two opposite equatorial sites of 'Jinshayou' pummelo peel were measured directly using a CR-400 colorimeter (Minolta Co., Osaka, Japan) following the protocol described by Mitalo et al. (2022). Both hue angle (h°) and color difference (ΔE) were calculated by the following two Hunter lab equations:

$h° = \arctan(b^*/a^*)$

$$\Delta E = \sqrt{(L^* - L_0^*)^2 + (a^* - a_0^*)^2 + (b^* - b_0^*)^2}$$

Where L_0, a_0, and b_0 were the readings at harvest (0 d), and L*, a*, and b* were the readings of each sampling time during storage period.

2.4 Evaluation of fruit decay incidence

The detailed method for evaluation of fruit decay rate has been previously described by Huang et al. (2021). The rate of fruit decay was evaluated as the number of decayed pummelo fruit with visible symptoms of pitted peel or pathogen incidence compared to the total number of pummelo fruit, and it was expressed as a percentage (%) after each storage period.

2.5 Determination of fruit weight loss

At 15-day intervals during storage at 20 ± 2°C, the weight loss of 'Jinshayou' pummelo fruit was recorded according to the protocol described by Baswal et al. (2020). The percentage (%) of WL rate was calculated compared to the initial fruit weight.

2.6 Assays of biochemical quality parameters

Total soluble solid (TSS) content in pummelo juice extracted from 10 fruit was determined with a digital refractometer (model: RA-250WE, Atago, Japan), calibrating with deionized water before each reading, and the results were expressed as a percentage (%). Titratable acidity (TA) content was analyzed in terms of citric acid by adding 4.0 grams extracted juice with two drops of 1% phenolphthalein in 40 mL of distilled water, and then it was titrated with 0.1 mol L^{-1} NaOH solution, and the results were calculated based on the NaOH consumption and expressed as %.

To estimate cell membrane permeability, electrolyte leakage (EL) was determined using a DDS-307A conductivity meter (Shanghai Rex., China) as described by Huang et al. (2021). The flesh tissue (5.0 grams) of juice sacs was stripped off, and then submerged in 40 mL of deionized water. Upon shaking the solution at 25°C for 30 min, the initial value (C0) was measured; subsequently, the final one (C1) was taken after the solution was exposed to a boiling water bath for 10 min. EL was reported as % from the ratio of C0 to C1.

For hydrogen peroxide (H_2O_2) content assay, a total of 2.0 g frozen sample was extracted with 5 mL of pre-cooled acetone and the homogenate was centrifuged (10 000 × *g* at 4°C for 20 min) to discard the residue. H_2O_2 content was determined using a specific detection kit (No: BC3590, Solarbio, Beijing, China) by monitoring the absorbance at 412 nm (Ackah et al., 2022), with the results reported as micromole per gram (μmol g^{-1}) on a frozen weight (FW).

Malondialdehyde (MDA) content was assayed using the TBA method as described by Bakpa et al. (2022) with a slight modification. Briefly, 2.0 g of frozen juice sac was extracted with 5 mL of 10% (*m/v*) TCA solution and centrifuged (10 000 × *g* at 4°C for 20 min). Afterwards, 2.0 mL of the supernatant was mixed by adding the same volume of 0.67% TBA (dissolved in 50 mM NaOH) solution, followed by boiling water bath for 20 min, and then quickly cooled in an ice bath. Finally, the absorbance of the supernatant was recorded at three specific wavelengths (450 nm, 532 nm, and 600 nm) using a UV-Vis spectrophotometer (model: TU-1950, Persee General Instrument Co., Ltd., Beijing, China), with the results were reported as millimole per gram (mmol g^{-1}) FW.

Quantitative determination of AsA content in pummelo fruit was carried out on juice sac samples according to the 2,6-dichlorophenol–indophenol (DPIP) dye titration method described by Huang et al. (2021), with *L*-AsA as the standard, where the AsA content was expressed as mg of AsA equivalent per 100 g of juice sac FW.

The glutathione (GSH) content of pummelo juice sac was determined using the 5,5'- dithiobis-(2-nitrobenzoic acid) reaction method, a protocol described by Nie et al. (2020), with 412 nm as the target wavelength, where the GSH content was reported as milligram per kilogram (mg kg^{-1}) FW.

Two grams of pummelo juice sac were homogenized with 8 mL of 1% HCl-methanol solution, followed by an extraction step at 4°C in the dark for 20 min, and vacuum filtered to remove the pumice. Following the Folin–Ciocalteu method and the $AlCl_3$ colorimetric method outlined by Nxumalo et al. (2022), both TPC and total flavonoids content (TFC) were measured at 760 nm and 510 nm, with GA and rutin as the standard, respectively, and the results of both TPC and TFC were expressed as mg equivalent per 100 g (mg 100 g^{-1}) of juice sac FW.

Two different assays were applied to assess the total antioxidant capacity in the juice sac of pummelo fruit: DPPH and hydroxyl radical (·OH) scavenging capacity assays. Determination of DPPH scavenging capacity was performed as described by Chen et al. (2022) with slight modifications. Briefly, 100 µL of the extracted juice sample was mixed with 1 mL of 0.1 mM DPPH solution, and allowed the mixture to stand in darkness for 30 min at 25°C before recording the absorbance at 517 nm. Adding 100 µL of deionized water in 1 mL of 0.1 mM DPPH solution was used as a control. The capacity to scavenge DPPH was expressed as percentage (%) and calculated by the following formula: (control OD_{517} - sample OD_{517})/control OD_{517} ×100.

The ·OH scavenging capacity was determined based on the SA–Fenton method as described by Yun et al. (2021) with slight modifications. Briefly, the juice supernatant was extracted from 0.5 g of pummelo juice sac was sample with 5 mL of 50% (*v/v*) ethanol. The reaction system consisted of 0.5 mL of 9 mM iron sulfate, 0.5 mL of 9 mM SA (dissolved in ethanol), 0.5 mL of juice supernatant, 2.5 mL of deionized water and 0.5 mL of 8.8 mM H_2O_2. After the water bath at 37°C for 20 min, the absorbance of the mixture reaction was determine at 410 nm. The ·OH scavenging capacity was expressed as percentage (%) and calculated with the formula as follows: (control OD_{410} - sample OD_{410})/control OD_{410} ×100.

2.7 Extraction and determination of ROS-scavenging enzymes activities

For the enzyme extraction and activity assay, all steps were carried out at 4°C. The extraction of crude enzyme was obtained by homogenizing 2.0 g of frozen juice sac powder with 8 mL of pre-cooled 100 mM phosphate buffer (pH 7.5, containing 5 mM DTT and 5% PVP) and removing the sediment by the centrifugation at 12 000 × *g* for 30 min, and the supernatant was collected for assaying ROS-scavenging enzymes [e.g., superoxide dismutase (SOD), catalase (CAT) and ascorbate peroxidase (APX), glutathione reductase (GR) and peroxide (POD)] activities.

SOD (EC 1.15.1.1) activity was determined *via* a specific SOD test kit (No: BC0170, Solarbio, Beijing, China) by detecting the absorbance of the reaction system at 560 nm. SOD activity was reported as U g^{-1}, where one unit (U) of SOD activity was equal to the photochemical reduction of nitroblue tetrazolium inhibited by 50% per minute. The activities of CAT (EC 1.11.1.6), APX (EC 1.11.1.11), and GR (EC 1.8.1.7) were measured as the description of Ackah et al. (2022) and Peng et al. (2022), and the results were reported as U g^{-1} FW, where one unit (U) of CAT, APX, and GR activities was defined as an increase in the absorbance by 0.01 per minute at 240 nm, 290 nm, and 340 nm, respectively. POD (EC 1.11.1.7) activity was monitored in accordance with the guaiacol oxidation method as reported by Nxumalo et al. (2022) with some modifications. Then, 200 µL of 0.5 M H_2O_2 (diluted with 50 mM phosphate buffer) was adding to trigger the reaction mixture for POD activity containing 3 mL of 25 mM guaiacol solution and 0.3 mL of crude enzyme. POD activity was expressed as U g^{-1}, where one unit (U) of POD activity was equal to the absorbance at 470 nm increased by 1 per minute.

2.8 RNA extraction and RT-qPCR analysis

The extraction of total high-quality RNA was carried out on 0.5 g of frozen juice sac powder from the control and 0.3% SA-treated pummelo fruit according to the cetyltrimethyl ammonium bromide (CTAB) method described by Landi et al. (2021). The integrity and quantification of the extracted RNA were determined using 1.0% agarose gel electrophoresis and based on the absorbance ratio at 260/280 nm in an ultramicro spectrophotometer (NanoDrop 2000, Wilmington, USA), respectively. The first-strand cDNA synthesis and qRT-PCR analysis of ROS-scavenging enzymes encoding genes were orderly performed following the procedures described by Chen et al. (2022). The *Actin* (Cg8g022300) gene was used as the internal control gene. Specific primers of *CmSOD* (Cg7g011780), *CmCAT* (Cg3g025260), *CmAPX* (Cg6g002810), *CmGR* (Cg5g018970), *CmPOD* (Cg2g001370), and *Actin* were designed with Primer 5.0 and listed in Supplementary Table 1. The transcript levels of the above-mentioned genes were quantified using the $2^{-\Delta\Delta Ct}$ method (Livak and Schmittgen, 2001).

2.9 Statistical analysis

All physico-biochemical parameters and gene expression data were acquired from three biological replicates (n = 3), each comprising a separate mixture of 10 pummelo fruit sampled per replicate. Duncan's multiple range test was applied to analyze the data using SPSS version 20.0. Significant differences among the control and SA treatments are highlighted with lowercase letters in Figure 1, and significant differences between both the control and 0.3% SA-treated fruit are highlighted with asterisks (**P*< 0.05 or ***P*< 0.01) in Figures 2-5.

3 Results

3.1 Effects of postharvest SA treatment on color performance, decay rate, weight loss, TSS content and TA level

Color is a pivotal factor which influences the acceptability of the fruit by consumers. Surface color of 'Jinshayou' pummelo

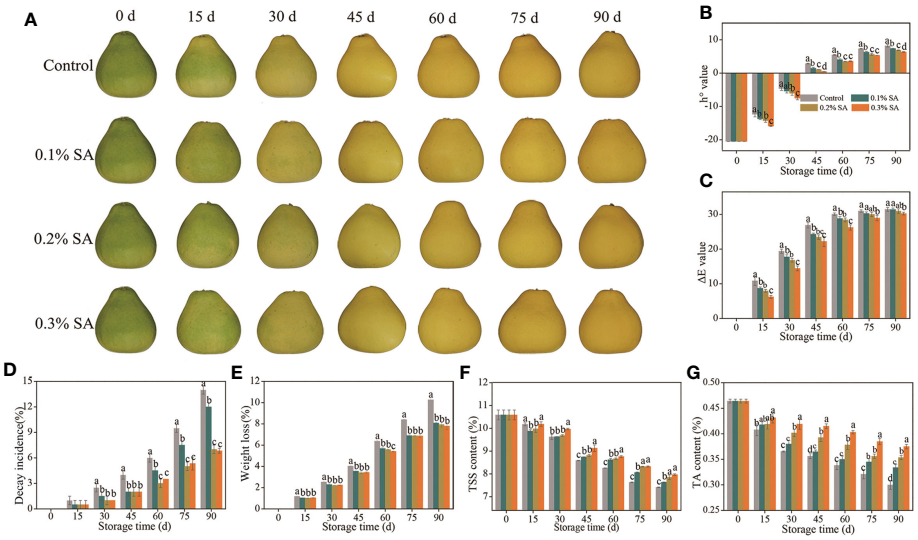

FIGURE 1
The mitigating effects of pre-storage SA treatment on color development **(A)**, decay incidence **(B)**, weight loss **(C)**, h° value **(D)**, ΔE value **(E)**, TSS content **(F)**, and TA content **(G)** of harvested 'Jinshayou' pummelo fruit. The different letters for each same sampling point indicate significant differences at $P< 0.05$ according to Duncan's multiple range test.

fruit turns from green to yellow during room temperature storage (Figure 1A). Both h° and ΔE values revealed a gradual increase in 'Jinshayou' pummelo fruit of three SA-treated and non-treated groups throughout the storage (Figures 1B, C). Nevertheless, the two increases in h° and ΔE value was significantly reduced by SA treatment in comparison with the control fruit surface. The inhibitory effect of pre-storage SA treatment was positively correlated with the SA-treated concentration, 0.3% SA-dipped treatment showed a significant delay on the increment of h° value in contrast with its 0.2% and 0.1% concentrations (Figures 1A–C).

A remarkable increase in decay incidence was observed in pummulo fruit with the prolongation of storage period from 30 to 90 d irrespective to the given SA-dipped treatment (Figure 1D). However, pre-storage treatment of SA dipping exhibited a significant inhibition in decay incidence compared to the control fruit throughout the storage period. This inhibitory effect until 90 d after the SA-dipped treatment, with the lowest decay incidence of 6.83% in the 0.3% SA-treated fruit, followed by the 0.2% and 0.1% SA-treated fruit, and finally the control (untreated) fruit, suggests that a beneficial effect of pre-storage treatment of SA dipping as a protective barrier avoiding postharvest pathogen infection or abiotic stress.

In general, fruit weight loss increased gradually throughout the storage period. The weight loss of pummulo fruit increased during the room temperature storage in case of all SA-dipped and control treatments (Figure 1E). Pre-storage treatment of SA dipping had no significant effect but delayed the weight loss percentage compared to the control fruit. At the end of storage (90 d), the highest weight loss of 10.27% was observed in control fruit, whereas the 0.3% SA-treated fruit showed the lowest weight loss of 7.61%.

The TSS content in pummelo fruit decreased continuously in all treatments, and this decline was effectively postponed by pre-

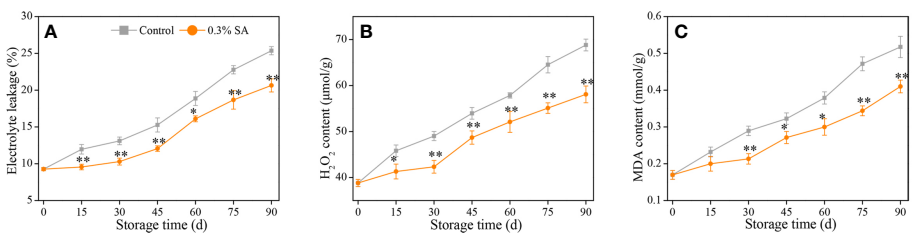

FIGURE 2
Variation in electrolyte leakage **(A)**, H_2O_2 content **(B)**, and MDA content **(C)** in the juice sac of 'Jinshayou' pummelo fruit treated with SA at 0.3% or untreated (control) during room temperature storage period. The asterisk of * ($P< 0.05$) or ** ($P< 0.01$) within the same sampling point denotes a significant difference between the control and 0.3% SA-treated group.

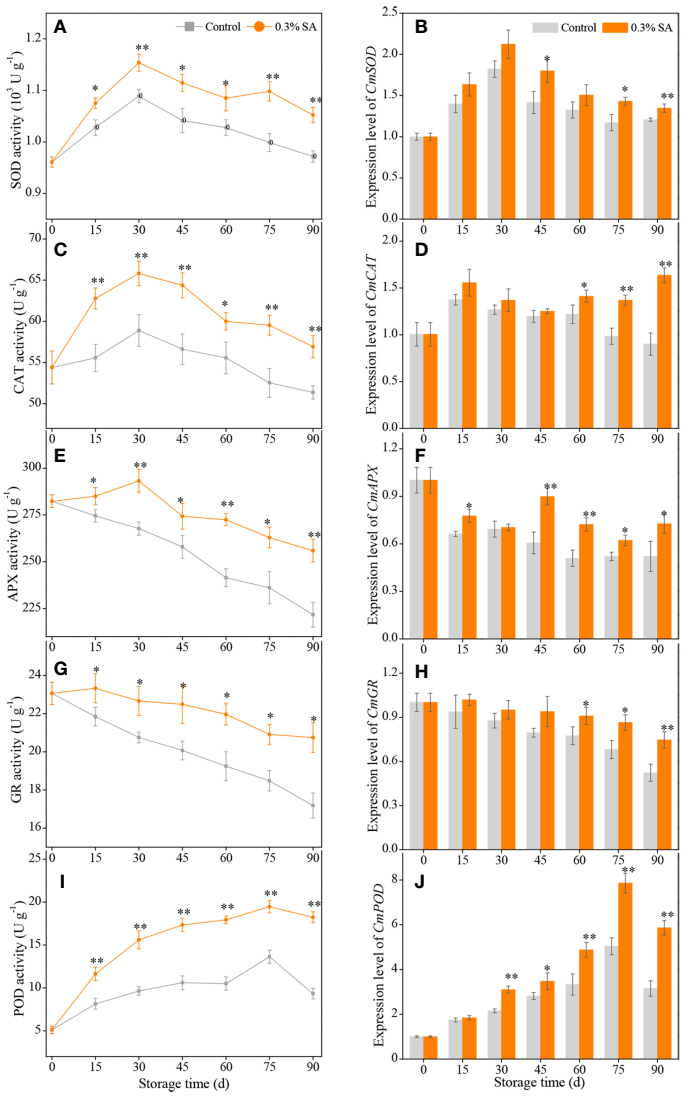

FIGURE 3
The activities and expression levels of SOD **(A, B)**, CAT **(C, D)**, APX **(E, F)**, GR **(G, H)**, POD **(I, J)** in the juice sac of 'Jinshayou' pummelo fruit treated with SA at 0.3% or untreated (control) during room temperature storage period. *β-actin* (Cg8g022300) was used as the internal control gene. The asterisk of * ($P< 0.05$) or ** ($P< 0.01$) within the same sampling point denotes a significant difference between the control and 0.3% SA-treated group.

storage treatment of SA dipping from 45 to 90 d (Figure 1F). At 90 d of storage, a reduction rate of TSS content reached 25.8% in the control fruit, while it was 22.5%, 20.0%, and 17.8% in 0.1%, 0.2%, and 0.3% SA-treated pummelo fruit, respectively. Significant differences were observed between the control and SA-treated fruit after 45 d of storage, with the most effective ability to reduce TSS degradation in the 0.3% SA-treated pummelo fruit. This characteristic of remained high TSS content is beneficial for maintaining the flavor quality and extending the storage life of pummelo fruit, because at the advanced stage of storage, once senescence stress has occurred, a rapid deterioration in fruit quality starts, resulting in serious quality losses.

At the beginning of storage (0 d), pummelo fruit showed the highest TA content (0.46%) which dropped continuously with the stretch of storage period. A rapid degradation of TA was recorded in the control fruit as compared to its slow degradation in 0.2% and 0.3% SA-treated fruit from 30 to 90 d (Figure 1G). The maximum TA loss in the control fruit was 34.8% compared to the minimum loss of 19.6% in pummelo fruit treated with 0.3% SA dipping. The decline of TA content in pummelo juice sacs was seen to be correlated to the senescence process of fruit,

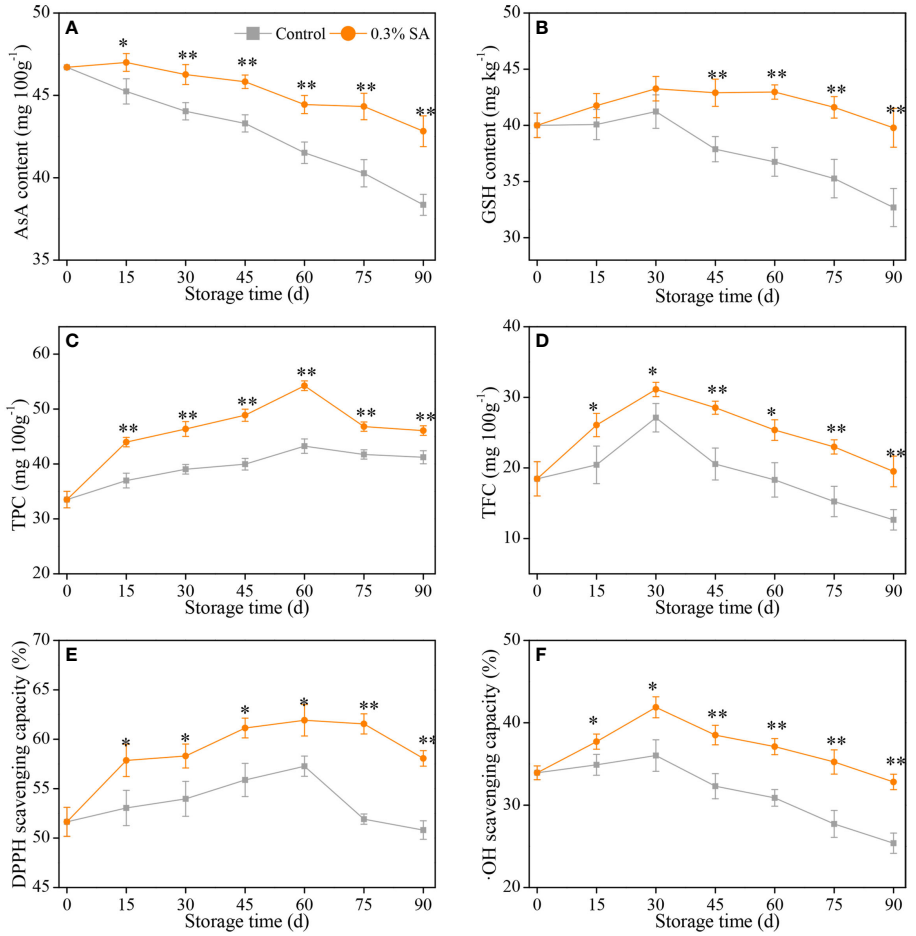

FIGURE 4
Variation in AsA content **(A)**, GSH content **(B)**, TP content **(C)**, TF content **(D)**, DPPH scavenging capacity **(E)**, and •OH scavenging capacity **(F)** in the juice sac of 'Jinshayou' pummelo fruit treated with SA at 0.3% or untreated (control) during room temperature storage period. The asterisk of * ($P< 0.05$) or ** ($P< 0.01$) within the same sampling point denotes a significant difference between the control and 0.3% SA-treated group.

and the 0.3% SA-dipped treatment showed the most effective suppression of delaying the TA decrease.

3.2 Effects of postharvest SA treatment on oxidative stress

The parameters of EL and H_2O_2 content usually reflected the damage caused by oxidative stress in harvested fruits and vegetables (Nie et al., 2020; Ackah et al., 2022; Chen et al., 2022). Both EL and H_2O_2 content in harvested pummelo fruit showed a rising trend over the course of 90 d of storage (Figures 2A, B). However, the control pummelo fruit recorded higher increases of EL and H_2O_2 content than the 0.3% SA-treated fruit. Pummelo fruit treated with 0.3% SA exhibited 24.7% lower EL along with 15.9% lower H_2O_2 content, respectively, than the control one at the end of storage. In addition, MDA content is a target indicator used for the judgment of the membrane lipid peroxidation's extent in plants under unfavorable conditions, including postharvest senescence stress (Ge et al., 2020; Sinha et al., 2022). As shown in Figure 2C, MDA content in the control fruit was displayed to gradually increase during the storage with its maximum level of 0.50 mmol g^{-1} at 90 d. MDA content in the 0.3% SA-treated fruit increased at a slower rate, with the overall MDA content being 19.7% lower than that of the control pummelo fruit from 30 to 90 d after the storage.

3.3 Effects of postharvest SA treatment on activities and expression levels of SOD, CAT, APX, GR and POD

During the storage at room temperature (20°C), ROS accumulation could lead to a decline in storage quality due to oxidative stress, as could the enzymatic antioxidant system,

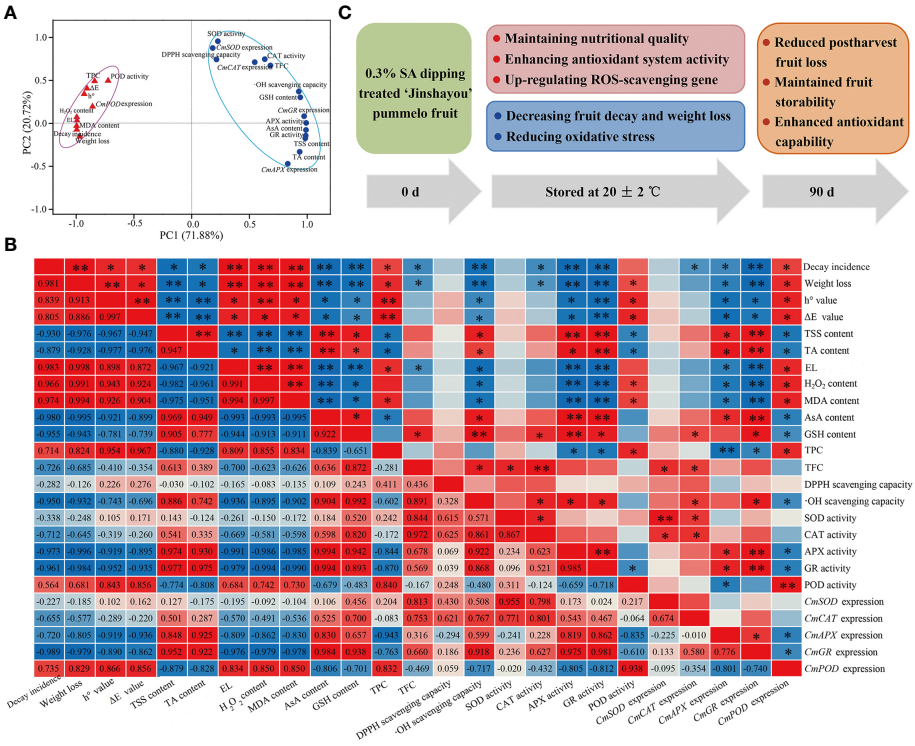

FIGURE 5
The PCA **(A)** and correlation analysis **(B)** of the ROS metabolism-related parameters in the control pummelo fruit stored at 20°C for 90 d. Correlation coefficients are shown in the lower triangle, while statistical significance (P < 0.05 or P < 0.01) is marked with * or ** in the upper triangle. A proposed model of the potential mechanism of pre-storage 0.3% SA treatment enhanced the storability and maintained higher redox state by regulating ROS-scavenging system in harvested 'Jinshayou' pummelo fruit **(C)**.

including SOD, CAT, APX, GR, and POD. As can be seen in Figure 3A, SOD activity in both treatments rose on the first 30 d of storage period and declined subsequently, but SOD activity in pummelo juice sac was enhanced by pre-storage 0.3% SA treatment, with 10.2% higher SOD activity than that in the control sample at 75 d. Pre-storage 0.3% SA treatment significantly increased the expression level of *CmSOD* at 45 d, 75 d, and 90 d, which were 26.8%, 22.2%, and 11.6% higher than those in the control pummelo juice sac, respectively (Figure 3B).

Two peaks of CAT activity in both treatments were assayed at 30 d of room temperature storage (Figure 3C). The maximum CAT activity in the 0.3% SA-treated pummelo juice sac was 1.13-fold higher compared with that in the control sample. Pre-storage 0.3% SA treatment also remarkably increased the expression level of *CmCAT* during the late 30 d of storage, which resulted in a higher overall *CmCAT* expression level by 42.7% compared to the control pummelo juice sac from 60 d to 90 d (Figure 3D).

APX activity in the control pummelo juice sac consistently decreased with the advancement of storage and reached its minimum value at the end of storage, while APX activity in the 0.3% SA-treated fruit slightly increased and peaked at 30 d, followed by a continuous decrease during the remaining storage period (Figure 3E). The levels of APX activity in the 0.3% SA-treated pummelo juice sac were much higher than those in the control over the entire storage period. Simultaneously, pre-storage 0.3% SA treatment remarkably up-regulated the expression level of *CmAPX* gene throughout the storage (except at 30 d time point, Figure 3F).

A gradual decrease in GR activity was observed in both treatments (Figure 3G). However, pummelo juice sac treated with 0.3% SA exhibited a higher GR activity during the entire storage period, resulting in a higher overall GR activity by 12.4% compared to the control treatment. The expression level of *CmGR* exhibited a trend similar to that of GR activity. Pre-storage 0.3% SA treatment prominently delayed the decline of *CmGR* expression level in pummelo juice sac during the late 30 d of storage period, with an overall *CmGR* expression level by 27.3% (Figure 3H).

POD activity in the control and 0.3% SA-treated pummelo juice sac increased gradually and reached the peak values of 13.62 ± 0.76 and 19.74 ± 0.92 U g^{-1} at 75 d and then dropped to 9.33 ± 0.61 and 18.23 ± 0.64 U g^{-1} at the end of storage (90 d), respectively (Figure 3I). Compared to the control treatment, significantly higher levels of POD activity were appeared in the 0.3% SA-treated pummelo throughout the room temperature

storage. Additionally, a higher *CmPOD* expression level was displayed in the 0.3% SA-treated pummelo juice sac than the control, with a noticeable discrepancy in the middle and late storage (Figure 3J).

3.4 Effects of postharvest SA treatment on ROS-scavenging compounds and antioxidant capacity

AsA is considered as not only a key primary component affecting citrus quality, but also one of the endogenous non-enzymatic antioxidants involved in the clearance of ROS over-accumulation (Nie et al., 2020; Serna-Escolano et al., 2021; Ackah et al., 2022). As illustrated in Figure 4A, the variations of AsA content in pummelo juice sac from both groups showed a declining trend with the increase of storage duration, with a more pronounced decline in AsA content of the control pummelo juice sac. Furthermore, the 0.3% SA-treated pummelo fruit had a notably AsA content than the control throughout the whole of storage. In general, AsA content of room temperature-stored pummelo fruit was decreased with increased storage period, but its decline was considerably mitigated by 0.3% SA treatment. In this sense, 0.3% SA-treated pummelo fruit exhibited a less reduction in AsA content, which is probably because that pre-storage 0.3% SA treatment retarded the AsA oxidation in pummelo juice sac by the oxidative stress.

In addition to AsA, GSH is another representative substrate in AsA-GSH system (Halliwell-Asada cycle), both of them perform a pivotal role in the AsA-GSH system together with other enzymatic antioxidant systems to maintain redox homeostasis in postharvest fruits, and their amount can directly indicate the fruits' ability to scavenge ROS (Hanaei et al., 2022; Peng et al., 2022). Figure 4B showed that GSH content in the control and 0.3% SA-treated fruit revealed the similar trend — i.e., a slight increase over the first 30 d of postharvest storage, followed by a gradual decrease. During the middle to late stage of storage, pre-storage 0.3% SA-dipped treatment remarkably delayed the decline of GSH content, which was 13.3% at 45 d, 16.9% at 60 d, 18.0% at 75 d, and 21.7% at 90 d higher compared with that in the control, respectively.

As the main secondary metabolites in plants, both phenolics and flavonoids are not only closely associated with the color conversion, flavor formation, and stress resistance of harvested fruits, but also protect them from over-produced ROS-caused oxidative damage (Ackah et al., 2022; Jiang et al., 2022). TPC is one of the important indexes to evaluate the antioxidant capacity of harvested fruits. Both groups reached a peak in TP content at 60 d, with that of the 0.3% SA-treated group being the highest level of 54.3 ± 0.9 mg/100g, while the highest level of TP content in the control group being 43.2 ± 1.3 mg/g, respectively (Figure 4C). As illustrated in Figure 4D, TFC of pummelo fruit remarkably rose on the first 30 d, and then decreased until to 90 d (the end of storage). It is worth to mention that pre-storage treatment of SA dipping remarkably delayed the decline of TF content, being an overall 1.36 times higher compared to the control pummelo fruit during the last 60 d of storage period. Similar to the overall variations of TPC and TFC, both DPPH and •OH scavenging capacity in two room temperature-stored pummelo juice sacs rose incrementally and peaked at 60 d and 30 d, respectively, followed by a decline (Figures 4E, F). Compared with the initial value at 0 d, the increases of two peak values in the 0.3% SA-treated pummelo juice sac was 9.0% and 17.3% higher than that in the control, showing that pre-storage 0.3% SA-dipped treatment had a positive influence on the increase of hydrophilic bioactive antioxidants and the maintenance of ROS-scavenging ability in 'Jinshayou' pummelo fruit during postharvest storage.

3.5 Correlation analysis

To understand the impact of 0.3% SA-dipped treatment in 'Jinshayou' pummelo fruit, both principal component analysis (PCA) and correlation analysis were applied to identify the ROS metabolism-related parameters that functionally referred to these measured parameters in pummelo fruit after 0.3% SA treatment. All 25 parameters linked to fruit postharvest ROS metabolism were mainly clustered into two main components (PC1: 66.719%; PC2: 20.72%, Figure 5A). The PC1 consisted of 10 parameters, including fruit decay rate, weight loss, h° value, ΔE value, electrolyte leakage, H_2O_2 content, MDA content, TPC, POD activity, and *CmPOD* expression (Figure 5A). PC2 showed a higher relationship factor for five nutritional/functional components (TSS, TA, AsA, GSH, and flavonoids) contents, DPPH scavenging capacity, •OH scavenging capacity, four ROS-scavenging enzymes activities, and their encode gene expression levels, showing a high negative correlation to postharvest storability loss (Figure 5B; $P< 0.05$ or 0.01). The loss of fruit postharvest storability is due to the imbalance of ROS homeostasis, and result in an increase of defective fruit as well as the degradation of fruit quality. Pre-storage SA treatment was effective to enhance the antioxidant capability and reduce postharvest loss of pummelo fruit during room temperature storage. A similar finding was reported by Nie et al. (2020) in that chitosan-coated treatment could maintain high levels of some antioxidants (enzymes: APX, GR, SOD, and CAT) and reduce the oxidative stress. PCA can be an effective means to assess the preservative effect of pre-storage SA treatment on 'Jinshayou' pummelo fruit as demonstrated by other reports in other horticultural products (Bakpa et al., 2022; Nxumalo et al., 2022). In the present study, fruit decay incidence was highly positively correlated with electrolyte leakage, H_2O_2 content, and MDA content, with the coefficients being 0.983, 0.966, and 0.974, respectively (Figure 5B, $P< 0.01$), because it is highly related to oxidative stress and ROS accumulation. Moreover, ROS-scavenging enzymes activities (SOD, CAT, APX, and GR) and expression levels of their encoding genes (*CmSOD*, *CmCAT*, *CmAPX*, and *CmGR*) exhibited high negative correlations with fruit decay rate and

oxidative stress-related parameters ($P< 0.05$ or 0.01). Other studies have also proved that ROS accumulation leads to membrane lipid deterioration and is highly negatively correlated with the activities of antioxidant enzymes during longan fruit storage (Chen et al., 2020). These findings well demonstrated that pummelo postharvest senescence was accompanied by a disability in antioxidant system and reduction in the overall quality, thus corroborating the intimate association between ROS metabolism and postharvest storability in 'Jinshayou' pummelo fruit during room temperature storage.

4 Discussion

Pummelo fruit, being a typical non-climacteric variety, is prone to a rapid decline in nutritional quality when stored at room temperature, thus limiting its storability. Numerous studies have revealed that pre-storage SA treatment prior to storage can delay postharvest senescence and quality deterioration of a variety of horticultural fruits, including apricot, blueberry, cornelian cherry, goji berry, papaya, pear, winter jujube, and tomato, as well as improve their resistance to abiotic stress (Dokhanieh et al., 2013; Hanif et al., 2020; Kumar et al., 2021; Zhang et al., 2021a; Jiang et al., 2022; Li et al., 2022; Sinha et al., 2022; Zhang et al., 2022). In this study, pre-storage application of SA was found to effectively in delaying fruit color change and decreasing h° and ΔE values, as well as reducing fruit decay and weight loss of harvested 'Jinshayou' pummelo fruit during storage at room temperature (Figures 1A–E). Pre-storage SA treatment at 0.3% was the more effective in terms of prolonging the storage duration to 90 d at 20°C. The protection of harvested fruit from color change and the inhibition of postharvest loss were observed when exogenous SA application was applied in varying concentrations; such as 2.0 mM SA on 'Patharnakh' pear (Adhikary et al., 2021), 0.5 mM SA on 'Taaptimjaan' wax apple (Supapvanich et al., 2017), and 0.05% SA on 'Dongzao' winter jujube (Zhang et al., 2022).

The deterioration of horticultural fruits' nutritional quality, mainly due to their own respiration rate, is a major cause for fruit flavor loss and is regarded as a key metric to evaluate their storability and postharvest freshness during storage (Lacerna et al., 2018; Haider et al., 2020; Nie et al., 2020). As harvested fruits undergo senescence, the soluble sugar and organic acids gradually degrade, thus delaying this process can help to maintain the fruit's flavor quality and extend its storage life (Chen et al., 2005; Baswal et al., 2020; Serna-Escolano et al., 2021). Both TSS and TA contents are essential metrics for assessing the maturity and ripeness process of horticultural fruit, particularly citrus fruit, which mainly determine the storability and overall flavor (Huang et al., 2021; Nxumalo et al., 2022). The data depicted in Figures 1F, G revealed that pre-storage 0.3% SA treatment can reduce the drop in TSS and TA content of 'Jinshayou' pummelo fruit throughout the storage period, as both levels are higher than the control and other two SA-treated fruit, which were in accordance with pre-storage treatment of SA to 'Kinnow' mandarin (Haider et al., 2020), 'Patharnakh' pear (Adhikary et al., 2021), 'Sabrosa' strawberry (Asghari and Hasanlooe, 2015), and 'Tupi' blackberry (Martínez-Camacho et al., 2022). Moreover, it was noted that 0.3% SA treatment displayed the most effective delay in the degradation of TSS and TA, from which the highest levels of TSS and TA content was obtained over the entire storage period.

Citrus fruits are stored at room temperature for too long, resulting in a loss of cell membrane integrity, which can be determined through EL, MDA accumulation and H_2O_2 production (Hanaei et al., 2022; Martínez-Camacho et al., 2022; Nxumalo et al., 2022). Prolonged exposure to senescence-elicited oxidative stress results in membrane lipid peroxidation. It is universally acknowledged that ROS-induced oxidative stress is a crucial factor leading to storability loss and quality deterioration of harvested fruits. ROS, especially H_2O_2, can cause the oxidation of unsaturated fatty acids, disrupting the cell membrane's integrity, eventually leading to membrane lipid peroxidation (Chen et al., 2020; Sinha et al., 2022). In pummelo fruit, the levels of electrolyte leakage, H_2O_2 content and MDA content in both treatments increased dramatically from 30 d onwards (Figure 2). Fruit senescence process advances due to oxidative stress caused by excessive ROS accumulation, which concomitantly give out a large amount of free radicals as by-products. In 'Majiayou' pummelo with red flesh, the accumulations of superoxide anions, H_2O_2, and MDA during room temperature storage was also reported by Nie et al. (2020), who pointed out that postharvest 1.5% chitosan treatment could reduce juice sac granulation stress by delaying ROS accumulation. Zhang et al. (2022) also ascertained that pre-storage treatment with 0.05% SA had a direct or indirect effect on the retardation of fruit respiration rate and senescence process, thereby decreasing the accumulation of ROS and maintaining postharvest quality of winter jujube. Pre-storage SA treatment also demonstrated its extraordinary capacity to scavenge over-produced ROS by enhancing the antioxidant system under oxidative stress.

It is a well-established notion that the maintenance of ROS homeostasis could decrease excess ROS accumulation and protects living cells from oxidative stress damage, which is vital for enhancing postharvest storability and maintaining overall quality in harvested fruits (Asghari and Hasanlooe, 2015; Huang et al., 2021; Ackah et al., 2022). SOD, CAT, APX, GR, and POD are pivotal antioxidant enzymes that share their responsibility for scavenging excess ROS, thus protecting plant cells against oxidative stress (Marschall and Tudzynski, 2016; Nie et al., 2020; Chen et al., 2022). Specially, SOD plays its pioneer role in the ROS-scavenging enzymatic antioxidant system, which can dismutate superoxide anion into O_2 and H_2O_2; subsequently, the disproportionated H_2O_2 is directly or indirectly decomposed into O_2 and H_2O_2 with the concerted effort from CAT, APX, GR, and POD (Siboza et al., 2017; Martínez-Camacho et al., 2022; Peng et al., 2022). Numerous studies have proved that pre-storage SA

treatment helps in maintaining or enhancing the antioxidant capacity in harvested fruits through the activation of antioxidant enzymatic system (Dokhanieh et al., 2013; Serna-Escolano et al., 2021; Zhang et al., 2021a). To reduce ROS-induced oxidative damage, plant cells initiate an enzymatic antioxidant system as a self-protective response. In this study, the higher levels of SOD, CAT, APX, GR, and POD activities was observed in the 0.3% SA-treated pummelo fruit; furthermore, the expression levels of these genes encoding *CmCAT*, *CmAPX*, *CmGR*, and *CmPOD* were up-regulated by 0.3% SA treatment in pummelo fruit (Figure 3), accompanying by the inferior H_2O_2 content and the lower MDA accumulation (Figure 2). The elimination of H_2O_2 and the less level of oxidative stress in pummelo juice sacs are dependent on the improvement of SOD, CAT, POD, APX, and GR activities, and the up-regulation of their encoding gene expressions. Other reports also indicated that elevated ROS-scavenging enzyme activities and up-regulated their encoding gene expressions contributed to the balance of ROS homeostasis and the maintenance of postharvest storability in 'Eureka' lemon (Siboza et al., 2017), 'Dahuang' apricot (Wang et al., 2015), 'Ningqi No. 5' goji berry (Zhang et al., 2021a), 'Cornelian' cherry (Dokhanieh et al., 2013), and 'Dongzao' winter jujube (Sang et al., 2022), and 'Majiayou' pummelo (Nie et al., 2020). Above findings explicitly showed that the maintained storability by exogenous SA treatment might be correlated with improvement of the fruit's own antioxidant enzymatic system. The findings in the present study plainly indicated that pre-storage 0.3% SA-dipped treatment increased ROS-scavenging enzymes activities and simultaneously up-regulated their encoding genes expression, thereby reducing ROS-caused oxidative stress in pummelo juice sacs. Thus, it could be inferred that 0.3% SA treatment contributed to the active function of enzymatic antioxidant system in 'Jinshayou' pummelo fruit, minimized the ROS-induced oxidative stress, and enhanced or maintained stress resistance in pummelo juice sacs, thereby reducing postharvest loss and extending storage life.

In addition to enzymatic antioxidant system, the non-enzymatic antioxidant system also has its irreplaceable role in reducing the oxidative senescence in harvested fruits (Supapvanich et al., 2017; Hanif et al., 2020; Nie et al., 2020). In higher plants, AsA and GSH are both representative substrates in AsA-GSH system (Halliwell-Asada cycle) for scavenging over-accumulated ROS in fruit, which maintains ROS homeostasis and delays cell senescence caused by oxidative stress (Serna-Escolano et al., 2021; Hanaei et al., 2022; Peng et al., 2022). Additionally, phenolics compounds are a class of plant secondary metabolites that perform a pivotal role in the color conversion, flavor formation, and stress resistance of harvested fruits, in conjunction with flavonoids, which protect them from the oxidative damage caused by the over-production of ROS (Ackah et al., 2022; Jiang et al., 2022). Therefore, high levels of antioxidants (AsA, GSH, phenolics, and flavonoids) contents are closely related to the fruit's resistance to postharvest senescence stress. This study showed that pummelo juice sacs treated by 0.3% SA dipping presented the higher levels of AsA content, GSH content, TPC, and TFC (Figures 4A–D) accompanied by superior DPPH and •OH radicals scavenging capacity (Figures 4E, F), which may occur thanks to higher levels of ROS-scavenging enzymes activities along with their encoding gene expression during room temperature storage (Figure 3). Haider et al. (2020) and Zhang et al. (2021b) found that high levels of AsA, phenolics and flavonoids were beneficial to enhance the antioxidation capacity of 'Kinnow' mandarin and 'Ningqi No. 5' goji berry to postharvest oxidative stress. Similar findings were also obtained for pre-storage SA treatment in 'Fino' lemon (Serna-Escolano et al., 2021), 'Cornelian' cherry (Dokhanieh et al., 2013), and 'Sabrosa' strawberry (Asghari and Hasanlooe, 2015). Therefore, our results showed that pre-storage 0.3% SA-dipped treatment had a positive influence on the increase of hydrophilic bioactive antioxidants, the improvement of ROS-scavenging ability to resist oxidative stress, the maintenance of overall quality, and the extension of the shelf life of 'Jinshayou' pummelo fruit.

5 Conclusion

In summary, pre-storage treatment of 0.3% SA dipping was found be to effective in reducing postharvest fruit loss and maintaining the overall quality of 'Jinshayou' pummelo fruit. This was mainly due to 0.3% SA enhancing the activities of ROS-scavenging enzymes, along with up-regulating their corresponding gene expressions, maintaining higher levels of TSS, TA, AsA, GSH, TFC, and free radical scavenging capacity, and decreasing fruit decay incidence. All of these contributed to reducing oxidative stress and stabilizing the ROS homeostasis in pummelo juice sacs, thereby maintaining postharvest storability and overall quality in 'Jinshayou' pummelo fruit (Figure 5C). These results indicate that pre-storage 0.3% SA treatment could potentially provide a feasible preservation technology in reducing postharvest loss and maintaining ROS metabolism, and thus delay postharvest senescence and extend storage life of 'Jinshayou' pummelo fruit after harvest.

Data availability statement

The original contributions presented in the study are included in the article/Supplementary Material. Further inquiries can be directed to the corresponding author.

Author contributions

QH: methodology, formal analysis, data curation, and writing-original draft. LH: methodology, investigation, and validation. JC: conceptualization, supervision, and funding acquisition. YZ: methodology, software, and investigation. WK: investigation and formal analysis. CC: conceptualization, supervision, project administration, and writing-review and

editing. All authors contributed to the article and approved the submitted version.

Funding

This work was supported by the Jiangxi Provincial and National Natural Science Foundation of China (20212BAB205011 and 32002104), and the Modern Agricultural Technology System of Jiangxi Province in China (JXARS-07).

Conflict of interest

The authors declare that the research was conducted in the absence of any commercial or financial relationships that could be construed as a potential conflict of interest.

Publisher's note

Supplementary material

The Supplementary Material for this article can be found online at: https://www.frontiersin.org/articles/10.3389/fpls.2022.1086375/full#supplementary-material

References

Ackah, S., Bi, Y., Xue, S., Yakubu, S., Han, Y., Zong, Y., et al. (2022). Post-harvest chitosan treatment suppresses oxidative stress by regulating reactive oxygen species metabolism in wounded apples. *Front. Plant Sci.* 13. doi: 10.3389/fpls.2022.959762

Adhikary, T., Gill, P. S., Jawandha, S. K., Bhardwaj, R. D., and Anurag, R. K. (2021). Browning and quality management of pear fruit by salicylic acid treatment during low temperature storage. *J. Sci. Food Agric.* 101 (3), 853–862. doi: 10.1002/jsfa.10692

Asghari, M., and Hasanlooe, A. R. (2015). Interaction effects of salicylic acid and methyl jasmonate on total antioxidant content, catalase and peroxidase enzymes activity in "Sabrosa" strawberry fruit during storage. *Sci. Hortic.* 197, 490–495. doi: 10.1016/j.scienta.2015.10.009

Bakpa, E. P., Zhang, J., Xie, J., Ma, Y., Han, K., and Chang, Y. (2022). Storage stability of nutritional qualities, enzyme activities, and volatile compounds of "Hangjiao no. 2" chili pepper treated with different concentrations of 1-methyl cyclopropene. *Front. Plant Sci.* 13. doi: 10.3389/fpls.2022.838916

Baswal, A. K., Dhaliwal, H. S., Singh, Z., Mahajan, B. V., and Gill, K. S. (2020). Postharvest application of methyl jasmonate, 1-methylcyclopropene and salicylic acid extends the cold storage life and maintain the quality of 'Kinnow' mandarin (*Citrus nobilis* l. X *C. deliciosa* l.) fruit. *Postharvest. Biol. Tech.* 161, 111064. doi: 10.1016/j.postharvbio.2019.111064

Belay, Z. A., and James Caleb, O. (2022). Role of integrated omics in unravelling fruit stress and defence responses during postharvest: A review. *Food Chem.: Molec. Sci.* 5, 100118. doi: 10.1016/j.fochms.2022.100118

Chen, C., Cai, N., Wan, C., Kai, W., and Chen, J. (2022). Carvacrol delays phomopsis stem-end rot development in pummelo fruit in relation to maintaining energy status and antioxidant system. *Food Chem.* 372, 131239. doi: 10.1016/j.foodchem.2021.131239

Chen, C., Peng, X., Chen, J., Gan, Z., and Wan, C. (2021). Mitigating effects of chitosan coating on postharvest senescence and energy depletion of harvested pummelo fruit response to granulation stress. *Food Chem.* 348, 129113. doi: 10.1016/j.foodchem.2021.129113

Chen, Y., Sun, J., Lin, H., Lin, M., Lin, Y., Wang, H., et al. (2020). Salicylic acid treatment suppresses *Phomopsis longanae* chi-induced disease development of postharvest longan fruit by modulating membrane lipid metabolism. *Postharvest. Biol. Tech.* 164, 111168. doi: 10.1016/j.postharvbio.2020.111168

Chen, K. S., Xu, C. J., Li, F., and Zhang, S. L. (2005). Postharvest granulation of 'Huyou' (*Citrus changshanensis*) fruit in response to calcium. *Isr. J. Plant Sci.* 53, 35–40. doi: 10.1560/9ekh-dm6c-yy7c-kpmd

Deng, J., Kong, S., Wang, F., Liu, Y., Jiao, J., Lu, Y., et al. (2020). Identification of a new *Bacillus sonorensis* strain KLBC GS-3 as a biocontrol agent for postharvest green mould in grapefruit. *Biol. Control* 151, 104393. doi: 10.1016/j.biocontrol.2020.104393

Dokhanieh, A. Y., Aghdam, M. S., Fard, J. R., and Hassanpour, H. (2013). Postharvest salicylic acid treatment enhances antioxidant potential of cornelian cherry fruit. *Sci. Hortic.* 154, 31–36. doi: 10.1016/j.scienta.2013.01.025

Ge, W., Zhao, Y., Kong, X., Sun, H., Luo, M., Yao, M., et al. (2020). Combining salicylic acid and trisodium phosphate alleviates chilling injury in bell pepper (*Capsicum annuum* l.) through enhancing fatty-acid desaturation efficiency and water retention. *Food Chem.* 327, 127057. doi: 10.1016/j.foodchem.2020.127057

Haider, S. A., Ahmad, S., Sattar Khan, A., Anjum, M. A., Nasir, M., and Naz, S. (2020). Effects of salicylic acid on postharvest fruit quality of "Kinnow" mandarin under cold storage. *Sci. Hortic.* 259, 108843. doi: 10.1016/j.scienta.2019.108843

Hanaei, S., Bodaghi, H., and Ghasimi Hagh, Z. (2022). Alleviation of postharvest chilling injury in sweet pepper using salicylic acid foliar spraying incorporated with caraway oil coating under cold storage. *Front. Plant Sci.* 13. doi: 10.3389/fpls.2022.999518

Hanif, A., Ahmad, S., Shahzad, S., Liaquat, M., and Anwar, R. (2020). Postharvest application of salicylic acid reduced decay and enhanced storage life of papaya fruit during cold storage. *J. Food Meas. Charact.* 14, 3078–3088. doi: 10.1007/s11694-020-00555-5

Huang, Q., Wan, C., Zhang, Y., Chen, C., and Chen, J. (2021). Gum arabic edible coating reduces postharvest decay and alleviates nutritional quality deterioration of ponkan fruit during cold storage. *Front. Nutr.* 8. doi: 10.3389/fnut.2021.717596

Jiang, B., Fang, X., Fu, D., Wu, W., Han, Y., Chen, H., et al. (2022). Exogenous salicylic acid regulates organic acids metabolism in postharvest blueberry fruit. *Front. Plant Sci.* 13. doi: 10.3389/fpls.2022.1024909

Khan, A., Azam, M., Shen, J., Ghani, M. A., Khan, A. S., Ahmad, S., et al. (2021). Overall quality maintenance of grapefruit during cold storage using pre-storage neem leaf extract dipping. *J. Food Meas. Charact.* 15, 1727–173610. doi: 10.1007/s11694-020-00752-2

Kumar, N., Tokas, J., Raghavendra, M., and Singal, H. R. (2021). Impact of exogenous salicylic acid treatment on the cell wall metabolism and ripening process in postharvest tomato fruit stored at ambient temperature. *Int. J. Food Sci. Tech.* 56, 2961–2972. doi: 10.1111/ijfs.14936

Lacerna, M., Bayogan, E. R., and Secretaria, L. (2018). Rind color change and granulation in pummelo [*Citrus maxima* (Burm. ex rumph.) merr.] fruit as influenced by 1-methylcyclopropene. *Int. Food Res. J.* 25, 1483–1488.

Landi, L., Peralta-Ruiz, Y., Lòpez, C., and Romanazzi, G. (2021). Chitosan coating enriched with *Ruta graveolens* l. essential oil reduces postharvest anthracnose of papaya (*Carica papaya* l.) and modulates defense-related gene expression. *Front. Plant Sci.* 12. doi: 10.3389/fpls.2021.765806

Li, Y., He, H., Hou, Y., Kelimu, A., Wu, F., Zhao, Y., et al. (2022). Salicylic acid treatment delays apricot (*Prunus armeniaca* l.) fruit softening by inhibiting ethylene biosynthesis and cell wall degradation. *Sci. Hortic.* 300, 111061. doi: 10.1016/j.scienta.2022.111061

Livak, K. J., and Schmittgen, T. D. (2001). Analysis of relative gene expression data using real-time quantitative PCR and the $2^{-\Delta\Delta CT}$ method. *Methods* 25, 402–408. doi: 10.1006/meth.2001.1262

Marschall, R., and Tudzynski, P. (2016). Reactive oxygen species in development and infection processes. *Semin. Cell Dev. Biol.* 57, 138–146. doi: 10.1016/j.semcdb.2016.03.020

Martínez-Camacho, J. E., Guevara-González, R. G., Rico-García, E., Tovar-Pérez, E. G., and Torres-Pacheco, I. (2022). Delayed senescence and marketability

index preservation of blackberry fruit by preharvest application of chitosan and salicylic acid. *Front. Plant Sci.* 13. doi: 10.3389/fpls.2022.796393

Mitalo, O. W., Asiche, W. O., Kang, S. W., Ezura, H., Akagi, T., Kubo, Y., et al. (2022). Examining the role of low temperature in Satsuma mandarin fruit peel degreening *via* comparative physiological and transcriptomic analysis. *Front. Plant Sci.* 13. doi: 10.3389/fpls.2022.918226

Nie, Z., Huang, Q., Chen, C., Wan, C., and Chen, J. (2020). Chitosan coating alleviates postharvest juice sac granulation by mitigating ROS accumulation in harvested pummelo (*Citrus grandis* l. osbeck) during room temperature storage. *Postharvest. Biol. Tech.* 169, 111309. doi: 10.1016/j.postharvbio.2020.111309

Nxumalo, K. A., Fawole, O. A., and Oluwafemi, O. S. (2022). Evaluating the efficacy of gum arabic-zinc oxide nanoparticles composite coating on shelf-life extension of mandarins (cv. kinnow). *Front. Plant Sci.* 13. doi: 10.3389/fpls.2022.953861

Peng, X., Zhang, Y., Wan, C., Gan, Z., Chen, C., and Chen, J. Y. (2022). Antofine triggers the resistance against *Penicillium italicum* in ponkan fruit by driving AsA-GSH cycle and ROS-scavenging system. *Front. Microbiol.* 13. doi: 10.3389/fmicb.2022.874430

Porat, R., Feng, X. Q., Huberman, M., Galili, D., Goren, R., and Goldschmidt, E. E. (2001). Gibberellic acid slows postharvest degreening of 'Oroblanco' citrus fruits. *Hortscience* 36, 937–940. doi: 10.21273/hortsci.36.5.937

Porat, R., Pavoncello, D., Peretz, J., Ben-Yehoshua, S., and Lurie, S. (2000). Effects of various heat treatments on the induction of cold tolerance and on the postharvest qualities of 'Star ruby' grapefruit. *Postharvest. Biol. Technol.* 18, 159–165. doi: 10.1016/s0925-5214(99)00075-7

Sang, Y., Liu, Y., Tang, Y., Yang, W., Guo, M., and Chen, G. (2022). Transcriptome sequencing reveals mechanism of improved antioxidant capacity and maintained postharvest quality of winter jujube during cold storage after salicylic acid treatment. *Postharvest. Biol. Tech.* 189, 111929. doi: 10.1016/j.postharvbio.2022.111929

Serna-Escolano, V., Martínez-Romero, D., Giménez, M. J., Serrano, M., García-Martínez, S., Valero, D., et al. (2021). Enhancing antioxidant systems by preharvest treatments with methyl jasmonate and salicylic acid leads to maintain lemon quality during cold storage. *Food Chem.* 338, 128044. doi: 10.1016/j.foodchem.2020.128044

Shi, Z., Yang, H., Jiao, J., Wang, F., Lu, Y., and Deng, J. (2019). Effects of graft copolymer of chitosan and salicylic acid on reducing rot of postharvest fruit and retarding cell wall degradation in grapefruit during storage. *Food Chem.* 283, 92–100. doi: 10.1016/j.foodchem.2018.12.078

Siboza, X. I., Bertling, I., and Odindo, A. O. (2017). Enzymatic antioxidants in response to methyl jasmonate and salicylic acid and their effect on chilling tolerance in lemon fruit [*Citrus limon* (L.) burm. f.]. *Sci. Hortic.* 225, 659–667. doi: 10.1016/j.scienta.2017.07.023

Sinha, A., Gill, P. P., Jawandha, S. K., Kaur, P., and Grewal, S. K. (2022). Salicylic acid enriched beeswax coatings suppress fruit softening in pears by modulation of cell wall degrading enzymes under different storage conditions. *Food Packag. Shelf.* 32, 100821. doi: 10.1016/j.fpsl.2022.100821

Supapvanich, S., Mitsang, P., and Youryon, P. (2017). Preharvest salicylic acid application maintains physicochemical quality of 'Taaptimjaan' wax apple fruit (*Syzygium samarangenese*) during short-term storage. *Sci. Hortic.* 215, 178–183. doi: 10.1016/j.scienta.2016.11.046

Vera-Guzmán, A. M., Aispuro-Hernández, E., Vargas-Arispuro, I., Islas-Osuna, M. A., and Martínez-Téllez, M. Á. (2019). Expression of antioxidant-related genes in flavedo of cold-stored grapefruit (*Citrus paradisi* macfad cv. Rio red) treated with pectic oligosaccharides. *Sci. Hortic.* 243, 274–280. doi: 10.1016/j.scienta.2018.08.035

Wang, Z., Ma, L., Zhang, X., Xu, L., Cao, J., and Jiang, W. (2015). The effect of exogenous salicylic acid on antioxidant activity, bioactive compounds and antioxidant system in apricot fruit. *Sci. Hortic.* 181, 113–120. doi: 10.1016/j.scienta.2014.10.055

Yun, Z., Gao, H., Chen, X., Chen, Z., Zhang, Z., Li, T., et al. (2021). Effects of hydrogen water treatment on antioxidant system of litchi fruit during the pericarp browning. *Food Chem.* 336, 127618. doi: 10.1016/j.foodchem.2020.127618

Zhang, W., Kang, J., Yang, W., Guo, H., Guo, M., and Chen, G. (2022). Incorporation of 1-methylcyclopropene and salicylic acid improves quality and shelf life of winter jujube (*Zizyphus jujuba* mill. cv. dongzao) through regulating reactive oxygen species metabolism. *Front. Nutr.* 9. doi: 10.3389/fnut.2022.940494

Zhang, H., Liu, F., Wang, J., Yang, Q., Wang, P., Zhao, H., et al. (2021a). Salicylic acid inhibits the postharvest decay of goji berry (*Lycium barbarum* l.) by modulating the antioxidant system and phenylpropanoid metabolites. *Postharvest. Biol. Tech.* 178, 111558. doi: 10.1016/j.postharvbio.2021.111558

Zhang, H., Ma, Z., Wang, J., Wang, P., Lu, D., Deng, S., et al. (2021b). Treatment with exogenous salicylic acid maintains quality, increases bioactive compounds, and enhances the antioxidant capacity of fresh goji (*Lycium barbarum* l.) fruit during storage. *LWT - Food Sci. Tech.* 140, 110837. doi: 10.1016/j.lwt.2020.110837

frontiers | Frontiers in Plant Science

TYPE Original Research
PUBLISHED 12 January 2023
DOI 10.3389/fpls.2022.1082041

OPEN ACCESS

EDITED BY
Shifeng Cao,
Zhejiang Wanli University, China

REVIEWED BY
Zhenfeng Yang,
Zhejiang Wanli University, China
Xingbin Xie,
Anhui Agricultural University, China

*CORRESPONDENCE
Junfeng Guan
junfeng-guan@263.net

†These authors have contributed equally to this work

SPECIALTY SECTION
This article was submitted to Crop and Product Physiology, a section of the journal Frontiers in Plant Science

RECEIVED 27 October 2022
ACCEPTED 15 December 2022
PUBLISHED 12 January 2023

CITATION
Li D, Li X, Cheng Y and Guan J (2023) Effect of 1-methylcyclopropene on peel greasiness, yellowing, and related gene expression in postharvest 'Yuluxiang' pear.
Front. Plant Sci. 13:1082041.
doi: 10.3389/fpls.2022.1082041

Effect of 1-methylcyclopropene on peel greasiness, yellowing, and related gene expression in postharvest 'Yuluxiang' pear

Dan Li[1,2†], Xueling Li[1†], Yudou Cheng[1] and Junfeng Guan[1*]

[1]Institute of Biotechnology and Food Science, Hebei Academy of Agriculture and Forestry Sciences, Shijiazhuang, China, [2]School of Life Science and Engineering, Handan University, Handan, China

'Yuluxiang' pear (*Pyrus sinkiangensis*) commonly develop a greasy coating and yellowing during storage. In this study, 1.0 μL L^{-1} 1-methylcyclopropene (1-MCP) was applied to 'Yuluxiang' pear to investigate its effects on fruit quality, peel wax composition, greasiness index, chlorophyll content, and the expression pattern of related genes during storage at ambient temperature (25°C). The results showed that 1-MCP treatment maintained higher fruit firmness and chlorophyll content, decreased respiration rate, and postponed the peak of ethylene production rate, lowered the greasy index of the peel. The main wax components of peel accumulated during storage, the principal ones being alkenes (C23, C25, and C29), fatty acids (C16, C18:1, and C28), aldehydes (C24:1, C26:1, and C28:1), and esters (C22:1 fatty alcohol-C16 fatty acid, C22:1 fatty alcohol-C18:1 fatty acid, C22 fatty alcohol-C16 fatty acid, C22 fatty alcohol-C18:1 fatty acid, C24:1 fatty alcohol-C18:1 fatty acid, and C24 fatty alcohol-C18:1 fatty acid), and were reduced by 1-MCP. 1-MCP also decreased the expression of genes associated with ethylene biosynthesis and signal transduction (*ACS1*, *ACO1*, *ERS1*, *ETR2*, and *ERF1*), chlorophyll breakdown (*NYC1*, *NOL*, *PAO*, *PPH*, and *SGR*), and wax accumulation (*LACS1*, *LACS6*, *KCS1*, *KCS2*, *KCS4*, *KCS10L*, *KCS11L*, *KCS20*, *FDH*, *CER10*, *KCR1*, *ABCG11L*, *ABCG12*, *ABCG21L*, *LTPG1*, *LTP4*, *CAC3*, *CAC3L*, and *DGAT1L*). There were close relationships among wax components (alkanes, alkenes, fatty acids, esters, and aldehydes), chlorophyll content, greasiness index, and level of expression of genes associated with wax synthesis and chlorophyll breakdown. These results suggest that 1-MCP treatment decreased the wax content of 'Yuluxiang' pear and delayed the development of peel greasiness and yellowing by inhibiting the expression of genes related to the ethylene synthesis, signal transduction, wax synthesis, and chlorophyll degradation.

KEYWORDS

pear, greasiness, chlorophyll, gene expression, wax, ethylene

Introduction

Ethylene is an important hormone in the regulation of fruit ripening and senescence and is involved in the process of wax biosynthesis and chlorophyll breakdown. Endogenous ethylene increases total wax content (Li et al., 2022) and stimulates chlorophyll breakdown (Cheng and Guan, 2014) in postharvest fruits. In contrast, 1-methycycloprone (1-MCP), an ethylene action inhibitor, represses wax accumulation and chlorophyll breakdown (Curry, 2008; Cheng et al., 2012; Cheng and Guan, 2014; Li et al., 2019; Lv et al., 2020; Zhao et al., 2020; Li et al., 2022).

As one of the important components of the cuticle, wax plays an essential role in the postharvest life of fruit, including fruit surface characteristics, water loss, and fungal infection. Thus, surface wax can affect the quality of the fruit's appearance. For example, alkane and fatty alcohols in wax can stabilize the three-dimensional structure of wax crystals, acting as inhibitors of peel greasiness in apples (Curry, 2008; Christeller and Roughan, 2016; Yang et al., 2017b), and also preventing the fruit surface from cracking in apples and cherries (Rios et al., 2015; Chai et al., 2020). Furthermore, aliphatic wax components (alkanes and aldehydes), when present at high concentrations, can form lamellar crystals and reduce fruit peel permeability in tomatoes and navel oranges (Leide et al., 2007; Leide et al., 2011; Liu et al., 2012; Petit et al., 2014; Wang et al., 2014).

The first step in fruit wax biosynthesis is the formation of a very long-chain fatty acid (VLCFA) (Samuels et al., 2008). In plastids, malonyl coenzyme A, as the donor of two-carbon units in $VLCFA_{n \leq 18}$ elongation cycles, is synthesized through the catalysis of acetyl-coenzyme A carboxylase (CAC) (Liu et al., 2015; Liu et al., 2016). In addition, several enzymes and transporters are involved in the biosynthesis of $VLCFA_{20 \leq n \leq 34}$ and their derivatives, such as long-chain acyl-CoA synthetase (LACS), β-ketoacyl CoA synthetase (KCS), β-ketoacyl CoA reductase (KCR), fatty acyl-CoA reductase (CER), ATP-binding cassette transporter G protein (ABCG), lipid transporter protein (LTP), and LTPG1 (glycosylphosphatidylinositol-anchored lipid transfer protein) (Teerawanichpan and Qiu, 2010; Bernard and Joubès, 2013; Zhang et al., 2020a).

The greasiness of peel is a physiological characteristic related to wax metabolism in some fruits during storage. Excess grease may reduce the quality of their appearance, and therefore their commercial value. More detailed studies focused on apples have shown that peel greasiness is associated with fruit maturity and is more obvious in fruits with advanced ripeness, and that it is caused by the accumulation of fluid wax components resulting from a state change from solid to liquid on fruit surface wax (Christeller and Roughan, 2016; Yang et al., 2017a; Yang et al., 2017b; Zhang et al., 2019b). 1-MCP, aminoethoxyvinylglycine (AVG), and dynamic controlled atmosphere treatments have been shown to slow the process of grease accumulation on peel, to reduce mobile-phase wax components, and to down-regulate the expression of wax-related genes in apples during storage (Ju and Bramlage, 2001; Curry, 2008; Dong et al., 2012; Yang et al., 2017a; Klein et al., 2020a; Klein et al., 2020b).

Fruit yellowing is closely related to chlorophyll degradation and is controlled by a series of enzymes, such as chlorophyllase (CLH), pheophorbide a oxygenase (PAO), red chlorophyll catabolite reductase (RCCR), pheophytinase (PPH), non-yellow coloring 1 (NYC1), NYC1-like (NOL), and stay-green (SGR). Chlorophyll degradation in peel of pear is retarded by 1-MCP through depression of the expression of *PAO*, *NYC*, *NOL*, and *SGR* (Cheng et al., 2012; Cheng and Guan, 2014; Zhao et al., 2020).

However, the mechanism by which 1-MCP regulates wax biosynthesis and greasiness in pear fruits is little known, and the relationship between greasiness and yellowing in particular is unclear. In this study, 'Yuluxiang' pear (*Pyrus sinkiangensis*), a recently extended cultivar in China that has a tendency to develop greasiness and yellowing during storage, was chosen to investigate response to 1-MCP treatment, and to explore the molecular mechanism of the effect of 1-MCP on wax accumulation, greasiness, and yellowing during storage.

Materials and methods

Materials and treatments

'Yuluxiang' pear fruits were harvested from Shenzhou City, Hebei Province, during the commercial harvest period (i.e., on 30 August 2016) and transported to the laboratory within 2 h after harvest. The fruits chosen were of similar size (average fruit weight: 249.55 g) and showed no evidence of disease or mechanical or insect damage, and divided into two groups. One group was treated with 1-MCP (1.0 μL L^{-1}) and the other with air (as the control) at 25 ± 1°C for 18 h (Dong et al., 2012); fruit were then stored at 25 ± 1°C.The fruit were sampled once a week to determine their fruit quality and wax content, and peel samples were immediately frozen with liquid nitrogen and then stored at −80°C for subsequent analysis.

Methods

Determination of fruit firmness and soluble solids content

Fruit firmness was measured with a fruit firmness tester (GY-4, Zhejiang, China) at the fruit equator, after peeling, and expressed in newtons (N). The soluble solids content (SSC) was measured with a digital refractometer (ATAGO PAL-1, Tokyo, Japan). Each experiment was carried out in triplicate, with five fruits used in each replicate.

Determination of peel greasiness index

The greasiness index was determined according to DeLong et al. (2004). The greasiness of the peel was divided into four grades. No greasiness, mild greasiness, moderate greasiness, and severe greasiness were classed as grade 0, grade 1, grade 2, and grade 3, respectively. The greasiness index was calculated using the formula:

$$\text{Greasiness index (GI)} = \Sigma\,(\text{number of fruit in each grade} \times \text{corresponding grade}) / (\text{highest grade} \times \text{total number of fruit})$$

Each experiment was carried out in triplicate, with 10 fruits used in each replicate.

Determination of chlorophyll content

Peel powder (0.5 g) was incubated in 15 mL of 80% (v/v) acetone solution at 25°C overnight. The chlorophyll (Chl) content was measured using the method described by Cheng et al. (2012), and the results were expressed as mg Chl g^{-1} fresh weight (FW). All measurements were performed in triplicate.

Determination of rates of respiration and ethylene production

The fruit were sealed in desiccators for 30 min at 25 ± 1°C, then 10 mL of gas was extracted and the carbon dioxide content determined using an infrared analyzer (HWF-1, Jiangsu Jintan Instrument Manufacturing Co. Ltd, China) for the calculation of the rate of respiration. After fruit sealing for 3 h, 1 mL of gas was mixed and extracted for the determination of the rate of ethylene production by gas chromatography (GC) (9790 II, Zhejiang Fuli Analytical Instrument Co. Ltd, China). Each experiment was carried out in triplicate, with 10 fruits used in each replicate.

Extraction and determination of wax components

The extraction of total wax was carried out using the method described by Wang et al. (2014). Fruit were divided among two containers and treated with chloroform for 30 s. Fruit extracted from the two containers were combined, and 400 µL of 0.5 µg μL^{-1} *N*-tetradecane (Accustadard Inc., New Haven, CT, USA) was added as an internal standard. The mixture was distilled using a rotary evaporator in a 40°C water bath and then dried with a slow nitrogen flow. The remaining substance was the total wax sample.

The wax sample was dissolved in pyridine, and incubated at 50°C for 30 min, following which 400 µL of *N*-*O*-trimethylsilyl trifluoroacetamide (TCI, Tokyo, Japan) was added and the sample incubated at 60°C for 40 min to enable a derivatization reaction to occur. The mixture was dried, and then re-dissolved in 2.5 mL of chloroform. The solution was filtered into a 1.5-mL headspace glass injection bottle with a filter membrane with a pore diameter of 0.22 µm, ready for wax determination.

The wax content was determined by gas chromatography–mass spectrometry (GC-MS). Wax components were separated in a capillary column (specification: 30 m × 0.25 mm, diameter × thickness). Helium was used as a carrier gas, and the flow rate setting was 1 mL min^{-1}. The heating program of GC was as follows: the initial temperature was 70°C for 1 min; subsequently the temperature was increased to 200°C at a rate of 10°C per min, and then to 300°C at a rate of 4°C per min for 20 min. The mass spectrum program was as follows: the injection port temperature was 250°C, the transmission line temperature was 250°C, the ion source temperature was 230°C, and the electron impact (EI) ion source was 70 eV, with a mass spectrum scanning range of 50–650 *m*/*z*. The wax component was identified by the mass spectrum library NIST09, and was expressed as µg cm^{-2}.

Ribonucleic acid extraction and real-time quantitative reverse transcription polymerase chain reaction analysis

RNA extraction was performed using the method reported by Gasic et al. (2004). The first strand of cDNA was synthesized by the Primescript™ RT reagent kit (Fischer Scientific, Waltham, MA, USA) with genomic DNA (gDNA) eraser. qRT-PCR was performed using an ABI 7500 quantitative PCR instrument (AppliedBiosystems, Foster City, CA, USA) and SYBR®Premix Ex Taq™ II kit (Tli RNaseH plus). The reaction system was as follows: 1 µL of forward primer and reverse primer (each at a concentration of 10 µmol L^{-1}), SYBR 10 µL, Rox 0.4 µL, ddH_2O 6.1 µL, and 12.5 ng of cDNA. The reaction procedure was 95°C for 15 s followed by 40 cycles of 95°C for 5 s and 60°C for 34 s. Relative gene expression was calculated according to the formula: $2^{-\Delta\Delta CT}$ (Livak and Schmittgen, 2001). *ACT2* was used to standardize the transcript levels of the qPCR product in tested genes. Expression of each gene at day 0 was recorded as "1". The specificity of primers was determined by the dissolution curve of qRT-PCR product. The primers of genes *LTPG1*, *LTP4*, *ACT2*, *ERS1*, *ETR2*, *CLH1*, *NYC1*, *RCCR*, *NOL*, *PPH*, and *SGR* were as reported in Wu et al. (2017); Li et al. (2017); Zhou et al. (2017), and Cheng and Guan (2014); the primers of the other genes were designed by Omega 2.0, and their sequences are shown in Table S1.

Data analysis

All assays included three replicates, and the results were expressed as mean ± standard error. One-way ANOVA was used for the analysis of data difference. Duncan's test ($\alpha = 0.05$) was used for multiple comparisons in SPSS 20.0 software (IBM, Armonk, NY, USA). Principal component analysis (PCA) and heatmap analysis were conducted using Origin 2021 software (OriginLab, Northampton, MA, USA).

Results

1-MCP treatment maintained higher fruit quality

Fruit firmness clearly decreased in fruits subjected to both treatments after 21 days of storage, but it was higher in 1-MCP-treated fruit than in control fruit at day 28 (Figure 1A). There was no significant difference in SSC between treatments during storage (Figure 1B). In addition, GI was lower in 1-MCP-treated fruit than in the control fruit during storage (Figure 1C). The contents of chlorophyll decreased in both treatments, but the decrease was delayed by 1-MCP (Figure 1D).

1-MCP treatment decreased the rates of respiration and ethylene production

The fruit showed an obvious ethylene production peak but no respiratory climacteric, although the lowest respiration rate was observed at day 6 in control fruit. The rate of respiration remained at a much lower level, and then slightly increased at day 24, in 1-MCP-treated fruit (Figure 2A). 1-MCP treatment significantly decreased the rate of ethylene production before day 18, and also delayed the appearance of its peak by 18 days (Figure 2B).

1-MCP treatment altered fruit wax composition and profile

The proportions of aliphatic wax components (alkanes, alkenes, fatty acid, ester, aldehydes, and fatty alcohols) and triterpenoids in 'Yuluxiang' pear were 39.4% and 51% at harvest (Table S1), respectively. Alkanes accounted for a higher proportion of wax than the other aliphatic components (Table S1). The above seven wax components accumulated in both treatments during storage, and the contents of alkenes, fatty acids, and esters were lower in 1-MCP-treated fruit than in control fruit (Table 1).

PCA showed that the contribution of total variance to PC1 and PC2 reached 86.2%. Fatty acids, esters, alkenes, and greasiness index were located on the positive axis of PC1 and on the negative axis of PC2. Fatty alcohols, triterpenoids, aldehydes, and alkanes were located on the positive axes of PC1 and PC2. However, chlorophyll content was on the negative axis of PC1 and the positive axis of PC2 (Figure 3A).

The positions of the control at day 7 and day 14 were on the positive axis of PC1, while 1-MCP treatment at day 7 and day 14 loaded on the negative axis of PC1. The positions of the control at day 21 and day 28 were located on the negative axis of PC2,

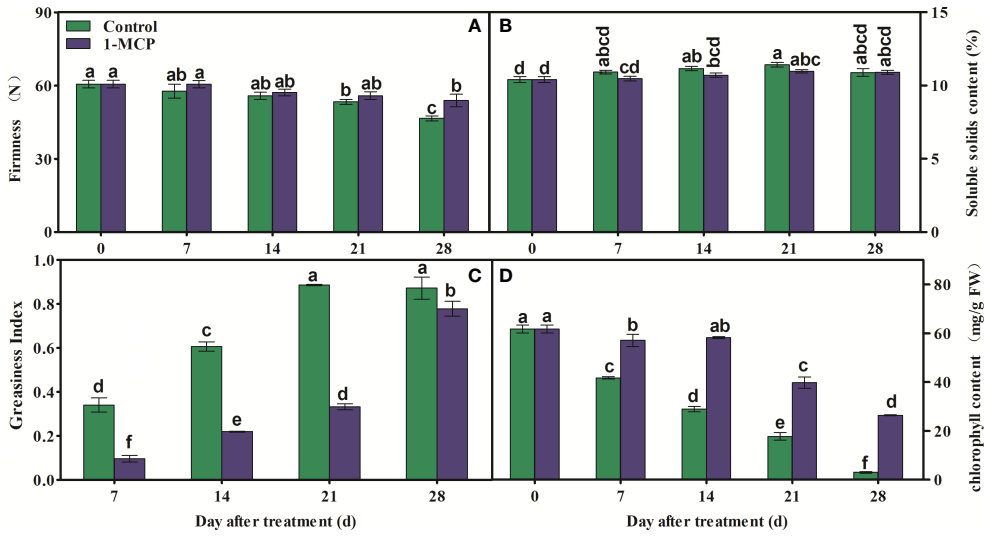

FIGURE 1
Effects of 1-MCP treatment on **(A)** fruit firmness, **(B)** soluble solids content (SSC), **(C)** greasiness index of peel, and **(D)** chlorophyll content in 'Yuluxiang' pear during storage. Data are mean ± SE ($n = 3$); values labeled with different letters represent a significant difference at $p<0.05$.

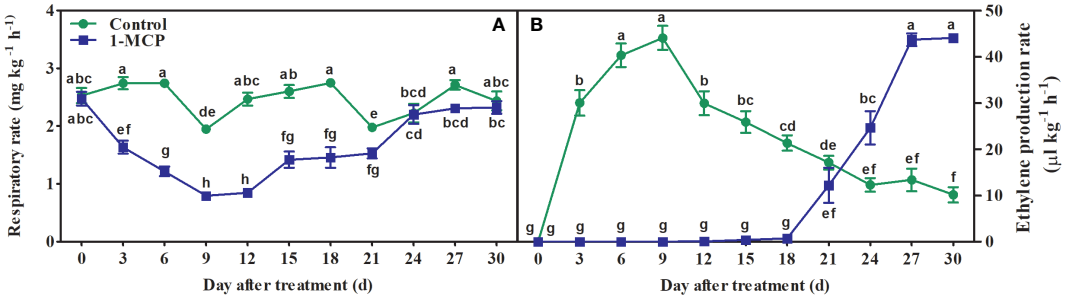

FIGURE 2
Effects of 1-MCP treatment on rates of **(A)** respiration and **(B)** ethylene production in 'Yuluxiang' pear during storage. Data are mean ± SE (n = 3); values labeled with different letters represent a significant difference at p<0.05.

TABLE 1 Effects of 1-MCP treatment on the seven components of wax on the fruit surface of 'Yuluxiang' pear during storage.

Treatments	Day after treatment (d)	Wax component (μg cm^{-2})						
		Alkanes	Alkenes	Fatty acids	Esters	Aldehydes	Fatty alcohols	Triterpenoids
Control	0	26.93 ± 5.43 **d**	1.11 ± 0.02 **f**	1.67 ± 0.25 **d**	1.86 ± 0.24 **d**	5.92 ± 4.13 **c**	3.94 ± 0.62 **d**	53.68 ± 21.01 **cd**
	7	40.6 ± 8.05 **ab**	13.32 ± 3.92 **c**	10.47 ± 3.63 **b**	28.12 ± 5.92 **c**	25.97 ± 5.72 **a**	8.75 ± 1.5 **ab**	78.72 ± 25.4 **abc**
	14	36.08 ± 2.42 **bc**	16.19 ± 3.89 **c**	11.33 ± 0.58 **ab**	22.76 ± 15.46 **c**	24.05 ± 4.13 **a**	6.73 ± 0.36 **c**	73.87 ± 12.38 **abcd**
	21	31.67 ± 0.87 **cd**	20.78 ± 0.97 **b**	9.27 ± 0.67 **b**	42.03 ± 2.64 **b**	22.02 ± 0.04 **ab**	7.23 ± 0.3 **bc**	46.78 ± 1.69 **d**
	28	45.89 ± 3.81 **a**	35.8 ± 1.16 **a**	13.51 ± 0.43 **a**	53.55 ± 5.43 **a**	22.9 ± 1.56 **a**	6.44 ± 1.17 **c**	88.24 ± 0.39 **ab**
1-MCP	0	26.93 ± 5.43 **d**	1.11 ± 0.02 **f**	1.67 ± 0.25 **d**	1.86 ± 0.24 **d**	5.92 ± 4.13 **c**	3.94 ± 0.62 **d**	53.68 ± 21.01 **cd**
	7	35.37 ± 3.67 **bc**	4.87 ± 0.96 **e**	2.28 ± 0.24 **d**	9.27 ± 2.09 **d**	20.47 ± 0.88 **ab**	8.8 ± 1.13 **ab**	80.08 ± 4.64 **abc**
	14	29.17 ± 0.72 **cd**	3.74 ± 0.76 **ef**	2.1 ± 0.63 **d**	11.2 ± 3.34 **d**	16.72 ± 1.23 **b**	6.3 ± 0.85 **c**	67.63 ± 21.22 **abcd**
	21	39.46 ± 3.78 **ab**	8.95 ± 1.2 **d**	5.84 ± 1.09 **c**	21.91 ± 0.73 **c**	23.68 ± 2.02 **a**	9.62 ± 2.19 **a**	59.03 ± 18.94 **bcd**
	28	43.98 ± 1.58 **a**	15.94 ± 1.41 **c**	11.42 ± 0.48 **ab**	39.02 ± 5.36 **b**	24.11 ± 1.21 **a**	7.02 ± 0.41 **bc**	89.76 ± 3.02 **a**

1-MCP, 1-methylcyclopropene. Data are mean ± SE (n = 3); values in the same column labeled with different letters represent a significant difference at p<0.05.

10.3389/fpls.2022.1082041

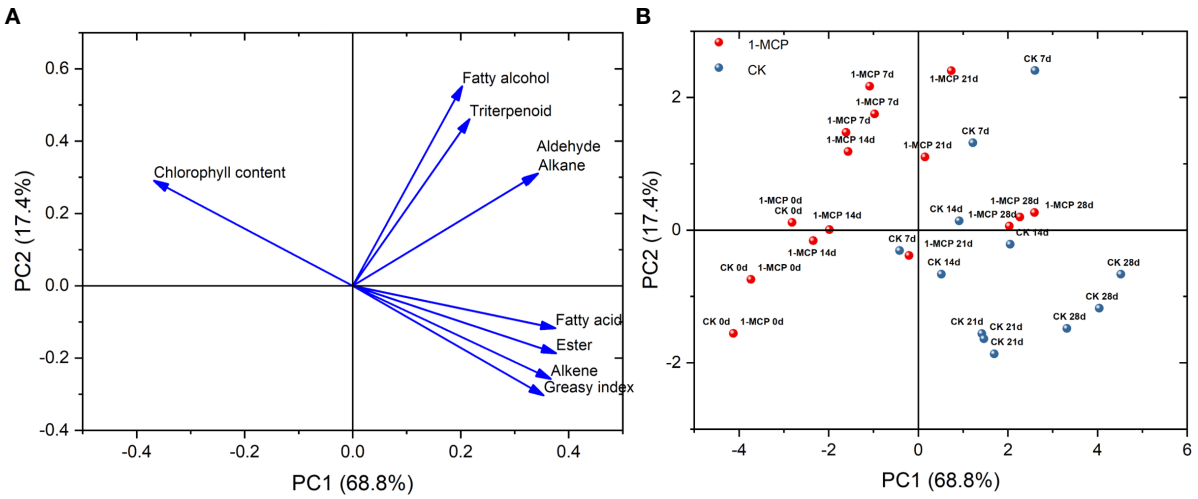

FIGURE 3
(A) Loading plot and **(B)** scoring plot of wax composition, greasiness index, and chlorophyll content based on PCA in control and 1-MCP-treated 'Yuluxiang' pear during storage.

while the positions of 1-MCP treatment on day 21 and day 28 were mainly on the positive axis of PC2 (Figure 3B).

Alkanes and alkenes with carbon chains of C21–C31, three fatty acids (C16, C18:1, and C28), aldehydes (C24–C34), fatty alcohols (C21–C30), six esters (C22:1 fatty alcohol-C16 fatty acid, C22:1 fatty alcohol-C18:1 fatty acid, C22 fatty alcohol-C16 fatty acid, C22 fatty alcohol-C18:1 fatty acid, C24:1 fatty alcohol-C18:1 fatty acid, and C24 fatty alcohol-C18:1 fatty acid), and seven triterpenoids were all detected in the surface wax of 'Yuluxiang' pear fruits (Figure S1). Among them, one alkane (C29), three alkenes (C23, C25, and C29), three fatty acids and six esters (see above), five aldehydes (C24:1, C26:1, C28:1, C32, and C34), two fatty alcohols (C22 and C24), and 28-oxours-12-en-3-yl acetate were the main components of wax (Fig S1). The contents of the major components of wax, three alkenes (C23, C25, and C29), three fatty acids (C16, C18:1, and C28), six esters, and three aldehydes (C24:1, C26:1, and C28:1), showed an upward trend in both treatments during storage; however, they were reduced by1-MCP treatment to different degrees (Figure S1 and Figure 4). No marked differences in the contents of alkane C29, aldehydes C32 and C34, fatty alcohols C22 and C24, and 28-oxours-12-en-3-yl acetate were found in either treatment during storage (Figures S1, 5).

1-MCP treatment regulated the expression pattern of genes associated with ethylene synthesis and signaling

The transcriptional levels of genes associated with ethylene synthesis (*ACS1*, *ACO1*) sharply increased during the first storage stage. Thereafter *ACS1* remained almost unchanged, while *ACO1* decreased in the control fruit, and both genes were down-regulated by 1-MCP. The expression in 1-MCP-treated fruit of genes encoding ethylene receptors (*ERS1*and *ETR2*) increased rapidly at first and then more slowly, before finally reducing. In control fruit, expression of *ERF1* quickly reached a maximum and then decreased before slowly increasing again. In comparison, peak expression of *ERF1* was delayed by 21 days in 1-MCP-treated fruit (Figure 6).

1-MCP treatment regulated the expression pattern of genes associated with chlorophyll degradation

The expression of *NYC1*, *NOL*, *PAO*, *PPH*, and *SGR* increased rapidly during storage (with the exception of *NYC1*, which showed a gradual increasing trend as storage time increased) and was down-regulated by 1-MCP. In contrast, the relative expression levels of *CLH1* and *RCCR* decreased during storage. In 1-MCP-treated fruit, the expression of *CLH1* was higher at day 7, while the expression of *RCCR* was lower at day 14 and higher at day 28 (Figure 7).

1-MCP treatment regulated the expression pattern of genes associated with wax synthesis and transduction

The *CAC* gene is involved in the biosynthesis of $VLCFA_{n \leq 18}$ in fruit wax. The present work showed that the expression of *CAC3* increased rapidly at first and then decreased. The

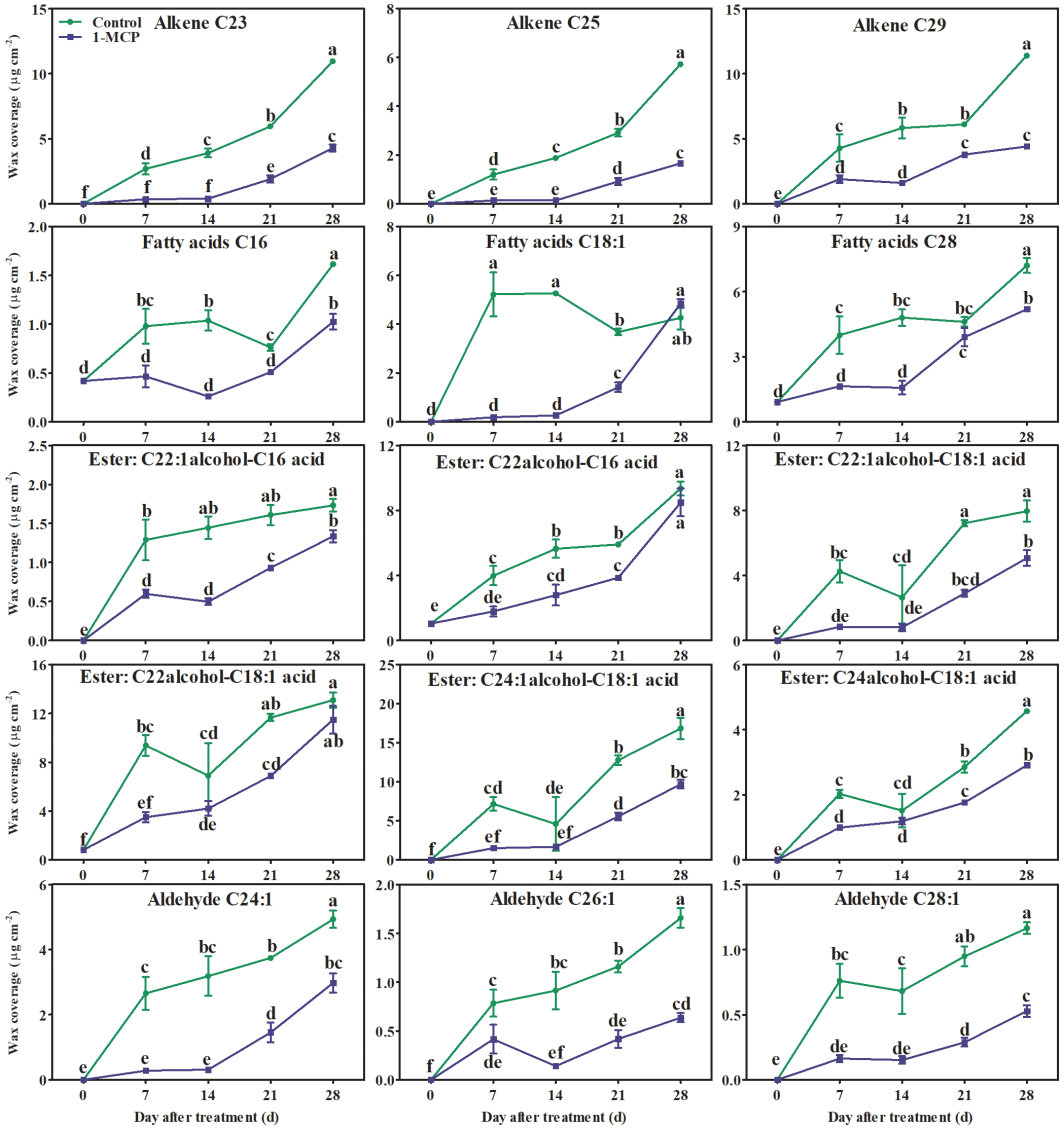

FIGURE 4
Effects of 1-MCP treatment on the principal components (alkenes, fatty acids, esters, and olefinic aldehydes) of wax on the surface of 'Yuluxiang' pear during storage. Data are mean ± SE (n = 3); values labeled with different letters represent a significant difference at p<0.05.

expression levels of *CAC3L* gradually increased in control fruits, but were reduced in fruit treated with 1-MCP.

The genes *LACS*, *KCS*, *KCR*, *CER*, *ABCG*, *LTP*, and *LTPG* encode important enzymes or transporters associated with the biosynthesis of VLCFA$_{20 \leq n \leq 34}$. Here, the expression of *KCS1*, *KCS4*, and *KCS11L* showed an upward trend in control fruit, but the expression of these genes was down-regulated by 1-MCP treatment (Figure 8). In contrast, the expression of *LACS1*, *LTP4*, *KCR1*, *ABCG12*, *ABCG11L*, and *ABCG21L* rapidly increased at first and then declined, at first somewhat sharply and then more gradually in the control fruit. The expression levels of *KCS2*, *KCS10L*, *FDH(KCS)*, *KCS20*, and *LTPG1* peaked midway through the experiment (day 14) and were also down-regulated by 1-MCP (Figure 8).

Correlation analysis between greasiness index, chlorophyll content, wax composition content, and expression levels of genes involved in wax synthesis and chlorophyll degradation

The expression levels of *ERS1*, *ACS1*, and *ETR2* showed a positive correlation with greasiness index and the contents in wax of alkanes, alkenes, fatty acids, esters, and aldehydes, but

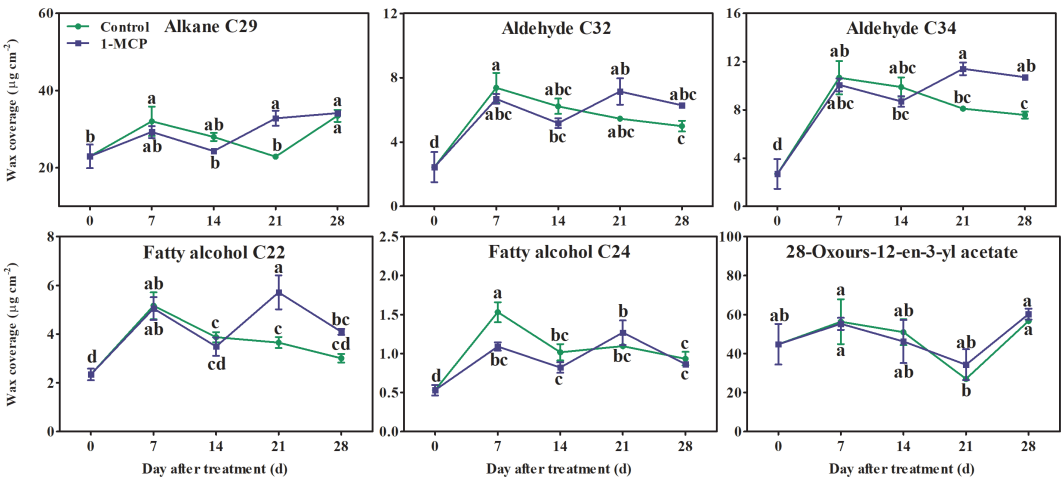

FIGURE 5
Effects of 1-MCP treatment on the principal components (alkanes, aldehydes, fatty alcohols, and triterpenoids) of wax on the surface of 'Yuluxiang' pear during storage. Data are mean ± SE (n = 3); values labeled with different letters represent a significant difference at p<0.05.

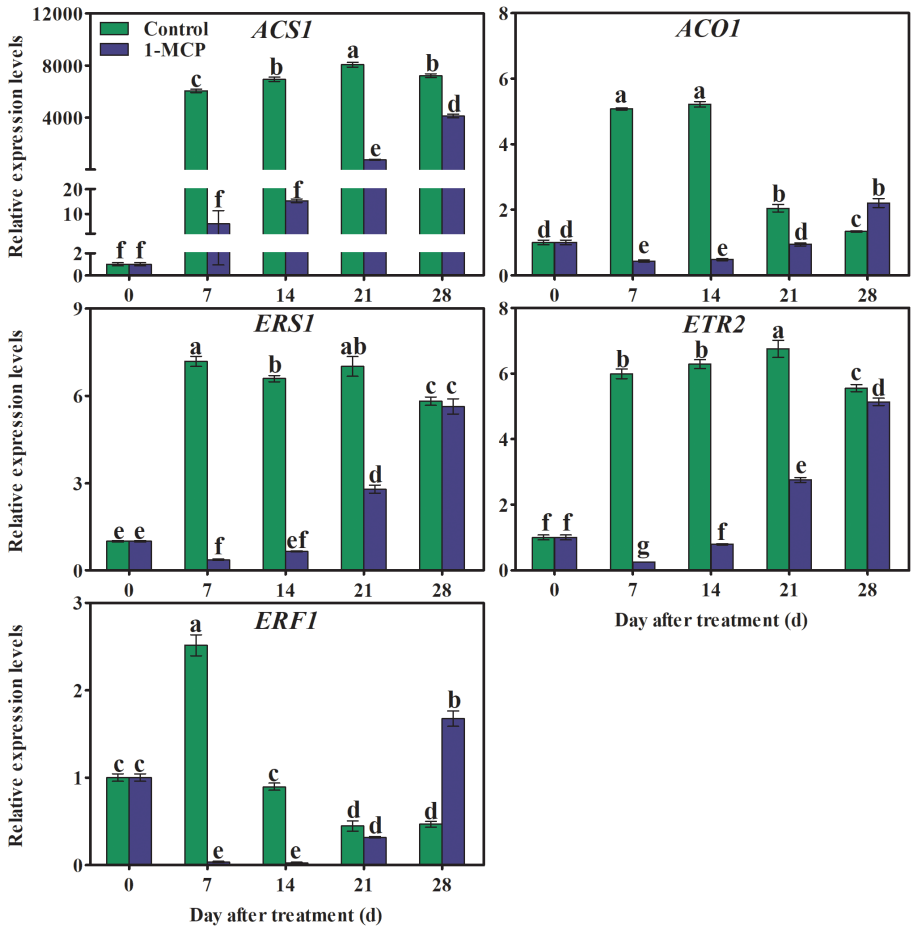

FIGURE 6
Effects of 1-MCP treatment on the expression levels of genes associated with ethylene biosynthesis (*ACS1* and *ACO1*), receptors (*ERS1* and *ETR2*), and signaling (*ERF1*) in the peel of 'Yuluxiang' pear during storage. Data are mean ± SE (n = 3); values labeled with different letters represent a significant difference at p<0.05.

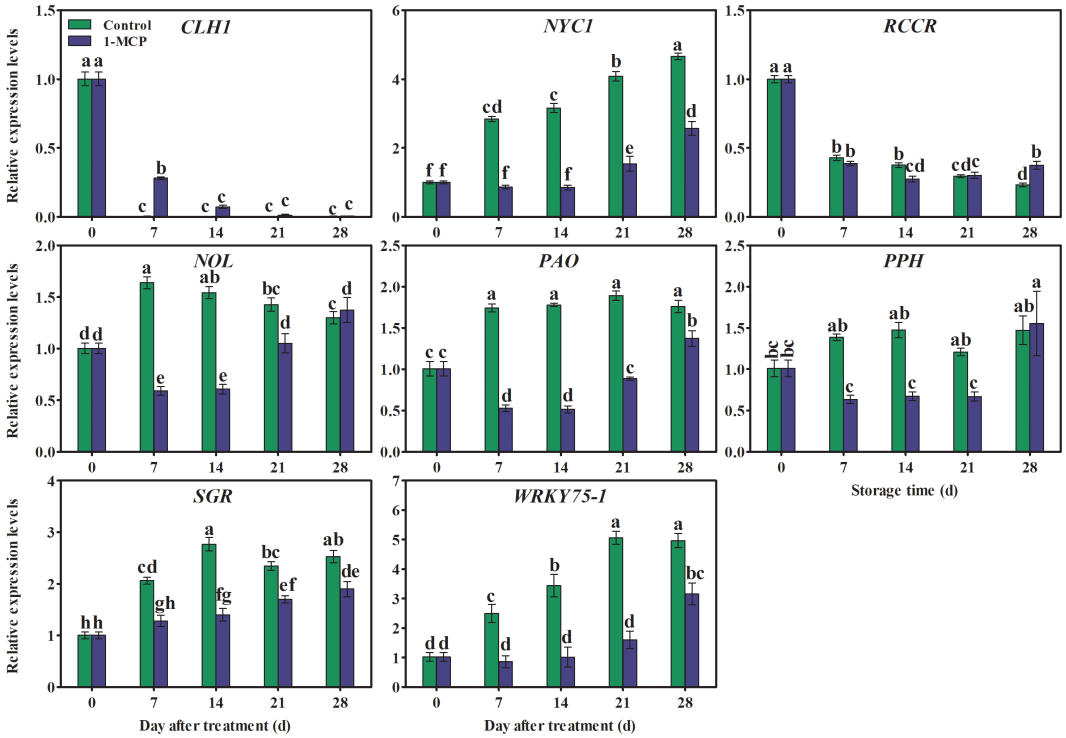

FIGURE 7
Effects of 1-MCP treatment on the expression pattern of genes associated with chlorophyll degradation in the peel of 'Yuluxiang' pear during storage. Data are mean ± SE (n = 3); values labeled with different letters represent a significant difference at p<0.05.

were negatively correlated with chlorophyll content (Figure 9A). In addition, the expression profiles of *ERF1* and *ACO1* were positively correlated with the fatty acid content of wax (Figure 9A). The expression levels of *CLH1* and *RCCR* showed a negative correlation with the greasiness index and the contents of fatty alcohols, aldehydes, esters, fatty acids, alkenes, and alkanes, but were positively correlated with chlorophyll content (Figure 9B). Expression levels of the *NYC1*, *NOL*, *PAO*, *PPH*, *SGR*, *LACS1*, *LACS6*, *KCS1*, *KCS2*, *KCS4*, *KCS11L*, *FDH*, and *KCS20* genes were positively correlated with the greasiness index, but the contents in wax of chemicals (such as aldehydes, esters, fatty acids, alkenes, and alkane) were negatively correlated with chlorophyll content (Figures 9B, C). In addition, there was no significant correlation between the expression of *PPH* and aldehyde content, or between the expression of *FDH* and *KCS20* and wax alkane content (Figures 9B, C). There was a positive correlation between the expression of three genes (*ABCG12*, *CAC3L*, and *DGAT1L*) and both greasiness index and the contents of some wax components (such as esters, fatty acids, and alkenes), but expression of the same three genes was negatively correlated with chlorophyll content (Figure 9C). Expression of the *CER10* and *LTPG1* genes was positively correlated with aldehyde content (Figure 9C). *LTP4* expression was positively correlated with fatty acid content (Figure 9C). Expression of *ABCG11L* was positively correlated with greasiness index and fatty acid content (Figure 9C). The relative expression levels of *ABCG21L* and *CAC3* showed a positive correlation with the contents of aldehydes and fatty acids, and expression of *CAC3* also showed a positive correlation with greasiness index (Figure 9C).

Discussion

In the present work, 1-MCP treatment decreased the greasiness index and inhibited the decline of fruit firmness and content of chlorophyll (Figures 1A, C). The content of chlorophyll was negatively correlated with the greasiness index and with the composition of the wax mobile phase (i.e., the contents of alkenes, fatty acids, esters, and aldehydes) (Figure 9A). The degradation of chlorophyll was found to be accompanied by the accumulation of wax and increased peel greasiness in 'Yuluxiang' pear.

Ethylene increases the fatty acid and ester content of wax, and also promotes the formation of wax, in apple (Contreras et al., 2016; Yang et al., 2017b; Li et al., 2022), whereas 1-MCP has the opposite effects (Li et al., 2022). In this work, 1-MCP

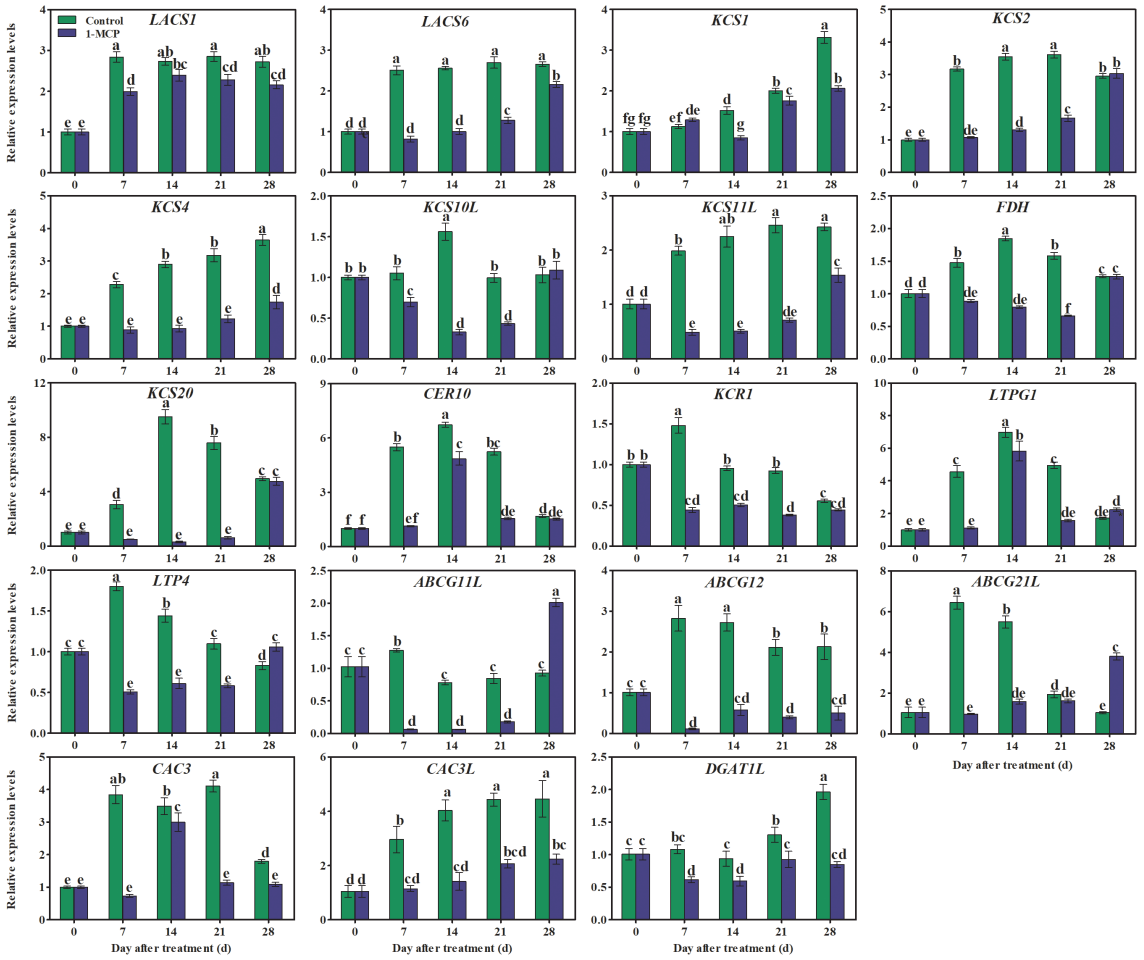

FIGURE 8
Effects of 1-MCP treatment on the expression pattern of genes associated with wax synthesis and transporter proteins in the peel of 'Yuluxiang' pear during storage. Data are mean ± SE (n = 3); values labeled with different letters represent a significant difference at p<0.05.

treatment inhibited the production of ethylene in fruit and delayed peak ethylene concentration (Figure 2B). A similar pattern was found in the expression of five ethylene-related genes (*ACS1*, *ACO1*, *ERS1*, *ETR2*, and *ERF1*) and 19 wax synthesis and transportation genes (*LACS1*, *LACS6*, *KCS1*, *KCS2*, *KCS4*, *KCS10L*, *KCS11L*, *FDH*, *KCS20*, *CER10*, *KCR1*, *LTPG1*, *LTP4*, *ABCG11L*, *ABCG12*, *ABCG21L*, *CAC3L*, *DGAT1L*, and *CAC3L*), and expression levels of these genes were also down-regulated by 1-MCP (Figures 6, 8). In addition, the changes in the contents of total fatty acids, esters, and alkenes were also consistent with the pattern of expression of ethylene-related genes and wax synthesis genes (Table 1; Figures 6, 8). Thus, it can be suggested that ethylene might be involved in regulation of the synthesis of wax in 'Yuluxiang' pear during storage.

It has been reported that the components of solid-phase wax on fruit surfaces, including alkanes and fatty alcohols, promote the morphogenesis of wax crystals (Wu et al., 2017; Yang et al., 2017b), while the components of mobile-phase wax, such as oleic acid and linoleic acid and their esters, are closely associated with peel greasiness in apples (Christeller and Roughan, 2016; Yang et al., 2017a; Yang et al., 2017b; Zhang et al., 2019b). In the present study, it was also found that the mobile-phase components (i.e., the three main fatty acids, six esters, three alkenes, and three aldehydes) accumulated during the development of peel greasiness in 'Yuluxiang' pear (Figures 1, 4, 9), and were reduced by 1-MCP (Figure 4). It has been reported that alkanes and fatty alcohols can contribute to the formation of wax crystals (Yang et al., 2017b). In this study, the proportions of alkanes and fatty alcohols were reduced in both control and 1-MCP-treated fruit, but their declines were retarded by 1-MCP (Table S2).

It has been shown that the *CAC1* and *CAC3* genes in apple, the *CAC* gene in the 'Newhall' orange mutant glossy, and two

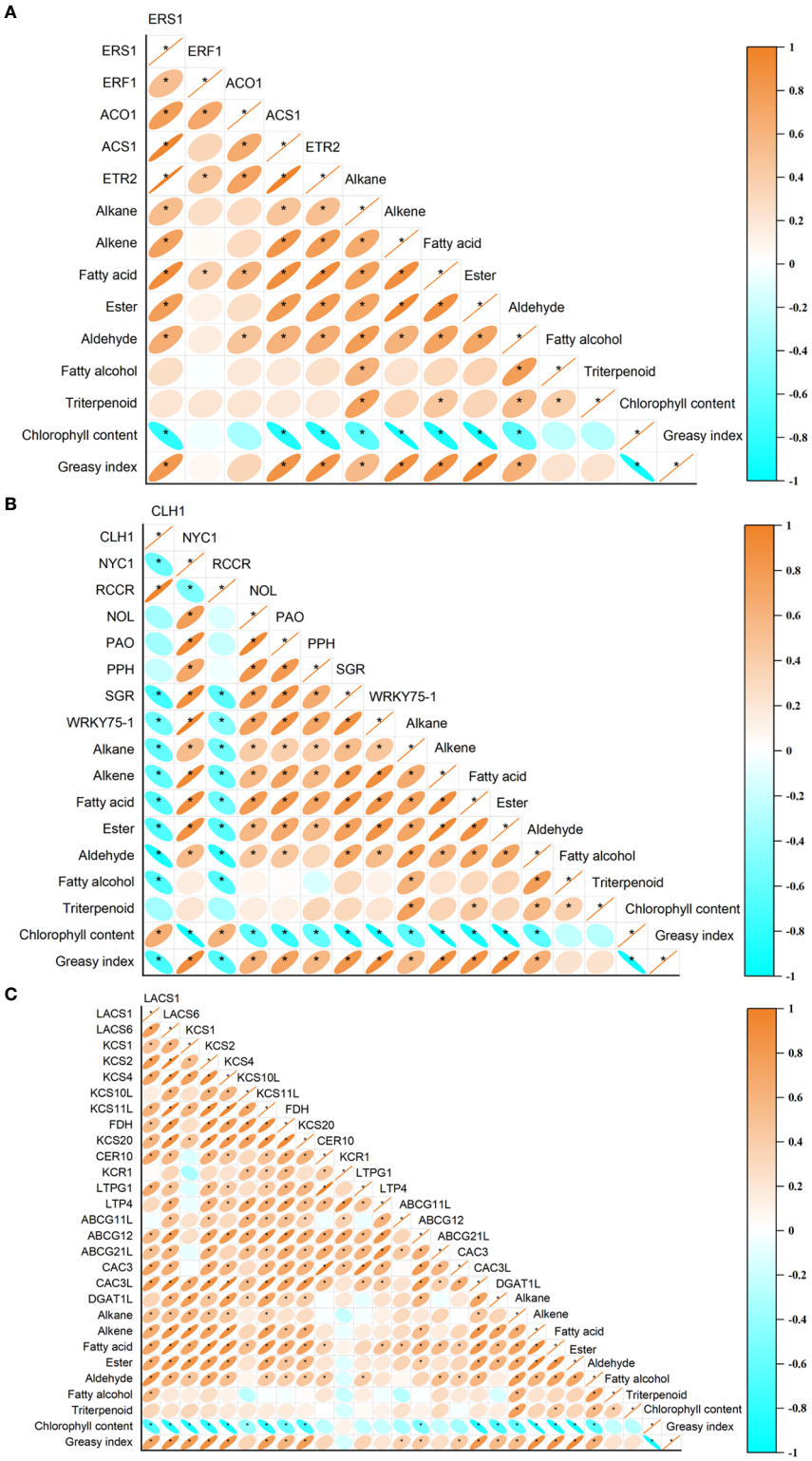

FIGURE 9
The relationships between peel greasiness index, chlorophyll content, and wax composition and **(A)** ethylene-related genes, **(B)** chlorophyll degradation genes, and **(C)** wax synthesis and transporter genes. The correlation significant level was set at $P<0.05$.

homologs of the *PbrCAC1* gene in 'Yuluxiang' pear are involved in the biosynthesis of VLCFA$_{n \leq 18}$ in wax (Liu et al., 2015; Yang et al., 2017a; Wu et al., 2019). Here the expression levels of *CAC3* and *CAC3L* were consistent with the changes in the amounts of two fatty acids (C16 and C18:1) in fruit wax (Figures 4, 8), and both genes were down-regulated by 1-MCP.

It has been reported that genes coding for fatty acid elongation enzymes (*LACS*, *KCS*, *KCR*, and *CER10*) and transport proteins (*ABCG* and *LTP*) are involved in the biosynthesis of C20–C34 fatty acids and their derivatives (Teerawanichpan and Qiu, 2010; Bernard and Joubès, 2013). The relatively high expression of *MdLACS2* and *MdKCS1* in apple, *SlCER6* in tomato, and *CsKCS1*, *CsABC*, and *CsLTP* in cucumber contributes to the accumulation of wax (Zhang et al., 2019a; Zhang et al., 2019c; Xiong et al., 2020; Zhang et al., 2020b). The *LACS1* gene, eight *KCS* genes (*KCS2*, *KCS4, KCS6*, *KCS9*, *KCS10*, *FDH1*, *KCS20*, and *CER60*), four *ABCG* genes (*CER5_1*, *CER5_2*, *WBC11_1*, and *WBC11_2*), and two *LTP* genes (*LTPG1* and *LTP4*) have all been linked to the accumulation of total wax and fatty acids in developing and ethephon-treated 'Yuluxiang' pear (Wu et al., 2019; Wu et al., 2020). In 'Newhall' navel orange, the levels of expression of two *KCS* genes (*KCS4* and *KCS2b*), two *ABCG* genes (*ABCG40* and *ABCG6*), and the *LTP1* gene were found to be correlated with the change in total wax content (Wan et al., 2020). In this study, lower quantities of three alkenes (C23, C25, and C29), C28 fatty acid, six esters, and three aldehydes were found in the surface wax of 1-MCP-treated fruit, and were also linked to the down-regulation of wax-related genes (Figure 8).

It is known that the protein DGAT1 possesses the structure domains of ester and diacylglycerol synthetase (Stöveken et al., 2005; Yen et al., 2005). The level of transcription of *DGAT1* mRNA was consistent with the content of the corresponding wax ester on the surface of pear fruits in cold storage (Wu et al., 2017). In this study, both the level of expression of *DGAT1L* and the ester content of peel were down-regulated by 1-MCP (Figure 8).

The process of ripening and senescence is delayed by 1-MCP treatment through inhibition of the ethylene signal and down-regulation of the expression of genes related to chlorophyll degradation (*RCCR2*, *NYC1*, *NYC3*, *NOL2*, *PPH*, *PAO*, *RCCR*, and *CLH*) in apple, pepper, and sweet cherry fruits (Lv et al., 2020; Du et al., 2021; Zhao et al., 2021). A study of the relationship between ethylene and fruit yellowing showed that 1-MCP delays chlorophyll degradation in 'Comice' pear by reducing ethylene production and the expression of chlorophyll catabolic signal genes, such as *PcPPH*, *PcNOL*, *PcSGR1*, and *PcPAO* (Zhao et al., 2020). In addition, 1-MCP inhibits the degreening induced by chlorophyll degradation in broccoli by down-regulating the expression of some chlorophyll degradation genes (Gómez-Lobato et al., 2012). In the present study, expression levels of chlorophyll degradation genes (*NYC1*, *NOL*, *PAO*, *PPH*, and *SGR*) were found to be lower in 1-MCP-treated fruit; as a result, chlorophyll content in 1-MCP-treated fruit remained high, and subsequent yellowing of the peel was delayed.

Correlation analysis suggested that chlorophyll content and associated gene expression were correlated with the expression of ethylene signal genes (*ACS1*, *ACO1*, *ERS1*, *ETR2*, and *ERF1*), and with the contents of major wax components and expression of related genes, which are closely related to the greasiness index (Figure 9).Thus, 1-MCP reduced the greasiness of 'Yuluxiang' pear during storage, by reducing the components of wax mobile-phase, and inhibited yellowing and the expression of chlorophyll breakdown pathway genes in peel, which are closely related to the ethylene signal function in 'Yuluxiang' pear.

Conclusion

1-MCP (1.0 μL L^{-1}) treatment significantly improved fruit firmness and chlorophyll content, reduced the components of mobile-phase wax (fatty acids, esters, alkenes, and aldehydes) and greasiness index, and also down-regulated the expression of genes associated with ethylene synthesis and signal (*ACS1*, *ACO1*, *ERS1*, *ETR2* and *ERF1*), wax synthesis and transduction (*LACS1*, *LACS6*, *KCS1*, *KCS2*, *KCS4*, *KCS10L*, *KCS11L*, *FDH*, *KCS20*, *CER10*, *KCR1*, *LTPG1*, *LTP4*, *ABCG11L*, *ABCG12*, *ABCG21L*, *CAC3*, *CAC3L*, and *DGAT1L*), and chlorophyll degradation (*NYC1*, *NOL*, *PAO*, *PPH*, and *SGR*). In this way, it repressed peel greasiness and yellowing in 'Yuluxiang' pear.

Data availability statement

The raw data supporting the conclusions of this article will be made available by the authors, without undue reservation.

Author contributions

JG: conceived and designed the experiments. DL and XL: performed the experiments. DL, XL and YC: analyzed the data. DL, JG, and YC wrote, reviewed and revised papers. All authors contributed to the article and approved the submitted version.

Funding

This work was funded by Key R & D plan of Hebei province (22327505D), and the HAAFS Agriculture Science and Technology Innovation Project (2022KJCXZX-SSS-3).

Conflict of interest

The authors declare that the research was conducted in the absence of any commercial or financial relationships that could be construed as a potential conflict of interest.

Publisher's note

All claims expressed in this article are solely those of the authors and do not necessarily represent those of their affiliated organizations, or those of the publisher, the editors and the reviewers. Any product that may be evaluated in this article, or claim that may be made by its manufacturer, is not guaranteed or endorsed by the publisher.

Supplementary material

The Supplementary Material for this article can be found online at: https://www.frontiersin.org/articles/10.3389/fpls.2022.1082041/full#supplementary-material

References

Bernard, A., and Joubès, J. M. (2013). *Arabidopsis* cuticular waxes: Advances in synthesis, export and regulation. *Prog. Lipid Res.* 52, 110–129. doi: 10.1016/j.plipres.2012.10.002

Chai, Y., Li, A., Chit Wai, S., Song, C., Zhao, Y., Duan, Y., et al. (2020). Cuticular wax composition changes of 10 apple cultivars during postharvest storage. *Food Chem.* 324, 126903. doi: 10.1016/j.foodchem.2020.126903

Cheng, Y., Dong, Y., Yan, H., Ge, W., Shen, C., Guan, J., et al. (2012). Effects of 1-MCP on chlorophll degradation pathway-associated genes expression and chloroplast ultrastructure during the peel yellowing of Chinese pear fruits in storage. *Food Chem.* 135, 415–422. doi: 10.1016/j.foodchem.2012.05.017

Cheng, Y., and Guan, J. (2014). Involvement of pheophytinase in ethylene-mediated chlorophylldegradation in the peel of harvested 'Yali'pear. *J. Plant Growth Regul.* 33, 364–372. doi: 10.1007/s00344-013-9383-z

Christeller, J. T., and Roughan, P. G. (2016). The novel esters farnesyl oleate and farnesyl linoleate are prominent in the surface wax of greasy apple fruit. *New Zeal. J. Crop Hortic.* 4, 164–170. doi: 10.1080/01140671.2016.1152979

Contreras, C., Tjellström, H., and Beaudry, R. M. (2016). Relationships between free and esterified fatty acids and LOX-derived volatiles during ripening in apple. *Postharvest Biol. Technol.* 112, 105–113. doi: 10.1016/j.postharvbio.2015.10.009

Curry, E. (2008). Effects of 1-MCP applied postharvest on epicuticular wax of apples (*Malus domestica* borkh.) during storage. *J. Sci. Food. Agric.* 88, 996–1006. doi: 10.1002/jsfa.3180

DeLong, J. M., Prange, R. K., and Harrison, P. A. (2004). The influence of pre-storage delayed cooling on quality and disorder incidence in 'Honeycrisp' apple fruit. *Postharvest Biol. Technol.* 34, 353–358. doi: 10.1016/j.postharvbio.2004.10.001

Dong, X., Rao, J., Huber, D. J., Chang, X., and Xin, F. (2012). Wax composition of 'Red fuji' apple fruit during development and during storage after 1-methylcyclopropene treatment. *Hortic. Environ. Biote.* 53, 288–297. doi: 10.1007/s13580-012-0036-0

Du, Y., Jin, T., Zhao, H., Han, C., Sun, F., Chen, Q., et al. (2021). Synergistic inhibitory effect of 1-methylcyclopropene (1-MCP) and chlorine dioxide (ClO_2) treatment on chlorophll degradation of green pepper fruit during storage. *Postharvest Biol. Technol.* 171, 111363. doi: 10.1016/j.postharvbio.2020.111363

Gasic, K., Hernandez, A., and Korban, S. S. (2004). RNA Extraction from different apple tissues rich in polyphenols and polysaccharides for cDNA library construction. *Plant Mol. Biol. Rep.* 22, 437–438. doi: 10.1007/BF02772687

Gómez-Lobato, M. E., Hasperué, J. H., Civello, P. M., Chaves, A. R., and Martínez, G. A. (2012). Effect of 1-MCP on the expression of chlorophll degrading genes during senescence of broccoli (*Brassica oleracea* l.). *Sci. Hortic.* 144, 208–211. doi: 10.1016/j.scienta.2012.07.017

Ju, Z., and Bramlage, W. J. (2001). Developmental changes of cuticular constituents and their association with ethylene during fruit ripening in 'Delicious' apples. *Postharvest Biol. Technol.* 21, 257–263. doi: 10.1016/S0925-5214(00)00156-3

Klein, B., Falk, R. B., Thewes, F. R., Anese, R. D. O., Santos, I. D. D., Ribeiro, S. R., et al. (2020a). Dynamic controlled atmosphere: Effects on the chemical composition of cuticular wax of 'Cripps pink' apples after long-term storage. *Postharvest Biol. Technol.* 164, 111170. doi: 10.1016/j.postharvbio.2020.111170

Klein, B., Ribeiro, Q. M., Thewes, F. R., Anese, R. D. O., Oliveira, F. D. C. D., Santos, I. D. D., et al. (2020b). The isolated or combined effects of dynamic controlled atmosphere (DCA) and 1-MCP on the chemical composition of cuticular wax and metabolism of 'Maxi gala' apples after long-term storage. *Food. Res. Int.* 140, 109900. doi: 10.1016/j.foodres.2020.109900

Leide, J., Hildebrandt, U., Reussing, K., Riederer, M., and Vogg, G. (2007). The developmental pattern of tomato fruit wax accumulation and its impact on cuticular transpiration barrier properties: Effects of a deficiency in a β-ketoacyl-coenzyme a synthase (*LeCER6*). *Plant Physiol.* 144, 1667–1679. doi: 10.1104/pp.107.099481

Leide, J., Hildebrandt, U., Vogg, G., and Riederer, M. (2011). The positional sterile (ps) mutation affects cuticular transpiration and wax biosynthesis of tomato fruits. *J. Plant Physiol.* 168, 871–877. doi: 10.1016/j.jplph.2010.11.014

Li, D., Cheng, Y., Dong, Y., Shang, Z., and Guan, J. (2017). Effects of low temperature conditioning on fruit quality and peel browning spot in 'Huangguan' pears during cold storage. *Postharvest Biol. Technol.* 131, 68–73. doi: 10.1016/j.postharvbio.2017.05.005

Li, F., Min, D., Ren, C., Dong, L., Shu, P., Cui, X., et al. (2019). Ethylene altered fruit cuticular wax, the expression of cuticular wax synthesis-related genes and fruit quality during cold storage of apple (*Malus domestica* borkh. c.v. starkrimson) fruit. *Postharvest Biol. Technol.* 149, 58–65. doi: 10.1016/j.postharvbio.2018.11.016

Liu, D., Yang, L., Wang, Y., Zhuang, X., Liu, C. , Liu, S., et al. (2016). Transcriptome sequencing identified wax-related genes controlling the glossy phenotype formation of 'Ganqi 3,' a bud mutant derived from wild-type "Newhall" navel orange. *Tree Genet. Genomes* 12, 55. doi: 10.1007/s11295-016-1017-8

Liu, D., Yang, L., Zheng, Q., Wang, Y., Wang, M., Zhuang, X., et al. (2015). Analysis of cuticular wax constituents and genes that contribute to the formation of 'glossy newhall', a spontaneous bud mutant from the wild-type 'Newhall' navel orange. *Plant Mol. Biol.* 88, 573–590. doi: 10.1007/s11103-015-0343-9

Liu, D. C., Zeng, Q., Ji, Q. X., Liu, C. F., Liu, S. B., and Liu, Y. (2012). A comparison of the ultrastructure and composition of fruits' cuticular wax from the wild-type 'Newhall' navel orange (*Citrus sinensis* [L.] osbeck cv. newhall) and its glossy mutant. *Plant Cell. Rep.* 31, 2239–2246. doi: 10.1007/s00299-012-1333-x

Livak, K. J., and Schmittgen, T. D. (2001). Analysis of relative gene expression data using real-time quantitative PCR and the $2^{-\Delta\Delta CT}$method. *Methods* 25, 402–408. doi: 10.1006/meth.2001.1262

Lv, J., Zhang, M., Bai, L., Han, X., Ge, Y., Wang, W., et al. (2020). Effects of 1-methylcyclopropene (1-MCP) on the expression of genes involved in the chlorophyII degradation pathway of apple fruit during storage. *Food Chem.* 308, 125707. doi: 10.1016/j.foodchem.2019.125707

Petit, J., Bres, C., Just, D., Garcia, V., Mauxion, J.-P., Marion, D., et al. (2014). Analyses of tomato fruit brightness mutants uncover both cutin-deficient and cutin-abundant mutants and a new hypomorphic allele of *GDSL lipase*. *Plant Physiol.* 164, 888–906. doi: 10.1104/pp.113.232645

Rios, J. C., Robledo, F., Schreiber, L., Zeisler, V., Lang, E., Carrasco, B., et al. (2015). Association between the concentration of n-alkanes and tolerance to cracking in commercial varieties of sweet cherry fruits. *Sci. Hortic.* 197, 57–65. doi: 10.1016/j.scienta.2015.10.037

Samuels, L., Kunst, L., and Jetter, R. (2008). Sealing plant surfaces: Cuticular wax formation by epidermal cells. *Annu.Rev. Plant Biol.* 59, 683–707. doi: 10.1146/annurev.arplant.59.103006.093219

Stöveken, T., Kalscheuer, R., Malkus, U., Reichelt, R., and Steinbüchel, A. (2005). The wax ester synthase/acyl coenzyme a: Diacylglycerol acyltransferase

from *Acinetobacter* sp. strain ADP1: characterization of a novel type of acyltransferase. *J. Bacteriol.* 187, 1369–1376. doi: 10.1128/jb.187.4.1369-1376.2005

Teerawanichpan, P., and Qiu, X. (2010). Fatty acyl-CoA reductase and wax synthase from euglena gracilis in the biosynthesis of medium-chain wax esters. *Lipids* 45, 263–273. doi: 10.1007/s11745-010-3395-2

Wang, J., Hao, H., Liu, R., Ma, Q., Xu, J., Chen, F., et al. (2014). Comparative analysis of surface wax in mature fruits between Satsuma mandarin (*Citrus unshiu*) and 'Newhall' navel orange (*Citrus sinensis*) from the perspective of crystal morphology, chemical composition and key gene expression. *Food Chem.* 153, 177–185. doi: 10.1016/j.foodchem.2013.12.021

Wan, H., Liu, H., Zhang, J., Lyu, Y., Li, Z., He, Yi., et al. (2020). Lipidomic and transcriptomic analysis reveals reallocation of carbon flux from cuticular wax into plastid membrane lipids in a glossy 'Newhall' navel orange mutant. *Hortic. Res.* 7, 1–18. doi: 10.1038/s41438-020-0262-z

Wu, X., Chen, Y., Shi, X., Qi, K., Cao, P., Liu, X., et al. (2020). Effects of palmitic acid (16:0), hexacosanoic acid (26:0), ethephon and methyl jasmonate on the cuticular wax composition, structure and expression of key gene in the fruits of three pear cultivars. *Funct. Plant Biol.* 47, 156–169. doi: 10.1071/FP19117

Wu, X., Shi, X., Bai, M., Chen, Y., Li, X., Qi, K., et al. (2019). Transcriptomic and gas chromatography-mass spectrometry metabolomic profiling analysis of the epidermis provides insights into cuticular wax regulation in developing 'Yuluxiang' pear fruit. *J. Agric. Food Chem.* 67, 8319–8331. doi: 10.1021/acs.jafc.9b01899

Wu, X., Yin, H., Chen, Y., Li, L., Wang, Y., Hao, P., et al. (2017). Chemical composition, crystal morphology and key gene expression of cuticular waxes of Asian pears at harvest and after storage. *Postharvest Biol. Technol.* 132, 71–80. doi: 10.1016/j.postharvbio.2017.05.007

Xiong, C., Xie, Q., Yang, Q., Sun, P., Gao, S., Li, H., et al. (2020). WOOLLY, interacting with MYB transcription factor MYB31, regulates cuticular wax biosynthesis by modulating *CER6* expression in tomato. *Plant J.* 103, 323–337. doi: 10.1111/tpj.14733

Yang, Y., Zhou, B., Wang, C., Lv, Y., Liu, C., Zhu, X., et al. (2017a). Analysis of the inhibitory effect of 1-methylcyclopropene on skin greasiness in postharvest apples by revealing the changes of wax constituents and gene expression. *Postharvest Biol. Technol.* 134, 87–97. doi: 10.1016/j.postharvbio.2017.08.013

Yang, Y., Zhou, B., Zhang, J., Wang, C., Liu, C., Liu, Y., et al. (2017b). Relationships between cuticular waxes and skin greasiness of apples during storage. *Postharvest Biol. Technol.* 131, 55–67. doi: 10.1016/j.postharvbio.2017.05.006

Yen, C.-L. E., Monetti, M., Burri, B. J., and Farese, R. V. (2005). The triacylglycerol synthesis enzyme DGAT1 also catalyzes the synthesis of diacylglycerols, waxes, and retinyl esters. *J. Lipid Res.* 46, 1502–1511. doi: 10.1194/jlr.M500036-JLR200

Zhang, C. L., Hu, X., Zhang, Y. L., Liu, Y., Wang, G. L., You, C. X., et al. (2020b). An apple long-chain acyl-CoA synthetase 2 gene enhances plant resistance to abiotic stress by regulating the accumulation of cuticular wax. *Tree Physiol.* 40, 1450–1465. doi: 10.1093/treephys/tpaa079

Zhang, Q., Qi, Y., Li, R., Yang, Y., Yan, D., Liu, X., et al. (2019b). Postharvest applications of n-butanol increase greasiness in apple skins by altering wax composition via effects on gene expression. *Postharvest Biol. Technol.* 155, 111–119. doi: 10.1016/j.postharvbio.2019.05.017

Zhang, J., Yang, J., Yang, Y., Luo, J., Zheng, X., Wen, C., et al. (2019a). Transcription factor *CsWIN1* regulates pericarp wax biosynthesis in cucumber grafted on pumpkin. *Front. Plant Sci.* 101564. doi: 10.3389/fpls.2019.01564

Zhang, Y. L., You, C. X., Li., Y. Y., and Hao, Y. J. (2020a). Advances in biosynthesis, regulation, and function of apple cuticular wax. *Front. Plant Sci.* 11. doi: 10.3389/fpls.2020.01165

Zhang, Y. L., Zhang, C. L., Wang, G. L., Wang, Y. X., Qi, C. H., Zhao, Q., et al. (2019c). The R2R3 MYB transcription factor MdMYB30 modulates plant resistance against pathogens by regulating cuticular wax biosynthesis. *BMC Plant Biol.* 19, 362. doi: 10.1186/s12870-019-1918-4

Zhao, H., Fu, M., Du, Y., Sun, F., Chen, Q., Jin, T., et al. (2021). Improvement of fruit quality and pedicel color of cold stored sweet cherry in response to pre-storage 1-methylcilopropene and chlorine dioxide treatments: Combination treatment of 1-MCP plus ClO_2 improves post-harvest quality of sweet cherry fruit. *Sci. Hortic.* 109806277. doi: 10.1016/j.scienta.2020.109806

Zhao, J., Xie, X., Wang, S., Zhu, H., Dun, W., Zhang, L., et al. (2020). 1-methylcyclopropene affects ethylene synthesis and chlorophyll degradation during cold storage of 'Comice'pears. *Sci. Hortic.* 260108865. doi: 10.1016/j.scienta.2019.108865

Zhou, S., Cheng, Y., and Guan, J. (2017). The molecular basis of superficial scald development related to ethylene perception and α-farnesene metabolism in 'Wujiuxiang' pear. *Sci. Hortic.* 216, 76–82. doi: 10.1016/j.scienta.2016.12.025

frontiers | Frontiers in Plant Science

TYPE Review
PUBLISHED 23 February 2023
DOI 10.3389/fpls.2023.1095967

OPEN ACCESS

EDITED BY
Shifeng Cao,
Zhejiang Wanli University, China

REVIEWED BY
Yuanyue Shen,
Beijing University of Agriculture, China
Qiaoli Xie,
Chongqing University, China

*CORRESPONDENCE
Bingzhu Hou
houbz@ibcas.ac.cn

SPECIALTY SECTION
This article was submitted to Crop and Product Physiology, a section of the journal Frontiers in Plant Science

RECEIVED 11 November 2022
ACCEPTED 01 February 2023
PUBLISHED 23 February 2023

CITATION
Liu J, Qiao Y, Li C and Hou B (2023) The NAC transcription factors play core roles in flowering and ripening fundamental to fruit yield and quality. *Front. Plant Sci.* 14:1095967. doi: 10.3389/fpls.2023.1095967

The NAC transcription factors play core roles in flowering and ripening fundamental to fruit yield and quality

Jianfeng Liu[1,2], Yuyuan Qiao[1,2], Cui Li[1,2] and Bingzhu Hou[1]*

[1]Key Laboratory of Plant Molecular Physiology, Institute of Botany, Chinese Academy of Sciences, Beijing, China, [2]University of Chinese Academy of Sciences, Beijing, China

Fruits are derived from flowers and play an important role in human food, nutrition, and health. In general, flowers determine the crop yield, and ripening affects the fruit quality. Although transcription factors (TFs) only account for a small part of plant transcriptomes, they control the global gene expression and regulation. The plant-specific NAC (NAM, ATAF, and CUC) TFs constitute a large family evolving concurrently with the transition of both aquatic-to-terrestrial plants and vegetative-to-reproductive growth. Thus, NACs play an important role in fruit yield and quality by determining shoot apical meristem (SAM) inflorescence and controlling ripening. The present review focuses on the various properties of NACs together with their function and regulation in flower formation and fruit ripening. Hitherto, we have a better understanding of the molecular mechanisms of NACs in ripening through abscisic acid (ABA) and ethylene (ETH), but how NACs regulate the expression of the inflorescence formation-related genes is largely unknown. In the future, we should focus on the analysis of NAC redundancy and identify the pivotal regulators of flowering and ripening. NACs are potentially vital manipulation targets for improving fruit quantity and quality.

KEYWORDS

flower, fruit ripening, NAC transcription factor, abscisic acid (ABA), ethylene

Introduction

Transcription factors (TFs) only account for a small quantity of genes in plant transcriptomes (less than 10%), but they control the global gene expression and regulation in plant development and adaptation. The plant-specific NAC (NAM, ATAF, and CUC) TFs constitute a large family, such as 101, 328, 138, and 280 members in tomato, rice, Arabidopsis and tobacco respectively (Liu G. S. et al., 2022). In general, the role of a TF is dependent on its binding to the cis-elements of the target genes, which are associated with nuclear localization, DNA binding, oligomerization, and gene expression. Because the NAC family exists from aquatic green algae to higher terrestrial plants, its members participate in the formation of the organ boundaries of plants transiting from vegetative growth to reproductive growth and are related to flower development and fruit ripening, which are essential to crop yield and quality

(Maugarny-Calès et al., 2016; Ma et al., 2017; Mathew and Agarwal, 2018; Forlani et al., 2021; Singh et al., 2021; Liu G. S. et al., 2022). Thereby, in recent years, much progress has been made toward understanding the molecular mechanisms regulated by NAC TFs in flower development (Guo et al., 2022; Liang et al., 2022; Liu X. et al., 2022; Wang et al., 2022; Ghissing et al., 2023) and fruit ripening (Fu B. L. et al., 2021; Gao et al., 2021; Kou et al., 2021; Gao et al., 2022; Li et al., 2022; Liu B. et al., 2022; Qi et al., 2022). In this review, we mainly summarize up-to-date advances on the basic properties, function, and action mechanisms of NACs in flower formation, flowering, and fruit ripening to improve our understanding of the molecular basis of crop yield and quality mediated by NAC TFs.

Specifically, we highlight that the NAC family includes no apical meristem (*NAM*), Arabidopsis transcription activator factors (*ATAF1*/*ATAF2*), and cup-shaped cotyledon (*CUC2*), which all contain a conserved amino acid (aa) sequence at the N-terminal with five subdomains, which not only possess versatile regulatory patterns at the DNA, RNA, and protein levels but also serve as activators or repressors through variable transcriptional regulatory regions at the C-terminal. Plant-specific NACs evolved from the streptophyte green algae to higher plants, concomitant with the transition of aquatic-to-terrestrial living and vegetative-to-reproductive growth, with a line of distinct NACs constituting a complex regulatory network linked to the phytohormones abscisic acid (ABA) and ethylene (ETH) that are essential to flowering and ripening. Thus, NACs are potentially important manipulation targets for improving fruit quantity and quality.

Basic traits of NAC transcription factors

In response to the aquatic-to-terrestrial environmental niches, the NAC family has shown gradual amplifications in gene size and diversity for the colony of land concurrently with the evolution of additional gene functions for water conductance, cell support, xylem/phloem differentiation, and vasculature formation, adaptive to land living in a sessile manner. Therefore, the present NACs in higher plants have developed a variety of structural and action traits, including DNA binding, nuclear localization, oligomerization/protein–protein interactions, and hierarchical regulatory patterns, using a conserved N-terminal NAC domain for target binding and a diverse C-terminal flexible region for regulating gene expression as activators or repressors.

NAC domain traits

NAC TFs have the conserved N-terminal NAC region with about 150 aa including both nuclear localization signal (NLS) and DNA binding regions, which are further divided into five subdomains designated from A to E (A, C, and D are more highly conserved compared to B and E) and a C-terminal region as a transcriptional regulatory/activation region (TRR and TAR, respectively) (Figure 1). In particular, members of the NAC family have a conserved domain fold containing one β-sheet flanked by an α-helical element, and the C-subdomain has a DNA recognition conserved motif sequence (WKATGT/NDK) that specifically binds to the developmental core CGT(GA) and the stress core CGTG (Mathew and Agarwal, 2018) (Figures 1B, E). In addition, NACs include activators and repressors for gene expression and repression, respectively, resulting from the NAC repression domain (NARD) in the D subdomain, such as the rice *NAC020* and *NAC026*, which show bifunctionality having both activation and repression properties (Mathew et al., 2016). In addition, NAC proteins have homodimers and heterodimers, and dimerization is required for stable DNA binding to post-transcriptional and translational modifications in target genes (Chen et al., 2016) (Figure 1B). In conclusion, the N-terminal region in NACs contains the repression domain, while the C-terminal region is the transactivation region to a large degree. These properties allow NACs to have multiple regulatory patterns at the transcriptional, post-transcriptional, and translational levels, serving as activators and repressors in response to developmental and environmental cues.

NAC localization traits

Most of the members of the NAC TF family are localized in the nucleus, although a few of them are situated in other organelles such as the plasma membrane (PM), the cytoplasm, and the endoplasmic reticulum (ER) (Olsen et al., 2005; Kim et al., 2006; Kim et al., 2007; Seo et al., 2008; Wang et al., 2016; Bhattacharjee et al., 2017). Notably, membrane-bound NACs may be anchored in membrane systems, including the PM, ER membrane, and nuclear membrane, in inactive forms. Stimulation by developmental or environmental cues promotes their release and trafficking from the membrane to the nucleus for the control of target gene expression in a common regulatory pattern (Kim et al., 2006; Kim et al., 2007; Seo et al., 2008; Wang et al., 2016; Bhattacharjee et al., 2017). Altogether, the multiple localizations and the translocation traits of NAC TFs implicate various biological functions and regulatory mechanisms in response to developmental and environmental cues.

NAC evolutionary traits

Environmental factors have played a vital role in the diversification of the NAC family, to a great extent, enabling higher plant survival and prosperity on land. Construction of a phylogeny tree based on the NAC family from green algae to higher plants can help to better understand the origin and expansion of NACs from their aquatic to terrestrial evolution (Mathew and Agarwal, 2018). Higher plant-specific NACs are potentially from the ancestral WRKY protein, concomitant with the transition from an aquatic to a terrestrial environment through two landmark expansions—the evolution of bryophytes from streptophytes, followed by the development of flowering angiosperm plants from vascular plants—which highlight the vital role of NACs in plant evolution (Yamasaki et al., 2013; Maugarny-Calès et al., 2016; Mathew and Agarwal, 2018).

The subfamily of *FaNAC035* (Moyano et al., 2018; Martín-Pizarro et al., 2021), a key regulator of strawberry fruit development and ripening, is a typical case. Phylogenetic analysis showed that this subfamily also followed the evolutionary relationships from aquatic to terrestrial, and some conserved motifs were discovered to be lost

10.3389/fpls.2023.1095967

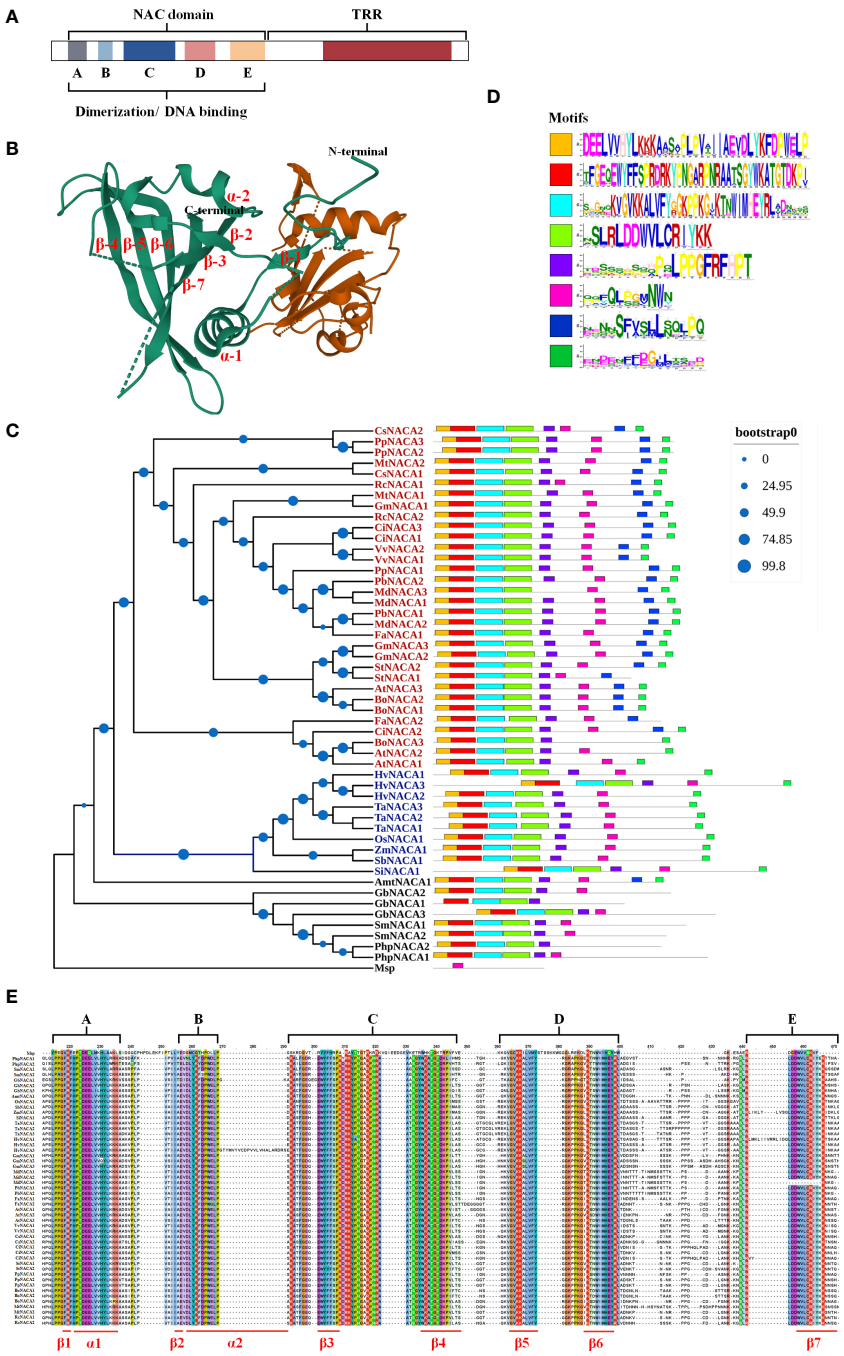

FIGURE 1
Basic traits of NAC (NAM, ATAF, and CUC) transcription factors (TFs). **(A)** Structure and function of NACs. **(B)** Three-dimensional structure of the Arabidopsis AtNAC019 protein homodimer. The AtNAC019 NAC domain crystal form IV is from the PDB database (PDB DOI: 10.2210/pdb4DUL/pdb). **(C)** Phylogenetic relationship of the NAC TFs. The homologous proteins of the strawberry NAC TF FaNACA2 (FaNAC035) (Martín-Pizarro et al., 2021) were found and verified in 24 species using BLAST and CDD tools, and a phylogenetic tree was constructed with reference to the evolutionary relationship of the NAC TF family in plants. The multiple sequence alignment, sequence pruning, model search, and phylogenetic tree construction were performed in Phylosuite_v1.2.2. The phylogenetic tree was obtained by applying the maximum likelihood method to a matrix of pairwise distances estimated using a JTT (Jones–Taylor–Thornton) model (bootstrap: ultrafast; no. of bootstraps: 10,000). *Blue letters* represent monocots and *red letters* represent dicots. *Msp*, *Mougeotia* sp.; *Php*, *Physcomitrella patens*; *Sm*, *Selaginella moellendorffii*; *Gb*, *Ginkgo biloba*; *Amt*, *Amborella trichopoda*; *Si*, *Setaria italica*; *Sb*, *Sorghum bicolor*; *Zm*, *Zea mays*; *Os*, *Oryza sativa*; *Ta*, *Triticum aestivum*; *Hv*, *Hordeum vulgare*; *At*, *Arabidopsis thaliana*; *Bo*, *Brassica oleracea*; *Ci*, *Citrus sinensis*; *Fa*, *Fragraria ananassa*; *St*, *Solanum tuberosum*; *Gm*, *Glycine max*; *MD*, *Malus domestica*; *Pb*, *Pyrus bretschneideri*; *Pp*, *Prunus persica*; *Vv*, *Vitis vinifera*; *Rc*, *Ricinus communis*; *Mt*, *Medicago truncatula*; *Cs*, *Cucumis sativus*. **(D)** The conserved motifs of all 51 sequences were queried online through the MEME website (https://meme-suite.org/meme/tools/meme). *Motif1* corresponds to the A and B subdomains in the NAC domain, *Motif2* contains the C subdomain, *Motif3* corresponds to the D subdomain, *Motif4* corresponds to the E domain, and *Motif5–Motif8* are the conserved motifs in the transcription regulatory region (TRR). **(E)** NAC domain consisting of five subdomains: three highly conserved (A, C, and D) and two diverse (B and E) subdomains.

when comparing ferns, gymnosperms, and angiosperms (Figures 1C–E). We supposed that four subdomains (motif1–motif4) appeared after the first evolutionary expansion; subsequently, the angiosperm NACs evolved to the conserved motif7 and motif8, with motif7 being conserved only in dicotyledons rather than in monocotyledons (Figures 1C, D). The number of genes also varies, with monocotyledons having only one member while dicotyledons have more than two members (Figure 1C). In brief, the gene numbers and conserved motifs are species-specific and have developed diverse functions in adapting to developmental and stress processes.

Based on wide phylogenetic analysis, the NAC family of green plants is divided into six major groups (groups I–VI) as follows: 1) the basal group I functions in water conduction and cell support; 2) the developmental group II, which includes *CUC1–CUC3* (*AtNAC054*, *AtNAC031*, and *AtNAC098*), function in shoot apical meristem (SAM) formation and cotyledon separation, associated with the ETH–auxin pathways; 3) group III has the transmembrane motif (TMM); 4) group IV functions in the timing control of several developmental processes, including flower evolution, such as *AtNAC034* for flowering time, *AtNAC009* for cell division, and *AtNAC042* for longevity; 5) group V regulates the stress responses; and 6) group VI has neo- and/or sub-functionalization in different plant species. In summary, NACs regulate many developmental and stress processes through phytohormones (Ooka et al., 2003; Ernst et al., 2004).

NAC hierarchical regulatory traits

Higher plants have developed multiple regulatory mechanisms to maintain a balance between the expression and turnover of NACs partly through NAC regulatory loops (Mathew and Agarwal, 2018). In the past years, significant progress has been made toward understanding the regulatory mechanisms of NACs in controlling their homeostasis at the DNA, RNA, and protein levels, including 1) transcriptional regulation by their upstream TFs to form messenger RNA precursors (pre-mRNAs) in the nucleus; 2) post-transcriptional regulation at the nucleotide level, including microRNA (miRNA)-mediated inhibition and/or splicing of pre-mRNAs and their transport from the synthesis site to the action sites; 3) post-translational regulation at the protein level, including the transfer of the cleave-mediated membrane-tethered proteins to the nucleus, which are associated with specific active groups, protein degradation by proteasome machinery, oligomerization, and protein interactions (Mathew and Agarwal, 2018).

Regarding the primary function of NACs in secondary cell wall thickening and xylem vessel element formation, the *NAC secondary wall thickening promoting factor2, NST2/AtNAC066*, and *ORE1* (*ORESARA1/AtNAC092*) are regulated by WRKY12 and EIN2 (ethylene-insensitive 2) (Wild and Krutzfeldt, 2010; Kim et al., 2014), while the secondary wall-associated NAC domain protein1, SND1/NAC012, appears autoregulatory in nature (Wang et al., 2011). In sweet potato (*Ipomoea batatas*), the homeostasis of *IbNAC1* is regulated by the competitive binding of two upstream TFs (the activator bHLH3 and the repressor bHLH4) to its promoter (Chen et al., 2016). Seven vascular-related NAC domains (AtVNDs) can induce the expression of *AtVND7* by binding to its promoter (Endo et al., 2015; Nakano et al., 2015).

NAC TFs have also evolved multiple post-transcriptional regulatory processes, including miRNA-mediated cleavage, alternative splicing, and *trans*-splicing, in regulating the transcripts of NAC functional genes, such as the microRNA164 (miR164)-mediated and organ boundary formation regulatory genes (e.g., *CUC1/AtNAC054, GOBLET/GOB*, and *SlNAM2*) (Samad et al., 2017), the petal size regulatory genes (e.g., *RhNAC100* in *Rosa hybrid*) (Pei et al., 2013), and the cell wall thickening genes (e.g., *PtrWND1B-s* and *PtrWND1B-l* in *Populus trichocarpa*) produced by intron-mediated alternative splicing of the wood-associated NAC TF1B (PtrWND1B) (Zhao et al., 2014).

Nuclear localization is a prerequisite for a protein to function as a TF; thus, NACs contain a bipartite NLS within the D subdomain. However, the Arabidopsis NTL4/AtNAC053 protein accumulates early in the ER, and its C-terminal portion may move to the nucleus after its cleavage from the ER (Kim et al., 2007), as confirmed by several similar reports on NACs targeted to the nucleus by homomerization/heteromerization (Seo et al., 2010; Ng et al., 2013; Lee et al., 2014; Mathew et al., 2016). These findings uncover an important regulatory mechanism of the activity of NACs from early PM/ER localization to nucleus translocation.

In addition, NACs participate in post-translational modifications through reversible acetylation and phosphorylation, protein–protein interactions, and ubiquitin-mediated proteolysis. For instance, the phosphorylation of the membrane-associated NTL6/AtNAC062 by SnRK2.8 (SNF1-related protein kinase) promotes the entry of NTL6 into the nucleus during drought conditions (Robertson, 2004; Kim et al., 2012; Guan et al., 2014). NAC proteins can form both homo- and heterodimers through the conserved β-sheet domain, which is influenced by the TRR/TAR (Zhu et al., 2012). The rice OsNAC29 and OsNAC31 independently interact with OsSLR1 (SLENDER RICE1), a repressor for OsMYB61, which promotes cellulose synthesis by increasing the transcripts of a cellulose synthase gene (Huang et al., 2015). The involvement of NAC1 in auxin signaling is ubiquitinated by SlNAT5, an E3 ubiquitin ligase, which leads to the degradation of NAC1 and the downregulation of the auxin signal in plant cells (Xie et al., 2002; Guo et al., 2015). In summary, NAC TFs have shown varied regulatory mechanisms at the transcriptional, post-transcriptional, translational, and post-translational levels.

NAC transcription factors regulate the transition from vegetative to reproductive growth and flower formation essential to crop yield

Flowering is a critical agricultural trait associated with fruit yield. Flower initiation and fusion congenitally occur within a single whorl of floral organs to form a connation or union, such as the union of sepals to form a calyx tube, the adnation of stamens and petals to form a corolla tube, and the connation of carpels to form the gynoecium (Ma et al., 2017; Phillips et al., 2020). In most angiosperms, the fusion of various floral organs to form diverse flowers and inflorescences

with different floral colors, sizes, shapes, scents, inflorescences, and flowering times that are linked to sepals/petals, stamens, and carpels —from free to fused structures, in addition to a spiral arrangement from the whorled corolla and androecium to a single flower or various inflorescences—is closely related to NAM/CUC3-mediated boundary formation through meristematic development and differentiation (Ma et al., 2017; Phillips et al., 2020).

In the primordium, the formation of distinct boundaries is a critical step to floral organ initiation. The meristematic activity between organs allows floral fusion, which is associated with the early identified genes that are key to boundary formation, separate lateral organ development, and floral fusion, such as the Arabidopsis *LOB* (*lateral organ boundaries*) and *Petunia hybrida NAM/CUC3* (*no apical meristem*), during the transition from vegetative to reproductive growth (Souer et al., 1996; Husbands et al., 2007). Indeed, variations in the expression of the *NAM/CUC3* genes correlate with the variations in fusion within floral organs due to *nam* mutants failing to initiate a SAM (Zhong et al., 2016). Similarly, the Arabidopsis genes *CUC1/CUC2* and *ATAF1/ATAF2* possess a mutant phenotype similar to the *nam* mutant. These mutations are associated with failure to initiate the SAM and defective to boundary formation, leading to the fusion of cotyledons and floral whorls (Aida et al., 1997). A distinct boundary is required for proper leaflet formation, as evidenced by a tomato *gob* (*goblet*) mutant similar to the *nam* (Berger et al., 2009). Taken together, the tomato *gob* mutant is phenotypically similar to the *nam/cuc3* mutants in both *Arabidopsis thaliana* and *P. hybrida*, in terms of failing to initiate the SAM and the presence of fused cotyledons and floral organs, suggesting a model to meet the requirements of higher *NAM/CUC3* expression to increase the separation of the structures and lower expression to promote organ fusion. To a large extent, the NAM/CUC3 family promotes the evolution of floral fusion phenotypes by controlling organ boundary formation (Phillips et al., 2020).

Interestingly, phylogenetic analyses based on comparative genomics across algae and higher plants showed that the NAC family might date back to streptophyte green algae (Maugarny-Calès et al., 2016). From the view of evolution, after the transition of NACs from algae to land organisms, they subsequently expanded throughout land plants, from 20–30 proteins in mosses and lycophytes to over 100 copies in various angiosperm species (Zhu et al., 2012; Pereira-Santana et al., 2015; Maugarny-Calès et al., 2016), among which NAM/CUC3 became a distinct subfamily while the NAM clade (NAM/CUC1/CUC2) was clustered as a sister group of the CUC3 proteins throughout angiosperms (Maugarny et al., 2016). The function of NACs in the formation of vascular tissues promotes flower diversification and makes plants more adaptable to various land environments through seed propagation, which is a landmark event in the evolution of land plants (Maugarny-Calès et al., 2016). In summary, the NAC family plays a pivotal role in the formation of the SAM, which is fundamental to flowering and post-flowering phylogenetic processes, including organ boundary formation, secondary wall thickening, floral development, flowering, embryo and seed development, and fruit development and ripening.

Indeed, the identification of the *nam* mutant and the evolution of the later redundant *CUC1/AtNAC054, CUC2/AtNAC098*, and *CUC3/AtNAC031* uncovered the specialization and diversification of NACs in the formation of embryos and flowers (Souer et al., 1996; Hibara et al., 2006; Raman et al., 2008). At the molecular level, CUC1 directly regulates the expression of *LSH3/LSH4* (*light-dependent short hypocotyls 3/4*) in shoot organ boundary cells, which are associated with the transition from shoot vegetative growth to flower reproductive growth (Takeda et al., 2011). It was further found that SlNAM2 participates in establishing the tomato flower whorl and sepal boundaries (Hendelman et al., 2013). In addition, CUC1–CUC3, NAM, and NH16 can suppress vegetable growth and, thus, promote establishment of the boundaries of the floral organs, such as petals, sepals, and stamens, of plants (Vroemen et al., 2003; Zhong et al., 2016). Therefore, NACs are important in the formation and the maintenance of the different meristem tissues for organ boundary formation and are essential to the transition from vegetative to reproductive growth, which is necessary for embryogenesis, seed formation, and fruit development.

Owing to the vital role of NACs in cell wall biosynthesis in higher plants, it is reasonable that some of the NAC TFs, such as NST1/AtNAC043, NST2/AtNAC066, and NST3/AtNAC012 (NAC secondary wall thickening promoting factors 1–3), positively regulate secondary wall thickening and, thus, function in *Arabidopsis silique* formation and anther dehiscence, which are also negatively regulated by AtNAC053, an anther indehiscence factor (Mitsuda et al., 2005; Shih et al., 2014). In addition, NARS1/NARS2 (NAC-regulated seed morphology1/2), also known as NAC2 and NAM, redundantly mediated Arabidopsis seed embryogenesis by regulating the development and degeneration of ovule integuments (Kunieda et al., 2008). Moreover, the three CUC proteins (CUC1–CUC3) are involved in the initiation and separation of ovules during Arabidopsis reproductive development. CUC1 and CUC2 determine the number of ovules, while CUC2 and CUC3 control organ separation (Gonçalves et al., 2015). Interestingly, NAM-B1 participates in the remobilization of nutrients from the vegetative tissue to grain formation in wheat (Waters et al., 2009). In addition, three rice NAC TFs, namely, OsNAC020, OsNAC026, and OsNAC023, were found to be strongly associated with seed size and grain yield (Mathew et al., 2016), as well as another NAC TF (RhNAC100) in ETH-promoted rose flower opening (Pei et al., 2013). Interestingly, a recent study has found loss of function in tomato OPEN STOMATA 1 (SlOST1), a protein kinase essential for ABA signaling and abiotic stress response. slost1 mutants also exhibited a late flowering phenotype under normal and drought stress conditions through SlOST1 interacting with and phosphorylating the NAC-type TF, VASCULAR PLANT ONE-ZINC FINGER 1 (SlVOZ1), providing insights into a novel strategy to balance drought stress response and flowering (Chong et al., 2022).

It is worth noting that, in the long-day (LD) model plant Arabidopsis, about 180 regulators have been confirmed to be involved in the control of flowering time, among which CONSTANS (CO) is a central activator, FLOWERING LOCUS C (FLC) is a central suppressor, and SQUAMOSA PROMOTER BINDING LIKE (SPL) is a positive TF, together with their downstream floral TFs, including FT (FLOWERING LOCUS T), SOC1 (SUPPRESSOR OF OVEREXPRESSION OF CO1), and AGL24 (AGAMOUS-like24) that activate the meristemic genes LFY (LEAFY), AP1 (APETALA1), SEP3 (SEPALLATA3), and FUL (FRUITFULL) (Blüemel et al., 2015). A more recent study has reported that strawberries (*Fragaria* sp.), a high-value horticultural

crop, initiate flowering during the short photoperiod and low temperatures in the autumn (Liang et al., 2022). With the onset of inflorescence, the SAM may undergo a leaf-to-flower primordium transformation through floral induction, during which SOC1, TFL1, AP1, and CUC2 are vital for floral initiation (Liang et al., 2022). The diversity of NAC proteins is critical for flower formation and fruit development in higher plants. Although much progress has been made toward understanding the molecular mechanisms underlying the formation of a terminal flower through a series of important genes (such as *LFY* and *AP1*) to control the transition from SAM to flower formation (Figure 2) (Ma et al., 2017), how NACs regulate the expression of these genes is poorly understood and needs to be urgently explored in the future.

NAC transcription factors regulate fruit ripening fundamental to quality formation

Fruits include seeds with flower accessories, and fruit ripening is essential to human food, nutrition, and health. Ripening is regulated by plant hormones, including ETH in climacteric fruits and ABA in non-climacteric fruits (Bai et al., 2021; Kou et al., 2021; Li S. et al., 2021). Using the model plant for climacteric fruits, tomato, much progress has been made toward understanding the molecular mechanisms of NACs in fruit ripening through the biosynthesis and activity of ETH and ABA (Bai et al., 2021; Kou et al., 2021; Li S. et al., 2021). As a precursor of ETH biosynthesis, methionine (Met) is transformed into *S*-adenosyl methionine (SAMe) by SAMS (SAMe synthetase), and then SAMe is converted to ETH by 1-aminocyclopropane-1-carboxylic acid synthase (ACS) and 1-aminocylopropane-1-carboxylic acid oxidase (ACO). The ripening signal is relayed through a series of ETH perception and signaling transduction events involving ETH receptors (ETRs), ethylene-insensitive 2 (EIN2), EIN3/EIN3-like, and ETH response factors (ERFs). Similarly, 9-*cis*-epoxycarotenoid dioxygenase (NCED) and ABA 8′-hydroxylase (CYP707A) are key enzymes in ABA homeostasis. The ABA perception and signaling components include PYR/PYL/RCAR receptors, type 2C protein phosphatase (PP2Cs), SNF1-related kinase subfamily 2 (SnRK2), and downstream TFs, such as the ABA-responsive element binding proteins (AREBs) and ABA-responsive element binding factors (ABFs) (Bai et al., 2021; Kou et al., 2021; Li S. et al., 2021).

Tomato is a model for studying the roles of NACs in fruit ripening

The first landmark finding for NAC function in ripening was from the non-ripening mutant (*nor*) of tomato (*Solanum lycopersicum*) fruit, known as *NAC-SlNOR*, which plays a central role in its ripening (Giovannoni, 2004). However, recent studies have considered that *nor* is a gain-of-function, rather than a loss-of-function, mutant of *SlNOR*, and SlNOR positively regulates fruit ripening by binding to the promoter of *SlACS2* as an activator (Wang et al., 2019; Gao et al., 2020). In addition, *SlNOR* is a direct target gene of SlRIN/SlMADS-RIN (RIPENING INHIBITOR) and SlAREB1 (a TF in ABA signaling). SlRIN and SlAREB1 bind to the *SlNOR* promoter to activate its expression and to promote the expression of *SlACS2/SlACS4* and *SlACO1* for ETH burst, suggesting that the *SlAREB1*-mediated transcriptional regulation of *SlNOR* is involved in the crosstalk between ETH and ABA in ripening (Fujisawa et al., 2013; Mou et al., 2018).

Later, many NAC proteins of *SlNOR* homologs were identified in ripening, such as SlNOR-like1 (SlNAC3/SlNAC4/SlNAC48) that favors ripening by binding to the promoter of multiple target genes involved in both ETH and ABA biosynthesis and signaling, including

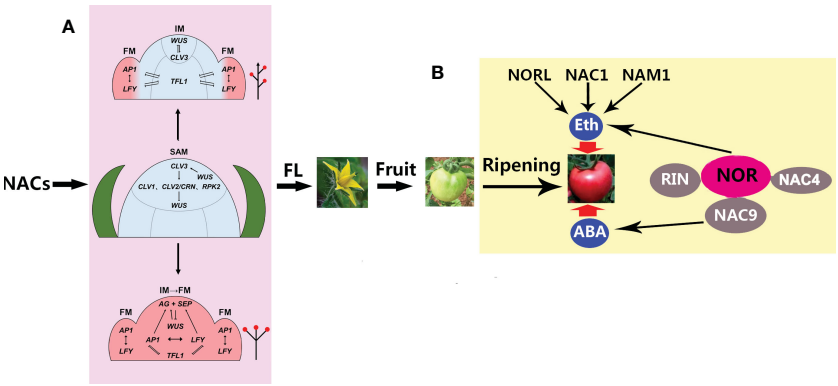

FIGURE 2
A model for the roles of NACs (NAM, ATAF, and CUC) in flower formation and ripening. **(A)** NACs control the transition of the shoot apical meristem (SAM) to the floral meristem (FM), including indeterminate inflorescence (*up arrow*) and determinate inflorescence (*down arrow*) (Ma et al., 2017). By controlling the relative expression levels of *TFL1* (TERMINAL FLOWER 1) and the FM identity genes, *AP1* and *LFY* (APETALA1 and LEAFY, respectively), in the distal inflorescence meristem (IM), the IM can remain meristematic and generate different numbers of FMs before converting to a terminal flower. A higher relative expression ratio prevents the expression of the FM identity genes *LFY* and *AP1* in the distal IM during the onset of indeterminate inflorescence. However, during determinate inflorescence development, the expression of the FM identity genes in the distal IM can evoke the expression of the C class AGAMOUS (*AG*) and E class SEPALLATA (*SEP*) genes, thus determining the floral fate of the apical meristem. *FL*, flowering. **(B)** NACs control tomato fruit ripening through ethylene (ETH) and abscisic acid (ABA), which are involved in NOR, NORL, RIN, NAM1, and NAC1/4/9. NOR, RIN, and NAC4/9 constitute an interaction complex in which NOR, together with NORL, NAC1, and NAM1, regulates ripening through ETH, while NAC9 regulates ripening through ABA. NOR, non-ripening mutant; NORL, NOR-like; NAM, no apical meristem; RIN ripening inhibitor.

SlACS2, *SlACS4*, *SlACS8*, *SlACO1*, *SlACO6*, *SlCYP707A1*, *SAPK3*, and *SlPYL9*. In particular, SlNAC9 interacts with SlPYL9 and SlAREB1 (Kou et al., 2016; Gao et al., 2018; Yang et al., 2021). In contrast, SlNAC1 (SlNAC033) can directly bind to the promoter regions of *SlACS2* and *SlACO1* and has multiple effects on tomato fruit ripening by inhibiting the biosynthesis of ETH while enhancing the expression of *SlNCED1* and *SlNCED2* for the accumulation of ABA (Ma et al., 2014; Meng et al., 2016). It has been reported that *SlNAC4* may be upstream of ETH biosynthesis by regulating the activities of SlRIN and SlNOR (Zhu M. et al., 2014). On the other hand, the expression of *SlNAC7* was induced by ETH and ABA during color breaking, and, together with *SlNAC6*, it induced the expression of *SlACS2*, *SlACS4*, *SlACO1*, *SlNCED1*, *SlNCED2*, *SlABA2*, and aldehyde oxidase (*SlAAO1/2*) (Zhu M. K. et al., 2014; Jian et al., 2021). Similarly, a recent report has shown that the new NAC, SlNAM1, is a positive regulator of ripening initiation by promoting the expression of *SlACS2* and *SlACS4* (Gao et al., 2021). In addition, an *Arabidopsis* NAC, JUNGBRUNNEN1 (*AtJUB1*), was overexpressed in tomatoes and resulted in dwarf plants and delayed ripening fruits by directly binding to a line of gene promoters of *GA3ox1* (*GA 3-oxidase 1*) and *DWF4* (*DWARF4*), which are responsible for the biosynthesis of both gibberellin (GA) and brassinosteroid (BR), and indirectly inhibited the expression of *ACS*, *ACO*, *SlERF.H15*, and *SlRIN* (Shahnejat-Bushehri et al., 2017).

Notably, a recent study has found that the NAC-NOR target gene encoding lipoxygenase (SlLOXC) is involved in fatty acid-derived volatile synthesis by epigenetics. NAC-NOR activated the expression of *SlDML2* (DNA demethylase 2) by directly binding to its promoter both *in vitro* and *in vivo* (Gao et al., 2022). On the other hand, the reduced NAC-NOR expression in the *sldml2* mutant was accompanied by the hypermethylation of its promoter, demonstrating a relationship between SlDML2-mediated DNA demethylation and NAC-NOR during tomato fruit ripening (Gao et al., 2022).

In summary, a series of NAC TFs constitute a complex regulation network in tomato fruit ripening, mainly through ETH and ABA homeostasis and signaling levels, confirming that the NAC family plays a central role in fruit ripening.

NACs play an important role in the ripening of many climacteric fruits

In addition to tomatoes, the NAC family also plays vital roles in many climacteric fruits. For instance, at least 13 NAC genes have been found during apple (*Malus domestica*) fruit ripening (Wang et al., 2011; Zhang et al., 2018; Migicovsky et al., 2021). In banana fruits (*Musa acuminata*), a total of six NACs (*MaNAC1–MaNAC6*) were associated with fruit ripening (Shan et al., 2012; Li et al., 2020; Shan et al., 2020; Wei et al., 2021). In pear fruits (*Pyrus pyrifolia*), 185 NACs were found in the genome, among which 1) *PpNAC56* may be related to fruit ripening (Ahmad et al., 2018); 2) *PpNAP1*, *PpNAP4*, and *PpNAP6* may regulate ripening through ETH and ABA; 3) *PpNOR* controls fruit ripening in a conservative manner, similar to *SlNOR*; and 4) PpNAC.A59 directly promotes *PpERF.A16* by binding to its promoter and facilitating the expression of *PpACS1* and *PpACO1*, confirming that it plays an important role in fruit ripening through ETH biosynthesis and signaling (Li et al., 2016; Ahmad et al., 2018; Guo et al., 2021; Tan et al., 2021).

Moreover, during ripening in papaya fruits (*Carica papaya* L.), CpEIN3a could interact with CpNAC2 to activate the biosynthesis of carotenoids, while CpNAC3 could interact with CpMADS4 to activate the expression of *pERF9* and *CpEIL5* (Fu et al., 2017; Fu C. C. et al., 2021). In apricot (*Prunus sibirica*) fruits, 102 NACs were identified in the genome, among which *PsNAC6/13/46/51/41/67/37/59* were highly expressed during the ripening stage (Xu et al., 2021). In kiwifruit (*Actinidia deliciosa*/*Actinidia chinensis*), *AcNAC2–AcNAC4* are positive regulators of ripening through ETH production, while *AdNAC2*/*AdNAC3* are promoted by methyl jasmonate (MeJA), suggesting a crosstalk between MeJA and ETH *via* AdNAC2 and AdNAC3 (Wang et al., 2020). In addition, the positive regulators of *AdNAC6* and *AdNAC7* in ripening are degraded by miR164, while this degradation is inhibited by ETH. Interestingly, the miR164–NAC pathway is conserved in both climacteric and non-climacteric fruits, including apple, pear, banana, peach, strawberry, citrus, and grape (Wang et al., 2020; Wu et al., 2020; Nieuwenhuizen et al., 2021).

Notably, a recent study has found that the NAC TF NOR is a master regulator of climacteric fruit ripening. Melon (*Cucumis melo*) (Rios et al., 2017) has climacteric and non-climacteric fruit ripening varieties, such as the climacteric and non-climacteric haplotypes CmNAC-NOR^{S,N} and CmNAC-NOR^{A,S}, respectively. A natural mutation in the transcriptional activation domain of CmNAC-NOR^{S,N} contributed to climacteric melon fruit ripening by directly activating its carotenoid, ETH, and ABA biosynthesis genes. In addition, *CmNAC-NOR* knockout in the climacteric-type melon cultivar "BYJH" completely inhibited fruit ripening, while ripening was delayed by 5–8 days in heterozygous *cmnac-nor* mutant fruits. Finally, *CmNAC-NOR* mediated the transcription of the "*CmNAC-NOR–CmNAC73–CmCWINV2*" module to enhance flesh sweetness. Altogether, the transcriptional activation activity of the climacteric haplotype, CmNAC-NOR^{S,N}, on these target genes was significantly higher than that of the non-climacteric haplotype, CmNAC-NOR^{A,S}, providing insights into the molecular mechanism of climacteric and non-climacteric fruit ripening in melon (Zhang et al., 2022). In addition, single-cytosine methylome analyses of a DNA demethylase ROS1 (*MELO3C024516*)-knockout mutant revealed changes in DNA methylation in the promoter regions of the key ripening genes, such as *ACS1*, *ETR1*, and *ACO1*, suggesting the importance of DNA demethylation in melon fruit ripening (Giordano et al., 2022). Thus, the NAC family participates in climacteric fruit ripening at multiple regulation levels.

NACs also play a role in the ripening of many non-climacteric fruits

Strawberry (*Fragaria ananassa*) is a non-climacteric model plant, and 112 *NAC* genes have been found in the genome, including six NACs, *FaNAC006/021/022/035/042/092*, related to fruit development and ripening. *FaNAC035*/*FaRIF* regulates ripening *via* ABA biosynthesis and signaling, demonstrating the presence of not only a *FaNAC035*-mediated crosstalk among various plant hormones but also a feedback mechanism between the ABA level and its signaling (Moyano et al., 2018; Martín-Pizarro et al., 2021). In addition,

FcNAC1 could participate in ripening regulation by responding to upstream hormone signals, such as those of ABA and auxin (Carrasco-Orellana et al., 2018).

In citrus (*Citrus reticulata*) fruits, an ABA-deficient mutant resulted from the abnormally high expression of *CrNAC036*, which bound to the C*rNCED5* promoter to inhibit its expression. On the other hand, CrMYB68 interacted with CrNAC036 to further inhibit *CrNCED5* expression, finally synergistically retarding fruit ripening (Zhu et al., 2020). Although CitNAC62 is located in the cytoplasm, the nucleus-localized CitWRKY1 may interact with CitNAC62 to promote its movement (Li et al., 2017). In jujube (*Ziziphus jujuba* Mill.) fruits, the NAC *LOC107435239* positively regulated the pericarp lignin accumulation during winter jujube fruit coloration by promoting the transcription of *F5H* (*ferulate 5-hydroxylase*), and *ZjNAC13/14/38/41* showed high expression levels during ripening (Li M. et al., 2021; Zhang Q. et al., 2021). In grape (*Vitis vinifera*) fruits, VvNAC26 interacted with VvMADS9 to induce the gene expression related to ETH and ABA biosynthesis, resulting in early fruit ripening, suggesting that *VvNAC26* promotes ripening by activating the levels of ETH and ABA (Zhang S. et al., 2021). In litchi (*Litchi chinensis*) fruits, *LcNAC13* and *LcR1MYB1* may antagonistically regulate the accumulation of anthocyanin during ripening (Jiang et al., 2019). In watermelon (*Citrullus lanatus*) fruits, *ClNAC68* positively regulated sucrose accumulation during ripening by directly binding to the promoters of both the *invertase* (*ClINV*) and *IAA-amino synthetase* (*ClGH3.6*) to inhibit their expression (Lv et al., 2016; Wang et al., 2021).

In summary, NAC TFs not only directly target genes encoding enzymes related to ripening parameters, softening, sugar, coloring, and aroma but also indirectly affect fruit ripening by regulating the homeostasis of ABA and ETH through conserved and specific mechanisms, which are closely related to fruit quality. ETH-controlled climacteric fruit ripening (such as in tomato) *via* NAC TFs is directly targeted to the ETH biosynthesis-related genes including *ACO* and *ACS*, while also involved in the interaction between ABA and ETH, mostly through ABA to activate *NOR* transcription and ETH synthesis. With regard to non-climacteric fruit ripening, a homolog of the tomato *NOR* in strawberry, the NAC TF FaNAC035/FaRIF, can promote ABA biosynthesis *via FaNCED3*. Thus, NAC TFs play a core role in the two ripening types through the interplay of ETH and ABA.

Conclusion

The plant-specific NAC TFs not only control the aquatic-to-terrestrial evolution through vasculature formation but also govern the transition from vegetative to reproductive growth through directing SAM differentiation. In addition, they constitute a complex regulatory network that regulates fruit ripening *via* ABA and ETH, improving our understanding of the molecular mechanisms of NACs in fruit ripening (Figure 2). Nevertheless, the mechanisms through which NACs regulate the inflorescence formation-related genes are largely unknown. Given that NAC TFs belong to a large family, more focus should be given to the analysis of their redundancy in order to identify pivotal players in the regulation of flowering and ripening. In addition, more attention should be paid to the regulatory network of NACs regulating the ripening of non-climacteric fruits. Finally, NACs are potentially important manipulation targets for improving fruit quantity and quality in the future, likely through water control.

Author contributions

BH planned the outline of the review. BH and JL collected the available literature and performed re-analyses. BH and JL completed the draft of the paper. YQ and CL compiled and corrected the references. All authors contributed to the article and approved the submitted version.

Funding

The authors gratefully acknowledge the support of the Beijing Natural Science Foundation (6214042) and the National Natural Science Foundation of China (32101769).

Conflict of interest

The authors declare that the research was conducted in the absence of any commercial or financial relationships that could be construed as a potential conflict of interest.

Publisher's note

References

Ahmad, M., Yan, X. H., Li, J. Z., Yang, Q. S., Jamil, W., Teng, Y. W., et al. (2018). Genome wide identification and predicted functional analyses of NAC transcription factors in Asian pears. *BMC Plant Biol.* 18, 214. doi: 10.1186/s12870-018-1427-x

Aida, M., Ishida, T., Fukaki, H., Fujisawa, H., and Tasaka, M. (1997). Genes involved in organ separation in arabidopsis: An analysis of the *cup-shaped cotyledon* mutant. *Plant Cell* 9, 841–857. doi: 10.1105/tpc.9.6.841

Bai, Q., Huang, Y., and Shen, Y. (2021). The physiological and molecular mechanism of abscisic acid in regulation of fleshy fruit ripening. *Front. Plant Sci.* 11. doi: 10.3389/fpls.2020.619953

Berger, Y., Harpaz-Saad, S., Brand, A., Melnik, H., Sirding, N., Alvarez, J. P., et al. (2009). The NAC-domain transcription factor GOBLET specifes leaflet boundaries in compound tomato leaves. *Development* 136, 823–832. doi: 10.1242/dev.031625

Bhattacharjee, P., Das, R., Mandal, A., and Kundu, P. (2017). Functional characterization of tomato membrane-bound NAC transcription factors. *Plant Mol. Biol.* 93, 511–532. doi: 10.1007/s11103-016-0579-z

Blüemel, M., Dally, N., and Jung, C. (2015). Flowering time regulation in crops-what did we learn from arabidopsis? *Curr. Opin. Biotechnol.* 32, 121–129. doi: 10.1016/j.copbio.2014.11.023

Carrasco-Orellana, C., Stappung, Y., Mendez-Yanez, A., Allan, A. C., Espley, R. V., Plunkett, B. J., et al. (2018). Characterization of a ripening-related transcription factor FcNAC1 from fragaria chiloensis fruit. *Sci. Rep.* 8, 10524. doi: 10.1038/s41598-018-28226-y

Chen, S. P., Kuo, C. H., Lu, H. H., Lo, H. S., and Yeh, K. W. (2016). The sweet potato NAC-domain transcription factor IbNAC1 is dynamically coordinated by the activator IbbHLH3 and the repressor IbbHLH4 to reprogram the defense mechanism against wounding. *PloS Genet.* 12, e1006397. doi: 10.1371/journal.pgen.1006397

Chong, L., Xu, R., Huang, P. C., Guo, P. C., Zhu, M. K., Du, H., et al. (2022). The tomato OST1-VOZ1 module regulates drought-mediated flowering. *Plant Cell* 34, 2001–2018. doi: 10.1093/plcell/koac026

Endo, H., Yamaguchi, M., Tamura, T., Nakano, Y., Nishikubo, N., Yoneda, A., et al. (2015). Multiple classes of transcription factors regulate the expression of *VASCULAR-RELATED NAC-DOMAIN7*, a master switch of xylem vessel differentiation. *Plant Cell Physiol.* 56, 242–254. doi: 10.1093/pcp/pcu134

Ernst, H. A., Olsen, A. N., Larsen, S., and Lo Leggio, L. (2004). Structure of the conserved domain of ANAC, a member of the NAC family of transcription factors. *EMBO Rep.* 5, 297–303. doi: 10.1038/sj.embor.7400093

Forlani, S., Mizzotti, C., and Masiero, S. (2021). The NAC side of the fruit: Tuning of fruit development and maturation. *BMC Plant Biol.* 21, 238. doi: 10.1186/s12870-021-03029-y

Fu, C. C., Chen, H. J., Gao, H. Y., Wang, S. L., Wang, N., Jin, J. C., et al. (2021). Papaya CpMADS4 and CpNAC3 co-operatively regulate ethylene signal genes *CpERF9* and *CpEIL5* during fruit ripening. *Postharvest. Biol. Technol.* 175, 111485. doi: 10.1016/j.postharvbio.2021.111485

Fu, C. C., Han, Y. C., Kuang, J. F., Chen, J. Y., and Lu, W. J. (2017). Papaya CpEIN3a and CpNAC2 co-operatively regulate carotenoid biosynthesis related genes *CpPDS2/4*, *CpLCY-e* and *CpCHY-b* during fruit ripening. *Plant Cell Physiol.* 58, 2155–2165. doi: 10.1093/pcp/pcx149

Fu, B. L., Wang, W. Q., Liu, X. F., Duan, X. W., Allan, A. C., and Grierson, D. (2021). An ethylene-hypersensitive methionine sulfoxide reductase regulated by NAC transcription factors increases methionine pool size and ethylene production during kiwifruit ripening. *New Phytol.* 2, 237–251. doi: 10.1111/nph.17560

Fujisawa, M., Nakano, T., Shima, Y., and Ito, Y. (2013). A large-scale identification of direct targets of the tomato MADS box transcription factor RIPENING INHIBITOR reveals the regulation of fruit ripening. *Plant Cell* 25, 371–386. doi: 10.1105/tpc.112.108118

Gao, Y., Fan, Z. Q., Zhang, Q., Li, H. L., Liu, G. S., Jing, Y., et al. (2021). A tomato NAC transcription factor, SlNAM1, positively regulates ethylene biosynthesis and the onset of tomato fruit ripening. *Plant J.* 108, 1317–1331. doi: 10.1111/tpj.15512

Gao, Y., Lin, Y., Xu, M., Bian, H., Zhang, C., Wang, J., et al. (2022). The role and interaction between transcription factor NAC-NOR and DNA demethylase SlDML2 in the biosynthesis of tomato fruit flavor volatiles. *New Phytol.* 235, 1913–1926. doi: 10.1111/nph.18301

Gao, Y., Wei, W., Fan, Z., Zhao, X., Zhang, Y., Jing, Y., et al. (2020). Re-evaluation of the nor mutation and the role of the NAC-NOR transcription factor in tomato fruit ripening. *J. Exp. Bot.* 71, 3560–3574. doi: 10.1093/jxb/eraa131

Gao, Y., Wei, W., Zhao, X., Tan, X., Fan, Z., Zhang, Y., et al. (2018). A NAC transcription factor, NOR-like1, is a new positive regulator of tomato fruit ripening. *Hortic. Res.* 5, 1–18. doi: 10.1038/s41438-018-0111-5

Ghissing, U., Kutty, N. N., Bimolata, W., Samanta, T., and Mitra, A. (2023). Comparative transcriptome analysis reveals an insight into the candidate genes involved in anthocyanin and scent volatiles biosynthesis in colour changing flowers of *Combretum indicum*. *Plant Biol. (Stuttg).* 25, 85–95. doi: 10.1111/plb.13481

Giordano, A., Santo Domingo, M., Quadrana, L., Pujol, M., Martin-Hernandez, A. M., and Garcia-Mas, J. (2022). CRISPR/Cas9 gene editing uncovers the roles of CONSTITUTIVE TRIPLE RESPONSE 1 and REPRESSOR OF SILENCING 1 in melon fruit ripening and epigenetic regulation. *J. Exp. Bot.* 73, 4022–4033. doi: 10.1093/jxb/erac148

Giovannoni, J. J. (2004). Genetic regulation of fruit development and ripening. *Plant Cell* 16, S170–S180. doi: 10.1105/tpc.019158

Gonçalves, B., Hasson, A., Belcram, K., Cortizo, M., Morin, H., Nikovics, K., et al. (2015). A conserved role for *CUP-SHAPED COTYLEDON* genes during ovule development. *Plant J.* 83, 732–742. doi: 10.1111/tpj.12923

Guan, Q., Yue, X., Zeng, H., and Zhu, J. (2014). The protein phosphatase RCF2 and its interacting partner NAC019 are critical for heat stress-responsive gene regulation and thermotolerance in *Arabidopsis*. *Plant Cell.* 26, 438–453. doi: 10.1105/tpc.113.118927

Guo, L., Li, Y., Zhang, C., Wang, Z., Carlson, J. E., Yin, W., et al. (2022). Integrated analysis of miRNAome transcriptome and degradome reveals miRNA-target modules governing floral florescence development and senescence across early- and late-flowering genotypes in tree peony. *Front. Plant Sci.* 13. doi: 10.3389/fpls.2022.1082415

Guo, Z. H., Zhang, Y. J., Yao, J. L., Xie, Z. H., Zhang, Y. Y., Zhang, S. L., et al. (2021). The NAM/ATAF1/2/CUC2 transcription factor PpNAC.A59 enhances *PpERF.A16* expression to promote ethylene biosynthesis during peach fruit ripening. *Hortic. Res.* 8, 209. doi: 10.1038/s41438-021-00644-6

Guo, W., Zhang, J., Zhang, N., Xin, M., Peng, H., Hu, Z., et al. (2015). The wheat NAC transcription factor TaNAC2L is regulated at the transcriptional and post-translational levels and promotes heat stress tolerance in transgenic *Arabidopsis*. *PloS One* 10, e0135667. doi: 10.1371/journal.pone.0135667

Hendelman, A., Stav, R., Zemach, H., and Arazi, T. (2013). The tomato NAC transcription factor *SlNAM2* is involved in flower-boundary morphogenesis. *J. Exp. Bot.* 64, 5497–5507. doi: 10.1093/jxb/ert324

Hibara, K., Karim, M. R., Takada, S., Taoka, K., Furutani, M., Aida, M., et al. (2006). *Arabidopsis CUP-SHAPED COTYLEDON3* regulates postembryonic shoot meristem and organ boundary formation. *Plant Cell* 18, 2946–2957. doi: 10.1105/tpc.106.045716

Huang, D., Wang, S., Zhang, B., Shang-Guan, K., Shi, Y., Zhang, D., et al. (2015). A gibberellin-mediated DELLA-NAC signaling cascade regulates cellulose synthesis in rice. *Plant Cell* 27, 1681–1696. doi: 10.1105/tpc.15.00015

Husbands, A., Bell, E. M., Shuai, B., Smith, H. M., and Springer, P. S. (2007). LATERAL ORGAN BOUNDARIES defines a new family of DNA-binding transcription factors and can interact with specific bHLH proteins. *Nucleic Acids Res.* 35, 6663–6671. doi: 10.1093/nar/gkm775

Jian, W., Zheng, Y., Yu, T., Cao, H., Chen, Y., Cui, Q., et al. (2021). SlNAC6, a NAC transcription factor, is involved in drought stress response and reproductive process in tomato. *J. Plant Physiol.* 264, 153483. doi: 10.1016/j.jplph.2021.153483

Jiang, G., Li, Z., Song, Y., Zhu, H., Lin, S., Huang, R., et al. (2019). LcNAC13 physically interacts with LcR1MYB1 to coregulate anthocyanin biosynthesis-related genes during litchi fruit ripening. *Biomolecules* 9, 135. doi: 10.3390/biom9040135

Kim, H. J., Hong, S. H., Kim, Y. W., Lee, I. H., Jun, J. H., Phee, B. K., et al. (2014). Gene regulatory cascade of senescence-associated NAC transcription factors activated by ETHYLENE-INSENSITIVE2-mediated leaf senescence signalling in *Arabidopsis*. *J. Exp. Bot.* 65, 4023–4036. doi: 10.1093/jxb/eru112

Kim, S. Y., Kim, S. G., Kim, Y. S., Seo, P. J., Bae, M., Yoon, H. K., et al. (2007). Exploring membrane-associated NAC transcription factors in *Arabidopsis*: implications for membrane biology in genome regulation. *Nucleic Acids Res.* 35, 203–213. doi: 10.1093/nar/gkl1068

Kim, Y. S., Kim, S. G., Park, J. E., Park, H. Y., Lim, M. H., Chua, N. H., et al. (2006). A membrane-bound NAC transcription factor regulates cell division in *Arabidopsis*. *Plant Cell* 18, 3132–3144. doi: 10.1105/tpc.106.043018

Kim, M. J., Park, M. J., Seo, P. J., Song, J. S., Kim, H. J., and Park, C. M. (2012). Controlled nuclear import of the transcription factor NTL6 reveals a cytoplasmic role of SnRK2.8 in the drought-stress response. *Biochem. J.* 448, 353–363. doi: 10.1042/BJ20120244

Kou, X., Liu, C., Han, L., Wang, S., and Xue, Z. (2016). NAC transcription factors play an important role in ethylene biosynthesis, reception and signaling of tomato fruit ripening. *Mol. Genet. Genomics* 291, 1205–1217. doi: 10.1007/s00438-016-1177-0

Kou, X., Zhou, J., Wu, C. E., Yang, S., Liu, Y., Chai, L., et al. (2021). The interplay between ABA/ethylene and NAC TFs in tomato fruit ripening: a review. *Plant Mol. Biol.* 106, 223–238. doi: 10.1007/s11103-021-01128-w

Kunieda, T., Mitsuda, N., Ohme-Takagi, M., Takeda, S., Aida, M., Tasaka, M., et al. (2008). NAC family proteins NARS1/NAC2 and NARS2/NAM in the outer integument regulate embryogenesis in *Arabidopsis*. *Plant Cell* 20, 2631–2642. doi: 10.1105/tpc.108.060160

Lee, S., Lee, H. J., Huh, S. U., Paek, K. H., Ha, J. H., and Park, C. M. (2014). The *Arabidopsis* NAC transcription factor NTL4 participates in a positive feedback loop that induces programmed cell death under heat stress conditions. *Plant Sci.* 227, 76–83. doi: 10.1016/j.plantsci.2014.07.003

Li, S., Chen, K., and Grierson, D. (2021). Molecular and hormonal mechanisms regulating fleshy fruit ripening. *Cells* 10, 1136. doi: 10.3390/cells10051136

Li, B., Fan, R., Yang, Q., Hu, C., Sheng, O., Deng, G., et al. (2020). Genome-wide identification and characterization of the NAC transcription factor family in *Musa acuminata* and expression analysis during fruit ripening. *Int. J. Mol. Sci.* 21, 634. doi: 10.3390/ijms21020634

Li, B. J., Grierson, D., Shi, Y., and Chen, K. S. (2022). Roles of abscisic acid in regulating ripening and quality of strawberry, a model non-climacteric fruit. *Hortic. Res.* 9, uhac089. doi: 10.1093/hr/uhac089

Li, M., Hou, L., Liu, S. S., Zhang, C. X., Yang, W. C., Pang, X. M., et al. (2021). Genome-wide identification and expression analysis of NAC transcription factors in *Ziziphus jujuba* mill. reveal their putative regulatory effects on tissue senescence and abiotic stress responses. *Ind. Crop Prod.* 173, 114093. doi: 10.1016/j.indcrop.2021.114093

Li, F., Li, J., Qian, M., Han, M., Cao, L., Liu, H., et al. (2016). Identification of peach NAP transcription factor genes and characterization of their expression in vegetative and reproductive organs during development and senescence. *Front. Plant Sci.* 7. doi: 10.3389/fpls.2016.00147

Li, S. J., Yin, X. R., Wang, W. L., Liu, X. F., Zhang, B., and Chen, K. S. (2017). Citrus CitNAC62 cooperates with CitWRKY1 to participate in citric acid degradation *via* up-regulation of *CitAco3*. *J. Exp. Bot.* 68, 3419–3426. doi: 10.1093/jxb/erx187

Liang, J., Zheng, J., Wu, Z., and Wang, H. (2022). Time-course transcriptomic profiling of floral induction in cultivated strawberry. *Int. J. Mol. Sci.* 23, 6126. doi: 10.3390/ijms23116126

Liu, G. S., Li, H. L., Grierson, D., and Fu, D. Q. (2022). NAC transcription factor family regulation of fruit ripening and quality: a review. *Cells* 11, 525. doi: 10.3390/cells11030525

Liu, B., Santo-Domingo, M., Mayobre, C., Martín-Hernández, A. M., Pujol, M., and Garcia-Mas, J. (2022). Knock-out of CmNAC-NOR affects melon climacteric fruit ripening. *Front. Plant Sci.* 13. doi: 10.3389/fpls.2022.878037

Liu, X., Zhang, L., and Yang, S. (2022). Analysis of floral organ development and sex determination in *Schisandra chinensis* by scanning electron microscopy and rna-sequencing. *Life (Basel).* 12, 1260. doi: 10.3390/life12081260

Lv, X., Lan, S., Guy, K. M., Yang, J., Zhang, M., and Hu, Z. (2016). Global expressions landscape of NAC transcription factor family and their responses to abiotic stresses in *Citrullus lanatus*. *Sci. Rep.* 6, 30574. doi: 10.1038/srep30574

Ma, N., Feng, H., Meng, X., Li, D., Yang, D., Wu, C., et al. (2014). Overexpression of tomato SlNAC1 transcription factor alters fruit pigmentation and softening. *BMC Plant Biol.* 14, 351. doi: 10.1186/s12870-014-0351-y

Ma, Q., Zhang, W., and Xiang, Q. Y. J. (2017). Evolution and developmental genetics of floral display–a review of progress. *J. Syst. Evol.* 55, 487–4515. doi: 10.1111/jse.12259

Martín-Pizarro, C., Vallarino, J. G., Osorio, S., Meco, V., Urrutia, M., Pillet, J., et al. (2021). The NAC transcription factor FaRIF controls fruit ripening in strawberry. *Plant Cell.* 33, 1574–1593. doi: 10.1093/plcell/koab070

Mathew, I. E., and Agarwal, P. (2018). May the fittest protein evolve: Favoring the plant-specific origin and expansion of NAC transcription factors. *Bioessays* 40, e1800018. doi: 10.1002/bies.201800018

Mathew, I. E., Das, S., Mahto, A., and Agarwal, P. (2016). Three rice NAC transcription factors heteromerize and are associated with seed size. *Front. Plant Sci.* 7. doi: 10.3389/fpls.2016.01638

Maugarny, A., Gonalves, B., Arnaud, N., and Laufs, P. (2016). CUC transcription factors: To the meristem and beyond. *Plant Transcription. Factors.*, 229–247.

Maugarny-Calès, A., Gonçalves, B., Jouannic, S., Melkonian, M., Ka-Shu Wong, G., and Laufs, P. (2016). Apparition of the NAC transcription factors predates the emergence of land plants. *Mol. Plant* 9, 1345–1348. doi: 10.1016/j.molp.2016.05.016

Meng, C., Yang, D. Y., Ma, X. C., Zhao, W. Y., Liang, X. Q., Ma, N. N., et al. (2016). Suppression of tomato SlNAC1 transcription factor delays fruit ripening. *J. Plant Physiol.* 193, 88–96. doi: 10.1016/j.jplph.2016.01.014

Migicovsky, Z., Yeats, T. H., Watts, S., Song, J., Forney, C. F., Burgher-MacLellan, K., et al. (2021). Apple ripening is controlled by a NAC transcription factor. *Front. Genet.* 12. doi: 10.3389/fgene.2021.671300

Mitsuda, N., Seki, M., Shinozaki, K., and Ohme-Takagi, M. (2005). The NAC transcription factors NST1 and NST2 of *Arabidopsis* regulate secondary wall thickenings and are required for anther dehiscence. *Plant Cell.* 17, 2993–3006. doi: 10.1105/tpc.105.036004

Mou, W., Li, D., Luo, Z., Li, L., Mao, L., and Ying, T. (2018). SlAREB1 transcriptional activation of NOR is involved in abscisic acid-modulated ethylene biosynthesis during tomato fruit ripening. *Plant Sci.* 276, 239–249. doi: 10.1016/j.plantsci.2018.07.015

Moyano, E., Martinez-Rivas, F. J., Blanco-Portales, R., Molina-Hidalgo, F. J., Ric-Varas, P., Matas-Arroyo, A. J., et al. (2018). Genome-wide analysis of the NAC transcription factor family and their expression during the development and ripening of the *Fragaria* × *ananassa* fruits. *PloS One* 13, e0196953. doi: 10.1371/journal.pone.0196953

Nakano, Y., Yamaguchi, M., Endo, H., Rejab, N. A., and Ohtani, M. (2015). NAC-MYB-based transcriptional regulation of secondary cell wall biosynthesis in land plants. *Front. Plant Sci.* 6. doi: 10.3389/fpls.2015.00288

Ng, S., Ivanova, A., Duncan, O., Law, S. R., Van Aken, O., De Clercq, I., et al. (2013). A membrane-bound NAC transcription factor, ANAC017, mediates mitochondrial retrograde signaling in *Arabidopsis*. *Plant Cell* 25, 3450–3471. doi: 10.1105/tpc.113.113985

Nieuwenhuizen, N. J., Chen, X. Y., Pellan, M., Zhang, L., Guo, L., Laing, W. A., et al. (2021). Regulation of wound ethylene biosynthesis by NAC transcription factors in kiwifruit. *BMC Plant Biol.* 21, 411. doi: 10.1186/s12870-021-03154-8

Olsen, A. N., Ernst, H. A., Lo Leggio, L., and Skriver, K. (2005). NAC transcription factors: Structurally distinct, functionally diverse. *Trends Plant Sci.* 10, 79–87. doi: 10.1016/j.tplants.2004.12.010

Ooka, H., Satoh, K., Doi, K., Nagata, T., Otomo, Y., Murakami, K., et al. (2003). Comprehensive analysis of NAC family genes in *Oryza sativa* and *Arabidopsis thaliana*. *DNA Res.* 10, 239–247. doi: 10.1093/dnares/10.6.239

Pei, H., Ma, N., Tian, J., Luo, J., Chen, J., Li, J., et al. (2013). An NAC transcription factor controls ethylene-regulated cell expansion in flower petals. *Plant Physiol.* 163, 775–791. doi: 10.1104/pp.113.223388

Pereira-Santana, A., Alcaraz, L. D., Castaño, E., Sanchez-Calderon, L., Sanchez-Teyer, F., and Rodriguez-Zapata, L. (2015). Comparative genomics of NAC transcriptional factors in angiosperms: implications for the adaptation and diversification of flowering plants. *PloS One* 10, e0141866. doi: 10.1371/journal.pone.0141866

Phillips, H. R., Landis, J. B., and Specht, C. D. (2020). Revisiting floral fusion: the evolution and molecular basis of a developmental innovation. *J. Exp. Bot.* 71, 3390–3404. doi: 10.1093/jxb/eraa125

Qi, X., Dong, Y., Liu, C., Song, L., Chen, L., and Li, M. (2022). The PavNAC56 transcription factor positively regulates fruit ripening and softening in sweet cherry (*Prunus avium*). *Physiol. Plant* 174, e13834. doi: 10.1111/ppl.13834

Raman, S., Greb, T., Peaucelle, A., Blein, T., Laufs, P., and Theres, K. (2008). Interplay of miR164, *CUP-SHAPED COTYLEDON* genes and *LATERAL SUPPRESSOR* controls axillary meristem formation in *Arabidopsis thaliana*. *Plant J.* 55, 65–76. doi: 10.1111/j.1365-313X.2008.03483.x

Ríos, P., Argyris, J., Vegas, J., Leida, C., Kenigswald, M., Tzuri, G., et al. (2017). ETHQV6.3 is involved in melon climacteric fruit ripening and is encoded by a NAC domain transcription factor. *Plant J.* 91, 671–683. doi: 10.1111/tpj.13596

Robertson, M. (2004). Two transcription factors are negative regulators of gibberellin response in the HvSPY-signaling pathway in barley aleurone. *Plant Physiol.* 136, 2747–2761. doi: 10.1104/pp.104.041665

Samad, A., Sajad, M., Nazaruddin, N., Fauzi, I. A., Murad, A., Zainal, Z., et al. (2017). MicroRNA and transcription factor: Key players in plant regulatory network. *Front. Plant Sci.* 8. doi: 10.3389/fpls.2017.00565

Seo, P. J., Kim, S. G., and Park, C. M. (2008). Membrane-bound transcription factors in plants. *Trends Plant Sci.* 13, 550–556. doi: 10.1016/j.tplants.2008.06.008

Seo, P. J., Kim, M. J., Park, J. Y., Kim, S. Y., Jeon, J., Lee, Y. H., et al. (2010). Cold activation of a plasma membrane-tethered NAC transcription factor induces a pathogen resistance response in *Arabidopsis*. *Plant J.* 61, 661–671. doi: 10.1111/j.1365-313X.2009.04091.x

Shahnejat-Bushehri, S., Allu, A. D., Mehterov, N., Thirumalaikumar, V. P., Alseekh, S., Fernie, A. R., et al. (2017). *Arabidopsis* NAC transcription factor JUNGBRUNNEN1 exerts conserved control over gibberellin and brassinosteroid metabolism and signaling genes in tomato. *Front. Plant Sci.* 8. doi: 10.3389/fpls.2017.00214

Shan, W., Kuang, J. F., Chen, L., Xie, H., Peng, H. H., Xiao, Y. Y., et al. (2012). Molecular characterization of banana NAC transcription factors and their interactions with ethylene signalling component EIL during fruit ripening. *J. Exp. Bot.* 63, 5171–5187. doi: 10.1093/jxb/ers178

Shan, W., Kuang, J. F., Wei, W., Fan, Z. Q., Deng, W., Li, Z. G., et al. (2020). MaXB3 modulates MaNAC2, MaACS1, and MaACO1 stability to repress ethylene biosynthesis during banana fruit ripening. *Plant Physiol.* 184, 1153–1171. doi: 10.1104/pp.20.00313

Shih, C. F., Hsu, W. H., Peng, Y. J., and Yang, C. H. (2014). The NAC-like gene *ANTHER INDEHISCENCE FACTOR* acts as a repressor that controls anther dehiscence by regulating genes in the jasmonate biosynthesis pathway in *Arabidopsis*. *J. Exp. Bot.* 65, 621–639. doi: 10.1093/jxb/ert412

Singh, S., Koyama, H., Bhati, K. K., and Alok, A. (2021). The biotechnological importance of the plant-specific NAC transcription factor family in crop improvement. *J. Plant Res.* 134, 475–495. doi: 10.1007/s10265-021-01270-y

Souer, E., van Houwelingen, A., Kloos, D., Mol, J., and Koes, R. (1996). The no apical meristem gene of *Petunia* is required for pattern formation in embryos and flowers and is expressed at meristem and primordia boundaries. *Cell* 85, 159–170. doi: 10.1016/s0092-8674(00)81093-4

Takeda, S., Hanano, K., Kariya, A., Shimizu, S., Zhao, L., Matsui, M., et al. (2011). CUP-SHAPED COTYLEDON1 transcription factor activates the expression of *LSH4* and *LSH3*, two members of the ALOG gene family, in shoot organ boundary cells. *Plant J.* 66, 1066–1077. doi: 10.1111/j.1365-313X.2011.04571.x

Tan, Q., Li, S., Zhang, Y., Chen, M., Wen, B., Jiang, S., et al. (2021). Chromosome-level genome assemblies of five *Prunus* species and genome-wide association studies for key agronomic traits in peach. *Hortic. Res.* 8, 213. doi: 10.1038/s41438-021-00648-2

Vroemen, C. W., Mordhorst, A. P., Albrecht, C., Kwaaitaal, M. A., and de Vries, S. C. (2003). The *CUP-SHAPED COTYLEDON3* gene is required for boundary and shoot meristem formation in *Arabidopsis*. *Plant Cell.* 15, 1563–1577. doi: 10.1105/tpc.012203

Wang, R., Tavano, E., Lammers, M., Martinelli, A. P., Angenent, G. C., and de Maagd, R. A. (2019). Re-evaluation of transcription factor function in tomato fruit development and ripening with CRISPR/Cas9-mutagenesis. *Sci. Rep.* 9, 1696. doi: 10.1038/s41598-018-38170-6

Wang, D., Wang, J., Wang, Y., Yao, D., and Niu, Y. (2022). Metabolomic and transcriptomic profiling uncover the underlying mechanism of color differentiation in *Scutellaria baicalensis* georgi. flowers. *Front. Plant Sci.* 3. doi: 10.3389/fpls.2022.884957

Wang, W. Q., Wang, J., Wu, Y. Y., Li, D. W., Allan, A. C., and Yin, X. R. (2020). Genome-wide analysis of coding and non-coding RNA reveals a conserved miR164-NAC regulatory pathway for fruit ripening. *New Phytol.* 225, 1618–1634. doi: 10.1111/nph.16233

Wang, J., Wang, Y., Zhang, J., Ren, Y., Li, M., Tian, S., et al. (2021). The NAC transcription factor ClNAC68 positively regulates sugar content and seed development in watermelon by repressing *ClINV* and *ClGH3.6*. *Hortic. Res.* 8, 214. doi: 10.1038/s41438-021-00710-z

Wang, D., Yu, Y., Liu, Z., Li, S., Wang, Z., and Xiang, F. (2016). Membrane-bound NAC transcription factors in maize and their contribution to the oxidative stress response. *Plant Sci.* 250, 30–39. doi: 10.1016/j.plantsci.2016.05.019

Wang, H., Zhao, Q., Chen, F., Wang, M., and Dixon, R. A. (2011). NAC domain function and transcriptional control of a secondary cell wall master switch. *Plant J.* 68, 1104–1114. doi: 10.1111/j.1365-313X.2011.04764.x

Waters, B. M., Uauy, C., Dubcovsky, J., and Grusak, M. A. (2009). Wheat (*Triticum aestivum*) NAM proteins regulate the translocation of iron, zinc, and nitrogen compounds from vegetative tissues to grain. *J. Exp. Bot.* 60, 4263–4274. doi: 10.1093/jxb/erp257

Wei, W., Yang, Y. Y., Su, X. G., Kuang, J. F., Chen, J. Y., Lu, W. J., et al. (2021). MaRTH1 suppression of ethylene response during banana fruit ripening and is controlled by MaXB3-MaNAC2 regulatory module. *Postharvest. Biol. Technol.* 182, 111707. doi: 10.1016/j.postharvbio.2021.111707

Wild, J. M., and Krützfeldt, N. O. (2010). Neocortical-like organization of avian auditory 'cortex'. commentary on Wang y, brzozowska-prechtl a, karten HJ, (2010): Laminar and columnar auditory cortex in avian brain. *Proc. natl. acad. sci. U.S.A.* 107:12676-12681. *Brain Behav. Evol.* 76, 89–92. doi: 10.1159/000320215

Wu, Y. Y., Liu, X. F., Fu, B. L., Zhang, Q. Y., Tong, Y., Wang, J., et al. (2020). Methyl jasmonate enhances ethylene synthesis in kiwifruit by inducing *NAC* genes that activate *ACS1*. *J. Agric. Food Chem.* 68, 3267–3276. doi: 10.1021/acs.jafc.9b07379

Xie, Q., Guo, H. S., Dallman, G., Fang, S., Weissman, A. M., and Chua, N. H. (2002). SINAT5 promotes ubiquitin-related degradation of NAC1 to attenuate auxin signals. *Nature* 419, 167–170. doi: 10.1038/nature00998

Xu, W. Y., Chen, C., Gou, N. N., Huang, M. Z., Wuyun, T. N., Zhu, G. P., et al. (2021). Genome-wide identification and expression analysis of NAC transcription factor family genes during fruit and kernel development in Siberian apricot. *J. Am. Soc Hortic. Sci.* 146, 276–285. doi: 10.21273/JASHS05007-20

Yamasaki, K., Kigawa, T., Seki, M., Shinozaki, K., and Yokoyama, S. (2013). DNA-Binding domains of plant-specific transcription factors: structure, function, and evolution. *Trends Plant Sci.* 18, 267–276. doi: 10.1016/j.tplants.2012.09.001

Yang, S., Zhou, J. Q., Watkins, C. B., Wu, C. E., Feng, Y. C., Zhao, X. Y., et al. (2021). NAC transcription factors *SNAC4* and *SNAC9* synergistically regulate tomato fruit ripening by affecting expression of genes involved in ethylene and abscisic acid metabolism and signal transduction. *Postharvest. Biol. Technol.* 178, 111555. doi: 10.1016/j.postharvbio.2021.111555

Zhang, S., Dong, R., Wang, Y., Li, X., Ji, M., and Wang, X. (2021). NAC domain gene VvNAC26 interacts with VvMADS9 and influences seed and fruit development. *Plant Physiol. Biochem.* 164, 63–72. doi: 10.1016/j.plaphy.2021.04.031

Zhang, Q. J., Li, T., Zhang, L. J., Dong, W. X., and Wang, A. D. (2018). Expression analysis of NAC genes during the growth and ripening of apples. *Hortic. Sci.* 45, 1–10. doi: 10.17221/153/2016-HORTSCI

Zhang, J., Li, M., Zhang, H., Gong, G., Wang, M., and Xu, Y. (2022). Natural variation in the NAC transcription factor NONRIPENING contributes to melon fruit ripening. *J. Integr. Plant Biol.* 64, 1448–1461. doi: 10.1111/jipb.13278

Zhang, Q., Wang, L., Wang, Z., Zhang, R., Liu, P., Liu, M., et al. (2021). The regulation of cell wall lignification and lignin biosynthesis during pigmentation of *Winter jujube*. *Hortic. Res.* 8, 238. doi: 10.1038/s41438-021-00670-4

Zhao, Y., Sun, J., Xu, P., Zhang, R., and Li, L. (2014). Intron-mediated alternative splicing of WOOD-ASSOCIATED NAC TRANSCRIPTION FACTOR1B regulates cell wall thickening during fiber development in *Populus* species. *Plant Physiol.* 164, 765–776. doi: 10.1104/pp.113.231134

Zhong, J., Powell, S., and Preston, J. C. (2016). Organ boundary NAC-domain transcription factors are implicated in the evolution of petal fusion. *Plant Biol.* 18, 893–902. doi: 10.1111/plb.12493

Zhu, M., Chen, G., Zhou, S., Tu, Y., Wang, Y., Dong, T., et al. (2014). A new tomato NAC (NAM/ATAF1/2/CUC2) transcription factor, SlNAC4, functions as a positive regulator of fruit ripening and carotenoid accumulation. *Plant Cell Physiol.* 55, 119–135. doi: 10.1093/pcp/pct162

Zhu, M. K., Hu, Z. L., Zhou, S., Wang, L. L., Dong, T. T., Pan, Y., et al. (2014). Molecular characterization of six tissue-specific or stress-inducible genes of NAC transcription factor family in tomato (*Solanum lycopersicum*). *J. Plant Growth Regul.* 33, 730–744. doi: 10.1007/s00344-014-9420-6

Zhu, F., Luo, T., Liu, C., Wang, Y., Zheng, L., Xiao, X., et al. (2020). A NAC transcription factor and its interaction protein hinder abscisic acid biosynthesis by synergistically repressing NCED5 in *Citrus reticulata*. *J. Exp. Bot.* 71, 3613–3625. doi: 10.1093/jxb/eraa118

Zhu, T., Nevo, E., Sun, D., and Peng, J. (2012). Phylogenetic analyses unravel the evolutionary history of NAC proteins in plants. *Evolution* 66, 1833–1848. doi: 10.1111/j.1558-5646.2011.01553.xs

frontiers | Frontiers in Plant Science

TYPE Original Research
PUBLISHED 22 March 2023
DOI 10.3389/fpls.2023.1072086

OPEN ACCESS

EDITED BY
C. Watkins,
Cornell University, United States

REVIEWED BY
Zhengke Zhang,
Hainan University, China
Xuewu Duan,
South China Botanical Garden (CAS), China

*CORRESPONDENCE
Jing-yi Wang
wangjingyi@itbb.org.cn
Ju-hua Liu
liujuhua@itbb.org.cn
Zhi-qiang Jin
18689846976@163.com

†These authors have contributed equally to this work and share first authorship

SPECIALTY SECTION
This article was submitted to Crop and Product Physiology, a section of the journal Frontiers in Plant Science

RECEIVED 19 October 2022
ACCEPTED 28 February 2023
PUBLISHED 22 March 2023

CITATION
Wang Z, Yao X-m, Jia C-h, Xu B-y, Wang J-y, Liu J-h and Jin Z-q (2023) Identification and analysis of lignin biosynthesis genes related to fruit ripening and stress response in banana (*Musa acuminata* L. AAA group, cv. Cavendish). *Front. Plant Sci.* 14:1072086. doi: 10.3389/fpls.2023.1072086

Identification and analysis of lignin biosynthesis genes related to fruit ripening and stress response in banana (*Musa acuminata* L. AAA group, cv. Cavendish)

Zhuo Wang[1,2,3†], Xiao-ming Yao[4†], Cai-hong Jia[1,2], Bi-yu Xu[1,2], Jing-yi Wang[1,2*], Ju-hua Liu[1,2,3*] and Zhi-qiang Jin[1,2,3*]

[1]Key Laboratory of Tropical Crop Biotechnology of Ministry of Agriculture and Rural Affairs, Institute of Tropical Bioscience and Biotechnology, Chinese Academy of Tropical Agricultural Sciences, Haikou, Hainan, China, [2]Hainan Academy of Tropical Agricultural Resource, Chinese Academy of Tropical Agricultural Sciences, Haikou, Hainan, China, [3]Sanya Research Institute of Chinese Academy of Tropical Agricultural Sciences, Sanya, Hainan, China, [4]Beijing Genomics Institute (BGI)-Sanya, Beijing Genomics Institute (BGI)-Shenzhen, Sanya, China

Background: Lignin is a key component of the secondary cell wall of plants, providing mechanical support and facilitating water transport as well as having important impact effects in response to a variety of biological and abiotic stresses.

Results: In this study, we identified 104 genes from ten enzyme gene families related to lignin biosynthesis in *Musa acuminata* genome and found the number of *MaCOMT* gene family was the largest, while *MaC3H*s had only two members. *MaPAL*s retained the original members, and the number of *Ma4CL*s in lignin biosynthesis was significantly less than that of flavonoids. Segmental duplication existed in most gene families, except for *MaC3H*s, and tandem duplication was the main way to expand the number of *MaCOMT*s. Moreover, the expression profiles of lignin biosynthesis genes during fruit development, postharvest ripening stages and under various abiotic and biological stresses were investigated using available RNA-sequencing data to obtain fruit ripening and stress response candidate genes. Finally, a co-expression network of lignin biosynthesis genes was constructed by weighted gene co-expression network analysis to elucidate the lignin biosynthesis genes that might participate in lignin biosynthesis in banana during development and in response to stresses.

Conclusion: This study systematically identified the lignin biosynthesis genes in the *Musa acuminata* genome, providing important candidate genes for further functional analysis. The identification of the major genes involved in lignin biosynthesis in banana provides the basis for the development of strategies to improve new banana varieties tolerant to biological and abiotic stresses with high yield and high quality.

KEYWORDS

lignin biosynthesis genes, banana, fruit ripening, stresses, co-expression networks, expression analysis

Introduction

Lignin is a complex and aromatic three-dimensional high molecular phenol polymer, which is widely distributed in nature, accounting for about 30% of the organic carbon in the biosphere (Campbell and Sederoff, 1996; Faraji et al., 2018). Lignin mainly exists in the secondary cell wall of all vascular plants and has many functions. For example, it can form an effective physical barrier against pathogens by cross-linking with the components of the cell wall (Lewis and Yamamoto, 1990). The lignin filled in the cellulose framework can also enhance the strength of plant cell wall and the bending resistance of stem, so as to improve the mechanical strength and lodging resistance of plant (Ahmad et al., 2020).

Lignin is mainly composed of three alcohol monomers, coniferyl, sinapyl and p-coumarin alcohol precursor, which are produced by coupling combination of oxidation of the p-hydroxycinnamic alcohol monomer, forming cinnamic acid through phenylalanine ammonia, and resulting in syringyl lignin (S), guaiacy lignin (G) and hyroxy-phenyl lignin (H) and other lignin monomer by a series of hydroxylation, methylation and reduction reaction, (Zhao and Dixon, 2011). These lignin monomers are finally dehydrogenated and polymerized into complex lignin complexes. The methoxylation level of S-, G- and H-type lignin monomers determines the lignin content and composition (Boerjan et al., 2003). In different plants, the content and composition of lignin are different. Generally, the lignins of pteriophyta and gymnosperm are mainly composed of G type lignin monomer and a small amount of H type lignin monomer. The dicotyledons in angiosperms are mainly composed of G-lignin monomer and S-lignin monomer, and the lignin in monocotyledons is a mixture of three monomers (Vanholme et al., 2010). Although the content and composition of lignin in different plants are different, the synthetic pathway is basically the same (Bonawitz and Chapple, 2010).

In most plants, there are mainly ten key enzyme gene families involved in lignin biosynthesis, including phenylalanine ammonia-lyase (PAL), cinnamate 4-hydroxylase (C4H), 4-coumarate: Co A ligase (4CL), hydroxycinnamoyl-Co A shikimate/quinate transferase (HCT), coumarate 3-hydroxylase (C3H), caffeoyl-Co A-O-methyltransferase (CcoAOMT), cinnamoyl Co A reductase (CCR), ferulate 5-hydroxylase (F5H), caffeic acid O-methyltransferase (COMT), cinnamyl alcohol dehydrogenase (CAD). Due to the increasing number of sequenced plant genomes, lignin biosynthesis genes have been identified in many plants, including *Arabidopsis* (Raes et al., 2003), *Populus trichocarpa* (Shi et al., 2010), Maize (Hu et al., 2009), Soybean (Baldoni et al., 2013), *Switchgrass* (Shen et al., 2013), *Eucalyptus grandis* (Carocha et al., 2015), Hard End Pear (Lu et al., 2015), Kenaf (Ryu et al., 2016), Pear (Cao et al., 2019), *Setaria viridis* (Ferreira et al., 2019), and Ramie (Tang et al., 2019).

Bananas (*Musa* spp.) are perennial monocotyledonous herbs that grow well in humid tropical and subtropical regions. In the banana pseudostem, the content of lignin in fiber is about 5-10%, lower than those of cellulose and hemicellulose (Komuraiah et al., 2014). Banana fruit is a popular tropical and subtropical fruit, and also is an important staple food for many people in tropical regions, rich in protein and carbohydrates (Aurore et al., 2009). As an important component of dietary fiber, lignin is an important index of quality of banana fruit and directly affects the fruit texture (Hamauzu et al., 1997; Happi Emaga et al., 2008). However, the expression pattern of lignin biosynthesis genes in banana fruit is rarely reported.

Cavendish banana is a triploid (AAA) banana cultivar formed by intraspecific hybridization in *Musa acuminata*. It is the most widely cultivated and commercialized variety (Perrier et al., 2011; Ploetz, 2015). After forming triploid, asexual propagation is the only reproductive mode of Cavendish banana, which leads to low environmental adaptability. Environmental stresses, such as drought (van Asten et al., 2011), low temperature (Kang et al., 2007), salt (Xu et al., 2014), and several devastating diseases (Heslop-Harrison and Schwarzacher, 2007) usually affect the yield and quality of the Cavendish banana fruits. Fusarium Wilt of Banana (FWB) is prevalent in main banana producing areas worldwide, which is seriously destructive for banana industry. It is a typical soil borne fungus disease caused by *Fusarium oxysporum* f. sp. *cubense* (Foc). Specifically, Cavendish banana is highly susceptible to Foc TR4 (Ploetz, 2006). Up to now, only a few genes have been cloned or used for expression analysis during Cavendish banana interacted with Foc TR4 (Wang et al., 2015; Wang et al., 2016). It is unclear about the roles of lignin biosynthesis gene in the process of fruit development, postharvest ripening and the response to stresses, especially those of the lignin biosynthesis genes involved in resistance to Foc TR4. This comprehensive study can increase our understanding of lignin biosynthesis genes of banana associated with fruit developmental and ripening processes and stresses responses and will establish a crucial foundation for future studies of genetic improvement in banana.

Materials and methods

Plant materials and treatments

Cavendish banana (*Musa acuminata* L. AAA group cv. Cavendish) fruits were harvested from the banana plantation of the Institute of Bioscience and Biotechnology (ITBB) of Chinese Academy of Tropical Agricultural Sciences (CATAS) (Wenchang, Hainan, 19.61N, 110.75E). The pulp of Cavendish banana fruit was harvested at 0, 20, and 80 DAF (day after flowering, DAF), which represented fruit developmental stages of budding, cutting flower, and harvest stages, respectively. During ripening stage, pulp of Cavendish banana fruit was harvested at 0, 8 and 14 DPH (day post-harvest, DPH) representing green, yellowish green, and yellow based on color of the fruit, respectively.

One month old Cavendish banana plantlets were grown under greenhouse conditions with 26°C and 80% humidity. Cavendish banana plantlets were irrigated with 300 mM NaCL and 200 mM mannitol for 7 days for salt and osmotic treatments, respectively. Cavendish banana plants were maintained at 4°C for 22 h for cold treatment. The leaves without main vein were harvested for analysis.

Fusarium Wilt of Banana (FWB) is prevalent in main banana producing areas worldwide, which is seriously destructive for banana industry. It is a typical soil borne fungus disease caused by *Fusarium*

oxysporum f. sp. *cubense* (Foc). Cavendish banana is highly susceptible to Foc TR4. Giant Cavendish Tissue Culture Variants (GCTCV, GC) have acquired resistance to TR4 through somaclonal variation (Hwang and Ko, 2004). GCTCV-119 is the best Foc TR4-resistant alternative cultivar for the Cavendish (Ploetz, 2015). Variety Pahang (PH) is a wild banana belonging to subspecies *Musa acuminata* ssp. *malaccensis*, and highly resistant to Foc TR4 (Zhang et al., 2018). The fungus was grown on potato dextrose agar medium and incubated for 5-7 days at 28°C. The roots of 2-month old susceptible cultivar Cavendish banana, resistant cultivar GCTCV-119 and variety Pahang were dipped in Foc TR4 spore suspension of 1.0×10^6 condia/mL, and the roots were harvested at 0 and 2 days post-infection (DPI) (Wang et al., 2012). All of the above samples were immediately frozen in liquid nitrogen and stored at -80°C.

Identification of lignin biosynthesis genes in the *Musa acuminata* genome and phylogenetic analyses

To analyze the genome-wide lignin biosynthesis genes, we first downloaded all gene coding protein sequences of *Musa acuminata* genome (DH Pahang) from the Banana Genome Hub (https://banana-genome-hub.southgreen.fr) (Martin et al., 2016). We compared genes related to lignin biosynthesis genes in the *Musa acuminata* genome with the genes annotated in genomes of rice (http://rice.uga.edu/index.shtml) and *Arabidopsis* (http://www.arabidopsis.org/). In the PAL and HCT gene families, we also selected representative genes to draw the phylogenetic tree, including *EsPAL* (ATD50344.1) from *Eucalyptus saligna*, *JcPAL* (XP_012077001.1) from *Jatropha curcas*, *HbPAL* (XP_021684949.1) from *Hevea brasiliensis*, *PtHCT1* (XP_024452069.1) from *Populus trichocarpa*, *PtHCT2* (XP_006368492.1), *NtHCT* (NP_001312552.1) and *NtHQT*(NP_001312079.1) from *Nicotiana tabacum*, and *CcHCT* (ABO47805.1) from *Coffea canephora*. We retrieved protein sequences of these gene families for homologue-based searches with the criteria: similarity > 80% and coverage > 80%. Then, we confirmed the presence of the conserved domain within all the protein sequences in CDD (http://www.ncbi.nlm.nih.gov/cdd/) databases in NCBI and removed members without complete domain. The full-length lignin biosynthesis genes protein sequences from *Musa acuminata*, rice, *Arabidopsis* and other woody plants were aligned using ClustalW. Relationships were assessed using a Maximum Likelihood evolutionary tree with 1,000 bootstrap replicates and were created using MEGA 6.0 software (Tamura et al., 2013). The accession number of identified lignin biosynthesis genes was listed in Supplementary Table 1. The molecular weight and isoelectric points of the lignin biosynthesis genes were predicted from the ExPASy database (http://expasy.org/). The sequence logo for lignin biosynthesis genes domain was created by WebLogo server (http://weblogo.berkeley.edu/logo.cgi).

Chromosome distribution and gene duplications

To determine the physical locations of lignin biosynthesis genes, the starting and ending positions of all lignin biosynthesis genes on each chromosome were obtained from the *Musa acuminata* genome database. MapInspect software was used to draw the images of the locations of the lignin biosynthesis genes (http://mapinspect.software.informer.com/). Tandem and segmental duplications were also identified according to the plant genome duplication database (Lee et al., 2012). Based on physical chromosomal location, homologous lignin biosynthesis genes on a single chromosome within 30 kb of each other were characterized as tandem duplication (Shiu and Bleecker, 2003; Du et al., 2013). Syntenic blocks were detected using MCSCAN (parameters: -a -e 1e-5 -s 5) (Wang et al., 2019), and all lignin biosynthesis genes located in the syntenic blocks were extracted. Circos (0.63) software was used to draw the images of the locations and synteny of the lignin biosynthesis genes (http://circos.ca/).

RNA-seq data processing and expression profiling during fruit development, post-harvest ripening and stresses response

Total RNAs were extracted using Eastep Super Total RNA Extraction Kit (Promega, Beijing, China). Five μg of total RNA from each sample was converted to cDNA using GoScript Reverse Transcription Mix (Promega, Beijing, China), and constructed the cDNA libraries using TruSeq RNA Library Preparation Kit v2, and then were sequenced on an IIIumina HiSeq 2000 platform (San Diego, CA, USA) using the IIIumina RNA-seq protocol. Two biological replicates were used for each sample. Gene expression levels were calculated as Reads Per Kilobases per Million reads (RPKM) (Mortazavi et al., 2008). Differentially expressed genes were identified with the mean of read count from two replicates for each gene (fold change ≥ 2) (Audic and Claverie, 1997). MeV 4.9 and Java Treeview software constructed the heat-map of genes according to the manufacturer's protocol. We analyzed the expression patterns of lignin biosynthesis genes during fruit development and postharvest ripening (0DAF, 20DAF, 80DAF-0DPH, 8DPH and 14DPH), and the response to abiotic (4°C for 22h, 300 mM NaCl for 7 days and 200 mM mannitol for 7 days) and biological (Roots of Cavendish banana, GCTCV-119 and Pahang varieties inoculated Foc TR4 after 2 days) stressors. All the data of RNA-seq had been uploaded to deposit in the CNSA (https://db.cngb.org/cnsa/) of CNGBdb with accession number CNP0000292. The accession numbers of all samples were listed in Supplementary Table 2.

Weighted gene co-expression network analysis

Gene expression patterns for all identified TFs and the lignin biosynthesis genes from fruits, leaves and roots tissues were used to construct the co-expression network using WGCNA (version 1.47) within the R platform (version 3.2.2) (Langfelder and Horvath, 2008). Genes whose expression had not been detected in all tissues were removed in advance. Soft thresholds were set according to the scale-free topology criterion adopted by Zhang and Horvath (2005).

An adjacency matrix was developed using the squared Euclidean distance values, and Pearson method was used to calculate the topological overlap matrix of unsigned network detection. Then, the co-expression coefficients greater than 0.50 between the target genes were selected. Finally, we extracted the co-expression network of lignin biosynthesis genes, and the network connections were visualized using cytoscape (Shannon et al., 2003). We enriched analysis of target genes using the Kyoto Encyclopedia of Genes and Genomes (KEGG) pathway.

Yeast one-hybrid assay

Yeast one-hybrid screening was performed using MatchmakerTM Gold Yeast One-Hybrid Library Screening System (Clontech, Dalian, China). The bait fragment (the 1481 bp fragment of MaC3H2 promoter) was cloned into the pAbAi vector. The MaC3H2-AbAi and p53-AbAi were linearized and transformed into Y1HGold to make a bait-reporter strain, respectively. Transformants were initially screened on plates containing SD medium without Ura (SD/-Ura) and added with 0-1000 ng/ml aureobasidin A (AbA) for auto-activation analysis. Full-length coding sequences of *MaMYB1* (Ma02_t00290.1), *MaMYB2* (Ma06_t05680.1), *MaMYB3* (Ma11_t11940.1), *MaNAC1* (Ma07_t06080.1) and *MabHLH1* (Ma07_t28500.1) were cloned into the pGADT7 (AD) prey vector and transferred into the bait-reporter yeast strain, respectively. Transformed Y1HGold were incubated on SD medium with 300 ng/ml AbA and without leucine (SD-Leu +AbA300) at 28°C for 3 days to test the interaction. pGADT7-Rec (AD-Rec-P53) and p53-promoter fragments were co-transformed into Y1HGold as positive controls, while the AD-empty and MaC3H2-AbAi were used as negative controls. The primers used for yeast one-hybrid assay were listed in Supplementary Table 3.

Dual luciferase reporter assay

Full-length coding sequences of the MaMYB1, MaMYB2, MaMYB3, MaNAC1 and MabHLH1 were inserted into the pGreen II 62-SK vector (SK), respectively, and the fragment of *MaC3H2* promoter was inserted into the pGreen II 0800-LUC vector. All the above constructs were transformed into *Agrobacterium tumefaciens* GV3101 using freeze-thaw method (Holsters et al., 1978). The dual luciferase assays were performed with *Nicotiana benthamiana* grown in green house for forty days. Agrobacterium cultures were prepared with infiltration buffer (10 mM $MgCl_2$, 10 mM MES and 150 mM acetosyringone, pH5.6) to an OD_{600} of 0.8. Agrobacterium culture mixtures of TF genes (5 ml) and promoter (95 µL) were infiltrated into the abaxial side of *Nicotiana benthamiana* leaves. Leaves were collected after two days infiltration for luciferase (LUC) and Renilla luciferase (REN) activities analyses using Dual-Luciferase Reporter Assay System (Promega, USA, E1910) with Modulus Luminometers (Promega). Luciferase activity was analyzed in three independent experiments with six replications for each assay.

Statistical analysis

Statistical analysis was performed using Student's t-test. The experimental results obtained were expressed as the means ± standard deviation (SD). P values<0.05 were considered statistically significant (*), and P values<0.01 were considered highly statistically significant (**).

Results

Identification of lignin biosynthesis genes in *Musa acuminata* genome

In total, 104 genes belonging to ten key enzyme gene families, including eight *MaPALs*, five *MaC4Hs*, eighteen *Ma4CLs*, three *MaHCTs*, two *MaC3Hs*, seven *MaCCoAOMTs*, twenty-four *MaCCRs*, four *MaF5Hs*, twenty-four *MaCOMTs* and ten *MaCADs* were identified in the *Musa acuminata* genome. In addition, we found 31 genes identified as 'like' genes (candidate genes excluded from *bona fide* clade), including 9 from *Ma4CLs*, 21 from *MaCCRs* and 1 from *MaCOMTs* (Supplementary Table 1). Gene names were based on the location of chromosomes. The gene ID, position, and protein physicochemical properties of all genes were shown in Supplementary Table 1.

In conservative domain analysis, we mainly compared the lignin biosynthesis genes from banana with genes from *Arabidopsis*. We found all genes contained the core conserved domains belonging to the features of gene family in the protein sequence. MaPALs contained the conserved motifs (GTITASGDLUPLSYIAG) (Figure 1A). MaC3Hs, MaC4Hs and MaF5Hs had cytochrome P450 conserved domains, such as proline rich region (PPGPKGLP), PERF conserved motif and heme-binding motif of CYP450 proteins (PFGSGRRSCP) (Figure 1B). In Ma4CLs, all of them contained conservative Box I (SSGTTGLPKGV) and Box II (GEICVRS) in the protein sequence (Figure 1C). We found *MaHCT*s genes contained the conserved active motif (HXXXDG) and conservative motif (DFGWGR) of acetyltransferase gene family (Figure 1D). Generally, the amino acid sequence of CCoAOMT gene family contains 8 conserved motifs, in which motif D, motif E, motif F, motif G and motif H are unique to the CCoAOMT family and are as the tag sequences (Zhao et al., 2004). We found all MaCCoAOMTs contained motif D, motif E, motif F, motif G and motif H (Figure 1E). In these sequences of COMT proteins, there were five amino acid conserved elements in proper order from the N-terminal to the C-terminal of the amino acid sequence (conservative motif 1: LVDGGGxG, conservative motif II: GINFDLPHV, conservative motif III: EHVGGDMF and conservative motif VI: NGKVI) (Ibrahim et al., 1998). In *Musa acuminata* genome, we found that 23 COMT genes had the above conserved domains (Figure 1F). Three *bona fide* MaCCRs (MaCCR1, MaCCR2 and MaCCR3) were identified to contain the conserved sequence (KNWYCYGK) belonging to CCR gene family (Figure 1G). Ten MaCAD proteins contained binding domain for the structurally important zinc (CX2CX2CX7C), NADPH (GxGGVG) and catalytic

10.3389/fpls.2023.1072086

FIGURE 1
Sequence logo of the lignin biosynthesis proteins motifs. The height of each amino acid represented the relative frequency of the amino acid at that position. **(A)** Phenylalanine ammonialyase(PAL), **(B)** coumarate 3-hydroxylase (C3H), cinnamate 4-hydroxylase (C4H) and ferulate 5-hydroxylase (F5H), **(C)** 4-coumarate: CoA ligase (4CL), **(D)** hydroxycinnamoyl-CoA shikimate/quinate transferase (HCT), **(E)** caffeoyl-CoA-O-methyltransferase (CcoAOMT), **(F)** caffeic acid Omethyltransferase (COMT), **(G)** cinnamoyl CoA reductase (CCR), **(H)** cinnamyl alcohol dehydrogenase (CAD).

Zn^{2+} binding motif (GHExxGxxxxxGxxV), which was the signature sequence of CAD genes (Figure 1H). The above results show that all 104 lignin biosynthesis genes have typical conserved domains of their respective gene families.

Phylogenetic analysis of lignin biosynthesis genes from *Musa acuminata* genome

Analyses of the evolutionary relationships of lignin synthetase genes from *Musa acuminata*, *Arabidopsis*, rice, and other plants have been functionally verified. The phylogenetic tree was analyzed by MEGA6 using the method with 1000 bootstrap replicates and the evolutionary distances were calculated using the Poisson correction method.

MaPAL family can be clearly divided into two groups. MaPAL1, MaPAL2, MaPAL3, MaPAL4, MaPAL5, MaPAL7 and MaPAL8 were clustered together with all PALs from *Arabidopsis* and rice. MaPAL6 was placed near the PALs from woody plants, such as EsPAL, JcPAL and HbPAL, indicating that the evolution of MaPALs is more conservative, MaPAL6 may have different origins from the other seven MaPALs (Figure 2A). In plants, 4CL can be divided into three clades, clade I is thought to be related to lignin synthesis, and clade II 4CL is thought to be related to flavonoid synthesis (Wei and Wang, 2004). The Ma4CLs can be divided into three clades, Ma4CL1, Ma4CL3, Ma4CL4, Ma4CL5, Ma4CL6, Ma4CL7 were located in clade I, Ma4CL2 and Ma4CL8 were located in clade II, and others were located in 4CL-like clade. Moreover, we also found that the Ma4CLs were often closer to Os4CLs and far away from At4CLs (Figure 2B). It is suggested that Ma4CL11, Ma4CL14, Ma4CL6 and Ma4CL7 may be related to lignin synthesis and formed after the differentiation of monocotyledons and dicotyledons. MaC4Hs can be divided into two clades: MaC4H, MaC4H3, MaC4H4, MaC4H5, MaC4H7, AtC4H, OsC4H1 and OsC4H2 which were located in same clade, while MaC4H1, MaC4H2, MaC4H6, OsC4H3 and OsC4H4 were located in the same clade (Figure 2C). MaC3Hs were more closely related to OsC3H than AtC3H1 and no member was close to AtC3H2 and AtC3H3 (Figure 2C). Those results indicate that the evolution of MaC4Hs and MaC3Hs may be formed after the differentiation of monocotyledons and dicotyledons. The members of MaF5Hs were clustered with the AtF5Hs, and far from OsF5Hs (Figure 2C), indicating that the differentiation of F5H gene is formed before the differentiation of monocotyledons and dicotyledons. Three MaHCTs were distributed in the same clade with OsHCT1 and OsHCT2, but far away from the HCTs from *Arabidopsis thaliana*, *Populus trichocarpa* (PtHCT1, PtHCT2), *Nicotiana tabacum* (NtHCT and NtHQT) and *Coffea canephora* (CcHCT), indicating that MaHCTs may be formed after differentiation of monocotyledons and dicotyledons (Figure 2C). CCoAOMTs can be mainly divided into two clades (Rakoczy et al., 2018). All seven MaCCoAOMTs were distributed in the same clade with OsCCoAOMT and AtCCoAOMT1 (Figure 2D). Similarly, all the MaCOMTs located with AtOMT1 and OsCOMT1 belonged to the Clade I, and only MaCOMT21 close to AtOMT-like11 and OsCOMT-like5 belonged to COMT-like (Figure 2D). *Bona fide*

10.3389/fpls.2023.1072086

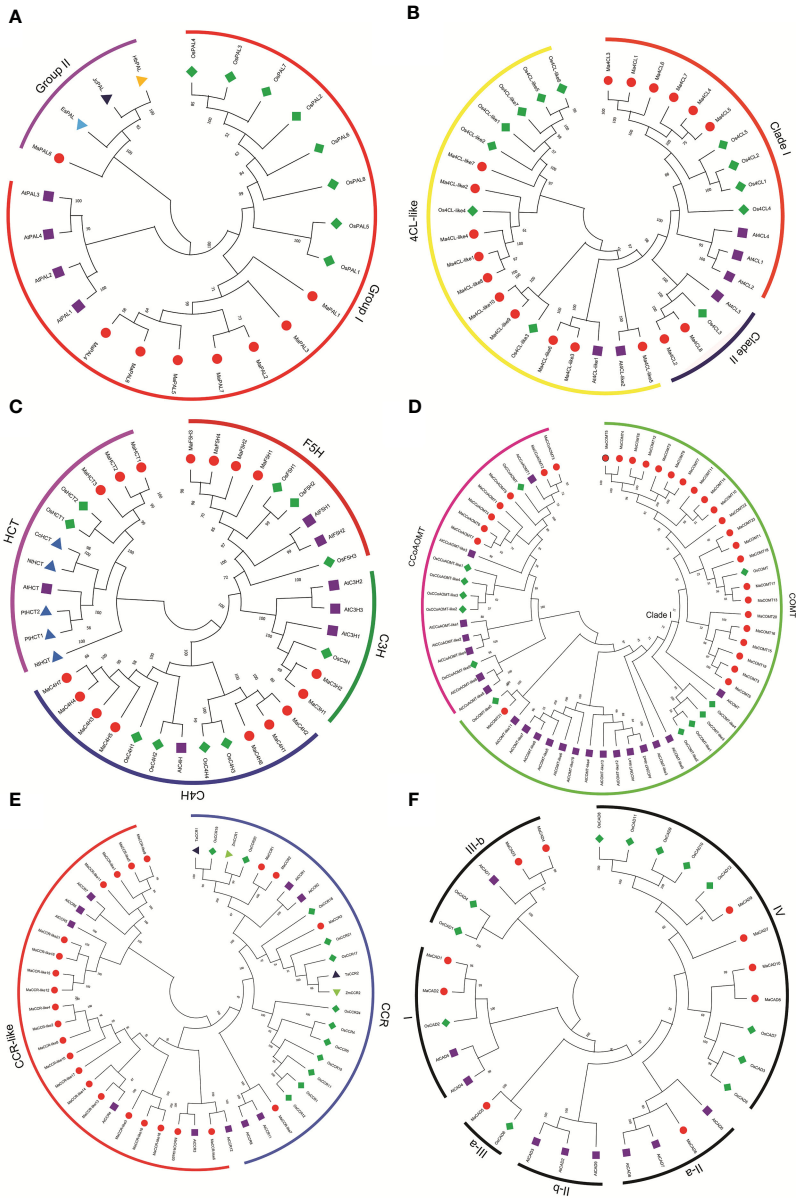

FIGURE 2
Phylogenetic relationship of lignin biosynthesis genes in *Musa acuminata* (red dot), *Arabidopsis* (purple square), rice (green diamond), and other plants (triangle). The Maximum Likelihood (ML) tree was drawn using MEGA 6.0 with 1000 bootstrap replicates. **(A)** Phenylalanine ammonialyase (PAL), **(B)** 4-coumarate: CoA ligase (4CL), **(C)** hydroxycinnamoyl-CoA shikimate/quinate transferase (HCT), coumarate 3-hydroxylase (C3H), cinnamate 4-hydroxylase (C4H) and ferulate 5-hydroxylase (F5H), **(D)** caffeic acid Omethyltransferase (COMT) and caffeoyl-CoA-O-methyltransferase (CcoAOMT), **(E)** cinnamoyl CoA reductase (CCR), **(F)** cinnamyl alcohol dehydrogenase (CAD).

CCR clade and CCR-like clade were contained in CCR gene family. In particular, MaCCR1 and MaCCR2 were closely related to TaCCR1, ZmCCR1, AtCCR1 and AtCCR2. MaCCR3 was grouped with ZmCCR2, TaCCR2, and PvCCR2 (Figure 2E). Thirty-one CADs were clearly divided into three classes (class I, class II and class III). MaCAD1 and MaCAD2 were located in class I (*bona fide* CAD clade) with AtCAD4, AtCAD5 and OsCAD2. MaCAD5, MaCAD6, MaCAD7, MaCAD8, MaCAD9 and MaCAD10 were distributed in class II. MaCAD3 and MaCAD4 were located in class III with AtCAD1, OsCAD1 and OsCAD4 (Figure 2F).

Chromosomal localization and gene duplication of lignin biosynthesis genes from *Musa acuminata* genome

In order to determine the distribution of lignin biosynthesis genes on the chromosome, the relative positions of 101 genes on the chromosome were identified according to their physical positions in the *Musa acuminata* genome database. Ma00_t01670.1, Ma00_t02580.1 and Ma00_t03560.1 were not anchored on the chromosome and were named *MaCOMT22*, *MaCOMT23* and

10.3389/fpls.2023.1072086

MaCAD10, respectively. As shown in Figure 3, although each of the 11 banana chromosomes contained lignin biosynthesis genes, the distribution appeared to be uneven. There were 17 members on chromosome 4 from 7 different gene families (*MaHCTs*, *Ma4CLs*, *MaCADs*, *MaC3Hs*, *MaCCRs*, *MaF5Hs* and *MaCOMTs*). There were 14 members on chromosome 9 from six families (*Ma4CLs*, *MaC4Hs*, *MaCADs*, *MaCCoAOMTs*, *MaCOMTs* and *MaPALs*), while only three genes on chromosome 3 were from three families (*Ma4CL6*, *MaCAD6* and *MaC4H2*). In the multi member gene families, eighteen *Ma4CLs* were widely distributed on the 10 chromosomes except for Chr10. Twenty-four *MaCCRs* were distributed on 6 chromosomes as follows Chr3, Chr4, Chr5, Chr6, Chr8 and Chr9. Most of *MaCOMTs* were only distributed on Chr2 and Chr9.

Segmental duplication, tandem duplication and retrotransposition are known to be key factors driving gene family expansion (Hurles, 2004; Freeling, 2009). In our study, 11 colinear genes pairs from nine gene families except for *MaC3Hs* were identified to be located in the synthetic blocks and belonged to segmental duplication (Figure 3 and Supplementary Table 4). It is worth noting that there were four *MaCADs* (*MaCAD1*, *MaCAD2*, *MaCAD3* and *MaCAD4*) with segmental duplication located in Block4_chr04, Block8_chr01 and Block8_chr04, indicating that the segmental duplication plays important roles in the expansion of *MaCADs*. We also found four tandem duplication gene clusters on Chr2, Chr8, Chr9 and Chr10. The number of gene clusters on chromosome 2 was the largest, containing 11 genes, and all of them were from *MaCOMT* gene family (Figure 3). We did not find the member belonging to retrotransposition among the 104 lignin biosynthesis genes. Based on our analysis, we propose that the expansion of lignin biosynthesis genes may be mainly *via* segment and tandem duplication during the *Musa acuminata* genome evolutionary processes.

Expression profile of lignin biosynthesis genes during Cavendish fruit development and the postharvest ripening stage

To analyze the expression profiles of lignin biosynthesis genes, RNA-Seq data were derived from the fruit development and ripening stages (Supplementary Table 2). We deleted 56 lignin biosynthesis genes with RPMK values less than 5 in 0DAF, 20DAF, 80DAF_0DPH, 8DPH and 14DPH. There were 25 and 26 lignin biosynthesis genes highly expressed at 0 DAF and 20 DAF (RPKM > 20), contributing about 24.04% and 25.00% of the total, respectively. In 0DAF and 20 DAF, the expression levels of *MaC3H2*, *MaC4H2*, *MaC4H5*, *MaCAD7*, *MaCCR-like17*, *MaCCR-like19*, *MaCCR-like2*, *MaCCR-like3*, *MaCCR-like4*, *MaCCR-like6*, *MaCCR-like7* and *MaPAL3* were more than 50 (RPKM>50). However, in 80 DAF-0

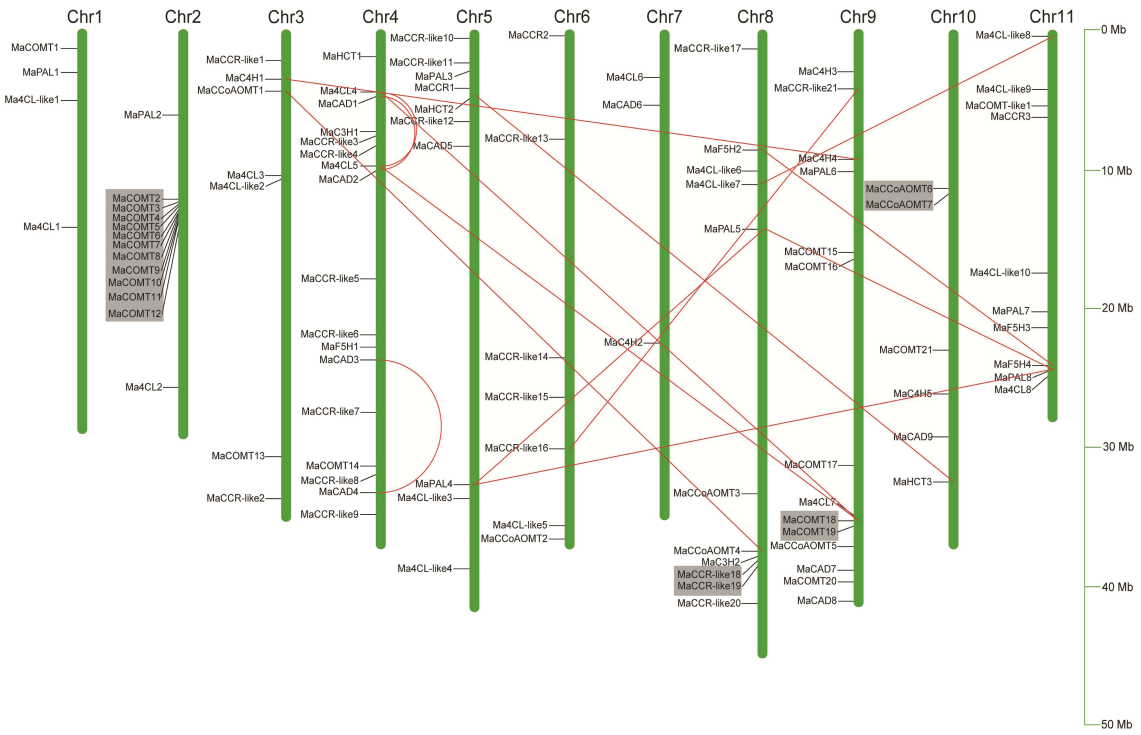

FIGURE 3
Localization of 102 lignin biosynthesis genes on eleven *Musa acuminata* genome chromosomes. The chromosomes were numbered between 1 to 11 and shown at the top of each chromosomes (Chr represented as bars). Chromosomal distances were given in Mb. Red line indicated segmental duplicated genes, and gray area indicated tandem duplicated genes.

10.3389/fpls.2023.1072086

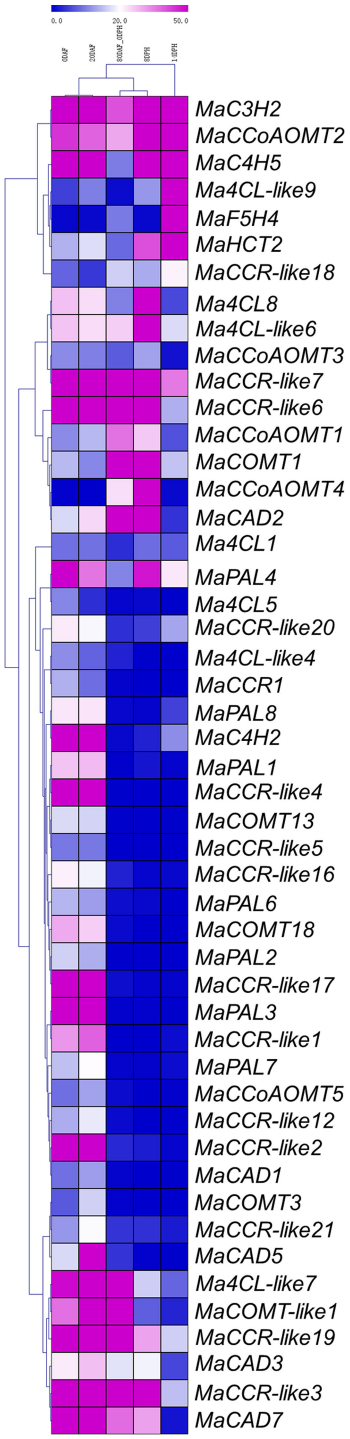

FIGURE 4
Expression patterns of lignin biosynthesis genes in different stages of fruit development and ripening. The heatmap with dendrogram was created based on the RPKM value of the lignin biosynthesis genes. Differences in gene expression changes were shown in color as the scale.

DPH, 8 DPH and 14 DPH, only 14, 16 and 10 genes were highly expressed (RPKM>20), respectively (Figure 4). The number of highly expressed genes during postharvest ripening was significantly less than that during fruit development. These results indicate that the lignin biosynthesis genes are expressed actively in the fruit development, which is closely related to the growth and development of banana fruit. It is worth noting that *MaC3H* gene family contained two copies (*MaC3H1* and *MaC3H2*) (Figure 3). During fruit development and ripening, we found that *MaC3H1* was not expressed in 11 transcriptome data and checked by RT-PCR (results not shown), while *MaC3H2* was constitutively expressed with high RPKM value (RPKM>40) (Supplementary Table 5), showing that only *MaC3H2* may have biological functions. We also found that the expression levels of *Ma4CL8*, *MaPAL4*, *MaC4H5*, *Ma4CL-like6*, *MaCCoAOMT2*, *MaCAD3*, *MaHCT2* and *MaCAD2* were increased gradually in 80DAF-0DPH, 8DPH and 14DPH, and some genes such as Ma4CL-like9, *MaHCT2*, *MaF5H4* and *MaC4H5* reached the highest level in 14DPH (RPKM>190) (Figure 4). The above results suggest that these lignin biosynthesis genes may play roles in the lignin synthesis during the postharvest process of banana fruit and participate in the quality formation.

The expression level of lignin biosynthesis genes in the Cavendish banana plantlets in response to osmotic, salt, and cold treatments

To analyze the expression profiles of lignin biosynthesis genes, RNA-Seq data were derived from Cavendish banana plantlets in response to osmotic, salt and cold treatments. To present the differentially expressed genes visually and exactly, we filtered out the genes with RPKM values less than 5 in the control or treatments. Cold treatment (4°C) caused the fifteen lignin biosynthesis genes were differentially expressed (log2 Ratio Cold/Control>1), among which eleven were up-regulated and four down-regulated (Figure 5 and Supplementary Table 6). Treatment with drought (200 mM mannitol) caused the eighteen genes were found to be differentially expressed (log2 Ratio Osmotic/Control > 1), among which nine were up-regulated and nine down-regulated (Figure 5 and Supplementary Table 6). Treatment with salt (300 mM NaCl) caused fourteen members were differentially expressed (log2 Ratio Salt/Control > 1), among which thirteen were up-regulated and one was down regulated (Figure 5 and Supplementary Table 6). It is worth noting that *MaPAL1*, *MaPAL3*, *MaPAL4*, *MaPAL7*, *MaC4H2* and *MaCCR9* were up-regulated during the drought, salt, and cold stresses. We found that forty-one genes were significantly differentially expressed under cold, drought and salt stresses, but nine genes were only involved in one of the abiotic stresses (Figure 5). Therefore, most of the genes were not differentially expressed in the responses to above stresses. For example, we did not find that *bona fide MaCCRs* was involved in the process of the responses to above abiotic stresses. Although several *MaCCR-likes* were found to be up-regulated under low temperature, drought and salt stresses, the function of *MaCCR-like* was not clear. Similarly, we also found that only one member of *MaCADs* was up-regulated under salt stress, other eight *MaCADs* were not differentially expressed during the responses to abiotic stresses. Moreover, in phylogenetic tree, the differentially expressed

10.3389/fpls.2023.1072086

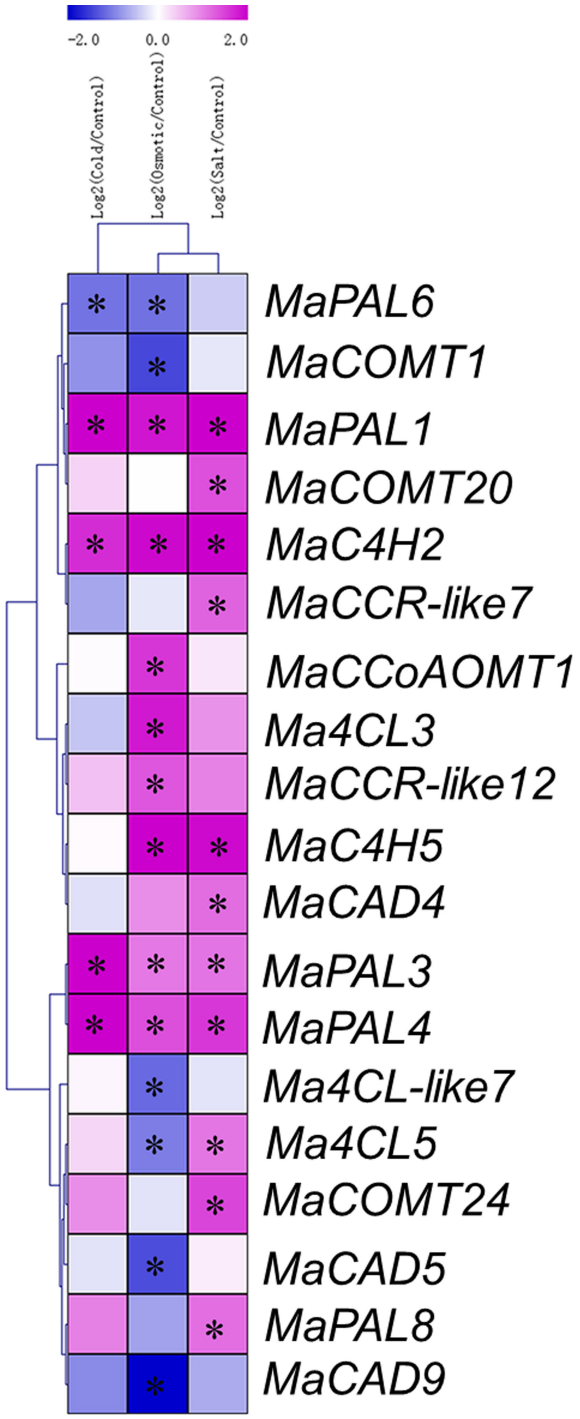

FIGURE 5
Expression patterns of lignin synthesis genes in response to cold, osmotic, and salt treatments in banana. The Log2-based fold change was used to create the heatmap. Differences in gene expression changes were shown in color as the scale. * Significant difference at $P < 0.01$.

MaCAD4 was closely related to *AtCAD1*, which played a partial role in the synthesis of lignin in *Arabidopsis* (Eudes et al., 2006). *MaCAD2* and *MaCAD3*, belonging to the group I (the *bona fide* CAD clade) (Figure 2), were not differentially expressed under the drought, salt and cold stresses (Figure 5). These results indicate that most of lignin synthesis genes are not involved in banana response to stresses, which may be one of the possible reasons for banana being more sensitive to abiotic stresses.

The expression level of lignin biosynthesis genes during the banana plantlets interacting with Foc TR4

The expression pattern of a gene is generally correlated with its function; hence, we analyzed the expression patterns of the lignin biosynthesis genes in susceptible and resistant varieties responding to Foc TR4 infection. To present the differentially expressed genes visually and exactly, we filtered out the genes with RPKM values less than 5 in the 0 DPI or 2 DPI. In variety Cavendish, there were only 11 differentially expressed genes (marked with black stars), of which only one was up-regulated and 10 down-regulated (Figure 6 and Supplementary Table 7). The results showed that lignin synthesis genes were not activated in susceptible varieties. In variety Pahang, there were 12 differentially expressed genes from seven gene families, all of which were up-regulated (Figure 6 and Supplementary Table 7), indicating that lignin biosynthesis genes were activated in banana responding to Foc TR4 infection. In variety GCTCV-119, we found 20 differentially expressed genes, 17 of which were up-regulated and 3 down-regulated (Figure 6 and Supplementary Table 7), indicating that most of the differentially expressed genes were activated. It is noteworthy that we found that the differentially expressed genes between Pahang and GCTCV-119 were not consistent, indicating that ploidy still has a great impact on the banana resistance to Foc TR4 infection. In general, our results indicate that these differentially expressed lignin biosynthesis genes are involved in banana resistance to Foc TR4 infection.

Based on RNA-seq data, 8 differentially expressed lignin biosynthesis genes were selected for RT-qPCR. The results showed that the expression patterns of the selected genes had the same trend and consistent results between RNA-seq data and RT-qPCR data (Figure 7).

Weighted gene co-expression network of lignin biosynthesis genes

To explore the functions, 104 lignin biosynthesis genes were selected as 'guide genes' to seek co-expressed genes using an RNA-Seq dataset from 11 different transcriptomes, including fruit development and ripening stages, banana plantlets response to osmotic, salt, and cold treatment, and banana roots inoculated with Foc TR4 (Supplementary Table 2). A total of 725 TFs were as the 'target nodes', whose expression patterns were closely correlated with 51 lignin biosynthesis genes from ten gene families, which were identified with weighted values larger than 0.5 (Supplementary Table 6). Following visualization using Cytoscape (Otasek et al., 2019), the co-expression network of lignin biosynthesis genes was divided into four modules. Module I-IV (purple, red, light blue and yellow, respectively) contained 37, 3, 4, 1 and 1 lignin biosynthesis

10.3389/fpls.2023.1072086

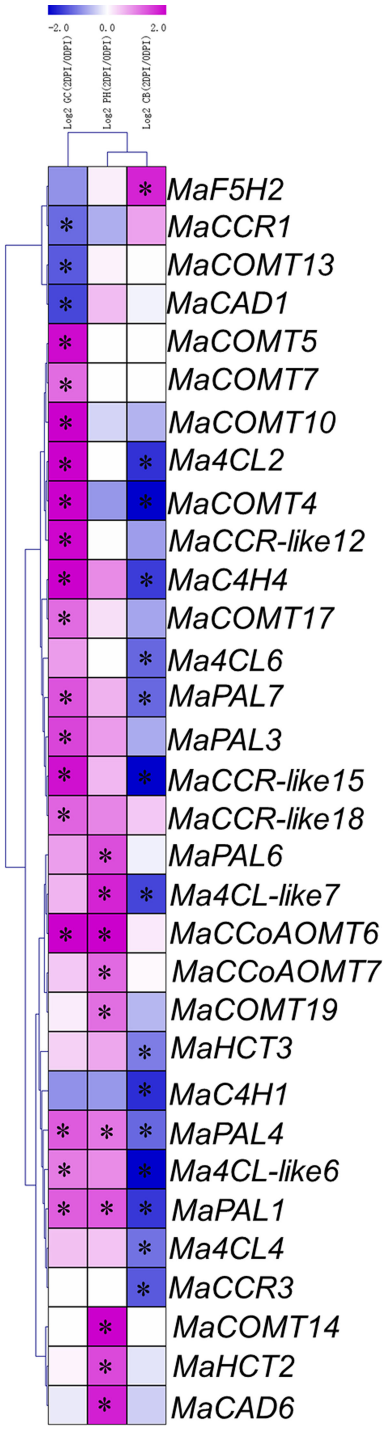

FIGURE 6
Expression patterns of lignin biosynthesis genes in Cavendish banana (CB), GCTCV-119 (GC) and Pahang (PH) inoculated with Foc TR4. The Log2-based fold change was used to create the heatmap. Differences in gene expression changes were shown in color as the scale.
* Significant difference at $P < 0.01$.

genes, respectively (Figure 8). The correlated TFs were in 68 different type TF classes, such as MYB, ERF, basic helix-loop-helix (bHLH), WRKY, C2H2, NAC, and LOB (Supplementary Table 8).

Verifying the interaction between promoter of *MaC3H2* and transcription factors in WGCNA using yeast one-hybrid

The -2000bp upstream sequence of *MaC3H2* was obtained by RT-PCR based on the sequence of *Musa acuminata* genome, the 1481bp promoter sequence was obtained by transcriptional active site prediction, and the main regulatory elements of *MaC3H2* promoter were predicted online by plantcare website. We found that there was conserved AC element (AC-I element, -1378bp) and MBS and MRE elements (-32 and -1066bp) bounding to MYB TF in the *MaC3H2* promoter sequence (Supplementary Table 3). The results show that *MaC3H2* may be closely related to lignin synthesis in banana.

We extracted the co-expression network of *MaC3H2* and found 36 transcription factors from 13 gene families were contained in the network, and *MaMYBs* had the largest number (10 *MaMYBs*) (Figure 9A). We further identified whether the *MaC3H2* promoter had a relationship with these transcription factors. Five transcription factors including *MaMYB1* (Ma03_t25780.1), *MaMYB2* (Ma09_t20280.1), *MaMYB3* (Ma11_t11940.1), *MaNAC1* (Ma07_t06080.1) and *MabHLH1* (Ma10_t14490.1) were verified by yeast one hybridization. Using the pGADT7-MaMYB1, pGADT7-MaMYB2, pGADT7-MaMYB3, pGADT7-MaNAC1, pGADT7-MabHLH1 vectors as effectors and using the pAbAi vector carrying *MaC3H2* promoter as a reporter, the Y1HGold yeast co-transformed with *MaC3H2* promoter-AbAi and pGADT7-MaMYB1, pGADT7-MaMYB2, pGADT7-MaMYB3, pGADT7-MaNAC1, pGADT7-MabHLH1 could grow normally on the SD/-Leu medium containing 300 ng/mL AbA, respectively, whereas the yeast carrying MaC3H2 promoter-AbAi and pGADT7 could not grow (Figure 9B), which proved that *MaMYB1*, *MaMYB2*, *MaMYB3*, *MaNAC1* and *MabHLH1* can definitely bind with the sequence of the *MaC3H2* promoter, respectively.

In the dual luciferase assay, the *MaC3H2* promoter-driven luciferase reporter and CaMV35S-driven *MaMYB1*, *MaMYB2*, *MaMYB3*, *MaNAC1* and *MabHLH1* effector were separately constructed and then co-infected tobacco leaf epidermal cells by *Agrobacterium-mediated* transformation (Figure 9C). *MaMYB1*, *MaMYB2*, *MaMYB3*, *MaNAC1* and *MabHLH1* were found to activate the activity of the *MaC3H2* promoter with a LUC/REN ratio higher than 2.12, 4.57, 3.81, 6.41 and 3.04-fold of empty vector (pGreen II 62-SK/pGreen II 0800-LUC), respectively, indicating that *MaMYB1*, *MaMYB2*, *MaMYB3*, *MaNAC1* and *MabHLH1* are activative effectors of *MaC3H2* gene expression (Figure 9D).

Discussion

Lignin is an important product of phenylpropane metabolism pathway and an important component of plant cell wall, playing crucial roles in maintaining normal development, enhancing overall mechanical strength and increasing stress resistance of plants (Zhao and Dixon, 2011). The systematic identification of the enzyme genes in the lignin biosynthesis pathway in *Musa acuminata*

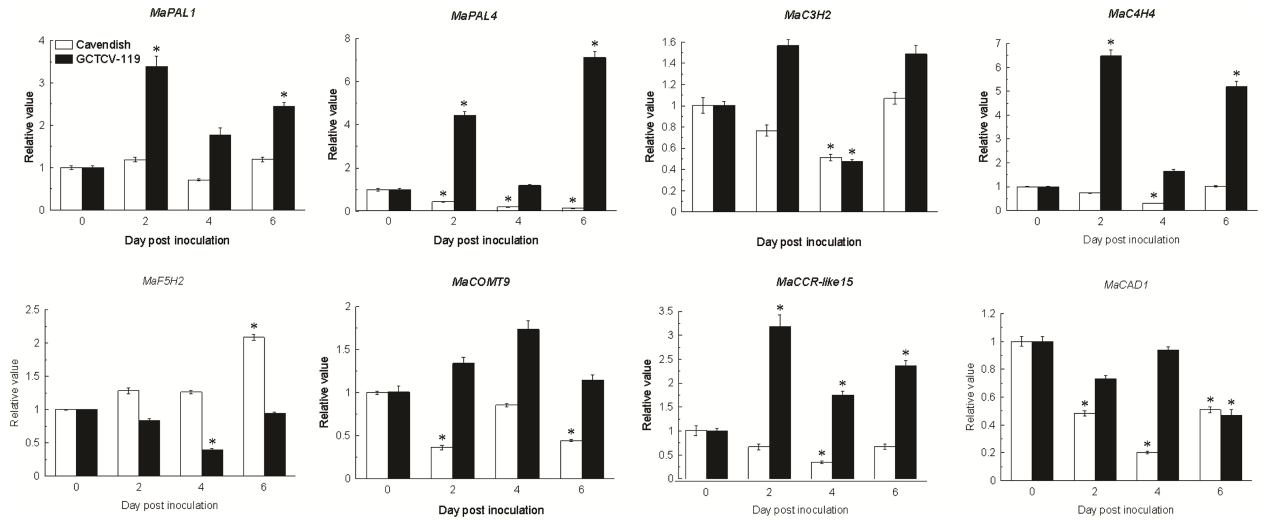

FIGURE 7
Expression patterns of lignin biosynthesis genes involving in plant-pathogen interaction pathway in Ba Xijiao and GCTCV-119 inoculated with Foc TR4 by qRT-PCR. The results are presented as differential relative transcript abundance. The data represent the mean ± standard deviation (SD) of three replicates. The y-axis shows the transcript fold-change relative to that in the control (0 DPI). * Significantly different from the control (0 DPI) at $P < 0.01$, respectively.

genome can provide important references for improving the content and composition of lignin to obtain ideal new varieties with good quality and strong resistance for banana industry. Generally, there are usually 10 enzyme gene families involved in lignin biosynthesis (Xu et al., 2009). So far, many important plants have identified genes for lignin biosynthesis enzyme, 56 genes encoding *bona fide* lignin biosynthesis enzymes in *Setaria viridis* genome (Ferreira et al., 2019), 37 genes in *Eucalyptus grandis* (Carocha et al., 2015), 34 genes in *Arabidopsis* (Raes et al., 2003), 35 genes in *Pyrus bretschneideri* (Cao et al., 2019). In this study, we totally identified 104 genes belonging to ten lignin biosynthesis gene families in *Musa acuminata* genome, and 73 genes encoding *bona fide* enzymes, which have been the highest number of *bona fide* lignin biosynthesis genes detected, to date. The characteristics of the number of encoding amino acids, isoelectric point, and molecular weight of the lignin biosynthesis genes are similar to previous results in *Arabidopsis* and other plants (Raes et al., 2003; Carocha et al., 2015; Cao et al., 2019).

Gene duplication is universal across all organisms and plays a key role in driving the evolution of genomes and genetic systems, and is closely related to translocation, insertion, inversion, deletion and duplication of small fragments, chromosome rearrangement and fusion after genome-wide duplication events (Simillion et al., 2004; Navajas-Pérez and Paterson, 2009). The *Musa acuminata* genome underwent three rounds of WGD (α/β/γ), resulting in a large number of collinear blocks in the *Musa acuminata* genome (D'Hont et al., 2012), and showed that the chromosomes of *Musa acuminata* genome had experienced multiple rounds of genome-wide duplication events. At the gene family level, we found that nine lignin biosynthesis gene from *Musa acuminata* genome underwent tandem or segmental duplication events except for *MaC3Hs* which have only two members and may be the reason leading the *Musa acuminata* genome has more gene members than those in *Arabidopsis* and rice. We found the number of *MaC4Hs*, *MaF5Hs*, *MaC3Hs*, *MaHCTs* and *MaCCoAOMTs* gene families was relatively small, which was not different from that in *Arabidopsis* and rice (Figure 2).

In the phylogenetic tree, MaPAL6 was divided into a subfamily with PALs of other woody plants (Figure 2). This is similar to the results of other species (Shi et al., 2010). 4CL gene family usually exists as a small gene family (Gui et al., 2011; Sun et al., 2013). There are four 4CL genes in *Arabidopsis* and five 4CL genes in rice, maize and *Populus* (Sun et al., 2013; Li et al., 2015; Rao et al., 2015; Xiong et al., 2019). In our results, we found eight 4CL genes were in *Musa acuminata* genome. Phylogenetic analysis show that 4CL in dicotyledons can be divided into two types. In type I, 4CL was mainly involved in lignin biosynthesis, while in type II, 4CL was often involved in flavonoids biosynthesis (Li et al., 2015). In *Musa acuminata* genome, we found six Ma4CLs in type I and two Ma4CLs in type II (Figure 2), indicating that the number of Ma4CL involved in lignin biosynthesis is more than that involved in flavonoid biosynthesis. During fruit development and postharvest ripening stages, we found that the RPKM value of *Ma4CL8* involved in flavonoid synthesis was significantly higher than that of *Ma4CL1*, *Ma4CL5* and *Ma4CL6* involved in lignin biosynthesis, and showed that the metabolism of flavonoids may be stronger than that of lignin in banana fruit (Figure 4). We also found that *Ma4CL3* and *Ma4CL5* involved in lignin synthesis were significantly differentially expressed in osmotic and salt stresses, while the *Ma4CL2* and *Ma4CL8* involved in flavonoid synthesis were not differentially expressed in low temperature, drought and salt stresses (Figure 5), indicating that *Ma4CLs* may be involved in Cavendish banana responding to abiotic stresses.

In plants, the COMT gene family usually comprises multiple members. For example, there are seven COMT genes in *Eucalyptus grandis* (Carocha et al., 2015), 25 in *Populus trichocarpa* (Shi et al.,

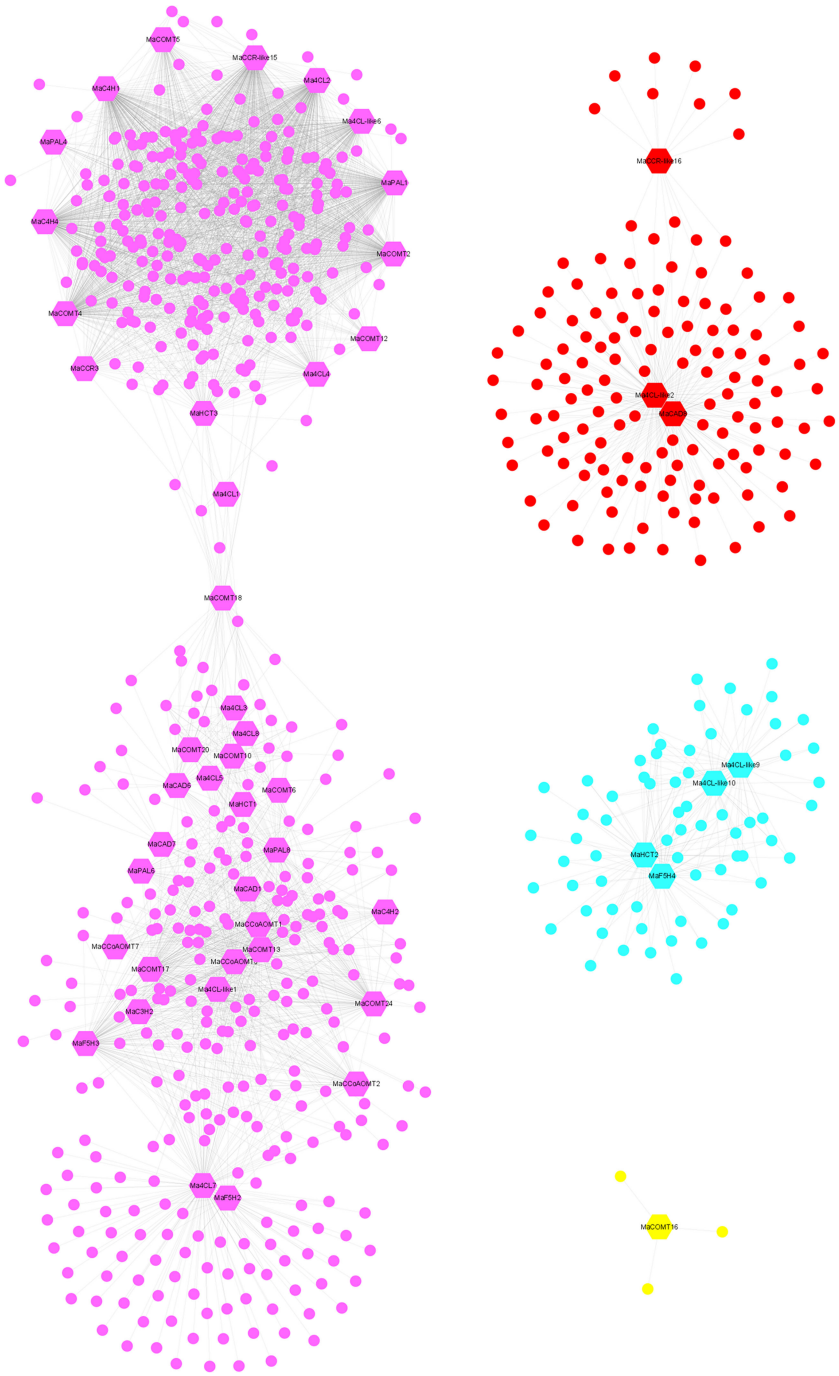

FIGURE 8
Co-expression network of banana generated using the lignin biosynthesis genes as guides. The network comprised 725 TF genes (nodes); the hexagon represented lignin biosynthesis genes.

2010) and 18 in *Arabidopsis thaliana* and 27 in *Vitis vinifera* (Liu et al., 2016). In our results, 24 MaCOMTs were detected in *Musa acuminata* genome. All the MaCOMTs were near by the *AtOMT1* (At5g54160.1) and *OsCOMT1* (Os08G06100) and located in clade I (Figure 2D). *AtOMT1* and *OsCOMT1* have been identified to participate in lignin biosynthesis in *Arabidopsis* and rice (Goujon et al., 2003; Raes et al., 2003; Vanholme et al., 2012; Dalmais et al., 2013; Koshiba et al., 2013). These results suggest that the MaCOMTs from *Musa acuminata* genome may have the ability to participate in lignin biosynthesis. In *Arabidopsis*, AtCCR1 is involved in constitutive lignification (Lauvergeat et al., 2001). ZmCCR1 and TaCCR1 may participate in developmental lignin deposition in secondary cell walls (Tamasloukht et al., 2011). TaCCR2 is actively undergoing lignification and involved in both G and S lignin synthesis (Ma and Tian, 2005). In phylogenetic tree, we found MaCCR1 and MaCCR2 were near by the ZmCCR1, TaCCR1, OsCCR19 and OsCCR20, and in this clade we also found AtCCR1. MaCCR3 was grouped with TaCCR2 (Figure 2E),

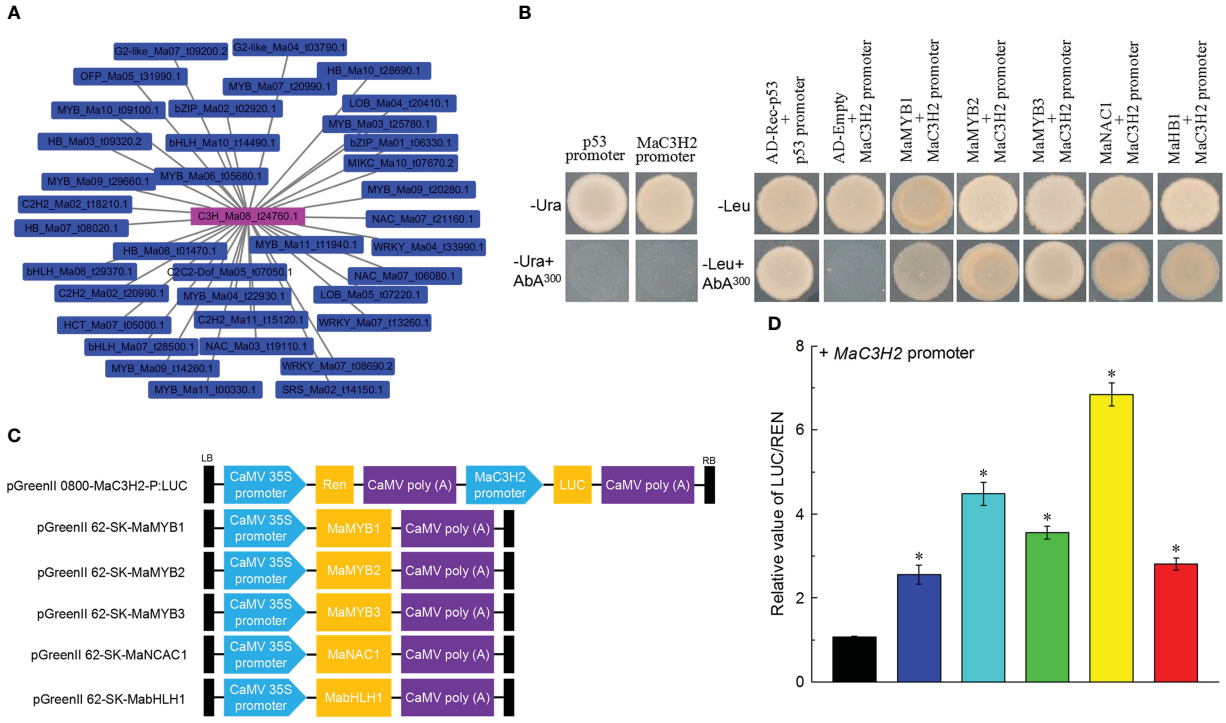

FIGURE 9
Identification of upstream regulatory transcription factors of MaC3H2. **(A)** Co-expression network of MaC3H2 by WGCNA. **(B)** Yeast one-hybrid assay of MaMYB1, MaMYB2, MaMYB3, MaNAC1 and MabHLH1 bind with MaC3H2 promoter. **(C)** Schematic diagrams of the effector and reporter constructs used for the dual LUC assay. **(D)** MaMYB1, MaMYB2, MaMYB3, MaNAC1 and MabHLH1 activate the MaC3H2 promoter in dual-luciferase assays. * Significant difference at $P < 0.01$.

suggesting that MaCCR1, MaCCR2 and MaCCR3 are probably involved in lignin biosynthesis or lignification of banana. CAD gene family can be divided into three classes according to homology and affinity for substrates (Ferreira et al., 2019). In *Arabidopsis*, the functional characteristics of AtCAD1, AtCAD4, AtCAD5 and OsCAD2 have been clear, and they are involved in the process of lignin synthesis (Sibout et al., 2005; Zhang et al., 2006; Barakat et al., 2009; Hirano et al., 2012). In our results, MaCAD1 and MaCAD2 also have high homology, and are in the same subgroup as AtCAD4 with AtCAD5. MaCAD3, MaCAD4 and AtCAD1 belonged to the same class (Figure 2F), indicating that MaCAD1, MaCAD2, MaCAD3 and MaCAD4 play roles in lignin biosynthesis of banana.

As the main component of dietary fiber, lignin content in fruit has a great impact on fruit quality. During fruit ripening, a large number of degradation of cell wall substances lead to the destruction of cell wall structure and increase the cell gap and the soft in pulp (Chaplin et al., 1990). During fruit development and ripening, we found that 49 genes of lignin synthesis were expressed (RPKM>5), accounting for 47.11% (104 of the total), 24 genes were highly expressed (RPKM>50), accounting for 23.08%, and *MaC3H2* and *MaCCR-like7* were constitutively expressed (RPKM>30) at all the time points. We also found *Ma4CL-like9*, *MaHCT2*, *MaF5H4*, *MaC4H5* and *MaCCoAOMT2* were highly expressed (RPKM>100) at 14 DPH. Our results show that most of lignin biosynthesis genes are involved in lignin biosynthesis and the quality formation during banana fruit development and ripening stage.

Lignin is an important part of vascular plant cell wall and mainly deposits in the secondary wall cells of vascular tissue, mechanical tissue and protective tissue. It provides mechanical support for cells and tissues, facilitates the long-distance transportation of water and minerals, and forms a physical barrier with cellulose to resist biological and abiotic stresses (Lewis and Yamamoto, 1990). During growth, Cavendish banana is vulnerable to drought (van Asten et al., 2011), low temperature (Kang et al., 2007) and salt (Xu et al., 2014), resulting in the reduction of fruit yield and quality. In our results, we found that most lignin biosynthesis genes from *Musa acuminata* genome had low RPKM value. Only 24 genes were differentially expressed after low temperature, drought or salt stress treatments, among which, 14 genes were differentially expressed in only one of the above three stresses (Figure 5). Therefore, the inactive gene expression of lignin biosynthesis genes may be the cause of more vulnerable to abiotic stresses in Cavendish banana. PAL is the key enzyme and rate limiting enzyme of phenylpropane metabolism. The products of phenylpropane metabolic pathway play an important role in plant growth and development and response to stresses (Harakava, 2005; Huang et al., 2010). In banana fruit, *MaPAL* participates in heat pretreatment inducing chilling tolerance during postharvest (Chen et al., 2008). In our results, we found that MAPALs were involved in the response to low temperature, drought and salt stresses. *MaPAL1*, *MaPAL3*, *MaPAL4* and *MaPAL7* were up-regulated and differentially expressed in Cavendish banana responding to

low temperature, drought and salt stresses, indicating that *MAPALs* are involved in Cavendish banana responding to abiotic stresses, and may have some redundancy in function, which is similar to the results of *AtPALs* in *Arabidopsis* (Huang et al., 2010).

Many studies have shown that lignin is involved in the construction of plant defense system, which is an important barrier for plants to prevent or reduce the invasion of pathogens (Boudet, 2000). In banana, treatment with elicitors from Foc R4 causes increased lignin deposition in roots of 'Williams' and 'Goldfinger' varieties, and higher contents of lignin are induced in the disease-resistant variety 'Goldfinger' (De Ascensao and Dubery, 2000). The lignin content accumulation of tolerance varieties is faster than that of susceptible varieties after inoculation with Foc TR4 (Van Den Berg et al., 2007). During Cavendish banana inoculated with Foc TR4, lignin biosynthesis genes such as *MAPALs*, *MaC4Hs*, *Ma4CLs* and *MaCADs* were significantly up-regulated and differentially expressed in cultivar Nongke No.1, which have acquired resistance to Foc TR4 through somaclonal variation from Cavendish banana (Wang et al., 2015). Up to now, GCTCV-119 is the best Foc TR4-tolerant alternative cultivar for the Cavendish (Ploetz, 2015). Pahang is highly resistant to Foc TR4 in the greenhouse and field trials, which is a wild germplasm that belongs to subspecies *Musa acuminata* ssp. *Malaccensis* (D'Hont et al., 2012; Zuo et al., 2018; Zhang et al., 2019). In our results, we found that 14 lignin biosynthesis genes were differentially expressed and significantly down-regulated in Cavendish banana variety, and only *MaF5H2* was significantly up-regulated, indicating that the expressions of lignin biosynthesis genes are not activated in susceptible variety responding to Foc TR4 infection. However, we found most lignin biosynthesis genes were significantly up-regulated and differentially expressed in both GCTCV-119 and Pahang varieties (Figure 6). Our results show that the expression of lignin biosynthesis genes is activated in banana resistance to Foc TR4 infection, which is consistent with the previous results (De Ascensao and Dubery, 2000; Van Den Berg et al., 2007).

WGCNA can identify functionally related or similar gene expression modules in high-throughput data, and we can consider gene function and its relationship from biological function as a whole, and we can specifically screen the co-expression modules with high biological significance with the target traits (Zhao et al., 2010). In our results, we found that 61.54% of lignin biosynthesis genes had co-expression network with 725 transcription factors from 68 gene families (Figure 8), suggesting that lignin biosynthesis genes may play important roles in the lignin biosynthesis for Cavendish banana during the growth or response to stresses. MYB, NAC (Nam, ataf1/2, CUC2) and LIM (LIN-11, ISL-1, MEC-3) transcription factors were related to the secondary wall synthesis (Zhao and Dixon, 2011). Overexpression of *MusaNAC68* can significantly reduce the expression of *MaPAL*, *Ma4CL*, *MaC4H*, *MaCOMT* and *MaCcOAMT*, resulting in reduced secondary wall thickness coupled with diminished lignin deposition (Negi et al., 2019). *MusaMYB31* as repressor of lignin biosynthesis in banana, overexpression of *MusaMYB31* in banana cultivar *Rasthali* (*Musa* cv. *Rasthali*) can reduce the deposition of lignin in Secondary wall (Tak et al., 2017). In the co-expression network, 97 *MaMYBs* and 34 *MaNACs* transcription factors were associated with lignin biosynthesis genes (Figure 8 and Supplementary Table 8), showing that these transcription factors may be candidate genes for regulating lignin biosynthesis in banana. WRKY and ERF transcription factors are widely involved in the process of plant responding to stresses (Rehman and Mahmood, 2015; Chen et al., 2018). Based on the whole gene family analysis, several *MabHLHs* were involved in banana resistance to Foc TR4 infection (Wang et al., 2020). In our results, we also found large number of *MaERFs* (88), *MabHLHs* (70) and *MaWRKYs* (59) transcription factors were associated with lignin biosynthesis genes (Figure 8 and Supplementary Table 8). P-coumarate 3-hydroxylase (C3H) determines the carbon source flow direction of lignin monomer and is also the rate limiting enzyme of phenylpropane pathway (Franke et al., 2002). Using yeast one hybrid and LUC activity assay, we also found that these transcription factors could bind with the promoter of *MaC3H2*, indicating that *MaMYB1*, *MaMYB2*, *MaMYB3*, *MaNAC1* and *MabHLH1* are active effectors of *MaC3H2* expression (Figure 9). In general, the above results suggest that these associated transcription factors in the co-expression network may play important roles in regulating lignin biosynthesis during fruit development, post-harvest ripening stages and response to stresses.

Conclusions

We have developed a comprehensive resource of gene families involved in lignin biosynthesis in *Musa acuminata* genome. A total of 101 lignin biosynthesis genes were located on 11 different chromosomes. Most gene families had segmental duplication, and tandem replication was the main way to expand the number of *MaCOMTs*. We found most lignin biosynthesis genes were not involved in banana responding to abiotic stresses, except for *MaPALs*. Finally, the co-expression network of lignin biosynthesis genes was constructed using WGCNA to elucidate the abundant upstream regulatory networks of lignin biosynthesis in Cavendish banana. This comprehensive study improves our understanding of the lignin biosynthesis genes associated with fruit development, ripening processes, and stress responses and will establish a foundation for future studies on genetic improvement in banana.

Data availability statement

All the data of RNA-seq have been uploaded to the CNSA (https://db.cngb.org/cnsa/) of CNGBdb with accession number CNP0000292. The accession numbers of all samples are listed in Supplementary Table 2.

Author contributions

The study was conceived by ZW, B-yX and Z-qJ. Z-mW, X-mY, C-hJ, J-yW, and J-hL analyzed the lignin biosynthesis gene's data from *Musa acuminata* genome and performed the bioinformatics analysis. ZW and C-hJ performed Foc TR4 inoculation, RNA isolation and qRT-PCR. ZW and J-yW wrote the manuscript. All authors contributed to the article and approved the submitted version.

Funding

This work was financially supported by Hainan Provincial Natural Science Fund Project (320LH020); National Key Research and Development Program of China (2019YFD1000903); National Nonprofit Institute Research Grant of CATAS (1630052022002); National Natural Science Foundation of China (31501624) and Modern Agro-industry Technology Research System (No. CARS-32).

Conflict of interest

The authors declare that the research was conducted in the absence of any commercial or financial relationships that could be construed as a potential conflict of interest.

Supplementary material

The Supplementary Material for this article can be found online at: https://www.frontiersin.org/articles/10.3389/fpls.2023.1072086/full#supplementary-material

References

Ahmad, I., Meng, X. P., Kamran, M., Ali, S., Ahmad, S., Liu, T. N., et al. (2020). Effects of uniconazole with or without micronutrient on the lignin biosynthesis, lodging resistance, and winter wheat production in semiarid regions. *J. Integr. Agr* 19 (1), 62–77. doi: 10.1016/S2095-3119(19)62632-8

Audic, S., and Claverie, J. M. (1997). The significance of digital gene expression profiles. *Genome Res.* 7 (10), 986–995. doi: 10.1101/gr.7.10.986

Aurore, G., Parfait, B., and Fahrasmane, L. (2009). Bananas, raw materials for making processed food products. *Trends Food Sci. Tech.* 20, 78–91. doi: 10.1016/j.tifs.2008.10.003

Baldoni, A., Von Pinho, E. V., Fernandes, J. S., Abreu, V. M., and Carvalho, M. L. (2013). Gene expression in the lignin biosynthesis pathway during soybean seed development. *Genet. Mol. Res.* 12, 2618–2624. doi: 10.4238/2013.February.28.2

Barakat, A., Bagniewska-Zadworna, A., Choi, A., Plakkat, U., DiLoreto, D. S., Yellanki, P., et al. (2009). The cinnamyl alcohol dehydrogenase gene family in populus: phylogeny, organization, and expression. *BMC Plant Biol.* 9, 26. doi: 10.1186/1471-2229-9-26

Boerjan, W., Ralph, J., and Baucher, M. (2003). Lignin biosynthesis. *Annu. Rev. Plant Biol.* 54, 519–546. doi: 10.1146/annurev.arplant.54.031902.134938

Bonawitz, N. D., and Chapple, C. (2010). The genetics of lignin biosynthesis: connecting genotype to phenotype. *Annu. Rev. Genet.* 44, 337–363. doi: 10.1146/annurev-genet-102209-163508

Boudet, A. M. (2000). Lignins and lignification: selected issues. *Plant Physiol. Bioch* 38, 81–96. doi: 10.1016/S0981-9428(00)00166-2

Campbell, M. M., and Sederoff, R. R. (1996). Variation in lignin content and composition (mechanisms of control and implications for the genetic improvement of plants). *Plant Physiol.* 110 (1), 3. doi: 10.1104/pp.110.1.3

Cao, Y., Li, X., and Jiang, L. (2019). Integrative analysis of the core fruit lignification toolbox in pear reveals targets for fruit quality bioengineering. *Biomolecules* 9, 504. doi: 10.3390/biom9090504

Carocha, V., Soler, M., Hefer, C., Cassan-Wang, H., Fevereiro, P., Myburg, A. A., et al. (2015). Genome-wide analysis of the lignin toolbox of eucalyptus grandis. *New Phytol.* 206, 1297–1313. doi: 10.1111/nph.13313

Chaplin, G. R., Buckley, M. J., and Lai, S. C. (1990). Differential softening and physico-chemical changes in the mesocarp of ripening mango fruit. *Symp. Trop. Fruit Int. Trade.* 269, 233–240. doi: 10.17660/ActaHortic.1990.269.30

Chen, J. Y., He, L. H., Jiang, Y. M., Wang, Y., Joyce, D. C., Ji, Z. L., et al. (2008). Role of phenylalanine ammonia-lyase in heat pretreatment-induced chilling tolerance in banana fruit. *Physiologia Plantarum* 132 (3), 318–328. doi: 10.1111/j.1399-3054.2007.01013.x

Chen, F., Hu, Y., Vannozzi, A., Wu, K., and Zhang, L. (2018). The WRKY transcription factor family in model plants and crops. *Crit. Rev. Plant Sci.* 36, 1–25. doi: 10.1080/07352689.2018.1441103

D'Hont, A., Denoeud, F., Aury, J. M., Baurens, F. C., Carreel, F., Garsmeur, O., et al. (2012). The banana (*Musa acuminata*) genome and the evolution of monocotyledonous plants. *Nature* 488, 213–217. doi: 10.1038/nature11241

Dalmais, M., Antelme, S., Ho-Yue-Kuang, S., Wang, Y., Darracq, O., d'Yvoire, M. B., et al. (2013). A tilling platform for functional genomics in brachypodium distachyon. *PloS One* 8, e65503. doi: 10.1371/journal.pone.0065503

De Ascensao, A. ,. R., and Dubery, I. ,. A. (2000). Panama Disease: cell wall reinforcement in banana roots in response to elicitors from *fusarium oxysporum* f. sp. cubense race four. *Phytopathology* 90, 1173–1180. doi: 10.1094/PHYTO.2000.90.10.1173

Du, D., Zhang, Q., Cheng, T., Pan, H., Yang, W., and Sun, L. (2013). Genome-wide identification and analysis of late embryogenesis abundant (LEA) genes in *Prunus mume*. *Mol. Biol. Rep.* 40 (2), 1937–1946. doi: 10.1007/s11033-012-2250-3

Eudes, A., Pollet, B., Sibout, R., Do, C. T., Séguin, A., Lapierre, C., et al. (2006). Evidence for a role of atcad 1 in lignification of elongating stems of *Arabidopsis thaliana*. *Planta* 225, 23–39. doi: 10.1007/s00425-006-0326-9

Faraji, M., Fonseca, L. L., Escamilla-Treviño, L., Barros-Rios, J., Engle, N., Yang, Z., et al. (2018). Mathematical models of lignin biosynthesis. *Biotechnol. Biofuels* 11 (1), 1–17. doi: 10.1186/s13068-018-1028-9

Ferreira, S. S., Simões, M. S., Carvalho, G. G., de Lima, L. G., Svartman, R. M., and Cesarino, I. (2019). The lignin toolbox of the model grass *Setaria viridis*. *Plant Mol. Biol.* 101, 235–255. doi: 10.1007/s11103-019-00897-9

Franke, R., Hemm, M. R., Denault, J. W., Ruegger, M. O., Humphreys, J. M., and Chapple, C. (2002). Changes in secondary metabolism and deposition of an unusual lignin in the ref8 mutant of *Arabidopsis*. *Plant J.* 30, 47–59. doi: 10.1046/j.1365-313X.2002.01267.x

Freeling, M. (2009). Bias in plant gene content following different sorts of duplication: tandem, whole-genome, segmental, or by transposition. *Annu. Rev. Plant Biol.* 60, 433–453. doi: 10.1146/annurev.arplant.043008.092122

Goujon, T., Sibout, R., Pollet, B., Maba, B., Nussaume, L., Bechtold, N., et al. (2003). A new *Arabidopsis thaliana* mutant deficient in the expression of O-methyltransferase impacts lignins and sinapoyl esters. *Plant Mol. Biol.* 51, 973–989. doi: 10.1023/A:1023022825098

Gui, J., Shen, J., and Li, L. (2011). Functional characterization of evolutionarily divergent 4-coumarate: coenzyme a ligases in rice. *Plant Physiol.* 157 (2), 574–586. doi: 10.1104/pp.111.178301

Hamauzu, Y., Chachin, K., Ding, C., and Kurooka, H. (1997). Differences in surface color, flesh firmness, physiological activity, and some components of loquat fruits picked at various stages of maturity. *Engei Gakkai zasshi.* 65, 859–869. doi: 10.2503/jjshs.65.859

Happi Emaga, T., Robert, C., Ronkart, S. N., Wathelet, B., and Paquot, M. (2008). Dietary fibre components and pectin chemical features of peels during ripening in banana and plantain varieties. *Bioresour Technol.* 99, 4346–4354. doi: 10.1016/j.biortech.2007.08.030

Harakava, R. (2005). Genes encoding enzymes of the lignin biosynthesis pathway in *Eucalyptus*. *Genet. Mol. Biol.* 28, 601–607. doi: 10.1590/S1415-47572005000400015

Heslop-Harrison, J. S., and Schwarzacher, T. (2007). Domestication, genomics and the future for banana. *Ann. Bot.* 100, 1073–1084. doi: 10.1093/aob/mcm191

Hirano, K., Aya, K., Kondo, M., Okuno, A., Morinaka, Y., and Matsuoka, M. (2012). OsCAD2 is the major CAD gene responsible for monolignol biosynthesis in rice culm. *Plant Cell Rep.* 31, 91–101. doi: 10.1007/s00299-011-1142-7

Holsters, M., De Waele, D., Depicker, A., Messens, E., Van Montagu, M., and Schell, J. (1978). Transfection and transformation of *Agrobacterium tumefaciens*. *Mol. Gen. Genet.* 163 (2), 181–187. doi: 10.1007/BF00267408

Hu, Y., Li, W., Xu, Y., Li, G., Liao, Y., and Fu, F. (2009). Differential expression of candidate genes for lignin biosynthesis under drought stress in maize leaves. *J. Appl. Genet.* 50, 213–223. doi: 10.1007/BF03195675

Huang, J., Gu, M., Lai, Z., Fan, B., Shi, K., Zhou, Y. H., et al. (2010). Functional analysis of the *Arabidopsis* PAL gene family in plant growth, development, and response to environmental stress. *Plant Physiol.* 153, 1526–1538. doi: 10.1104/pp.110.157370

Hurles, M. (2004). Gene duplication: the genomic trade in spare parts. *PloS Biol.* 2, E206. doi: 10.1371/journal.pbio.0020206

Hwang, S. C., and Ko, W. H. (2004). Cavendish Banana cultivars resistant to fusarium wilt acquired through somaclonal variation in Taiwan. *Plant Dis.* 88, 580–588. doi: 10.1094/PDIS.2004.88.6.580

Ibrahim, R. K., Bruneau, A., and Bantignies, B. (1998). Plant O-methyltransferases: molecular analysis, common signature and classification. *Plant Mol. Biol.* 36, 1–10. doi: 10.1023/A:1005939803300

Kang, G., Wang, Z., Xia, K., and Sun, G. (2007). Protection of ultrastructure in chilling-stressed banana leaves by salicylic acid. *J. Zhejiang Univ. Sci. B.* 8, 277–282. doi: 10.1631/jzus.2007.B0277

Komuraiah, A., Kumar, N. S., and Prasad, B. D. (2014). Chemical composition of natural fibers and its influence on their mechanical properties. *Mech. Compos. Mater.* 50 (3), 359–376. doi: 10.1007/s11029-014-9422-2

Koshiba, T., Hirose, N., Mukai, M., Yamamura, M., Hattori, T., Suzuki, S., et al. (2013). Characterization of 5-hydroxyconiferaldehyde O-methyltransferase in *Oryza sativa*. *Plant Biotechnol.* 30, 157–167. doi: 10.5511/plantbiotechnology.13.0219a

Langfelder, P., and Horvath, S. (2008). WGCNA: an r package for weighted correlation network analysis. *BMC Bioinf.* 9, 559. doi: 10.1186/1471-2105-9-559

Lauvergeat, V., Lacomme, C., Lacombe, E., Lasserre, E., Roby, D., and Grima-Pettenati, J. (2001). Two cinnamoyl-CoA reductase (CCR) genes from *Arabidopsis thaliana* are differentially expressed during development and in response to infection with pathogenic bacteria. *Phytochemistry* 57, 1187–1195. doi: 10.1016/S0031-9422(01)00053-X

Lee, T. H., Tang, H., Wang, X., and Paterson, A. H. (2012). PGDD: a database of gene and genome duplication in plants. *Nucleic Acids Res.* 41, D1152–D1158. doi: 10.1093/nar/gks1104

Lewis, N. G., and Yamamoto, E. (1990). Lignin: occurrence, biogenesis and biodegradation. *Annu. Rev. Plant Physiol. Plant Mol. Biol.* 41, 455–496. doi: 10.1146/annurev.pp.41.060190.002323

Li, Y., Kim, J. I., Pysh, L., and Chapple, C. (2015). Four isoforms of *Arabidopsis* 4-Coumarate:CoA ligase have overlapping yet distinct roles in phenylpropanoid metabolism. *Plant Physiol.* 169, 2409–2421. doi: 10.1104/pp.15.00838

Liu, X., Luo, Y., Wu, H., Xi, W., Yu, J., Zhang, Q., et al. (2016). Systematic analysis of O-methyltransferase gene family and identification of potential members involved in the formation of O-methylated flavonoids in citrus. *Gene* 575 (2), 458–472. doi: 10.1016/j.gene.2015.09.048

Lu, G., Li, Z., Zhang, X., Wang, R., and Yang, S. (2015). Expression analysis of lignin-associated genes in hard end pear (*Pyrus pyrifolia* whangkeumbae) and its response to calcium chloride treatment conditions. *J. Plant Growth Regul.* 34, 251–262. doi: 10.1007/s00344-014-9461-x

Ma, Q. H., and Tian, B. (2005). Biochemical characterization of a cinnamoyl-CoA reductase from wheat. *Biol. Chem.* 386, 553–560. doi: 10.1515/BC.2005.065

Martin, G., Baurens, F. C., Droc, G., Rouard, M., Cenci, A., Kilian, A., et al. (2016). Improvement of the banana '*Musa acuminata*'reference sequence using NGS data and semi-automated bioinformatics methods. *BMC Genomics* 17, 243. doi: 10.1186/s12864-016-2579-4

Mortazavi, A., Williams, B. A., McCue, K., Schaeffer, L., and Wold, B. (2008). Mapping and quantifying mammalian transcriptomes by RNA-seq. *Nat. Methods* 5 (7), 621–628. doi: 10.1038/nmeth.1226

Navajas-Pérez, R., and Paterson, A. H. (2009). Patterns of tandem repetition in plant whole genome assemblies. *Mol. Genet. Genomics* 281, 579–590. doi: 10.1007/s00438-009-0433-y

Negi, S., Tak, H., and Ganapathi, T. R. (2019). Overexpression of *MusaNAC68* reduces secondary wall thickness of xylem tissue in banana. *Plant Biotechnol. Rep.* 13 (2), 151–160. doi: 10.1007/s11816-019-00524-5

Otasek, D., Morris, J. H., Bouças, J., Pico, A. R., and Demchak, B. (2019). Cytoscape automation: empowering workflow-based network analysis. *Genome Biol.* 20, 185. doi: 10.1186/s13059-019-1758-4

Perrier, X., Langhe., E., Donohue, M., Lentfer, C., Vrydaghs, L., Bakry, F., et al. (2011). Multidisciplinary perspectives on banana (*Musa* spp.) domestication. *Proc. Natl. Acad. Sci. U S A.* 108, 11311–11318. doi: 10.1073/pnas.1102001108

Ploetz, R. ,. C. (2006). Fusarium wilt of banana is caused by several pathogens referred to as fusarium oxysporum f. sp. cubense. *Phytopathology* 96, 653–656. doi: 10.1094/PHYTO-96-0653

Ploetz, R. C. (2015). Fusarium wilt of banana. *Phytopathology* 105, 1512–1521. doi: 10.1094/PHYTO-04-15-0101-RVW

Raes, J., Rohde, A., Christensen, J. H., de, V., Peer, Y., and Boerjan, W. (2003). Genome-wide characterization of the lignification toolbox in *Arabidopsis*. *Plant Physiol.* 133, 1051–1071. doi: 10.1104/pp.103.026484

Rakoczy, M., Femiak, I., Alejska, M., Figlerowicz, M., and Podkowinski, J. (2018). Sorghum CCoAOMT and CCoAOMT-like gene evolution, structure, expression and the role of conserved amino acids in protein activity. *Mol. Genet. Genomics* 293 (5), 1077–1089. doi: 10.1007/s00438-018-1441-6

Rao, G., Pan, X., Xu, F., Zhang, Y., Cao, S., Jiang, X., et al. (2015). Divergent and overlapping function of five 4-coumarate/coenzyme a ligases from *Populus tomentosa*. *Plant Mol. Biol. Rep.* 33, 841–885. doi: 10.1007/s11105-014-0803-4

Rehman, S., and Mahmood, T. (2015). Functional role of DREB and ERF transcription factors: regulating stress-responsive network in plants. *Acta Physiol. Plant* 37, 178. doi: 10.1007/s11738-015-1929-1

Ryu, J., Kwon, S. J., Sung, S. Y., Kim, W. J., Kim, D. S., Ahn, J. W., et al. (2016). Molecular cloning, characterization, and expression analysis of lignin biosynthesis genes from kenaf (*Hibiscus cannabinus* l.). *Genes Genom.* 38 (1), 59–67. doi: 10.1007/s13258-015-0341-y

Shannon, P., Markiel, A., Ozier, O., Baliga, N. S., Wang, J. T., Ramage, D., et al. (2003). Cytoscape: a software environment for integrated models of biomolecular interaction networks. *Genome Res.* 13, 2498–2504. doi: 10.1101/gr.1239303

Shen, H., Mazarei, M., Hisano, H., Escamilla-Trevino, L., Fu, C., Pu, Y., et al. (2013). A genomics approach to deciphering lignin biosynthesis in switchgrass. *Plant Cell.* 25, 4342–4361. doi: 10.1105/tpc.113.118828

Shi, R., Sun, Y. H., Li, Q., Heber, S., Sederoff, R., and Chiang, V. L. (2010). Towards a systems approach for lignin biosynthesis in populus trichocarpa: transcript abundance and specificity of the monolignol biosynthetic genes. *Plant Cell Physiol.* 51, 144–163. doi: 10.1093/pcp/pcp175

Shiu, S. H., and Bleecker, A. B. (2003). Expansion of the receptor-like kinase/Pelle gene family and receptor-like proteins in *Arabidopsis*. *Plant Physiol.* 132, 530–543. doi: 10.1104/pp.103.021964

Sibout, R., Eudes, A., Mouille, G., Pollet, B., Lapierre, C., Jouanin, L., et al. (2005). CINNAMYL ALCOHOL DEHYDROGENASE-c and -d are the primary genes involved in lignin biosynthesis in the floral stem of arabidopsis. *Plant Cell.* 17, 2059–2076. doi: 10.1105/tpc.105.030767

Simillion, C., Vandepoele, K., Saeys, Y., and Van de Peer, Y. (2004). Building genomic profiles for uncovering segmental homology in the twilight zone. *Genome Res.* 14, 1095–1106. doi: 10.1101/gr.2179004

Sun, H., Li, Y., Feng, S., Zou, W., Guo, K., Fan, C., et al. (2013). Analysis of five rice 4-coumarate: coenzyme a ligase enzyme activity and stress response for potential roles in lignin and flavonoid biosynthesis in rice. *Biochem. Bioph Res. Co.* 430 (3), 1151–1156. doi: 10.1016/j.bbrc.2012.12.019

Tak, H., Negi, S., and Ganapathi, T. R. (2017). Overexpression of *MusaMYB31*, a R2R3 type MYB transcription factor gene indicate its role as a negative regulator of lignin biosynthesis in banana. *PloS One* 12, e0172695. doi: 10.1371/journal.pone.0172695

Tamasloukht, B., Wong Quai Lam, M. S., Martinez, Y., Tozo, K., Barbier, O., Jourda, C., et al. (2011). Characterization of a cinnamoyl-CoA reductase 1 (CCR1) mutant in maize: effects on lignification, fibre development, and global gene expression. *J. Exp. Bot.* 62, 3837–3848. doi: 10.1093/jxb/err077

Tamura, K., Stecher, G., Peterson, D., Filipski, A., and Kumar, S. (2013). MEGA6: molecular evolutionary genetics analysis version 6.0. *Mol. Biol. Evol.* 30, 2725–2729. doi: 10.1093/molbev/mst197

Tang, Y., Liu, F., Xing, H., Mao, K., Chen, G., Guo, Q., et al. (2019). Correlation analysis of lignin accumulation and expression of key genes involved in lignin biosynthesis of ramie (*Boehmeria nivea*). *Genes (Basel).* 10, 389. doi: 10.3390/genes10050389

van Asten, P. J. A., Fermont, A. M., and Taulya, G. (2011). Drought is a major yield loss factor for rainfed East African highland banana. *Agr Water Manage.* 98, 541–552. doi: 10.1016/j.agwat.2010.10.005

Van Den Berg, N., Berger, D. K., Hein, I., Birch, P. R., Wingfield, M. J., and Viljoen, A. (2007). Tolerance in banana to fusarium wilt is associated with early up-regulation of cell wall-strengthening genes in the roots. *Mol. Plant Pathol.* 8, 333–341. doi: 10.1111/j.1364-3703.2007.00389.x

Vanholme, R., Demedts, B., Morreel, K., Ralph, J., and Boerjan, W. (2010). Lignin biosynthesis and structure. *Plant Physiol.* 153, 895–905. doi: 10.1104/pp.110.155119

Vanholme, R., Morreel, K., Darrah, C., Oyarce, P., Grabber, J. H., Ralph., J., et al. (2012). Metabolic engineering of novel lignin in biomass crops. *New Phytol.* 196, 978–1000. doi: 10.1111/j.1469-8137.2012.04337.x

Wang, Z., Jia, C., Li, J., Huang, S., Xu, B., and Jin, Z. (2015). Activation of salicylic acid metabolism and signal transduction can enhance resistance to fusarium wilt in banana (*Musa acuminata* l. AAA group, cv. *Cavendis*). *Funct. Integr. Genomics* 15, 47–62. doi: 10.1007/s10142-014-0402-3

Wang, Z., Jia, C., Wang, J., Miao, H., Liu, J., Chen, C., et al. (2020). Genome-wide analysis of basic helix-loop-helix transcription factors to elucidate candidate genes related to fruit ripening and stress in banana (*Musa acuminata* l. AAA group, cv. *Cavendish*). *Front. Plant Sci.* 27, 11:650. doi: 10.3389/fpls.2020.00650

Wang, Z., Li, J., Jia, C., Li, J., Xu, B., and Jin, Z. (2016). Molecular cloning and expression of four phenylalanine ammonia lyase genes from banana interacting with fusarium oxysporum. *Biol. Plantarum.* 60, 1–10. doi: 10.1007/s10535-016-0619-1

Wang, Z., Miao, H., Liu, J., Xu, B., Yao, X., Xu, C., et al. (2019). *Musa balbisiana* genome reveals subgenome evolution and functional divergence. *Nat. Plants.* 5, 810–821. doi: 10.1038/s41477-019-0452-6

Wang, Z., Zhang, J., Jia, C., Liu, J., Li, Y., Yin, X., et al. (2012). *De novo* characterization of the banana root transcriptome and analysis of gene expression under *Fusarium oxysporum* f. sp. *Cubense* tropical race 4 infection. *BMC Genomics* 13, 650. doi: 10.1186/1471-2164-13-650

Wei, X. X., and Wang, X. Q. (2004). Evolution of 4-coumarate: coenzyme a ligase (4CL) gene and divergence of larix (*Pinaceae*). *Mol. Phylogenet. Evo.* 31 (2), 542–553. doi: 10.1016/j.ympev.2003.08.015

Xiong, W., Wu, Z., Liu, Y., Li, Y., Su, K., Bai, Z., et al. (2019). Mutation of 4-coumarate: coenzyme a ligase 1 gene affects lignin biosynthesis and increases the cell wall digestibility in maize *brown midrib5* mutants. *Biotechnol. Biofuels.* 12, 82. doi: 10.1186/s13068-019-1421-z

Xu, Y., Hu, W., Liu, J., Zhang, J., Jia, C., Miao, H., et al. (2014). A banana aquaporin gene, *MaPIP1.1*, is involved in tolerance to drought and salt stresses. *BMC Plant Biol.* 14, 59. doi: 10.1186/1471-2229-14-59

Xu, Z., Zhang, D., Hu, J., Zhou, X., Ye, X., Reichel, K. L., et al. (2009). Comparative genome analysis of lignin biosynthesis gene families across the plant kingdom. *BMC Bioinf.* 10 (Suppl 11), S3. doi: 10.1186/1471-2105-10-S11-S3

Zhang, L., Cenci, A., Rouard, M., Zhang, D., Wang, Y., Tang, W., et al. (2019). Transcriptomic analysis of resistant and susceptible banana corms in response to infection by *Fusarium oxysporum* f. sp. cubense tropical race 4. *Sci. Rep.* 9, 8199. doi: 10.1038/s41598-019-44637-x

Zhang, B., and Horvath, S. (2005). A general framework for weighted gene co-expression network analysis. *Stat. Appl. Genet. Mol. Biol.* 4. Article17. doi: 10.2202/1544-6115.1128

Zhang, K., Qian, Q., Huang, Z., Wang, Y., Li, M., Hong, L., et al. (2006). GOLD HULL AND INTERNODE2 encodes a primarily multifunctional cinnamyl-alcohol dehydrogenase in rice. *Plant Physiol.* 140, 972–983. doi: 10.1104/pp.105.073007

Zhang, L., Yuan, T., Wang, Y., Zhang, D., Bai, T., Xu, S., et al. (2018). Identification and evaluation of resistance to *Fusarium oxysporum* f. sp. *cubense* tropical race 4 in *Musa acuminata* pahang. *Euphytica* 214. Article number: 106. doi: 10.1007/s10681-018-2185-4

Zhao, Q., and Dixon, R. A. (2011). Transcriptional networks for lignin biosynthesis: more complex than we thought? *Trends Plant Sci.* 16, 227–233. doi: 10.1016/j.tplants.2010.12.005

Zhao, W., Langfelder, P., Fuller, T., Dong, J., Li, A., and Hovarth, S. (2010). Weighted gene coexpression network analysis: state of the art. *J. Biopharm. Stat.* 20, 281–300. doi: 10.1080/10543400903572753

Zhao, H., Sheng, Q., Lv, S., Wang, T., and Song, Y. (2004). Characterization of three rice CCoAOMT genes. *Chin. Sci. Bull.* 49, 1602–1606. doi: 10.1360/04wc0225

Zuo, C., Deng, G., Li, B., Huo, H., Li, C., and Hu, C. (2018). Germplasm screening of *Musa* spp. for resistance to *Fusarium oxysporum* f. sp. cubense tropical race 4 (Foc TR4). *Eur. J. Plant Pathol.* 151, 723–734. doi: 10.1007/s10658-017-1406-3

Frontiers in
Plant Science

Cultivates the science of plant biology and its applications

The most cited plant science journal, which advances our understanding of plant biology for sustainable food security, functional ecosystems and human health.

Discover the latest Research Topics

See more →

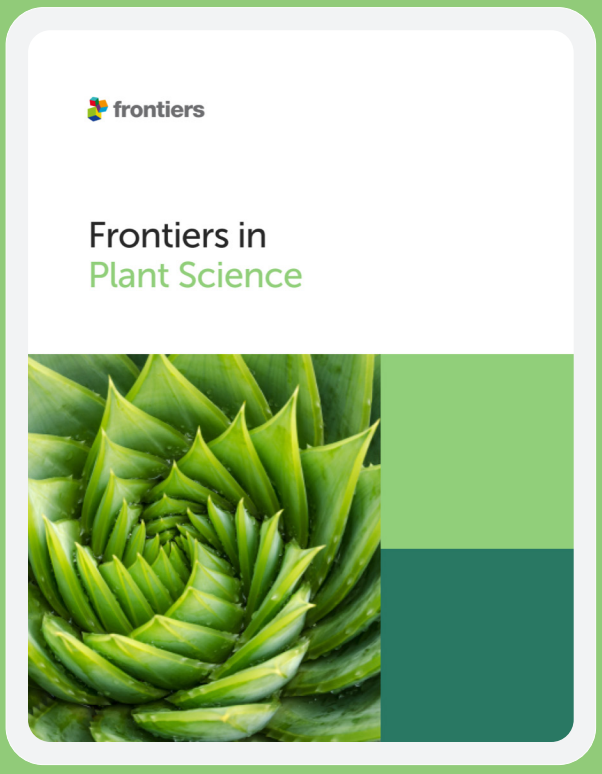

Frontiers

Avenue du Tribunal-Fédéral 34
1005 Lausanne, Switzerland
frontiersin.org

Contact us

+41 (0)21 510 17 00
frontiersin.org/about/contact